



THE UNIVERSITY *of* EDINBURGH

This thesis has been submitted in fulfilment of the requirements for a postgraduate degree (e.g. PhD, MPhil, DClinPsychol) at the University of Edinburgh. Please note the following terms and conditions of use:

- This work is protected by copyright and other intellectual property rights, which are retained by the thesis author, unless otherwise stated.
- A copy can be downloaded for personal non-commercial research or study, without prior permission or charge.
- This thesis cannot be reproduced or quoted extensively from without first obtaining permission in writing from the author.
- The content must not be changed in any way or sold commercially in any format or medium without the formal permission of the author.
- When referring to this work, full bibliographic details including the author, title, awarding institution and date of the thesis must be given.

**The regulation of Type III Secretion in
Enterohaemorrhagic *Escherichia coli***

Xuefang Xu



Thesis presented for the degree of Doctor of Philosophy

The University of Edinburgh

2011

Declaration

The research presented in this thesis is entirely my own work unless otherwise stated in the text. The material contained in this thesis has not been submitted for any other degree or professional qualification in any University.

Xuefang Xu

Acknowledgments

I would like to thank my supervisor Prof. David Gally for his guidance, support and ingenious ideas in my whole PhD. I fell so lucky to have David Gally as my supervisor. He is always there when I need help and kind to me. He not only takes his responsibility as a supervisor, but also cares about student life. He encouraged me to have own ideas in research and showed me how to do the research. In the beginning of PhD, I totally don't know how to do the research and what is research. But now, I have my own interest and thinking in research. That's a huge work to turn a student into a potential scientist. But he made it. He spent lots time on my thesis as well. I can't say more to express my appreciation to him.

Many thanks also go to all the staff and students of the ZAP lab, LBEP and MPRL groups. I would like to separately thank to Sean McAteer in the ZAP lab for his hard work making Stx2 conjugated K12 strain so we would publish the paper. He answers every question I encountered and helps me to solve difficulties I met. I thank honour student Chris Simpson and visiting student Pilar for the LEE1-GFP measurement work. Also special thanks to Dai Wang, Tracy Dransfield, Tracy Rosser, Allen Flockhart for the support and guidance in the beginning of my PhD. A big thank you to Jai Tree for making the *cII* plasmids and help with CGH work. Thanks also goes to Gill, Bethan, Prerna, Eliza, Robyn, Caitriona, Nouri, you make the lab a fun place to work and best friends I have ever made in the lab. I also acknowledge Darren Shaw for statistical analysis.

I would also like to thank all my friends who supported me throughout the five years I have been studying in Edinburgh. It wouldn't be possible to list them all here, but I would like to specially thank Xiaojun Liu and his wife Wei Zhou, Rui Zhang, Lina Ma, Ye Liu, Xin Jin and his girlfriend Yue Kang, Jianing and her husband Huizhong, Li Sha, Hui Zhang, Yijing Chen, Qianmin Gao, Eric, Long Ma, Ao Zhang, Liang Liang, Libing Xue with his girlfriend Lily, Zhaoyuan Li and his wife Pin Liu and their lovely daughter Xing Zi, Ailing Zhang and his husband Xiaozhong Zheng, Qi Ma and his wife Xiaoqin, Kun Zhao, Yang Zhang and her boyfriend Sanliang Lin for their friendship and love. A big thank you to my flatmate Zejun Yan. I would like to thank him for his constant support and for the proof reading of my thesis.

I would like to acknowledge the China Scholarship council and College of Medicine and Veterinary Medicine for funding my PhD.

Finally, my family, Dad and Mum, my brother Longgang Xu, deserve a separate big thank you for believing in me and supporting me in every step of my life. I owe all my accomplishments and achievements to them.

Contents

Title page	i
Declaration	ii
Acknowledgments	iii
Contents	v
List of abbreviations	
1.1 <i>Escherichia coli</i> background	2
1.2 Pathogenic <i>E. coli</i>	2
1.3 Enterohaemorrhagic <i>E. coli</i> (EHEC)	4
1.4 <i>E. coli</i> O157:H7	6
1.4.1 Serotyping of <i>E. coli</i>	6
1.4.2 Phage-typing of <i>E. coli</i> O157:H7	9
1.4.3 Clinical impact of Shiga-toxigenic <i>E. coli</i> infections	11
1.4.4 Epidemiology of <i>E. coli</i> O157:H7	14
1.4.4.1 Sources of <i>E. coli</i> O157:H7 infection	14
1.4.4.2 Transmission of <i>E. coli</i> O157:H7	14
1.4.5 Infection models of <i>E. coli</i> O157:H7	16
1.4.6 Evolution of <i>E. coli</i> O157:H7	16
1.4.6.1 Evolution of <i>E. coli</i> O157:H7	16
1.4.6.2 The evolution of phage	18
1.5 A/E lesions	19
1.6 The LEE and Type III secretion	20
1.6.1 LEE	20
1.6.2 T3SS	22
1.6.2.1 Introduction to T3SS	22
1.6.2.2 Basal apparatus of the T3SS	24
1.6.2.3 Translocon of T3SS	25
1.6.2.4 Secreted translocon and effectors encoded by LEE	26
1.6.2.5 Non-LEE-encoded effectors secreted by T3SS	28
1.7 The regulation of Type III secretion	30
1.7.1 Regulation inputs into the LEE	30
1.7.1.1 The regulators encoded on LEE	30
1.7.1.2 The regulation of aerobic/anaerobic respiration and impact on T3S	32
1.7.2 Timing of secretion	33
1.7.3 The non LEE encoded regulators	34
1.8 Shiga- like toxin (Stx) and Stx phage	35
1.8.1 Introduction	35
1.8.2 The lytic and lysogenic decision of bacteria phage lambda (λ)	39
1.8.3 The regulation of Stx phage	41
1.8.4 The role of CII	43
1.9 Research background and aims of this project	46
2 Chapter 2 Materials and Methods	48
2.1 Bacterial strains, media & plasmids	48
2.2 Primers used in this work	53
2.3 DNA manipulation	58
2.3.1 DNA agarose electrophoresis	58

2.3.2	PCR purification.....	59
2.3.3	DNA sequencing	59
2.3.4	DNA sequence analysis.....	60
2.3.5	Purification of DNA from gel	60
2.3.6	Plasmids DNA extraction and purification	60
2.3.7	Electro-transformation.....	61
2.3.7.1	Preparation of competent cell	61
2.3.7.2	Electro-transformation	61
2.3.8	Chemical transformation.....	62
2.3.8.1	Preparation of calcium-chloride competent bacteria.....	62
2.3.8.2	Chemical transformation.....	63
2.4	Construction of mutants.....	63
2.4.1	The construction of ZAP198 mutants in genes involved in aerobic and anaerobic respiration	63
2.4.1.1	Preparation of electrocompetent hyper-rec EHEC carrying λ -Red functions on pKM201	64
2.4.1.2	Electro-transformation of PCR products into EHEC strains containing pKM201.....	64
2.4.2	The creation of LEE1 promoter constructs.....	65
2.4.2.1	Constructs for allelic exchange	67
2.4.2.2	The construction of mutants for LEE1 constructions.....	68
2.4.2.3	Testing aTc induction efficiency by TetR using GFP measurement	69
2.4.3	The construction of EDL933 mutants in Stx1&2 phage and <i>cII</i> genes.....	70
2.4.3.1	Constructs for allelic exchange.	70
2.4.3.2	Mutant construction	70
2.5	Quantification of population fluorescence levels	72
2.6	Preparation of bacterial and epithelial cell cultures for infection assays	72
2.7	Bacterial infection assays and immunofluorescence microscopy.....	73
2.8	Comparative genomic hybridization (CGH)	73
2.9	PCR to identify Stx2 and Stx2c phage	74
2.10	Preparation of secreted proteins and bacterial fractions for protein analyses	74
2.11	Sodium dodecyl sulphate-polyacrylamide gel electrophoresis (SDS-PAGE)	75
2.12	Colloidal coomassie blue staining of SDS-PAGE gels	75
2.13	Western blotting.....	76
2.14	Statistical analysis	77
2.14.1	Statistical analysis in Chapter 3	77
2.14.2	Statistical analysis in Chapter 7	77
3	Chapter 3 The T3SS & respiration regulation.....	78
3.1	Introduction	79
3.2	Results	80
3.2.1	The deletion of <i>E. coli</i> O157 respiration regulators.....	80
3.2.1.1	The construction of an <i>arcA</i> deletion.....	80
3.2.1.2	<i>fnr</i> deletion.....	83
3.2.1.3	<i>narX</i> deletion.....	85
3.2.1.4	<i>narP</i> deletion.....	87
3.2.2	Growth of ZAP198 and mutant strains	89
3.2.3	Cell binding assay of ZAP198 and mutant strains on EBL cells.....	91
3.2.4	A/E lesion formation by ZAP198 and isogenic strains with deletions in specific respiration-associated genes	93
3.2.5	T3S level in ZAP198 and the respiration regulation mutants	95
3.3	Discussion	97

4	Chapter 4 The Construction of an Inducible LEE1 Promoter.....	102
4.1	Introduction	103
4.2	Results	108
4.2.1	Construction of an <i>E. coli</i> O157:H7 strain with <i>tetR</i> exchanged into the <i>lac</i>	108
4.2.1.1	Replacement of <i>lacZY</i> with the <i>sacBkan</i> cassette in ZAP198 (Step 1 Fig. 4.2)	108
4.2.1.2	The exchange of the <i>sacBkan</i> cassette with PN25& <i>tetR</i> at <i>lacZY</i> (Step 2 Fig. 4.2).	111
4.2.1.2.1	The construction of a plasmid suitable for the exchange of the <i>sacBkan</i> cassette with PN25TetR at <i>lac</i>	111
4.2.1.2.2	The exchange of <i>sacBkan</i> cassette with <i>tetR</i>	113
4.2.2	Testing aTc induction of GFP expression in ZAP1213.....	114
4.2.2.1	The construction of pXLS03	115
4.2.2.2	GFP measurement following aTc induction	116
4.2.3	Creation of strains with LEE1 promoter replaced by <i>tet</i> promoter in ZAP1213	119
4.2.3.1	First exchange: The exchange of the LEE1 promoter with <i>sacBkan</i> cassette producing intermediate strains for both constructions (Step 3, Fig. 4.2)	122
4.2.3.1.1	The construction of plasmids suitable for the exchange of the LEE1 promoter with <i>sacBkan</i> cassette.....	122
4.2.3.2	The exchange of the LEE1 promoter with <i>sacBkan</i> cassette	125
4.2.3.3	The second exchange: the exchange of the <i>sacBkan</i> cassette with <i>tet</i> promoter (Step 4, Fig. 4.2)	127
4.2.3.3.1	The construction of plasmids suitable for the exchange of the <i>sacBkan</i> cassette with <i>tet</i> promoter	127
4.2.3.3.2	The exchange of the <i>sacBkan</i> for the <i>tet</i> promoter	129
4.2.3.4	Testing induction of the <i>tet</i> promoter in ZAP1213 with the LEE1 promoter replaced by the two <i>tet</i> promoter constructs.....	131
4.2.4	The control of T3S in ZAP1327	133
4.3	Discussion	136
5	Chapter V Phage Regulation of T3S.....	141
5.1	Introduction	142
5.2	Results	144
5.2.1	Comparative genomic hybridization of PT 21/28 and PT 32 strains	144
5.2.2	Identification of Stx2 and Stx2c phage.....	147
5.2.3	T3S levels in PT 21/28 and PT 32 strains	150
5.2.3.1	EspD and EscJ levels in PT 21/28 and PT32 strains.....	150
5.2.3.2	LEE1 promoter expression levels in PT 21/28 and PT32 strains.....	150
5.2.4	Comparison of T3S expression in the presence and absence of Stx phages....	152
5.2.4.1	Comparison of EDL933 and TUV93-0.....	152
5.2.4.2	Plasmid constructs to create deletion mutants	156
5.2.4.3	Construction of Stx phage deletion strains in EDL933.....	159
5.2.5	Repression of LEE1 promoter activity in <i>E. coli</i> K12 transduced with a Stx2 bacteriophage.....	166
5.2.6	The lysogeny regulator CII can repress type III secretion	170
5.2.6.1	Constructs for allelic exchange	173
5.2.6.2	Strain construction.....	175
5.3	Discussion	179
6	Chapter 6 Conclusion.....	188
7	References.....	195

List of abbreviations

AAF	aggregative adherence fimbriae
A/E	attaching and effacing
AMP	Ampicillin
Arc	aerobic respiration control system
Avr	avirulence
aTc	anhydrotetracycline
β	Beta
BFP	bundle-forming pilus
Bp	base pairs
X-gal	bromo-chloro-indolyl-galactopyranoside
BSA	bovine serum albumin
CAM	Chloramphenicol
CDS	coding sequence
CFA	colonisation factor antigen
CL	confluent lysis
CFU	colony forming units
CGSC	Coli Genetic stock centre
CGH	comparative genomic hybridization
DAF	decay-accelerating factor
DAEC	diffusely adherent <i>E. coli</i>
DMEM	Dulbecco's modified eagle medium
DNA	deoxyribonucleic acid
<i>E. coli</i>	<i>Escherichia coli</i>
EAEC	enteroaggregative <i>Escherichia coli</i>
EAST1	enteroaggregative <i>E. coli</i> ST1
EDTA	ethylenediamine tetraacetic acid
EHEC	enterohaemorrhagic <i>Escherichia coli</i>
EIEC	enteroinvasive <i>Escherichia coli</i>

EPEC	enteropathogenic <i>Escherichia coli</i>
ETEC	enterotoxigenic <i>Escherichia coli</i>
Esp	<i>Escherichia coli</i> secreted protein
Esc	<i>Escherichia coli</i> secretion
FBS	fetal bovine serum
Fnr	fumarate, nitrate reduction protein
g	gram
GFP	green fluorescent protein
GrlA	global regulator of <i>LEE</i> activator
GrlR	global regulator of <i>LEE</i> repressor
h	hour(s)
H	flagellar antigen
HC	haemorrhagic colitis
H-NS	histone-like protein
HTH	helix-turn-helix
HUS	haemolytic uremic syndrome
IE	integrative elements
IHF	integration host factor
IPRAVE	international partnership research award in veterinary epidemiology
IPTG	isopropyl β -D-1-thiogalactopyranoside
K	capsular antigen
KAN	kanamycin
kb	kilobase pairs
kDa	kilodalton
λ	lambda
LB	Luria-Bertani
LEE	locus of enterocyte effacement
Ler	<i>LEE</i> encoded regulator
LPS	lipopolysaccharide
LT	heat-labile
M	molar

Map	mitochondrion-associated protein (Map),
Mb	mega base
MEM	minimal essential medium
mg	milligram (10^{-3} gram)
min	minute(s)
ml	millilitre (10^{-3} litre)
mM	millimolar (10^{-3} molar)
Nar	nitrate reductase
Nle	non-LEE encoded effectors
ng	nanogram (10^{-9} gram)
NM	non-motile
NUT	Nitrogen utilization
O	somatic antigen
OD ₆₀₀	optical density at 600 nm
OIs	O-islands
OL	opaque lysis
ORFs	open reading frames
PAI	pathogenicity islands
PBS	phosphate buffered saline
pch	<i>perC</i> -homologous
PCR	polymerase chain reaction
PFA	paraformaldehyde
PFGE	pulsed-field gel electrophoresis
PT	phage type
RNA	ribonucleic acid
rpm	revolutions per minute
SDS	sodium dodecyl sulphate
SCL	semi-confluent lysis
SDS-PAGE	sodium dodecyl sulphate-polyacrylamide gel electrophoresis
Sep	secretion of <i>E. coli</i> proteins
ShET1	<i>Shigella</i> enterotoxin 1

S-loops	Sakai-specific sequence
SSC	saline-sodium citrate
ST	heat-stable
STEC	Stx-producing strains of <i>Escherichia coli</i>
Stx	Shiga toxin
T3SS	type III secretion system
TBE	Tris-borate/EDTA
Tc	tetracycline
TCA	trichloroacetic acid
TetR	Tet repressor
TetA	Tet activator
TFB	transformation buffer
Tir	translocated intimin receptor
TRITC	tetramethyl rhodamine isothiocyanate
Tris	Trishydroxymethylaminomethane
μg	microgram (10 ⁻⁶ gram)
μl	microlitre (10 ⁻⁶ litre)
μM	micromolar (10 ⁻⁶ molar)
V	volt

List of figures

- Fig. 1.1 Pathogenic schema of diarrhoeagenic *E. coli*
- Fig. 1.2 Transmission diagram of *E. coli* O157:H7
- Fig. 1.3 Evolution model for *E. coli* O157:H7
- Fig. 1.4 A/E lesion caused by *E. coli* in rabbit intestinal epithelial cells
- Fig. 1.5 Genetic organization of *LEE*
- Fig. 1.6 Schematic representation of the EPEC/EHEC type III secretion apparatus
- Fig. 1.7 EspA stain of ZAP198
- Fig. 1.8 SDS PAGE gel of T3 secreted protein profile
- Fig. 1.9 Summary of the regulation of the *LEE* genes in *E. coli* O157:H7
- Fig. 1.10 Circular synthetic plot of phage Stx2c: circular representation of the CDS of phage Stx2c and related proteins in the other phages
- Fig. 1.11 Schematic diagram of lysis and lysogeny in λ phage
- Fig. 1.12 Fig. 1.12 Lambda immunity region.
- Fig. 1.13 Schematic diagram of regulation of CII
- Fig. 2.1 Summary of *tet* promoter inducing system
- Fig. 3.1 Structure diagram of *arcA* locus and primers in ZAP198 and *arcA* mutant
- Fig. 3.2 PCR for generation of the deletion cassette with *arcA*, *fnr*, *narX*, *narP* regions and for screening of *arcA* recombinati
- Fig. 3.3 Structure diagram of *fnr* locus and primers in ZAP198 and *fnr* mutant
- Fig. 3.4 PCR screening of recombinant colony 1
- Fig. 3.5 Structure diagram of *narX* locus and primers in ZAP198 and *narX* mutant
- Fig. 3.6 PCR screening of colonies for replacement of *narX* with a CAM cassette
- Fig. 3.7 Structure diagram of *narP* locus and primers in ZAP198 and *narP* mutant
- Fig. 3.8 Screening of colonies for deletion of *narP*
- Fig. 3.9 Time of two generation of four mutants and wild type (ZAP198)
- Fig. 3.10 Cell binding of *E. coli* O157: H7 ZAP198 and isogenic mutants in *arcA*, *fnr*, *narX* and *narP*.
- Fig. 3.11 A/E lesion formation by ZAP198 and defined respiration-associated mutants
- Fig. 3.12 SDS-PAGE analysing supernatant proteins of ZAP198 and isogenic mutants deleted for specific respiration-associated genes
- Fig. 4.1 Schematic description of tetracycline (Tc) resistance

Fig. 4.2 Four steps used to construct an inducible LEE1 promoter, each step indicating one allelic exchange process

Fig. 4.3 A: Structure diagram of *lacYZ* locus and primers in ZAP198, B: Structure diagram of *sacBkan* cassette and primers in *lacYZ* mutant

Fig. 4.4 PCR for screening the *sacBkan* cassette

Fig. 4.5 PCR for screening the *lacZY* genes

Fig. 4.6 PCR for screening the outside *lacZY* genes using 5-*lacI* and 3-*lacA*

Fig. 4.7 PCR for screening the conjunction of *lacI* and *sacBkan* cassette

Fig. 4.8 PCR for PN25&*tetR* from PZS4Int-*laci/tetR* plasmid

Fig. 4.9 *Bam*H I digestion of PN25&*tetR* in pAJR27

Fig. 4.10 Structure diagram of *tetR* and primers in ZAP1213

Fig. 4.11 PCR screening for PN25&*tetR*

Fig. 4.12 PCR screening for outside *lacZY*

Fig. 4.13 LacZ&Y was replaced by PN25-tetR with *lacI* upstream and *lacA* downstream

Fig. 4.14 PCR synthesis of *tetO1*

Fig. 4.15 *Xba*I digestion for *tetO1* cloning

Fig. 4.16 aTc induction for Tet repressor with *tetO1* operator

Fig. 4.17 Genetic organization of *LEE1* promoter

Fig. 4.18 Genetic organization of first construction

Fig. 4.19 Genetic organization of second construction

Fig. 4.20 PCR for downstream flanking region fragments for first and second constructions

Fig. 4.21 *Xba*I and *Bam*H I digestion for downstream cloning

Fig. 4.22 PCR for upstream flanking region fragment for first and second constructions

Fig. 4.23 *Xma*I and *Bam*H I digestion for upstream cloning

Fig. 4.24 *Bam*H I digestion for *sacBkan* cassette cloning

Fig. 4.25 A: Structure diagram of LEE1 promoter locus and primers in ZAP198, B: Structure diagram of *sacBkan* cassette and primers in ZAP1327

Fig. 4.26 PCR for testing inside LEE1 promoter

Fig. 4.27 PCR for S/K cassette

Fig. 4.28 PCR for testing the junction of *sacBkan* cassette

Fig. 4.29 PCR for Tet promoter synthesis

Fig. 4.30 PCR for testing Tet promoter cloning for 1st construction

Fig.4.31 PCR for testing Tet promoter cloning for 2nd construction

Fig. 4.32 Structure diagram of *tet* promoter and primers in ZAP1327 with LEE1 promoter replaced by *tet* promoter

Fig. 4.33 PCR for *sacBkan* cassette for exchange *sacBkan* cassette for *tet* promoter

Fig. 4.34 PCR for Tet repressor

Fig. 4.35 PCR crossing junction of *tet* promoter and chromosome

Fig. 4.36 SDS-PAGE gel results

Fig. 4.37 Anti-EspD Western Blotting results

Fig. 4.38 Measurement of LEE1 promoter activity in ZAP1327

Fig. 4.39 RT-PCR measurement of *ler* expression levels in EHEC strains ZAP198, ZAP1004 and ZAP1327

Fig. 4.40 Western blot of EspD secretion in ZAP1327 with and without Ler

Fig. 5.1 Analysis of CGH data for Stx2 phage for PT 21/28 and PT 32

Fig. 5.2 Western blot analysis of a subset of PT21/28 and PT32 strains

Fig. 5.3 Relative fluorescence levels from a LEE1-GFP reporter construct transformed into 20 PT21/28 and 20 PT32 strains with levels measured at OD₆₀₀=1

Fig. 5.4 LEE1-GFP expression levels compared between strains containing either one or both Stx2 or Stx2c prophages

Fig. 5.5 Western blot analysis of paired *E. coli* O157 and O26 strains

Fig. 5.6 LEE1-GFP measurement of the same strain sets as in Fig 5.5

Fig 5.7 A minimum of three values were determined from the expression curves for OD₆₀₀=0.9 and plotted in Fig 5.7. $p<0.001$ for the TUV strains and $p=0.001$ for the EDL strains compared

Fig. 5.8 LEE1-GFP expression of *E. coli* O26 pair of strains

Fig. 5.9 pIB307 with the *z1449* digestion with *Bam*H I and *Hind* III

Fig. 5.10 pXLS11 digested by *Bam*H I and *Sal* I to check for cloning the downstream flanking region of *z1449*

Fig. 5.11 pXLS13 digested by *Bam*H I to demonstrate the insertion of the *sacBkan* cassette.

Fig. 5.12 pIB307 with *stxI* upstream flanking region inserted; digested with *Bam*H I *Hind* III

Fig. 5.13 pXLS12 digested by *Bam*H I and *Sal* I to cut out the downstream flanking region of *stxI*

Fig. 5.14 pXLS16 digested by *Bam*H I to detect *sacBkan* cassette.

Fig. 5.15 pIB with the *stx2* upstream flanking region inserted; digested with *Bam*H I and *Hind* III

Fig. 5.16 pXLS15 digested by *Bam*H I and *Sal* I to show the insertion of the *stx2* downstream flanking region.

Fig. 5.17 Schematic diagram of strains construction

Fig. 5.18 Structure diagram of *z1449* locus and primers in EDL933

Fig. 5.19 Structure diagram of *z1449* locus and primers in ZAP1321

Fig. 5.20 Structure diagram of *Stx2* phage locus and primers in EDL933

Fig. 5.21 Structure diagram of *Stx1* phage locus and primers in EDL933

Fig. 5.22 Structure diagram of *Stx1* phage locus and primers in ZAP1326

Fig. 5.23 Internal PCR of *z1449*

Fig. 5.24 External PCR of *z1449*

Fig. 5.25 PCR of *sacBkan* cassette for exchange of *z1449* for *sacBkan* cassette

Fig. 5.26 PCR of junction of *Stx2* using primer pair *wrbA* and *intW*

Fig. 5.27 PCR of junction of *Stx2* using primer pair *z1503* and *z1504*

Fig. 5.28 PCR of inside of *Stx2* using primer pair *stx2F* and *stx2R*

Fig. 5.29 PCR of left end and right end of *Stx1* phage

Fig. 5.30 PCR of outside of *Stx1*

Fig. 5.31 PCR of inside of *Stx1* with primers *stx1 5'* and *stx1 3'*

Fig. 5.32 PCR of *sacBkan* cassette

Fig. 5.33 LEE1-GFP measurement of K12 and K12 *Stx2*⁺

Fig. 5.34 LEE1-GFP measurement of K12 and K12 *Stx2*⁺ with plasmids *ler*

Fig. 5.35 6xHis-tagged *Ler* levels were compared with *RecA* in the different strains western blotting from whole cell samples taken at OD₆₀₀=0.9

Fig. 5.36 Western blot detection of *EspD* from bacterial supernatants and *EscJ* & *RecA* from whole cell samples

Fig. 5.37 Western blot analysis of the same proteins from *E. coli* EDL933 and an strain from which both the *Stx1* phage *cII* gene and the *Stx2 cII* gene

Fig. 5.38 LEE1-GFP measurement of EDL933, TUV93-0 and TUV *Stx1&2cII* deletion

Fig. 5.39 *z3357* downstream flanking region inserted into pIB307 digested by *Bam*H I and *Hind* III

Fig. 5.40 pXLS10 digested by *Bam*H I and *Sal* I

Fig. 5.41 PXLS14 digested by *Bam*H I

Fig. 5.42 Structure diagram of *z3357* locus and primers in EDL933

Fig. 5.43 Structure diagram of *z3357* (replaced by *sacBkan* cassette) locus and primers in ZAP1324

Fig. 5.44 External PCR of *z1449* in ZAP1323

Fig. 5.45 PCR of *sacBkan* cassette in ZAP1323

Fig. 5.46 Internal PCR of *z3357* in ZAP1324

Fig. 5.47 PCR of *sacBkan* cassette in ZAP1324

Fig. 5.48 Internal PCR of *z3357* in ZAP1324

Fig. 5.49 Schematic diagram showing that the integrated Shiga toxin prophage represses type III secretion (T3S) by blocking Ler activation at LEE1

Fig. 5.50 Schematic diagram showing that the repressive control of the Stx prophage is overridden by the activity of activators such as Ler, and PchA/B

Fig. 5.51 A model for EHEC interaction with the epithelium

List of tables

Table 1.1. General outbreaks of infectious intestinal disease (IID), foodborne general outbreaks of IID, and foodborne general outbreaks of STEC O157 infection, England and Wales, 1992 – 2002

Table 1.2. Serotypes characteristic of the diarrheagenic *E. coli* categories

Table 1.3. Comparison of the proportion of phage types between cases of culture positive indigenous human *E. coli* O157 cases reported to HPS and cattle isolates during the same periods of the Scottish Executive Environment and Rural Affairs Department (SEERAD)

Table 1.4. HUS and EHEC infection in the Europe and USA with Germany excluded

Table 2.1. Bacterial strains associated with this work

Table 2.2. Plasmids used in the study

Table 2.3. Oligonucleotide primers used in this study

Table 5.1. EHEC O157:H7 PT21/28 and PT32 strains and properties

Abstract

Enterohaemorrhagic *Escherichia coli* (EHEC) strains are associated with gastrointestinal and severe systemic disease in humans. EHEC O157:H7 is the most common serotype causing human infections in North America and the UK. Human infections mainly originate from cattle, through either direct contact with infected animals or indirectly through contamination of food or water with animal faeces. From the sequencing of EHEC O157 strains, it is clear that the genomes contain multiple prophages, many of them cryptic, which define this *E. coli* pathotype. These regions include the locus of enterocyte effacement (LEE) which is a critical horizontally acquired pathogenicity island and encodes a type III secretion system (T3SS). The T3SS translocates effector proteins into epithelial cells that enable tight attachment to these host cells and also modify innate responses and other cellular functions to promote persistence in the animal host. The T3SS is essential for the colonisation of cattle by EHEC O157 where it is localised to the terminal rectum. The regulation of T3S is complex with many regulators and environmental factors already identified. Previous work has demonstrated marked variation in the levels of T3S among EHEC O157 strains. The aim of this research was to further investigate the regulation of T3S towards two objectives: (1) to understand the localisation of EHEC O157 at the terminal rectum of cattle; (2) to understand the strain variation in T3S. (1) In relation to rectal and mucosal colonisation, established aerobic/anaerobic regulators were investigated including *arcA*, *fnr*, *narX*, *narQ*. Briefly, *arcA*, *fnr*, *narX*, *narQ* were deleted in an *E. coli* O157 strain ZAP198 by lambda red recombination. Apart from the *fnr* mutant which showed lower levels of T3S, the remaining mutants displayed similar T3S protein levels compared to the wild type strain. In addition, no significant changes in adherence and A/E lesion formation capacity were measured for the mutants following interaction with bovine epithelial cells. (2) Strain secretion variation was approached in two ways; the first was to control expression from the *LEE1* operon, required for T3S expression, in order to both induce expression and examine the importance of downstream regulation. The second was to investigate variation in T3S between different phages types of EHEC O157. While attempts to construct an inducible T3SS were not successful, intermediate strains made in the process have been useful to dissect how regulators being studied in the laboratory control T3S. The main novel insights from the research have come from examining T3S in different EHEC

O157 phage types. We found that the average level of T3S in PT 21/28 strains was lower than in PT 32 strains. Interestingly, most (90%) of PT 21/28 strains contained both Stx2 and Stx2c phages. In contrast, only 28% of PT 32 strains had both phages. Taken together, this raised the possibility that Stx phage integration might have a repressive impact on T3SS regulation in *E.coli* O157:H7. This hypothesis was addressed using a number of different approaches. Deletions of Stx phages were constructed and these had increased levels of T3S when compared to the parental strains. This phage regulation of T3SS was confirmed in an *E. coli* K12 background by examining an induced LEE1 reporter in the presence and absence of a transduced Stx2 phage. In addition, it was shown that deletion of the CII phage regulator led to increased T3S and may contribute to the Stx phage repression reported above. This work demonstrates for the first time that Stx phage integration represses T3S expression. It is proposed that this control may limit immune exposure of this critical colonisation factor and that the repression actually allows activation by prophage encoded regulators, including PchA/B, that co-ordinate T3S and non LEE-encoded effector expression to promote epithelial cell colonisation.

Chapter 1

Introduction

1.1 *Escherichia coli* background

Escherichia coli (*E. coli*) is a facultative anaerobic Gram-negative bacterium that colonises neonates within a short time of birth (Bettelheim *et al.*, 1974). It was named after Theodore Escherich who first isolated and described it in 1885 from the faeces of healthy individuals in Germany (Wasteson, 2001). Usually, most *E. coli* strains are harmless and co-exist with the host in the gut. These *E. coli* strains can benefit the host by protecting it from infection by pathogenic bacteria (Reid *et al.*, 2001) and synthesizing Vitamin K₂ in the host intestine (Bentley & Meganathan, 1982). However, *E. coli* strains can also cause diseases due to reduced immunity of the host or the evolution of more pathogenic *E. coli* strains (Nataro & Kaper, 1998).

1.2 Pathogenic *E. coli*

Enteric infection outbreaks caused by bacterial pathogens remain a problem in industrialized countries and developing nations (Fang, 2005). These infections and outbreaks have a significant health and economic impact on humans and animals, and are especially severe for the young, elderly and immuno-compromised. Most of the reported outbreaks are associated with pathogenic bacteria belonging to the *Enterobacteriaceae*. The *Enterobacteriaceae* contain many common bacterial pathogens that cause a range of intestinal and systemic illness from food- or water-borne outbreaks worldwide. The key genera in the *Enterobacteriaceae* include: *Salmonella*, *Shigella*, *Yersinia* and *Escherichia*.

Many pathogenic *E. coli* are considered as emerging pathogens and are involved in human clinical diseases such as acute intestinal disease and haemolytic uremic syndrome - HUS (Garmendia *et al.*, 2005; Kaper *et al.*, 2004). Six categories of pathogenic *E. coli* have been well-described: enteropathogenic *E. coli* (EPEC), enterohaemorrhagic *E. coli* (EHEC), enteroinvasive *E. coli* (EIEC), enterotoxigenic *E. coli* (ETEC), diffusely adherent *E. coli* (DAEC) and enteroaggregative *E. coli* (EAEC) (Nataro & Kaper, 1998). Although the six pathovars show differences in their genome and other aspects, they share similar pathogenic mechanisms and can cause overlapping clinical outcomes (Kaper *et al.*, 2004) (Fig. 1.1).

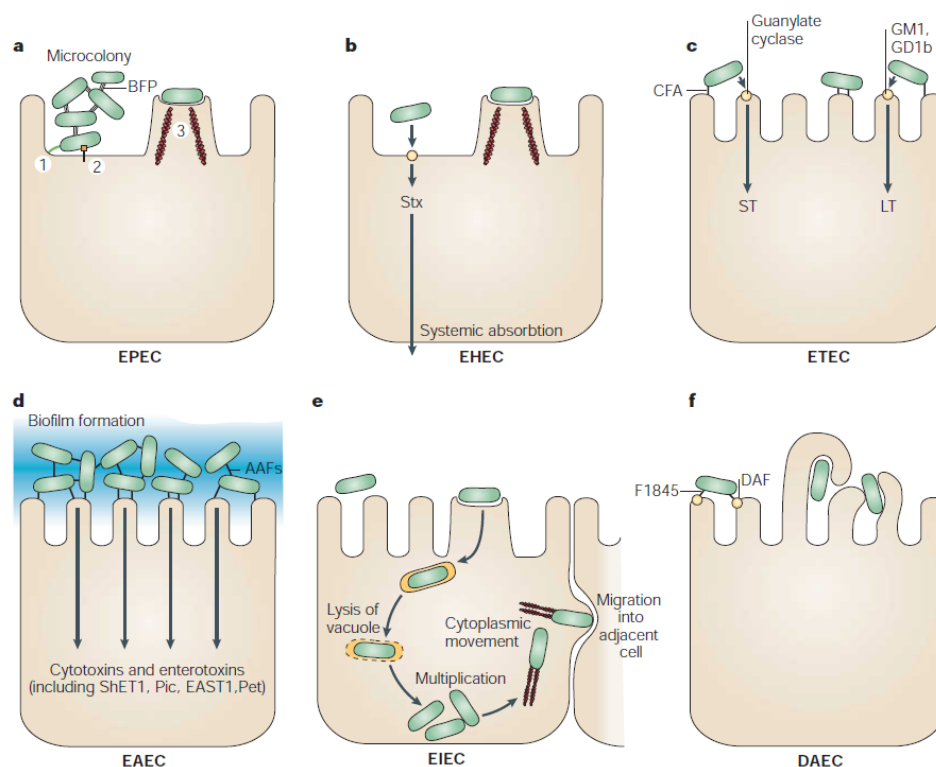


Fig. 1.1 **Pathogenic scheme for diarrhoeagenic *E. coli*.** (originally from Kaper *et al.*,2004) Each type of diarrhoeagenic *E. coli* has its own unique features in the interaction with eukaryotic cells. Interactions with a target cell for these six categories of pathogenic *E. coli* are shown above. These summaries are mainly from the results of *in vitro* work and will not fully represent the host responses in humans. **a.** Illustration for EPEC: EPEC adhere to small bowel enterocytes, destroy the normal microvillar brush border, forming the typical attaching and effacing (A/E) lesion. Cytoskeletal derangement was accompanied by diarrhoea and inflammatory response. Three features are identified: i. Initial adhesion; ii. Protein translocation by a type III secretion system (T3SS); iii. Pedestal formation. **b.** Illustration for EHEC: Similarly, A/E lesions exist in EHEC, but found in the colon. The distinguishing characteristic of EHEC is the production of Shiga toxin (Stx). The systemic absorption of Stx induces potentially life-threatening complications. **c.** Illustration for ETEC: ETEC strains adhere to small bowel enterocytes like EPEC and results in watery diarrhoea by the secretion of heat-labile (LT) and/or heat-stable (ST) enterotoxins. **d.** Illustration for EAEC: EAEC attaches to small and large bowel epithelia in a thick biofilm. The distinguishing feature of EAEC is the secretion of enterotoxins and cytotoxins. **e.** Illustration for EIEC: EIEC targets the colonic epithelial

cell, lyses the phagosome and moves through the cell by nucleating actin microfilaments. Following attaching and invading, EIEC might move laterally through the epithelium by direct cell-to-cell spread or might stay and then re-enter the baso-lateral plasma membrane. **f.** Illustration for DAEC: DAEC induces a characteristic signal transduction effect in small bowel enterocytes. This effect increases the growth of long finger-like cellular projections, which wrap around the bacteria. BFP, bundle-forming pilus; CFA, colonization factor antigen; AAF, aggregative adherence fimbriae; EAST1, enteroaggregative *E. coli* ST1; LT, heat-labile enterotoxin; ShET1, *Shigella* enterotoxin 1; ST, heat-stable enterotoxin; DAF, decay-accelerating factor.

1.3 Enterohaemorrhagic *E. coli* (EHEC)

EHEC are a subset of Stx-producing strains of *Escherichia coli* (STEC), which are associated with reported incidences of infection and severe disease. As an emerging pathogen, EHEC was identified as a distinct type of pathogenic *E. coli* from two main outbreaks. (i) EHEC was first reported by Riley and co-workers when *E. coli* O157:H7 was isolated from a food-borne outbreak associated with watery diarrhoea and bloody diarrhoea in 1982 (Riley *et al.*, 1983). This disease was associated with haemorrhagic colitis (HC), which results from colonization of the intestinal mucosa and subsequent toxin release. (ii) The second outbreak was reported by Karmali (Karmali *et al.*, 1983) in 1983, who observed the sporadic cases of HUS with faecal cytotoxin and cytotoxin-producing *E. coli* in stools. HUS is characterized by the triad of acute renal failure, thrombocytopenia, and microangiopathic haemolytic anemia; and it is typically preceded by a bloody diarrhoeal illness. EHEC strains are characterized by many specific virulence determinants such as Shiga-toxin and locus of enterocyte effacement (LEE).

A geographic distribution of EHEC infection was found, being more common in northern than southern states of the United States and more common in western than eastern Canada (Nataro & Kaper, 1998). The most often implicated EHEC serotype in outbreaks and sporadic cases of infection is *E. coli* O157:H7 (Karmali, 1989; Paton & Paton, 1998; Riley *et al.*, 1983). Between 1 January 1992 and 31 December 2002, 44 of the 1645 food borne general outbreaks of infectious intestinal disease were caused by Shiga toxin-

producing *E. coli* O157 according to the reports to the Health Protection Agency Communicable Disease Surveillance Centre in UK (Gillespie *et al.*, 2005)(Table 1.1).

Table 1.1. General outbreaks of infectious intestinal disease (IID), foodborne general outbreaks of IID, and foodborne general outbreaks of EHEC O157 infection, England and Wales, 1992 – 2002.

Year	All	Foodborne (%)	STEC O157 (%)
1992	373	224 (60)	3 (1.3)
1993	454	225 (50)	6 (2.7)
1994	490	192 (39)	0
1995	837	183 (22)	5 (2.7)
1996	733	165 (23)	7 (4.2)
1997	591	222 (38)	4 (1.8)
1998	610	121 (20)	4 (3.3)
1999	515	92 (18)	7 (7.6)
2000	656	96 (15)	6 (6.3)
2001	526	70 (13)	1 (1.4)
2002	1225	55 (4)	1 (1.8)
Total	7010	1645	44 (2.7)

1.4 *E. coli* O157:H7

More than 100 different serotypes of EHEC have been identified as human pathogens such as O26:H11, O86:H34, O111:H8, O113:H21, O117:H14 and O157:H7 (Bettelheim *et al.*, 2000). One way to identify *E. coli* O157:H7 in microbiological procedures is the lack of capacity of most isolates to ferment sorbitol (Mead & Griffin, 1998). However, several sorbitol-fermenting, Stx-producing O157:H- strains were also isolated from patients with HUS in Germany (Gunzer *et al.*, 1992). The recovery rate of *E. coli* O157:H7 on SMAC agar can be improved by prior enrichment in selective broth. GN Broth Hajna and trypticase soy broth supplemented with cefixime (50 ng/ml) and vancomycin (40 mg/ml) were both used with success (Karch *et al.*, 1996; Sanderson *et al.*, 1995). Due to the resistance to cefixime and tellurite, SMAC agar containing cefixime and tellurite (CT-SMAC agar) is also commonly used to isolate Stx-producing *E. coli* O157:H7 (Zadik *et al.*, 1993). Among outbreaks and sporadic cases (Friedrich *et al.*, 2007; Garg *et al.*, 2005), *E. coli* O157:H7 is the most commonly isolated EHEC in the USA and UK and accounts for more than 90% of clinical cases.

1.4.1 Serotyping of *E. coli*

A serological system, known as the Kauffman scheme (Kauffmann, 1947), was introduced for *E. coli* classification in 1947. *E. coli* are serotyped on the basis of three types of surface antigen including the somatic (O) antigen (O-specific lipopolysaccharides on the outer membrane), the flagellar (H) antigen, and capsular (K) antigen (Ewing, 1972; Lior *et al.*, 1996). So far, a total number of 170 different types of O antigen have been identified, each of which represents a serogroup. Each “serotype” of an isolate is distinguished by a specific combination of O and H antigens such as *E. coli* O157:H7. The K characterization comes from the process described below. If an isolated *E. coli* strain did not agglutinate with O antisera but did so when the culture was heated, it was then defined to have a capsular or K antigen. Specific serogroups can be associated with certain clinical syndromes (Table 1.2). However, this association doesn’t indicate that certain serologic antigens always confer virulence (Gunzer *et al.*, 1992).

Table 1.2. Serotypes characteristic of the diarrhoeagenic *E. coli* categories (Nataro & Kaper, 1998)

Category	Serogroup	Associated H antigen(s)
ETEC	O6	H16
	O8	H9
	O11	H27
	O15	H11
	O20	NM
	O25	H42, NM
	O27	H7
	O78	H11, H12
	O128	H7
	O148	H28
	O149	H10
	O159	H20
	O173	NM
EPEC	O55	H6, NM
	O86	H34, NM
	O111	H2, H12, NM
	O119	H6, NM
	O125	H21
	O126	H27, NM
	O127	H6, NM
	O128	H2, H12
	O142	H6
EHEC	O26	H11, H32, NM
	O157	H7
	O111	H8, NM
	O113	H21
	O117	H14

Category	Serogroup	Associated H antigen(s)
EAEC	O3	H2
	O15	H18
	O44	H18
	O86	NM
	O77	H18
	O111	H21
	O127	H2
	O?	H10
EIEC	O28	NM
	O29	NM
	O112	NM
	O124	H30, NM
	O136	NM
	O143	NM
	O144	NM
	O152	NM
	O159	H2, NM
	O164	NM
	O167	H4, H5, NM

NM: strains of *E. coli* O157:H7 that have lost the flagella H antigen become non-motile and are designated “NM”. ?: O antigen untypeable by conventional methods.

1.4.2 Phage-typing of *E. coli* O157:H7

E. coli O157:H7 or O157:NM (non-motile) are well recognized pathogen serotypes and cause diarrhoeal diseases and other syndromes such as haemorrhagic colitis (HC) and haemolytic uremic syndrome (HUS). Although serotyping is an important tool to initially characterize isolates, more discriminatory methods are needed to relate strains in an outbreak and to determine if particular subtypes are more likely to be associated with disease. Phage-typing schemes are used to trace the source of epidemics and classify pathogenic *E. coli* strains. In fact, the phage-typing scheme for Stx-producing *E. coli* O157:H7 has been successfully developed and applied in the investigation of the epidemiology of *E. coli* O157:H7 infections (Khakhriaa & Liora, 1990). Phage typing is usually carried out by the plaque assay technique. Briefly, a lawn of tested bacteria is cultured on an agar plate. The plate is divided into several distinct quadrants and labelled. Each quadrant is then inoculated with respective phage and incubated. Identification of lytic activity is then recorded by formation of plaques, which are the clear zones resulted from the lysis of the bacterial cells. 62 phage types were reported according to the geographical distribution in Canada. In contrast, 66 types were identified by using these 16 phages in Britain (Smith & Scotland, 1993). A Wellcome Foundation International Partnership Research Award in Veterinary Epidemiology (IPRAVE) study revealed that phage type (PT) 21/28 is the main phage type found from 952 farms (Table 1.3). Consistent with this, PT 21/28 has been the main O157 phage type isolated from human infections in the United Kingdom over the last decade (Table 1.3).

Table 1.3. Comparison of the proportion of phage types between cases of culture positive indigenous human *E. coli* O157 cases reported to HPS and cattle isolates during the same periods of the Scottish Executive Environment and Rural Affairs Department (SEERAD) (Pearce *et al.*, 2009)

Phage Type	Human Cases (Proportion)		Cattle Isolates (Proportion)	
	SEERAD	IPRAVE	SEERAD	IPRAVE
PT2	51 (0.109)	23 (0.071)	181 (0.147)	50 (0.098)
PT21/28	320 (0.634)	232 (0.718)	722 (0.587)	257 (0.504)
PT32	22 (0.047)	7 (0.022)	145 (0.118)	85 (0.167)
PT4	19 (0.041)	9 (0.028)	67 (0.0054)	6 (0.012)
PT8	31 (0.067)	22 (0.068)	56 (0.046)	51 (0.100)
'Other' PTs ^a	25 (0.053)	30 (0.093)	60 (0.049)	61 (0.120)

^aIncludes PT34, PT14, PT31, PT33, PT54, RDNC and untypeable

1.4.3 Clinical impact of Shiga-toxigenic *E. coli* infections

STEC can cause a wide range of clinical symptoms that include asymptomatic infection, mild-non bloody diarrhoea, HC (bloody diarrhoea), HUS, thrombocytopenic purpura and death (Boyce *et al.*, 1995). The first Pennington report is about a serious *E. coli* O157:H7 outbreak in 1996. The outbreak, which killed 21 people and infected 400 people, was traced to a butcher's shop in Wishaw, Lanarkshire. The second Pennington report about *E. coli* O157:H7 referred to an outbreak in South Wales in 2005. This large outbreak infected 150 people and one child died (Agency, 2005). *E. coli* O157:H7 accounts for a small proportion of all food-borne cases (1996 [USA] 3 per 100,000); however, it is an important threat to public health with the potential for large-scale outbreaks and the serious complications associated with infections, including rare fatalities. The most lethal STEC outbreak occurred recently (May 2011) in northern Germany caused by an O104:H4 serotype. In this case over 823 HUS cases have come from over 3,688 EHEC infection cases with 42 fatalities in Germany (as of 22nd June 2011). Other European countries have reported a total of 31 HUS cases (1 fatal) and 73 EHEC cases (none fatal) (Table 1.4). The suspected source of this outbreak is locally produced bean sprouts. The sequence of the outbreak strain was cracked rapidly in China by high-technology methods. This strain belongs to an EAEC strain carrying Stx phages from EHEC, which then means the infection can cause HC and HUS. In this case the high number of HUS cases may result from higher levels of Shiga toxin release due to enhanced adherence or invasion by the EAEC 'carrier' strain.

Table1.4. HUS and EHEC infection in the Europe and North America as of 22nd June

Country	HUS		EHEC		Comments
	Cases	Deaths	Cases	Deaths	
Austria	1	0	3	0	
Canada	0	0	1	0	
Czech Republic	0	0	1	0	A tourist from the United States who had travelled in Germany
Denmark	9	0	13	0	
France	0	0	2	0	
Germany	823	29	2865	13	
Greece	0	0	1	0	A German tourist
Luxembourg	1	0	1	0	
Netherlands	4	0	5	0	
Norway	0	0	1	0	Contact with a German in Norway
Poland	2	0	1	0	
Spain	1	0	1	0	
Sweden	17	1	33	0	
Switzerland	0	0	5	0	
United Kingdom	3	0	3	0	
USA	3	0	2	0	3 HUS cases (all confirmed) and 2 EHEC cases (one confirmed and one suspected)
Total	864	30	2938	13	

Note. There are 3802 HUS and EHEC cases in total, including 43 fatalities.

The main clinical impact comes from the production of Shiga toxins (Stx) or Verotoxins. Please see section 1.8.1 for a detailed introduction to the bacteriophages that encode the genes for these toxins. Stx produced by the bacteria is initially present in the intestine but then enters the general circulation. In polarized intestinal epithelial cells in vitro, Stx moves across the epithelial cell monolayer without obvious cellular disruption in an energy-requiring and saturable manner (Acheson, 1992). In addition, damage of the intestinal epithelium cells by Stx, bacterial lipopolysaccharide (LPS), or other inflammatory mediators could also assist translocation of the toxin into the bloodstream. This theory is supported by the observation that patients with bloody diarrhea due to *E. coli* O157:H7 are more likely to develop HUS than those with non-bloody diarrhea (Griffin, 1995). Once Stx is in the general circulation, potentially trafficked by granulocytes (Te Loo *et al.*, 2000), it binds to Gb3 expressing endothelial cells lining blood vessels in renal glomeruli and other capillaries in the body, including the brain. The activity of the toxin is described in section 1.8.1 but leads to endothelial cell death. Platelets try and repair this damage but fibrin fibres and clots can block the capillaries leading to ‘shredding’ of red blood cells; this and immune complex deposition can block the capillaries leading to a restriction in oxygen transfer to the local tissues and tissue death. In the kidney this accounts for HUS and kidney failure. HC is caused by *E. coli* O157:H7 colonization of the intestinal mucosa and subsequent toxin release in the intestinal tract.

1.4.4 Epidemiology of *E. coli* O157:H7

1.4.4.1 Sources of *E. coli* O157:H7 infection

Ruminants, especially cattle and sheep, are considered to be the main common source of human infection with *E. coli* O157:H7 (Hancock *et al.*, 1994; Orskov *et al.*, 1987). It is carried asymptomatically in the intestine of ruminants and shed in their faeces. In cattle, *E. coli* O157:H7 colonises at the terminal rectum and does not cause any obvious disease (Naylor *et al.*, 2005). Prevalence studies in Scotland revealed that 23% of herds and 7.9% of cattle shed *E. coli* O157:H7 in their faeces indicating a considerable environmental risk to humans, particularly by animals shedding high levels of the bacterium (Strachan *et al.*, 2006). In these cattle, some of them were defined as ‘super-shedders’ with $\geq 10^4$ colony forming units per g (CFU.g⁻¹) and low-shedders with $< 10^2$ CFU.g⁻¹. Preventing colonisation of *E. coli* O157:H7 in cattle or reducing shedding levels excreted by cattle are approaches being investigated to limit the threat to public health.

1.4.4.2 Transmission of *E. coli* O157:H7

E. coli O157:H7 can be transmitted through (i) food and water, (ii) animal-to-human contact, and (iii) person-to-person contact (Fig. 1.2). Among them, food-borne transmission is probably responsible for most infections.

(i) Ingestion of raw or undercooked contaminated foods, particularly of bovine origin such as ground beef (hamburgers) and unpasteurized milk, is the most common route of transmission of *E. coli* O157:H7. Contamination either directly from faeces or indirectly, through rinsing or preparation procedures, can happen. For example, an outbreak traced back to packed spinach occurred in United States in 2006 causing the infection of 200 people in which 31 (16%) developed HUS.

(ii) Infections through direct animal contact during farm visits have been reported with *E. coli* O157:H7 (Renwick *et al.*, 1993; Shukla *et al.*, 1995). In the United Kingdom, animal contacts are also associated with infections as there are a large number of educational farm visits annually, particularly by school children (Smith, 1998). Infections can be

caused by direct contact with farm animals and their faeces. An outbreak was caused by visiting a ‘petting’ farm in 2009 leading to 93 people contracting EHEC O157 (Committee, 2010). Kidney complications occurred in many of the children.

(iii) Another transmission route is person-to-person spread, which can easily happen in settings of poor hygiene or in families where children may have diarrhoea. Transmission is made more likely by the extremely low infectious dose of *E. coli* O157:H7.

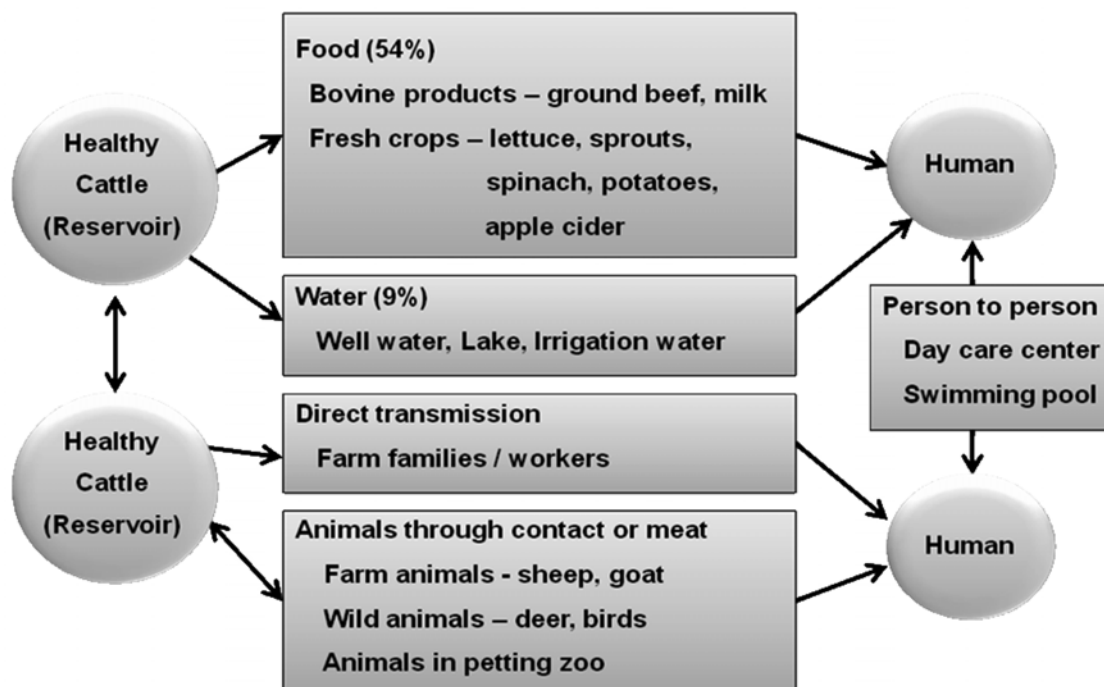


Fig. 1.2 Transmission diagram of *E. coli* O157:H7 (originally from Lim *et al.*, 2010). This diagram shows that healthy cattle are the main reservoir of *E. coli* O157:H7. Contaminated food and water linked with cattle are major sources for human infections. Animal contact or person to person also could be important transmission routes.

1.4.5 Infection models of *E. coli* O157:H7

Many infection models of *E. coli* O157:H7 have been developed to study its pathogenesis, covering *in vitro* cell culture, small animal and large animal systems. Most of the *in vitro* methods were used to investigate the adherence of the EHEC strains to epithelial cells or Stx effects on cells. Small animals such as mice (Eaton *et al.*, 2008; Karpman *et al.*, 1997; Kurioka *et al.*, 1998; Mohawk *et al.*, ; Shimizu *et al.*, 2003), rats (Zotta *et al.*, 2008), and rabbits (Garcia *et al.*, 2006), were mainly used for the study of *E. coli* O157:H7 infection and disease. Larger animals including cows (Dean-Nystrom *et al.*, 2008), chickens (Beery *et al.*, 1985; Sueyoshi & Nakazawa, 1994), pigs (Tzipori *et al.*, 1986), baboons (Taylor *et al.*, 1999), macaques (Kang *et al.*, 2001), and dogs (O'Brien, 1998) have also been reported as infection models for EHEC. A/E lesions in the gastrointestinal tract have been detected in infected animals such as rabbits, chickens, gnotobiotic piglets, infant calves, and macaques (O'Brien, 1998). In addition, HUS-like disease has occurred naturally in dogs and rabbits (Cowan *et al.*, 1997; Garcia *et al.*, 2002; O'Brien, 1998).

1.4.6 Evolution of *E. coli* O157:H7

1.4.6.1 Evolution of *E. coli* O157:H7

The published evolution of *E. coli* O157:H7 is accompanied by stepwise acquisition or loss of virulence and phenotypic traits (Feng *et al.*, 1998). Early evolution involved genetic exchange, competition, and selection. An evolutionary model demonstrated the evolution pathway of *E. coli* O157:H7 strains (Fig. 1.3) (Feng *et al.*, 2007). This model is based on the molecular typing (PCRs, PFGE eg) and genetic studies. O55:H7 that ferments sorbitol (SOR) and is β -glucuronidase positive (GUD+) is considered to be an ancestor strain of *E. coli* O157:H7. As time goes on, this O55:H7 acquired Stx2 phage producing a closer ancestor of *E. coli* O157:H7. By analyzing a sequenced O55:H7 Stx2⁺ strain, it was thought that *E. coli* O157:H7 derived from its ancestor strains (O55:H7 Stx2⁺) around 400 years ago by using a new clock rate (Zhou *et al.*, 2010). Some strains, such as EOR-37 and LSU61, were left as the uncertain due to the contradictory molecular typing results (Feng *et al.*, 2007). LSU61 is an O157 strain that is SOR⁺ and have many traits proposed for the A3 intermediate. If it is A3 intermediate, it would be related to A2, A4

and A5. However, only 60% similarity to A2, A4 and A5 clonal complexes by PFGE profile.

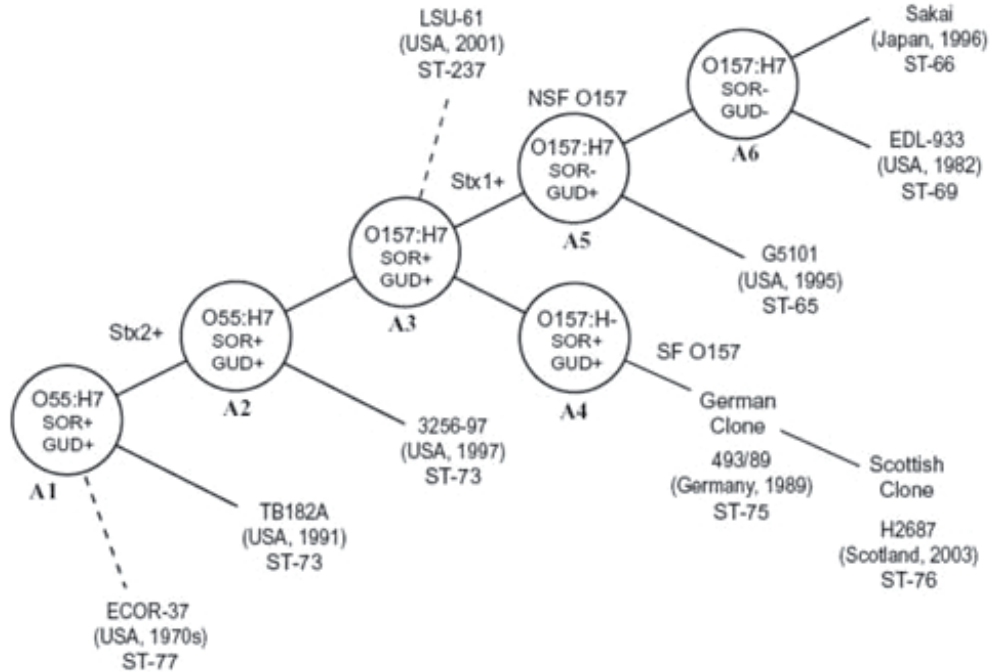


Fig. 1.3 Evolution model for *E. coli* O157:H7 (originally from Feng *et al.*, 2007).

Strains are named in evolutionary order. It shows the evolution pathway of O157:H7 from O55:H7 by acquiring Stx2 and Stx1 phage with SOR and GUD changes. For some strains, the position on the model still remains to be determined and they are shown with dashed lines.

It was apparent from genome analysis that *E. coli* O157:H7 contains more prophages and virulence determinants than the non-pathogenic laboratory strain *E. coli* K12. For example, *E. coli* O157:H7 (EDL933) and K12 (MG1655) share 4.1 Mb of 'backbone' sequence. 1,387 additional genes were detected in the EDL933 strain. These include genes encoding candidate virulence factors, prophages, and alternative metabolic functions (Perna *et al.*, 2001). In total, 1.34 Mb of designated 'O-island' DNA, comprised of 177 O-islands were specific to EDL933. Similarly, 1.4 Mb of O157 Sakai-specific sequence (S-loops) was identified in the Sakai strain (Hayashi *et al.*, 2001). There were 1,600 genes found in this specific sequence, including 18 prophages (Sp1-18), 6 prophage-like elements (SpLE1-6) and other potentially horizontally-acquired regions.

Significantly, most virulence determinants are present in these regions which include the Stx 1 phage and Stx2 prophages (Ogura *et al.*, 2006).

Based on the 29 *E. coli* genome sequences, it was concluded that the genomes of all EHEC strains are much larger than those of the non-EHEC strains (Ogura *et al.*, 2009). These EHEC strains (O157, O26, O111, and O103) contain virulence genes for Shiga toxins and many other factors. Moreover, it was found that the genes associated with T3SS were grouped into three different types: integrative elements (IE) (the locus of enterocyte effacement), which encodes the T3SS; SpLE3-like IEs and lambdoid phages, which carry numerous T3SS effector genes and other T3SS-related genes.

1.4.6.2 The evolution of phage

Phage and bacteria have co-evolved and interactions between them continue to drive their evolution and the emergence of new pathogens, as is evident from the recent STEC O104:H4 outbreak in Germany. Some phages have been separate from bacterial genomes for millions of years. Then, some phages stayed independently in the environment. Alternatively, some of them were integrated with host bacteria again. Some other phage might be generated recently. Horizontal gene transfer (HGT) by transduction is the main mechanism involved in phage integration with a bacterial genome. The additional genetic elements encoded by these prophages can provide various novel capacities for the bacterium, such as niche adaptation and virulence (Filee *et al.*, 2003; Canchaya *et al.*, 2003). Genetic defects, such as deletions or disruptions, are detected in the prophages. Therefore, these prophages can become 'cryptic and potentially are not functional as mobile genetic elements. However, it was recently revealed that many of these defective prophages, including the Stx1 phage, are inducible through the activity of other prophages (Asadulghani *et al.*, 2009). This was confirmed by the release of many different prophage sequences from the *E. coli* O157:H7 genome. Furthermore, some of these sequences could be transferred to other *E. coli* strains producing novel pathogenic *E. coli* strains. Interestingly, it was found new Stx1 phages are produced by recombination between the existing Stx1 and Stx2 phages.

Little research was done on this phage evolution. DNA sequencing and sequence comparison, as the only tool to study the early phage status, was used. Till now, 200 phage genomes have been sequenced with a total number of 1031 defined phages. No consensus model of phage is reported. Although vertical and horizontal evolution models and combination of the two have been introduced, the base of these models is limited by the number of sequenced phages used in model construction (Canchaya *et al.*, 2003).

1.5 A/E lesions

In 1987, Knutton and his co-workers demonstrated the accumulation of electron dense material under attached bacteria when carrying out infection assays on human intestinal biopsy material (Knutton *et al.*, 1987)(Fig. 1.4). Knutton also reported that fluorescein-labelled phalloidin could be used to visualise the electron-dense material under attached EPEC and EHEC bacteria on mucosal surfaces and this staining corresponded in size and position with each adherent bacterium (Knutton *et al.*, 1989). Therefore, this specific phalloidin staining could be applied to screen for genes that were responsible for these attaching and effacing (A/E) lesions via random mutagenesis.

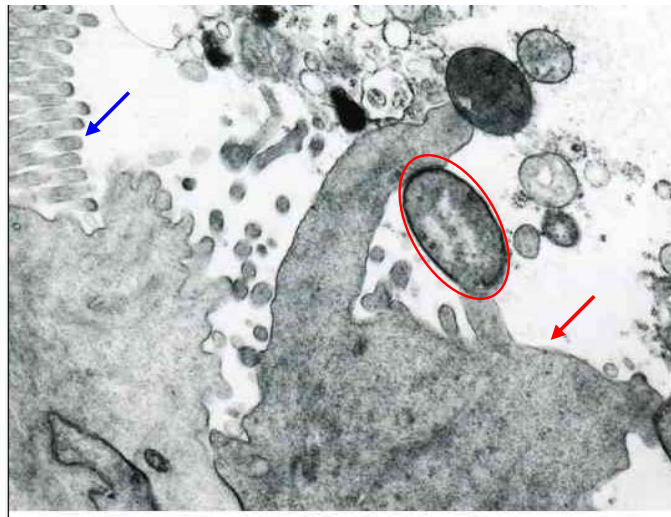


Fig. 1.4 A/E lesion caused by *E. coli* in rabbit intestinal epithelial cells (originally from Goosney *et al.*, 1999), bacteria is shown by circle in red, microvilli is suggested by arrow in blue, effacement of microvilli is indicated by arrow in red. The brush border in the intestine was removed by *E.coli* which attached the host intestinal epithelium.

EHEC colonizes the intestinal mucosa and causes A/E lesions following bacterial attachment to the host intestinal epithelium. These are characterized by effacement of the brush border and actin polymerization underneath the bacteria. After infection, EHEC can subvert host cell signal transduction pathways and utilize host cytoskeletal/membrane components for localization (Frankel *et al.*, 1998). The adherent bacteria assemble on formed pedestals at the surface of one pole of the bacterium by polymerization of the eukaryotic cytoskeletal protein actin (Knutton *et al.*, 1987). The forming of A/E lesions depends on T3SS (Jarvis *et al.*, 1995), the outer membrane adhesive protein intimin (Jerse *et al.*, 1990) and the translocated intimin receptor (Tir), which is translocated into the host cell (Kenny *et al.*, 1997). All these elements are encoded in a pathogenicity island termed the ‘locus of enterocyte effacement’ – LEE (McDaniel *et al.*, 1995).

1.6 The LEE and Type III secretion

1.6.1 LEE

Besides a core genome structure shared between commensal and pathogenic strains, pathogenic strains also acquire other genes on pathogenicity islands (PAI) that allow niche adaptation and enhance virulence. The locus of enterocyte effacement or LEE is one critical PAI encoding a T3SS, various translocators and effectors, the outer-membrane protein intimin (Hacker & Kaper, 2000; Jerse *et al.*, 1990) and its receptor, termed the translocated intimin receptor (Tir). EHEC and EPEC, along with many other pathogenic Gram negative bacteria, utilize a T3SS to secrete and inject bacterial effector proteins into the cytosol of host cells. A/E lesion formation results from this process (Zhang *et al.*, 2004).

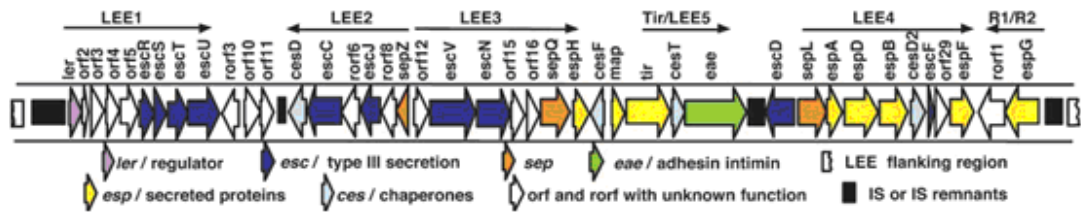


Fig. 1.5 Genetic organization of LEE (originally from Deng *et al.*, 2004)

The whole LEE contains 5 main operons (LEE1-5). There are 54 open reading frames in these five operons. *ler* is the first gene of LEE1 operons. Each open reading frames are represented by arrow with different color indicating different function.

The LEE is around 43kb in size and is composed of 54 open reading frames (ORFs) that form five main operons (LEE1-5) (Elliott *et al.*, 1998). LEE1-3 encode components of the basal apparatus of the T3SS including EscC, J, R, S, T, U, V (Bustamante *et al.*, 2001; Garmendia *et al.*, 2005; Sperandio *et al.*, 2003) (Fig. 1.5). LEE4 encodes EspA, B, D, F (Crane *et al.*, 2001; Daniell *et al.*, 2001; Delahay *et al.*, 1999; Hartland *et al.*, 2000; Knutton *et al.*, 1998; Kresse *et al.*, 1999; Neves *et al.*, 1998; Wachter *et al.*, 1999), SepL (Kresse *et al.*, 2000) and EscF (Wilson *et al.*, 2001). LEE5 encodes an outer membrane adhesin called intimin, its translocated receptor Tir, and a Tir chaperone known as CesT (Sanchez-SanMartin *et al.*, 2001). Tir is located at the host cell plasma membrane and forms a hairpin-like structure which binds with intimin (Kenny *et al.*, 1997). Following

the assembly of the type III basal apparatus and EspA needle complex, EspB and Tir are translocated to the host epithelial cell where Tir is integrated into the plasma membrane. The binding of Tir with intimin on the bacterial surface is responsible for the rearrangement of the host cell cytoskeleton and subsequent formation of A/E lesions during infection with *E. coli* O157:H7 (Roe *et al.*, 2003b; Sperandio *et al.*, 2002). SepL is required for the formation of intact translocation apparatus and the secretion of Esp proteins (Kresse *et al.*, 2000). SepD is the only protein that was revealed to interact with SepL by yeast two-hybrid system and is considered to have an associated function with SepL (Creasey *et al.*, 2003).

1.6.2 T3SS

1.6.2.1 Introduction to T3SS

The Gram negative pathogenic bacteria: *Yersinia spp.*, *Salmonella spp.*, *Shigella spp.*, EPEC and EHEC all can express specific but related T3SSs. Pathogenic bacteria utilize this system to translocate proteins and effectors into the host cell. *Yersinia* and *Shigella* possess a short needle complex to inject T3 effectors into host cells. However, EHEC and EPEC use a different T3SS in which a filament structure extends to its needle. It is not clear why this additional structure is required. But it may act as an initial adhesin (Ebel *et al.*, 1998) and may allow the secretion system to penetrate through mucus or past microvilli. A model of the T3S system of EHEC O157 is illustrated in Fig. 1.6.

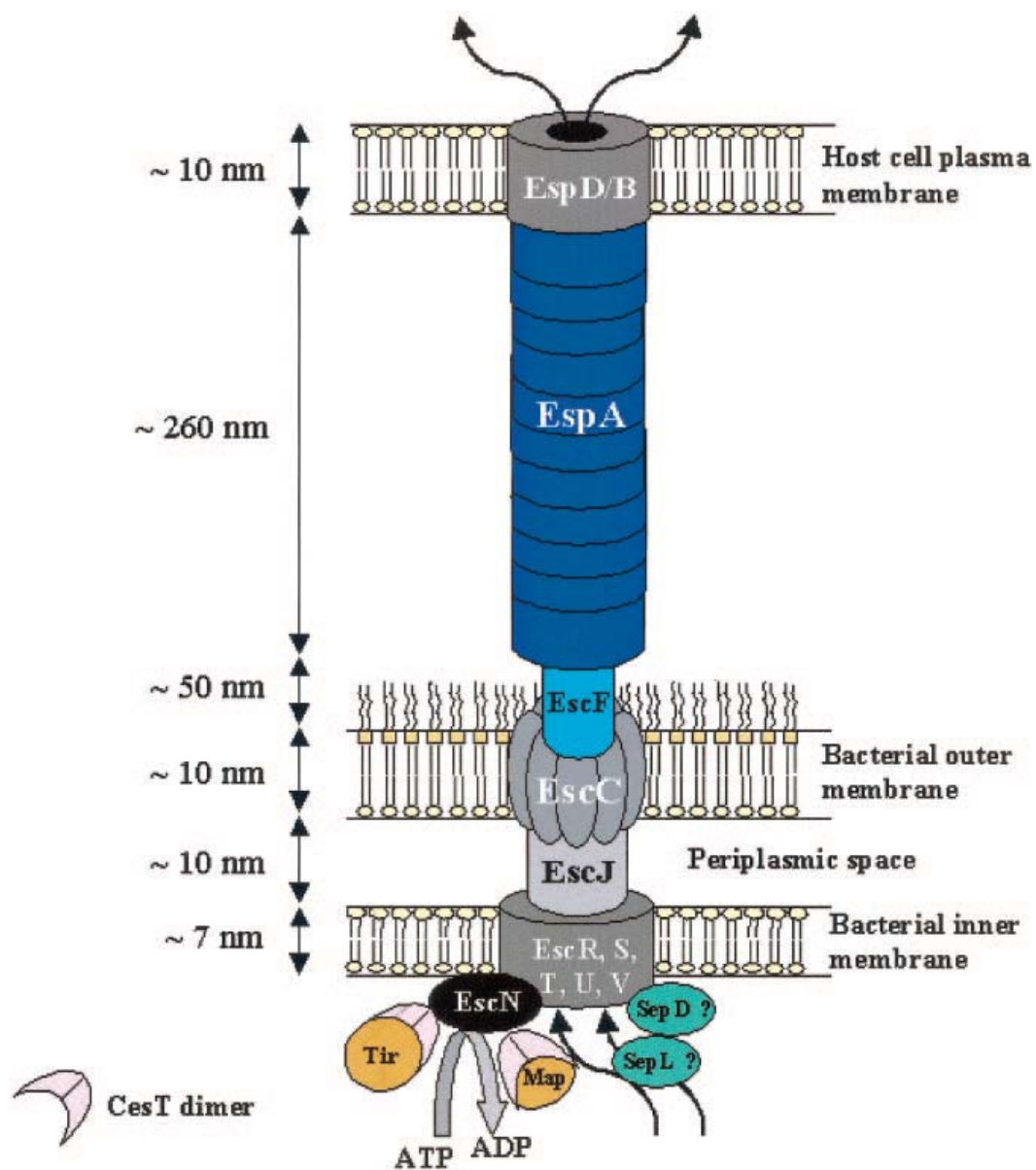


Fig. 1.6 Schematic representation of the EPEC/EHEC type III secretion apparatus.

(originally from Garmendia *et al.*, 2005). See text for details. The basal apparatus is composed of EscR, EscS, EscT, EscU and EscV proteins. EscF contains the needle structure connecting the bacteria and host cells. EspA is considered as the filament. EspB and EspD assemble the pore at the end of the filament.

1.6.2.2 Basal apparatus of the T3SS

The basal apparatus of the T3S system in EHEC O157 is mainly encoded by LEE1-3 operons. EscD (Pas), EscQ, EscR, EscS, EscT, EscU and EscV are the main contents for the inner membrane (Gauthier *et al.*, 2003; Kresse *et al.*, 1998; Ogino *et al.*, 2006). Moreover, EscC and EscV are considered to be the main components of the outer and inner membrane ring structures, respectively. These two proteins form a large annular complex. The effectors and molecules are transported through this structure across the membrane (Hueck, 1998)(Fig. 1.6). By nuclear magnetic resonance, it was revealed that EscJ is composed of two structured domains connected by a linker forming a bridge across the periplasm. This needle complex connects the outer and inner membrane (Crepin *et al.*, 2005). EscN, as the cytoplasm located ATPase, energizes the translocation of T3SS by interacting with membrane-bound components of the type III apparatus (Gauthier *et al.*, 2003). EscN is required in EscC insertion. Therefore, it was believed that energy might be needed for EscC localization. EscC is one of the family of proteins (secretins) which are associated with translocating large molecules across the outer membrane (Hueck, 1998). However, the secretion and function of EscC require not only the general secretion pathway but also other components of the type III apparatus (Gauthier *et al.*, 2003). It was revealed that EscJ is a large 24-subunit ‘ring’ superstructure that might bridge the membrane-associated rings of the T3S system (Crepin *et al.*, 2005). In addition, T3S system and flagella share high levels of homology in the proteins of the basal apparatus (Pallen *et al.*, 2005a). Following assembly of basal apparatus, the needle complex can be switched to assemble. EscF encoded by LEE4 operon is considered to be the main component of needle structure in EHEC and EPEC

(Fig. 1.6). EspA assembly is essential for T3SS. One end of the EspA filament connects with the EscF needle (Larzabal *et al.*, 2010). Previous research revealed that YscU (EHEC EscU homologue) regulates the forming of needle complex in *Yersinia*. It's also found that translocation and secretion by T3SS were blocked in EscU mutation (Tree *et al.*, 2009b). This evidence indicated that EscU is likely involved in the switch to formation of the later needle complex.

1.6.2.3 Translocon of T3SS

With the needle structure in position, the translocon begins to assemble. The translocon is encoded on LEE4 operon. EspA composes the main filament extension. It was confirmed by the staining with antibodies on the surface of the bacterium (Fig. 1.7). EspB and EspD are considered to make up the pore at the end of the EspA filament. EspB&D are similar in size and are the main T3 secreted proteins that can be detected in EHEC supernatants under T3S conditions (Fig. 1.8). It was observed that EspD may have multiple activities: to influence the length of the EspA filament; to promote adhesion during early stages of infection; and to generate the translocation pore into host cells once contact has been established (Daniell *et al.*, 2001).

In addition, the deletion of *SepL* and *SepD* caused the failure of the export of the EspA translocon (O'Connell *et al.*, 2004; Wang *et al.*, 2008). This indicated that *SepL* and *SepD* are essential for translocator. *SepL* and *SepD* also disrupted the secretion of T3 effectors.

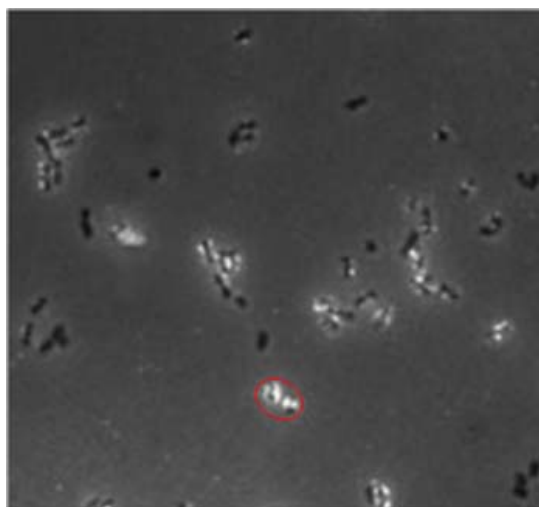


Fig. 1.7 EspA stain of ZAP198 (originally from Naylor *et al.*, 2005), EspA staining is indicated by circle in red. It shows some of the bacteria are stained with EspA antibody with fluorescence (highlighted). Unstained bacteria keeps dark.

1.6.2.4 Secreted translocon and effectors encoded by LEE

LEE4 is responsible for effector proteins including EspA, B, D, F, SepL and EscF. The regulation of LEE4 was investigated by Andrew Roe and his co-workers (Roe *et al.*, 2003b). The report demonstrated that the expression of EspA filament was heterogeneous in all of the tested EHEC O157 strains isolated from bovine and human disease. The proportion of the bacterial population expressing EspA filaments was consistent with the secreted EspD levels. High EspD-secreting strains had a higher proportion of bacteria expressing EspA filaments than low EspD-secreting trains. The regulation of individual bacterium to express EspA filaments was not controlled at the level of LEE1-4 operon transcription. LEE4 translocon expression is regulated by a posttranscriptional mechanism, which controls the translation of *LEE4-espADB* mRNA. A classic T3 secreted protein profile is shown in Fig. 1.8. EspA, B, D secretion level is demonstrated with a precipitation control (BSA).

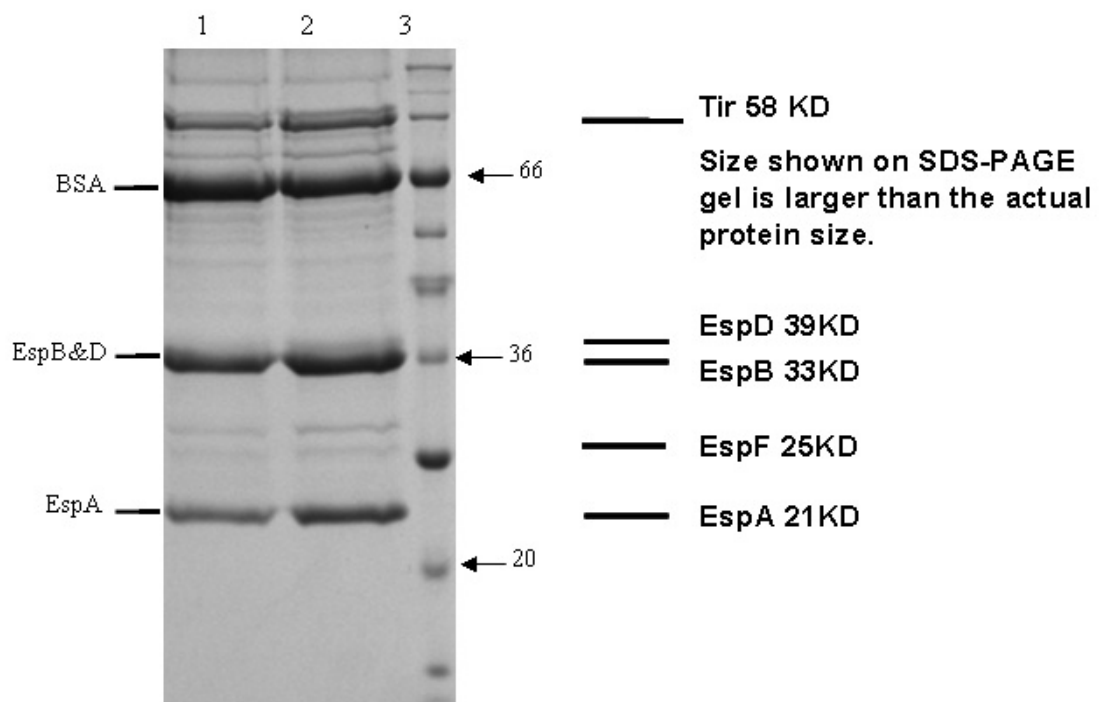


Fig. 1.8 SDS PAGE gel of T3 secreted protein profile

1-2: Supernatant protein samples (prepared as described in Materials and Methods, section 2.10), 3: Wide range molecular weight marker (Sigma), number indicates beside is in KD. Precise sizes of secreted proteins are shown on the right. The gel was prepared, run, and stained as described in Materials and Methods section 2.11.

Other LEE-encoded effectors, which are involved in modulating the host cytoskeleton in EHEC, have also been identified including the mitochondrion-associated protein (Map), SepZ, EspH, EspF, EspO and EspZ. Each of them is briefly discussed below.

Map was named for its localization to mitochondria via a N-terminal targeting sequence (Kenny & Jepson, 2000). Map has three distinct and independent functions: firstly, in the initial stages of EHEC infection, Map plays an important role in the transient formation of filopodium-like structures at the sites of bacterial infection; secondly, it assists the cellular ability of *E. coli* O157:H7 by triggering the formation of misshapen mitochondria, mitochondrial swelling, and damage (Kenny & Jepson, 2000); finally, Map is responsible for the disruption or alteration of tight junctions and intestinal barrier function that is independent of mitochondrial targeting (Dean & Kenny, 2004). Two new members of Map protein family were discovered, which were named as EspM1 and EspM2 (Ando *et al.*, 2007).

EspH is found on the host cell membrane and affects the structure of the host actin cytoskeleton, which in turn affects filopodia and pedestal formation (Tu *et al.*, 2003). SepZ is the most recently observed LEE-encoded effector. However, no evidence has been shown that its translocation was associated with a specific phenotype or function.

EspF is a proline-rich effector protein since it contains four proline-rich repeats in EHEC (Viswanathan *et al.*, 2004). It has been reported that EspF can disrupt the intestinal barrier function, increase membrane permeability and induce the release of the toxic protein cytochrome *c* (McNamara *et al.*, 2001; Nagai *et al.*, 2005; Nougayrede & Donnenberg, 2004). Map and EspF have similar functions in disruption of intestinal barrier in the presence of intimin (Dean & Kenny, 2004).

It was recently revealed that EspO can strengthen the adherence of host cells to the basement membrane by interacting with integrin-linked kinase (Kim *et al.*, 2009). It also plays a role in inhibiting the turnover of focal adhesion in cell motility by blocking the phosphorylation of focal adhesion kinase and paxillin.

EspZ has a similar function as EspO in preventing host cell detachment by interacting with host protein CD98 and enhancing phosphorylation of focal adhesion kinase (FAK) and 3-kinase (Akt), which reinforces the stability of focal adhesins during infection (Shames *et al.*, 2010).

Despite the secreted effectors encoded by local LEE operons, many non-LEE-encoded effectors (Nles) were recently reported by using homology searches to identify homologous proteins (Pallen *et al.*, 2005b; Pallen *et al.*, 2005c). A large number of Nles are identified in EHEC O157 by comparing with other T3S organisms such as plant pathogen *Pseudomonas syringae*. Twenty eight of these predicted effectors were confirmed by experiments as detailed below.

1.6.2.5 Non-LEE-encoded effectors secreted by T3SS

NleG family: NleG proteins have many homologues secreted by T3S system in EHEC O157:H7 strain. These effectors belong to a U-Box E3 ubiquitin ligase family. NleG binding and autoubiquitination activity was decreased by the alanine substitutions of UBE2D2 residues Arg5 and Lys63 (Wu *et al.*, 2010). The NleG effectors are likely related to the turnover of host cell proteins and/or other type III effectors by the cell proteasome via the host cell ubiquitination pathway (Wu *et al.*, 2010).

NleA-F: Secreted by T3SS, NLeA is translocated into the host cells, localizes in the host Golgi apparatus and is required for EHEC virulence (Gruenheid *et al.*, 2004). In contrast, NleB and NleE prevent the activation of NF- κ B by inhibiting I κ B degradation and p65 nuclear translocation (Nadler *et al.*, 2010; Newton *et al.*, 2010; Vossenkamper *et al.*, 2010). In addition, NF- κ B involves the regulation of cytokine gene expression; however, NleC can block the function of NF- κ B which increases the secretion of effectors (Pearson *et al.*, 2011). Finally, NleB homologs and NleE-F encoded within prophages are translocated into eukaryotic cells by T3S system (Tobe *et al.*, 2006).

Other effectors: Besides the effectors described above, one effector secreted by *E. coli*, protein J (EspJ), is located in the CP-933U phage and has an effect on TTSS and virulence in EHEC (Dahan *et al.*, 2005). Although EspJ is not essential for A/E lesion activity *in vivo* and *vitro*, EspJ has an effect on the dynamics of clearance of the pathogen from the host's intestinal tract. This suggests its role in host survival and pathogen transmission (Dahan *et al.*, 2005). Other effectors include NleD, EspW and EspV. EspV is a short protein having a similar function as avirulence (Avr) A effector (Napoli & Staskawicz, 1987).

In conclusion, T3SS comprises a basal apparatus with its protein components present in both inner and outer bacterial membrane, and a needle complex known as the translocon, which allows the injection of effector proteins through the host cell membrane (Roe *et al.*, 2003b) .

1.7 The regulation of Type III secretion

1.7.1 Regulation inputs into the LEE

LEE gene expression is regulated in a complex way and it responds to many regulators and environmental factors such as pH value, glucose, iron and temperature (Laaberki *et al.*, 2006). The expression of the secretion system is a multi-step process controlled by the genes and signals illustrated in Fig. 1.9.

1.7.1.1 The regulators encoded on LEE

The LEE encoded regulator (*ler*) is located within the LEE itself and its transcription has been shown to be regulated both positively and negatively by two other regulatory proteins expressed from the LEE; the global regulator of LEE activator (GrlA) (LEE-encoded Orf10) and global regulator of LEE repressor (GrlR) (LEE-encoded Orf11) (Deng *et al.*, 2004). As shown in Fig. 1.9, besides these regulators, the response to environmental factors, which are, in part, mediated through *perC*-homologous (*pch*) A,B,C in *E. coli* O157:H7, can also induce up-regulation of the T3S (Spears *et al.*, 2006). Through PchA, B, C, the LEE activator (Ler and GrlA) and repressor (GrlR) proteins are stimulated and therefore T3S expression level is affected.

Ler is a 15 kDa protein encoded by the first gene of LEE1 and it directly regulates genes

within the LEE and elsewhere in the genome. Ler is considered as an anti-repressor protein by displacing the histone-like protein (H-NS) which acts as an inhibitor on LEE2/LEE3 promoters (Bustamante *et al.*, 2001). In addition, *ler* also plays an essential role in up-regulating the LEE4 promoter (Elliott *et al.*, 2000). Since most of the genes that are important for A/E lesions are regulated by *ler*, the *ler* regulator is crucial for control of the whole T3SS.

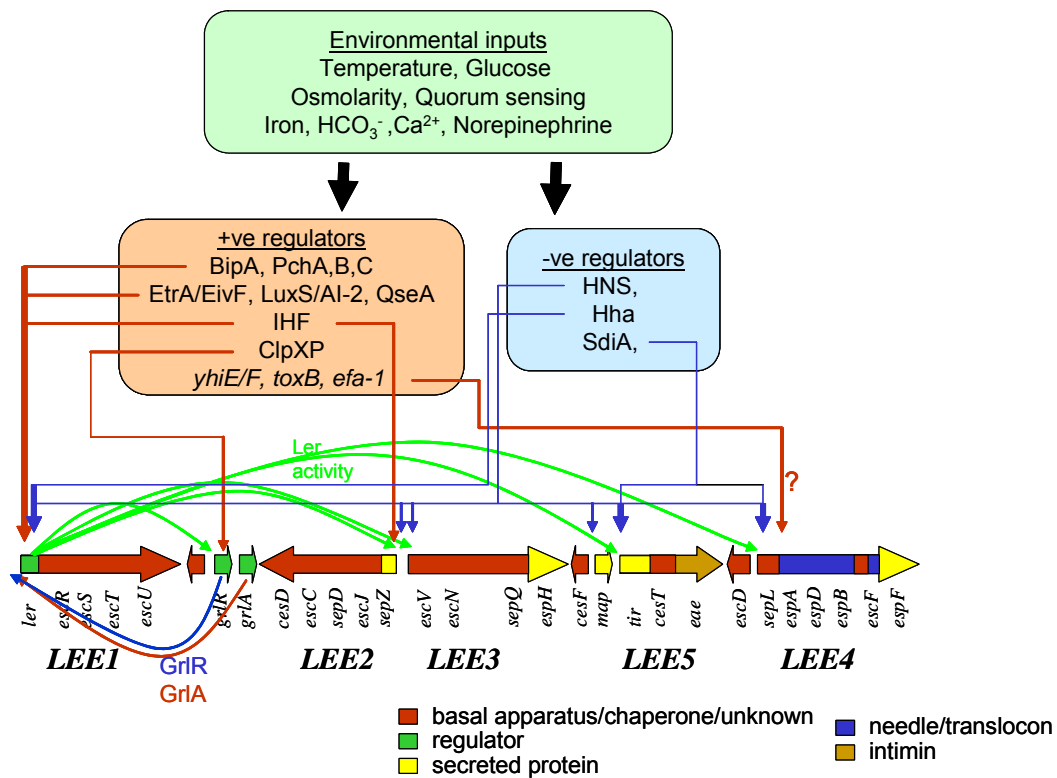


Fig. 1.9 Summary of the regulation of the LEE genes in *E. coli* O157:H7 (originally from Spears *et al.*, 2006)

This diagram shows that T3SS is regulated at multiple levels by many factors. Positive regulators are shown in red square. Negative regulators are shown in blue square. The effect on *ler* can be transferred to the later operons. Regulators are represented in green. Basal apparatus chaperone and unknown genes are indicated in red. Secreted effectors are

shown in yellow. Needle and translocon are indicated in blue. Itimin is represented in brown.

GrlA is a positive regulator of LEE expression encoded by *orf11*, whereas GrlR acts as a negative regulator on LEE expression encoded by *orf10* (Fig. 1.5). They both have an effect on the upstream *ler* and lead to regulation of LEE expression through *ler*. GrlR is considered to achieve the effect on LEE gene expression by interacting with GrlA (Deng *et al.*, 2004).

1.7.1.2 The regulation of aerobic/anaerobic respiration and impact on T3S

E. coli possesses a large number of sensing/ regulation systems for the rapid response to the availability of oxygen and presence of other electron acceptors (Guest JR, 1996; Gunsalus, 1992; Park & Gunsalus, 1995; Unden *et al.*, 1995). The adaptive responses are co-ordinated by a group of global regulators including a one component fumarate, nitrate reduction (Fnr) protein, and the two-component aerobic respiration control (Arc) system (Gunsalus, 1992; Lin & Iuchi, 1991; Lynch & Lin, 1996). The Arc system is a two-component regulatory system including ArcA, the cytosolic response regulator, and ArcB, the transmembrane histidine kinase sensor. Fnr is mainly active during anaerobic growth. It activates and represses target genes in response to anaerobiosis. Moreover, the response to nitrate and nitrite is regulated by the nitrate reductase (Nar) two-component regulatory systems (Bearson *et al.* 2002),. NarX and NarQ sense then respond to nitrate and/or nitrite by auto-phosphorylating the conserved histidyl residue in the transmitter module. Phosphoryl transfer to the conserved aspartyl residue in the receiver domain of the response regulators NarL and NarP results in activation or repression of target operon transcription. In the absence of nitrate and nitrite, NarX sensor acts as a phospho-NarL phosphatase. A similar relationship between the NarQ sensor and phospho-NarP is presumed.

According to Ando and coworkers report (Ando *et al.*, 2007), the activation of the

anaerobic respiratory system accelerates the maturation of a functional TTS apparatus. Previous research in ZAP lab identified the terminal rectum (TR) as the principal site of *E. coli* O157:H7 colonisation in the bovine gut (Naylor *et al.*, 2003). Colonisation of this site is associated with high-level shedding individuals (super-shedders) and these animals are responsible for maintenance of *E. coli* O157:H7 in the host population (Matthews *et al.*, 2006). An overall aim within the Edinburgh research group is to investigate the molecular basis of this tropism. *E. coli* O157:H7 requires the locus of enterocyte effacement (LEE) pathogenicity island for colonisation of the bovine TR (Naylor *et al.*, 2005). If this system is deleted, EHEC O157 does not colonise cattle. A hypothesis that I wanted to test with this research is whether the tropism is driven by when the secretion system is expressed in the animal. This would be a relatively simple question to address if the T3SS regulation was well understood and therefore easy to manipulate.

1.7.2 Timing of secretion

After the assembly of the translocon, the secretion of effector proteins starts. It has been reported that there are extensive ordered synergistic and antagonistic relationships in the secretion of T3S effectors and that the order of secreted effectors matters (Cain *et al.*, 2008). In EPEC, the translocation of effectors was shown to follow the order: Tir>EspZ>EspF>EspH> EspG > Map, based on the translocation efficiency (Mills *et al.*, 2008). It is considered that the T3S effectors function co-ordinately within the host cell and this different translocation efficiency leads to a hierarchy in effector translocation (Ghosh, 2004); (Tu *et al.*, 2003) and therefore activity in the cell.

Secretion of effectors seems to be in an ordered process that is dictated by intracellular concentration of each effector and affinity for cytoplasmic chaperones. The function of many T3 secreted proteins requires a chaperone protein which binds to the secreted effector protein. For example, Tir translocated into host cells mediates the A/E effect in which a chaperone protein, CesT, is involved in the maximizing the efficiency of Tir delivery to the T3SS (Abe *et al.*, 1999; Elliott *et al.*, 1999). Another protein, SepD is also essential for the secretion of T3S effectors and A/E formation by binding with SepL. The deletion of SepD leads to the failure of secretion.

1.7.3 The non LEE encoded regulators

PerC family: Seven homologues of PerC are encoded within O-islands (Ois) in EHEC including PchA-E, PchX and PchY. The *pch* genes include three different classes based on sequence similarity. The *pchA*, *pchB* and *pchC* belong to one class sharing a high similarity in sequence. These three prophage-encoded genes are all positive regulators of LEE1 and in turn of other LEE encoded genes (Iyoda & Watanabe, 2004). It was also revealed PchA-C facilitates the activation of the genes encoded on OIs (Porter *et al.*, 2005). PchA is repressed by the RcsBCD phospho-relay system. However, RcsB serves as a positive regulator of LEE transcription through the activation of another OI encoded regulator, GrvA, an EHEC-specific activator of *ler* (Tobe *et al.*, 2005). In addition, the different expression of *pchA*, *pchB* and *pchC* is also controlled by the stringent response. This regulation is responsible for the up-regulation of T3S level under different physiological conditions, such as the growth-regulated expression of LEE in batch culture (Nakanishi *et al.*, 2006). The other two classes of *pch* genes are *pchD* and *pchE*. The function of these two genes is not clear, it was demonstrated that *pchD* and *pchE* cannot activate LEE1 expression in a K12 background and these are both smaller variant proteins than PchA/B (Porter *et al.*, 2005). Recent studies have shown that PchA and/or Ler bind to and activate transcription of many genes encoding effectors outside the LEE and horizontally-acquired genes coding for virulence factors by transcriptional profiling and chromatin immuno-precipitation (Abe *et al.*, 2008). The key issue is that *pch* genes are usually encoded on prophage regions that also encode non LEE-encoded effector proteins. The Pch family induce the expression of these effectors at the same time ensuring the T3SS is also produced, thereby enabling their export and impact of that integrated region. These regions also encode phage secretion regulators (Psr) that appear to repress the main LEE-encoded effectors to allow the Nles to compete for translocation (Tree *et al.*, 2011).

***pch* adjacent genomic region:** As described above, *pch* genes are involved in the co-ordination of LEE expression. Interestingly, it was recently observed that in contrast

with the highly conserved *pch* genes, a *pch* adjacent genomic region (*pch* AGR) showed extensive variation by genomic study (Yang *et al.*, 2009). The pattern of this variation is largely correlated with phylogenic marker distribution on the chromosome. In addition, by quantitative analysis of transcriptional LEE1 promoter, the variation of *pch* AGR was proved to be pivotal in absolute levels and patterns of LEE1 transcription. *pch* AGR variation is responsible for the diversity of LEE expression patterns. Other OI encoded regulators were also found in David Gally laboratory such as Ecs1581 (not published).

QseA regulator: T3S is also regulated by the host hormones epinephrine and norepinephrine (Epi/Ne) via the quorum-sensing regulator QseA, which controls the transcription level of *ler* and *grlA*. Furthermore, QseA is in turn regulated by the signals from Epi/Ne and inducer-3 (AI-3) through the two-component system consisting of *qseC* and *qseB* (Sperandio *et al.*, 2003).

1.8 Shiga- like toxin (Stx) and Stx phage

1.8.1 Introduction

Phages play an important role in the evolution and virulence of many pathogens such as *E. coli*, *C. botulinum*, *S. aureus* *P. aeruginosa*, etc (Brussow *et al.*, 2004). Genome sequencing has really clarified just to what extent the evolution of particular bacteria is inter-related with that of bacteriophages. Many bacteriophages carry additional ‘cargo’ genes (also termed morons or lysogenic conversion genes). These genes are not necessarily required for the phage life cycle, so why are they present in the bacteriophages? In fact, many of the cargo genes encode potential or proven virulence factors. They are considered to contribute to a change of phenotype or fitness of the lysogenized bacterium. Consequently, these resultant strains are more competitive in the host or other environments; this may also mean more pathogenic in humans.

Stx-producing EHEC are responsible for human HC and HUS associated with Stx activity (Besser *et al.*, 1999). Mortality and morbidity are linked to the activity of this potent toxin in patients infected with *E. coli* O157:H7 as described in section 1.4.3. There

are two major immunologically non-cross-reactive groups in the Stx toxin family, Stx1 and Stx2 (Mainil *et al.*, 1987). Stx2 contains multiple subtypes such as Stx2c and Stx2e. A single EHEC strain may produce Stx1, Stx2 or both, and sometimes even multiple forms of Stx2.

Although Stx1 and Stx2 are similar in mode of action, structure and general characteristics, there are no cross neutralization effects between them. The prototypical Stx1 and Stx2 toxins share 57% homology in amino acid sequence in the A subunit and 60% in the B subunit (Jackson *et al.*, 1987). Stx1 from different origins has more than 99% homology in nucleotide sequence, whereas Stx2 shows more variations and is sub-classified into Stx2c, Stx2d2, Stx2vhb, Stx2e, etc (Fig. 1.10).

A Subunit

Stx2d2	1	MKCLF KW VLCLLLGFSSVSYSREPTIDFSTQ Q SYVSSLNSIRTEISTPLEHISQ G TTSVSVINHTPPGSYFAVDIRGLDVY Q ARFDHLRLII EQ NNLYVAGFVNTAINTFYRFSDFTHI
P1332	1L.....
P1334	1
P1330	1
CL-15	1
CVM9322	1
CVM9557	1
CVM9584	1
CVM3605	1
CVM3676	1
CVM3880	1
CVM3961	1
CVM3939	1
CVM3541	1
CVM3639	1
CVM3756	1
CVM3962	1
Stx2c	1
Stx2	1
Stx2d2	121	SVPGVTTVSMITDSSYTTLQ R VAALERSGMQISRHSLVSSYLALMEFSGNTMTRDASRAVLRFTVTAEALRFRQIQREFRQALSETAPVYTIMPGDVLTLNWGRISNVLPEYRGEDGV
P1332	121
P1334	121
P1330	121
CL-15	121
CVM9322	121
CVM9557	121
CVM9584	121
CVM3605	121
CVM3676	121
CVM3880	121
CVM3961	121
CVM3939	121
CVM3541	121
CVM3639	121
CVM3756	121
CVM3962	121
Stx2c	121
Stx2	121
Stx2d2	241	RVGRISFN N ISAILGTAVILNCH H QGARSVRVAVNEESQ PE CQITGDRPVIKINNTLWESNTAAFLNRKSQ S LYTT C
P1332	241
P1334	241
P1330	241
CL-15	241
CVM9322	241
CVM9557	241
CVM9584	241
CVM3605	241D.....F.....K
CVM3676	241D.....F.....K
CVM3880	241D.....F.....K
CVM3961	241D.....F.....K

Fig. 1.10 Alignment of predicted amino acid sequences of the A subunit of Stx2 variants with the published sequences of Stx2dact of STEC strain B2F1 (Stx2d2) (GenBank accession no. AF479829) and Stx2 (GenBank accession no. AB035143) (Zheng, 2008). Dots indicate residues identical to those in Stx2dact. Residues Ser313 and Glu319 in the A subunit and residues Asn35 and Asp43 in the B subunit, which distinguish Stx2d from Stx2, are indicated by bold type and underlining.

Stx1 from EHEC is identical to Shiga toxin from *Shigella dysenteriae* type 1. The basic A-B subunit structure in all members of the Shiga toxin family is retained. Stx1 is comprised of an A subunit of ~32 kDa and five B subunits of ~7.5 kDa each. Furthermore, the single 32 kDa A subunit consists of a 28 kDa peptide (A1) and a 4 kDa peptide (A2), and the A1 and A2 combine through a disulfide bond. The A1 peptide contains the enzymatic activity, while the A2 peptide is responsible for linking the A subunit to a pentamer of 7.5 kDa B subunit. The B subunits recognize a specific glycolipid receptor, globotriaosylceramide (Gb3), on the surface of eukaryotic cells. The Gb3 receptor is the main binding target for Stx; while the Stx2e variant uses Gb4 as its receptor. These receptors can be found on the surface of cultured human renal epithelial cells, human platelets, erythrocytes and some other cell types. Once the toxin is bound to the cell membrane, the holotoxin is internalized by endocytosis through coated pits and delivered to the trans-Golgi network apparatus. The toxin is then transported to the endoplasmic reticulum and finally to the cytosol (Sandvig & van Deurs, 1994). In the cytoplasm, the A subunit cleaves the 28S rRNA of the eukaryotic ribosome, and this leads to the inhibition of protein synthesis (Law, 2000). The consequent prevention of protein synthesis results in the death of cells that possess the Gb3 (or Gb4 for Stx2e) receptor, such as renal intestinal epithelial cells, endothelial cells, Vero and HeLa cells.

Epidemiological data demonstrated that Stx2 has a more important role than Stx1 in the development of HUS (Griffin, 1995). It was revealed that *E. coli* O157:H7 strains that carry Stx2 alone are more likely to be associated with HUS than strains producing Stx1 alone or both (Pickering *et al.*, 1994). It has been also reported for both cultured renal endothelial cells (Louise & Obrig, 1995) and mice (Wadolkowski *et al.*, 1990) that Stx2 is critical for renal damage, but not Stx1. As mentioned above, although Stx1 and Stx2 share commonality in structure and general biochemical characteristics, significant differences in amino acid sequence within the A subunit can lead to differences in toxin activity in mice (Melton-Celsa *et al.*, 1996).

1.8.2 The lytic and lysogenic decision of bacteria phage lambda (λ)

In the evolution of EHEC strains, there are many phages obtained by integrating with the host genome. When the phages enter the bacteria, a decision between lysis or lysogeny is made. Two key features are characterized in the lytic and lysogenic development pathway. Firstly, following the infection by the phage, a decision between lysis or lysogeny is made depending on environmental signals and the number of infecting phages per cell (Oppenheim *et al.*, 2005). Secondly, the lysogenic state is very stable and only responds to SOS induction.

If the bacteria follow the lytic pathway, phage can reproduce as package virions; then the replicated phages are released by lysis. Alternatively, if the lysogeny pathway is activated, phage DNA is integrated into the host genome, which is accompanied by the switch-off of the lytic pathway. Moreover, the prophage DNA is replicated with the host chromosome in the later cell division and also contributes immunity to the host cell against other phage infections. Normally, the lysogenic state is very stable. However, DNA damage can arise in some extreme conditions. When the SOS response is induced as a result of DNA damage, the switch from lysogeny to lysis state is turned on as a result of CI autocleavage mediated by activated RecA. This is confirmed by the low spontaneous prophage induction in a *recA* mutant (Morelli *et al.*, 2009). Host cell lysis is followed after the replication of phage. At the same time, few of these induced host cells can enter an abortive lytic cycle in which the prophage DNA is lost and host cells are cured of the phage (curing) (Fig. 1.11).

CI and Cro regulation proteins control the lytic or lysogenic development with a bistable genetic switch system. The CI regulator sustains the lysogenic state by controlling the expression of three promoters P_L , P_R and P_{RM} ; while the Cro protein regulates lytic development by inhibiting the level of CII, which activates *cI* transcription.

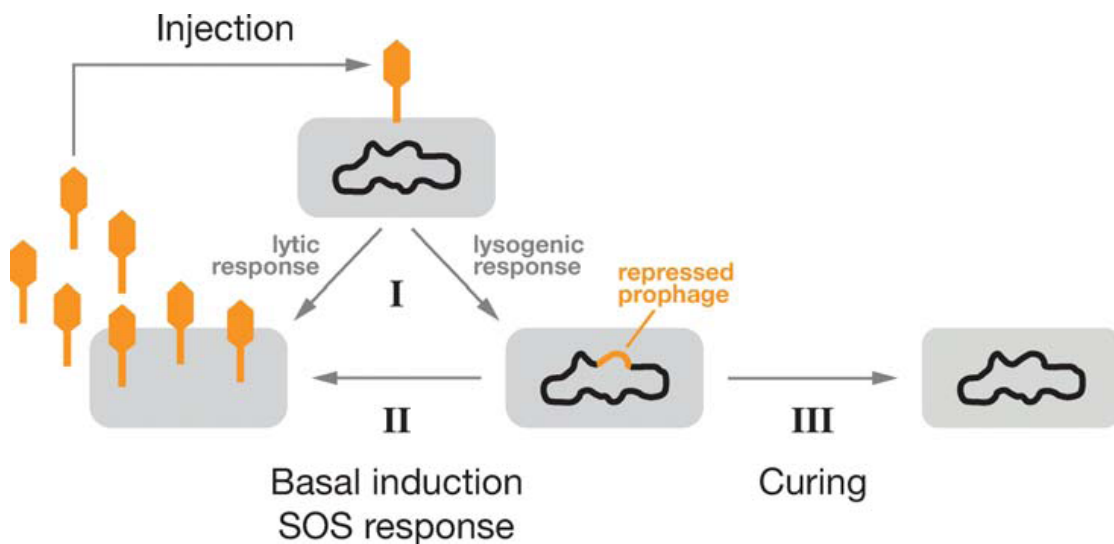


Fig. 1.11 Schematic diagram of lysis and lysogeny in λ phage (originally from Oppenheim *et al.*, 2005). It shows the lytic and lysogenic pathway of phage. In the lytic process, phage is released due to bacteria lysis by producing package virions. In lysogenic pathway, phage is integrated to bacteria chromosome. The integrated phage genes are reproduced with bacteria cell life cycles. This integrated phage can also be released by curing.

An immunity system is usually used by lambda like phage to prevent the multiple infections of lysogens. The CI protein is essential in this immunity system. CI keeps a certain level of expression which represses other phage genes involved in the integration into the host genome and lytic replication cycle. Consequently, the integrase from incoming lambda like phage is inhibited resulting in a single lysogen in the host bacteria (Ptashne, M. 2004). However, multiple lysogens were found in Stx phage Φ 24_B and confirmed by the transcription expression of anti-repressor *ant* using RT-PCR (Fogg *et*

al., 2007). This superinfection leads to an increase of intracellular recombination of Stx prophages and in turn enhanced virulence (Fogg *et al.*, 2010). Fogg and his co-workers also demonstrated that additional lambda phages were detected following formation of a lambda lysogen. This result was confirmed by Southern hybridization and quantitative PCR. In addition, phage immunity mutation was excluded by analysis of the complete immunity region in the integrated lysogens.

Lambda phages including Stx coding phages share a similar genomic structure. The centre region of regulatory circuitry termed immunity region. This immunity region usually locates between N to O gene on lambda and contains two genes encoding specific DNA binding proteins, CI and Cro, and six operator sites to which CI and Cro bind (Degnan *et al.*, 2007). By comparing eight lambdoid phages including three Stx producing phage, high similarity was observed in the immunity region. These immunity region sequences are usually well conserved (Fattah *et al.*, 2000). However, it was proposed that the difference in the immunity region might account for the different phage lysis patterns leading to the different phage types.

1.8.3 The regulation of Stx phage

In the sequenced genome of *E. coli* O157:H7 strain EDL933, Stx1 and Stx2 are encoded by two different prophages: CP-933V & BP-933W (Karch *et al.*, 1999; Unkmeir & Schmidt, 2000). The sequences of these prophages show a high degree of homology to that of phage lambda (Karch *et al.*, 1999). So, Stx1 and Stx2 phage all belong to the λ phage family. The Phages in the λ family have a similar genome structure and are regulated by the same mechanisms (Fig. 1.12).

Stx genes are usually found immediately downstream of the Q gene. So Stx will be produced at the end of the lytic process when naive bacteriophages are produced. Stx expression is usually repressed in lysogenic bacteria. However, once the phage lytic program is induced, transcription initiates at early promoters P_L and P_R and this results in Stx expression or release through terminating and anti-terminating transcription (Fig. 1.12) (Fogg *et al.*, 2010). Transcription elongation begins with the λ -encoded anti-

termination protein N. In the beginning, the N protein binds at the RNA site 'N utilization' (NUT) and activates transcription that initiates at P_R . As a result of the switch of this transcription, terminators were overridden and antiterminator protein Q was activated. According to sequence and structure analysis, there are three parts in the NUT site, including BOXA, which is considered to interact with NusB and ribosomal protein S10 (NusE), a spacer region, and a stem-loop structure, BOXB, which interacts with N and NusA (Chattopadhyay *et al.*, 1995; Mogridge *et al.*, 1995). When the NUT RNA is synthesized, the various proteins associated with the NUT sequences combine together with the RNA polymerase (RNAP), forming a complex that overrides downstream transcription termination signals.

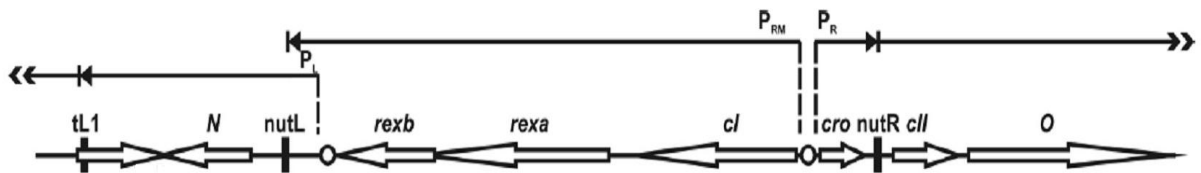


Fig. 1.12 Lambda immunity region. Closed boxes represents transcription terminator regions. Open circles indicates OL and OR operator binding regions. Transcription is indicated by black arrows raised above the genetic map. \Rightarrow represents transcripts that extend beyond the border; \Rightarrow indicates transcript termination. (Fogg *et al.*, 2010)

When P_R promoter is activated, the anti-terminator protein Q is produced. Q recognizes a DNA sequence, the *qut* site, partly within P_R' (Guo & Roberts, 2004), which allows transcription to proceed. Stx expression is turned on as a result of Q protein binding at P_R' which promote the read through (Neely & Friedman, 1998). Because Q production requires transcription from the early P_R promoter that is in turn stimulated by N protein, the anti-terminator N protein is required for Stx expression.

1.8.4 The role of CII

The switch to the lysogenic process needs a set of conditions, including integration of DNA, repression of the early promoters, and inhibition of lytic gene expression (Oppenheim *et al.*, 2005). CII is essential in this process. Int and CI are activated by CII, which turns on *pI* and *pRE* promoters. Antiterminator Q is repressed by CII through *paQ* promoter. CII recognizes these promoters by binding to a direct repeat TTGC-N6-TTGC sequence on the promoter. The N6 region location in these promoters corresponds to the -35 position. The mechanism of the activation of the three promoters by CII remains unclear.

The structure of CII protein has been revealed recently (Datta *et al.*, 2005a; Datta *et al.*, 2005b; Jain *et al.*, 2005). The quaternary structured CII is composed of two nearly equivalent dimers. Each monomer has a helix-turn-helix DNA binding motif. However, it was proved that only two of the four monomers are involved in the binding with direct repeat sequence. The *pI*, *pRE*, and *paQ* promoters belong to Xis, CII, and Q protein coding sequence, respectively. When CII is induced, it activates the *pI* promoter. This promoter is responsible for the activation of Int and repression of Xis. Xis is a DNA-binding protein that binds as a trimer to its DNA binding site and interacts cooperatively with Int for excision. Int is required for both the integrative and excisive reactions. The integration host factor (IHF) is also required for efficient integration. Therefore, following the activation of *pI* promoter, CII promotes the lysogenic integration by switching on the synthesis of Int, which helps the integration and repressing Xis protein.

CII is essential in the decision of lysis or lysogeny. The regulation of CII is in response to many factors (Herman *et al.*, 1993) (Hoyt *et al.*, 1982) (Kihara *et al.*, 1997; Rattray *et al.*, 1984; Shotland *et al.*, 1997). CII is controlled at multi-levels as detailed below (Fig. 1.13); (i) The transcription level of *cII* is repressed by CRO and CI through binding to *oR*. At the same time, *cII* transcription is activated by antitermination N factor that acts at *NUTR*. High expression of CII is only detected shortly before the repression of CRO and CI. (ii) The translation of CII is stimulated by IHF (Hoyt *et al.*, 1982). Although the mechanism

is not clear, IHF is considered to activate the translation by binding to the upstream of CII (Mahajna *et al.*, 1986; Peacock & Weissbach, 1985). (iii) CII mRNA is degraded by OOP RNA which is a 77-nucleotide major transcript synthesized from bacteriophage lambda. OOP RNA is an antisense complementary to the 3' end of *cII* mRNA. Therefore, it binds to *cII* mRNA. A double-stranded RNA is formed as a result of binding. This double-stranded RNA is recognized and cleaved by RNase III (Krinke & Wulff, 1990; Krinke *et al.*, 1991). *cII* mRNA is reduced rapidly by RNase III. (iv) CII protein is also degraded rapidly by ATP-dependent protease FtsH (Shotland *et al.*, 1997; Kihara *et al.*, 1997; Greenblatt *et al.*, 1998). It was reported that *ftsH* mutations resulted in an increased stabilization of CII and in turn lysogenic frequency was increased as well (Banuett *et al.*, 1986). FtsH acts at the C-terminal of CII leading to the rapid proteolysis of CII (Datta *et al.*, 2005b; Kobiler *et al.*, 2002). (v) Cro is inhibited by CI RNA which acts as antisense to *cro*. This was confirmed in *ftsH* host mutant, in which the repression of Cro and high concentration of CII were found. (vi) CIII, a 54-residue long peptide, functions as an activator of CII by repressing the FtsH protease (Herman *et al.*, 1997; Kobiler *et al.*, 2002; Kornitzer *et al.*, 1991).

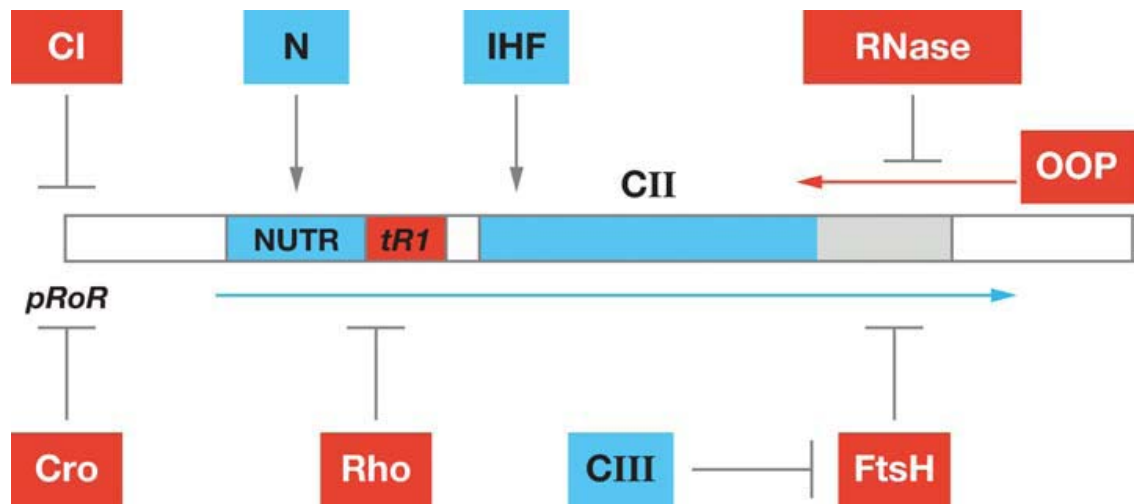


Fig. 1.13 Schematic diagram of regulation of CII (originally from Oppenheim *et al.*, 2005)

The CII repressors are indicated in red. The *cII* gene, promoter and CII activator are depicted in blue. The direction of CII is labeled in blue with a red arrow for OOP. CII is inhibited by CI and Cro at transcription level. *tR1*, the promoter of *cII*, is repressed by Rho factor which leads to the reduction of *cII* transcription. The antiterminator N is required for the transcription initiation of *cII* by acting on NUTR site. The OOP RNA, as an antisense RNA, decreases CII mRNA stability via RNase III cleavage function. FtsH is essential in rapid degradation of CII protein by binding at the the C terminus of CII.

1.9 Research background and aims of this project

Previous research in the Zoonotic and Animal Pathogens Laboratory (ZAP Lab) has shown that EHEC O157:H7 strains vary significantly in their capacity to secrete LEE T3SS proteins (Roe *et al.*, 2003b). For example, secretion of T3S proteins is much higher in TUV93-0 (Stx negative derivative of EDL933) compared to EDL933 (contains both Stx1 and Stx2 phages). This leads to the possibility that Stx phages may have an effect on T3S expression. The basis to this variation is unclear.

It is also evident that particular strains are more likely to be associated with human infections than others. As the main reservoir, cattle play a key role in human infection via food contamination or direct exposure. From a large survey of 430 farms, some cattle were defined as super-shedders with $\geq 10^4$ colony forming units per g⁻¹ (CFU.g⁻¹) and some as low-shedders with $< 10^2$ CFU.g⁻¹ (Chase-Topping *et al.*, 2007a). Interestingly, PT 21/28 was found to be more common in the super-shedders and PT 32 was more often detected in the low-shedders. The basic hypothesis is that higher shedding levels from cattle may make it more likely to be the strains which will end up infecting humans. As T3S is essential for cattle colonisation, it is proposed that:

1. Oxygen sensing regulation of T3S may account for the tropism of EHEC O157:H7 for the terminal rectum of cattle. Oxygen level might vary in the different parts of gastrointestinal tract. This could lead to the colonization tropism of terminal rectum in the cattle due to the variation in T3SS expression in the intestine.
2. Variation in the regulation of T3S is associated with variation in excretion level of EHEC O157:H7 from colonized cattle.

This PhD was focused on addressing these two areas: (1) to understand the localisation of EHEC O157 at the terminal rectum of cattle; (2) to understand the strain variation in T3S.

(1) In relation to rectal and mucosal colonisation, established aerobic/anaerobic regulators were investigated including *arcA*, *fnr*, *narX*, *narQ*. Then the T3S levels, adherence efficiency and A/E lesion formation were measured in these four mutants.

(2) Strain secretion variation was approached in two ways; the first was to control expression from the LEE1 operon, required for T3S expression, in order to both induce expression and examine the importance of downstream regulation. The second was to investigate variation in T3S between different phage types of EHEC O157.

2 Chapter 2 Materials and Methods

2.1 Bacterial strains, media & plasmids

Details of the strains and plasmids in this work are shown in Table 2.1 and 2.2. Bacteria were cultured either in Luria-Bertani (LB) broth or Minimal Essential Medium with 25 mM Hepes modification (MEM-Hepes) (Sigma-Aldrich). Glucose was added to MEM-

Hepes to give a final concentration of 0.2%. Antibiotics were included when required at the following concentrations: chloramphenicol (CAM) 20 µg ml⁻¹, kanamycin (KAN) 50 µg ml⁻¹, Ampicillin (AMP) 100 µg ml⁻¹. Other chemicals added to media were bromo-chloro-indolyl-galactopyranoside (X-gal) 20 µg ml⁻¹ (dissolved in dimethylformamide) and Isopropyl β-D-1-thiogalactopyranoside (IPTG) 2µg ml⁻¹.

Table 2.1. Bacterial strains associated with this work

Strain	Details	Source
ZAP198	<i>E. coli</i> O157:H7 Nalidixic acid resistant, Shiga toxin-negative	(Naylor <i>et al.</i> , 2003)
ZAPΔ <i>arcA</i>	<i>arcA</i> replaced with CAM cassette in ZAP198	<i>This study</i>
ZAPΔ <i>fnr</i>	<i>fnr</i> replaced with CAM cassette in ZAP198	<i>This study</i>
ZAPΔ <i>narX</i>	<i>narX</i> replaced with CAM cassette in ZAP198	<i>This study</i>
ZAPΔ <i>narP</i>	<i>narP</i> replaced with CAM cassette in ZAP198	<i>This study</i>
ZAP1212	<i>lacYZ</i> replaced with <i>sacBkan</i> cassette in ZAP198	<i>This study</i>
ZAP1213	<i>lacYZ</i> replaced with PN25& <i>tetR</i> in ZAP198	<i>This study</i>
ZAP1238	<i>E. coli</i> O26 Stx2+	(Mellmann <i>et al.</i> , 2008)
ZAP1239	<i>E. coli</i> O26 Stx2-	(Mellmann <i>et al.</i> , 2008)
EDL933	<i>E. coli</i> O157:H7 EDL933, Stx1+ Stx2+	<i>Lab stock</i>
TUV93-0	EDL933 with excised Stx1 and Stx2 phages	(Campellone <i>et al.</i> , 2007)
Strain	Details	Source
ZAP1321	EDL933 <i>z1449(cII_{stx2})<>sacBkan</i> . Constructed by allelic exchange using pXLS13 (Table 2.2)	<i>This study</i>
ZAP1322	EDL933ΔBP-933W (Stx2 phage) by allelic	<i>This study</i>

	exchange of ZAP1321 using pXLS15 (Table 2.2)	
ZAP1323	ZAP1321 Δ z1449	<i>This study</i>
ZAP1324	ZAP1323 z3357 $\langle\rangle$ sacBkan	<i>This study</i>
ZAP1325	ZAP1324 Δ z3357-delete	<i>This study</i>
ZAP1326	ZAP1322 CP-933V $\langle\rangle$ sacBkan	<i>This study</i>
Sakai stx2A::kan	Sequenced <i>E. coli</i> O157:H7 Sakai strain with a kanamycin cassette replacing the stx2A toxin gene (Sp5 stx2::KmR)	(Dahan <i>et al.</i> , 2004)
TUV+Stx2	TUV93-0 containing a marked Stx2 phage conjugated from Sakai stx2A::kan via JC5029 as described in Material and Methods	<i>This study</i>
AAEC185	Laboratory K-12 strain for plasmid cloning	(Blomfield <i>et al.</i> , 1991)
<i>E. coli</i> K12 MG1655 (Nal ^R)	Spontaneous NalR derivative from <i>E. coli</i> K12 MG1655.	<i>Provided by Prof.M.Masters, University of Edinburgh</i>
<i>E. coli</i> K12 MG1655 (Sp5 stx2::KmR)	Generated by transduction from the Sakai stx2A::kan strain	<i>This study</i>
JC5029	Hfr strain	<i>Coli Genetic stock centre (CGSC)</i>
<i>E. coli</i> O157:H7 PT21/28 and PT32 bovine isolates	18 strains isolated as part of an international partnership in veterinary epidemiology (IPRAVE) project 2001-2006. Further information is provided in Table 5.1.	(Chase-Topping <i>et al.</i> , 2007b)
<i>E. coli</i> O157:H7 PT21/28 and PT32 human isolates	20 strains provided by Dr. Lesley Allison from the <i>E. coli</i> reference laboratory, Edinburgh. Further information is provided in Table 5.1.	(Chase-Topping <i>et al.</i> , 2007b)

Table 2.2. Plasmids used in the study

Plasmid	Details	Source
pIB307	pMAK705-based vector for allelic exchange; temperature-sensitive replicon	(Blomfield et al., 1991)
pAJR27	Andrew J.Roe provided, <i>lacIA</i> flanking regions from <i>E. coli</i> O157 (ZAP1) cloned into pIB307	(Roe et al., 2003b)
pAJR33	Andrew J.Roe provided, <i>lacIA</i> flanking regions cloned into pIB307 with <i>sacBkan</i> cassette	(Roe et al., 2003b)
PZS4Int-laci/tetR	Commercial vector	Expressys
pKC26	pACYC184 with GFP fusion	(Holden et al., 2007)
pTP883	The <i>cat</i> gene cloned into pTP809 originally from pBR322	(Murphy et al., 2000)
pKM201	Temperature sensitive <i>Red-gam</i> expressing plasmids.	(Murphy & Campellone, 2003)
pXLS01	<i>ler</i> with 567 bp of the promoter region was amplified with primer pair Ct- <i>ler</i> -SalI and Nt- <i>ler</i> -PstI, cloned into pWSK29 with <i>Sal</i> I and <i>Pst</i> I	This study
pXLS02	PN25& <i>tetR</i> amplified from PZS4Int-laci/tetR inserted into pAJR27 at <i>Bam</i> H I site	This study
pXLS03	<i>tet</i> promoter inserted into <i>Xba</i> I site in pKC26	This study
pXLS04	LEE1 promoter flanking regions for first construction amplified from EDL933 and cloned into pIB307	This study
pXLS05	LEE1 promoter flanking regions for second construction amplified from EDL933 and cloned into pIB307	This study
Plasmid	Details	Source

pXLS06	<i>sacBkan</i> cassette was cloned into pXLS04 at <i>BamH</i> I site	<i>This study</i>
pXLS07	<i>tet</i> promoter was cloned into pXLS04 at <i>BamH</i> I	<i>This study</i>
pAJR32	Source of <i>sacBkan</i> cassette	(Porter <i>et al.</i> , 2004)
pBAD/His A	Expression vector designed for regulated, dose-dependent recombinant protein expression and purification in <i>E. coli</i>	<i>Invitrogen</i>
pBAD-N	Amplified with primers JTstx2.N.F. <i>Nco</i> I and JTstx2.N.R. <i>Hind</i> III from EDL933 and cloned via <i>Nco</i> I and <i>Hind</i> III sites in pBAD/His A.	<i>This study</i>
pBAD-CRO	Amplified with primers JTstx2.CRO.F. <i>Nco</i> I and JTstx2.CRO.R. <i>Hind</i> III from EDL933 and cloned via <i>Nco</i> I and <i>Hind</i> III sites in pBAD/His A.	<i>This study</i>
pBAD-CI	Amplified with primers JTstx2.CI.F. <i>Nco</i> I and JTstx2.CI.R. <i>Hind</i> III from EDL933 and cloned via <i>Nco</i> I and <i>Hind</i> III sites in pBAD/His A.	<i>This study</i>
pBAD-CII	Amplified with primers JTstx2.CII.F. <i>Nco</i> I and JTstx2.CII.R. <i>Hind</i> III from EDL933 and cloned via <i>Nco</i> I and <i>Hind</i> III sites in pBAD/His A.	<i>This study</i>
pBAD-Q	Amplified with primers JTstx2.cl.Q. <i>Nco</i> I and JTstx2.Q.R. <i>Hind</i> III from EDL933 and cloned via <i>Nco</i> I and <i>Hind</i> III sites in pBAD/His A.	<i>This study</i>
pAJR70	pACYC184 containing <i>egfp</i>	(Blomfield <i>et al.</i> , 1991)
pAJR71	LEE1 promoter fusion	(Blomfield <i>et al.</i> , 1991)
Plasmid	Details	Source
pXLS10	z3357(<i>cII_{stx1}</i>) flanking regions amplified from	<i>This study</i>

	EDL933 and cloned into pIB307 as described in Material and Methods (used to make ZAP1325)	
pXLS11	<i>z1449</i> (<i>cII_{stx2}</i>) flanking regions from EDL933 cloned into pIB307 as described in Material and Methods (used to make ZAP1323 & pXLS13)	<i>This study</i>
pXLS12	Stx1 phage (CP-933V) flanking regions from EDL933 cloned into pIB307 as described in Material and Methods (used to make pXLS16)	<i>This study</i>
pXLS13	<i>z1449</i> flanking regions from EDL933 cloned into pIB307 with <i>sacBkan</i> cassette (used to make ZAP1321)	<i>This study</i>
pXLS14	<i>z3357</i> flanking regions from EDL933 cloned into pIB307 with <i>sacBkan</i> cassette (used to make ZAP1324)	<i>This study</i>
pXLS15	Stx2 phage (BP-933W) flanking regions from EDL933 cloned into pIB307 as described above in Material and Methods (used to make ZAP1322)	<i>This study</i>
pXLS16	Stx1 phage (CP-933V) flanking regions from EDL933 cloned into pIB307 with <i>sacBkan</i> cassette (used to make ZAP1326)	<i>This study</i>

2.2 Primers used in this work

Table 2. 3. Oligonucleotide primers used in this study. Standard letters represents the original target sequence, capital letters represents the additional sequence and underlined capital letter represents introduced enzyme restriction site.

Primer	Detail	Source
5-KO- <i>ArcA</i>	ggacttttgacttctctgtttcgatttagttggcaatttaggtagcaaacGCG GCCGCATGAGACGTTGAT	This study
3-KO- <i>ArcA</i>	ataaaaacggcgctaaaaagcgccgttttttgacgggtgtaaagccgaG CGGCCGCTTTCGAATTTCTGC	This study
5-KO- <i>Fnr</i>	Ctaaaaagatgttaaaattgacaaatatcaattacggcttgagcagacct GCGGCCGCATGAGACGTTGAT	This study
3-KO- <i>Fnr</i>	tcagaaaaatttaatatgatgacagaaggatagtgagttatgcggaaaaa GCGGCCGCTTTCGAATTTCTGC	This study
5-KO- <i>NarX</i>	cacattcattaagggtattgtctcatttaaagcctgaaggaagaggttac GCGGCCGCATGAGACGTTGAT	This study
3-KO- <i>NarX</i>	ttcgagcatcggtgatcgtaatcagcaggatagtagccggttctga GCGGCCGCTTTCGAATTTCTGC	This study
5-KO- <i>NarP</i>	caacgtacgtcaaacataatgattctaataaaacctcaggagactact GCGGCCGCATGAGACGTTGAT	This study
3-KO- <i>NarP</i>	gcaggagagtaaataaaaaggcccgatggtgatgccatcgggctattt GCGGCCGCTTTCGAATTTCTGC	This study
5- <i>ArcA</i>	cagaccccgacattcttate	This study
3- <i>ArcA</i>	cttcagatcaccgcagaagc	This study
5-up- <i>ArcA</i>	cgggtcctgagggaagtaccc	This study
3-down- <i>ArcA</i>	gctggtggtggcgctggccggc	This study
3- <i>Fnr</i>	ggcaacgttacgcgtatgacc	This study
5-up- <i>Fnr</i>	cggaattctctgctgtaagggttg	This study
3-down- <i>Fnr</i>	gtcctggtaggatcgataac	This study
Primer	Detail	Source
5- <i>NarX</i>	cgttgtctctctccgctcacc	This study
3- <i>NarX</i>	gggtatctccttgacgtctg	This study

5-up- <i>NarX</i>	ccgggtatgggtatacttcag	This study
3-down- <i>NarX</i>	gttcattgccgggcatattgag	This study
5- <i>NarP</i>	cctgaagcaacgccttttcag	This study
3- <i>NarP</i>	gcgcagtagattgcgaatatg	This study
5-up- <i>NarP</i>	gatccaaagcgaacgacaa	This study
3-down- <i>NarP</i>	cctttgagcagcagcgatttg	This study
5- <i>lacI</i>	ggccgattcattaatgcagctg	This study
3- <i>lacA</i>	caacttctgatggatgcgagtg	This study
5- <i>lacZ</i>	gcattttaaatctcactcggc	This study
3- <i>lacY</i>	gccctggaaaccgatgcttc	This study
5- <i>PN25</i> -BamHI	AAAAAGGATCCtcgagggaaatcataaaaaattatttgc	This study
3- <i>PN25</i> -BamHI	AAAAAGGATCCttaagaccactttcacatttaagtg	This study
5-Tetpromoter- XbaI	AAAATCTAGAtccctatcagtgatagagattgacatccctatca gtgatagagatac	This study
3-Tetpromoter- XbaI	AAAATCTAGAggtcagtcgctcctgctgatgtgctcagtat ctctatcactgatagg	This study
5-GFP	ggccaacactgtcactactttgac	This study
3-GFP	gtttgtgtccgagaatgtttccatc	This study
5- <i>LEE1</i> up FR XmaI	AACCCGGGgcagcatctaaactaaagatgc	This study
3- <i>LEE1</i> UP FR BamHI	CCGGATCCcccaggagcttacataagtaag	This study
5- <i>LEE1</i> down FR 1 st BamHI	CCGGATCCtaatagcttaaaatattaaag	This study
5- <i>LEE1</i> down FR 2 nd BamHI	CCGGATCCcttaaaatattaaagcatgcg	This study
Primer	Detail	Source
3- <i>LEE1</i> down FR XbaI	CCTCTAGAgactcagtgctcttattag	This study
5- <i>LEE1</i> test	cttatgtaagctcctgggga	This study

3- <i>LEE1</i> test	gtgagataacgtttatctatca	This study
5-Tet promoter BamHI 1 st	AAAAGGATCCctatcagtgatagagattgacatccctatcag	This study
3-Tet promoter BamHI 1 st	GGGGGATCCgtatctctatcactgataggatgtcaatctc	This study
5-Tet promoter BamHI 2 nd	AAAAGGATCCctatcagtgatagagattgacatccctatcag tgatag	This study
3-Tet promoter BamHI 2 nd	GGGGGATCCgatgtgctcagtatctctatcactgataggga tgtcaa	This study
5-PIB test	gtcataagtgcggcgacgatag	This study
3-PIB test	cagtagtaggtgaggccgttg	This study
<i>stx2</i> up 5'	aaaaaGGATCCgacatgttgaaacgatggcac	This study
<i>stx2</i> up 3'	gggggAAGCTTcgagcaatagacagttcttcc	This study
<i>stx2</i> down 5'	aaaaaGGATCCcaatatgtccgtacatggaataa	This study
<i>stx2</i> down 3'	aaaaaGAGCTCgatggcttttgacgagcttaa	This study
<i>stx1</i> up 5'	aaaaaGGATCCcacgcgcgtaacgtgacag	This study
<i>stx1</i> up 3'	gggggAAGCTTcgacacgggtattggcaatag	This study
<i>stx1</i> down 5'	aaaaaGGATCCcgagatcaaacgtggatcg	This study
<i>stx1</i> down 3'	aaaaaGTCGACgttcgattttcacgcacca	This study
<i>z1449</i> up 5'	aaaaaGAGCTCcaaacaacatcaacgttttagaa	This study
<i>z1449</i> up 3'	aaaaaGGATCCttcttaagatttccaatag tgaa	This study
<i>z1449</i> down 5'	aaaaaGGATCCgggaattactggatcaatcc	This study
<i>z1449</i> down 3'	cccccAAGCTTgaaagatcgtttctggctg	This study
<i>z3357</i> up 5'	aaaaaGTCGACctttctgttcttaactcgtag	This study
<i>z3357</i> up 3'	aaaaaGGATCCttgttaattttctatattgatattg	This study
Primer	Detail	Source
<i>z3357</i> down 5'	aaaaaGGATCCgggaattactggatcaatccac	This study
<i>z3357</i> down 3'	gggggAAGCTTgtcgttttctggctggcaga	This study
Stx1 phage (CP933-V) left end		
yehU	cacatctgctgaagcagcagc	This study

Z3305	gcgatacagatctcaacacgc	This study
Stx1 phage (CP933-V) right end		
intV	atcacgaacagatagaactcc	This study
yehV	agcgtctgggcggggaatcc	This study
stx2 phage (BP933-W) left end		
wrbA	cgcctgtctggtcgaggaagg	This study
intW	tacaatgttatggtgatgg	This study
stx2 phage (BP933-W) right end		
z1503	tttttcctcgcccataacc	This study
z1504	cggaaatagagataacacgagg	This study
SLT-I-1	cagtaatgtggtggcgaag	(Blomfield <i>et al.</i> , 1991)
SI-1	cgcctgctatttcactgagc	(Blomfield <i>et al.</i> , 1991)
z1449 5'	gctattttcacaatggacattc	This study
z1449 3'	tcagaattgcatatcaattgc	This study
z1449 external 5'	cacgcataaccttcaactagc	This study
z1449 external 3'	ctgtggattgatccagtaattc	This study
z3357 5'	aaaaaGAATTCtcagaattgcatatcaattgc	This study
z3357 3'	aaaaaCCATGGatggcacaagcaagctacag	This study
z3357 external 5'	gtcataatgaatcctgtggatt	This study
Primer	Detail	Source
z3357 external 3'	ggtgtgccgtataactcaa	This study
SacB 5'	gcaactcaagcgtttgcgaaag	This study
SacB 3'	ggcttgatgggccagttaaag	This study
stx2 5'	gcgggtttatttgcattagc	(Blomfield <i>et al.</i> , 1991)

stx2 3'	tcccgtaaccttcactgta	(Blomfield <i>et al.</i> , 1991)
stx2c 5'	gcgggtttatttgcattagt	(Blomfield <i>et al.</i> , 1991)
stx2c 3'	agtactcttttcggccact	(Blomfield <i>et al.</i> , 1991)
Ct-ler-Sall	aaaaaGTCGACtcattgttaaatttttcagcgg	This study
Nt-ler-PstI	aaaaaCTGCAGgtatcatatagcatcatatagtg	This study
JTstx2.N.F.NcoI	ggCCATGGcacgcagaactcagtt	This study
JTstx2.N.R.HindIII	ggAAGCTTtcacctcgccgtcagttgtt	This study
JTstx2.CRO.F.NcoI	ggCCATGGaaaatcttgatgagcc	This study
JTstx2.CRO.R.HindIII	ggAAGCTTttatgcagccagaaggttct	This study
JTstx2.CI.F.NcoI	ggCCATGGttcagaatgaaaaagt	This study
JTstx2.CI.R.HindIII	ggAAGCTTtcacgaacttttcagccact	This study
JTstx2.CII.F.NcoI	ggCCATGGaacaacaagttacag	This study
JTstx2.CII.R.HindIII	ggAAGCTTtcagaattgcatatcaattt	This study
JTstx2.Q.F.NcoI	ggCCATGGgtgatatccggcaggttc	This study
JTstx2.Q.R.HindIII	ggAAGCTTttacgatcgtaaactatttttcg	This study

2.3 DNA manipulation

2.3.1 DNA agarose electrophoresis

To detect and separate DNA fragments, DNA agarose electrophoresis was carried out as described below. The required concentration of agarose (Melford) was added to Tris borate EDTA (TBE), the volume was dependent on the the size of gel. 1 litre of TBE contains 0.09 M Tris base, 0.09 M boric acid and 0.002 M EDTA disodium salt dissolved in dH₂O. The agarose solution was heated in a micro-wave for 2-5 min to dissolve the

agarose. The solution was cooled down in water and added with 10,000 x Safe view (NBS biologicals). DNA samples were loaded in gel wells after mixing with 6 x DNA loading buffer (Fermentas). An appropriate DNA marker: 100 bp or 1Kb ladder (Fermentas) was also loaded into an additional well. After running at 100 volts for 40 min (depending on the size of expected DNA), the gels were analyzed and photographed with ultra violet light using the Flowgen Multi-Image cabinet and Image Capture software. Fig. 5.10 and Fig. 5.13 are shown in high contrast.

2.3.2 PCR purification

In order to purify specific PCR product, a GeneJET™ PCR Purification Kit (Fermentas), was used after the PCR process. One volume of the binding buffer was added to one volume of PCR product. The mixture was then removed to a GeneJET™ purification column in a collection tube and centrifuged at 13,000 rpm (revolutions per minute) for 30-60 s. The flow-through was discarded. Then 700 µl wash buffer was added to the column with centrifugation at 13,000 rpm for 30-60 s. Discarding the flow-through, the column was centrifuged at 13,000 rpm for 1 min again to remove any residual wash buffer. The spin column was placed in a clean 1.5 ml micro-centrifuge tube and 50 µl of elution buffer added to the centre of the column. The column was incubated at room temperature for 1 min and centrifuged at 13,000 rpm for 1 min. The elution tube contained the purified PCR product was stored at -20 °C.

2.3.3 DNA sequencing

Nucleotide sequencing was performed in The Gene Pool, School of Biological Sciences, University of Edinburgh. 1 µl primer (3.2 pmol/µl) was mixed with 5 µl DNA for sequencing. ABI Prism Big Dye terminator cycle sequencing kit version 3.1 (Applied Biosystems) was used. Reaction results were analyzed on an ABI 3730 DNA sequencer.

2.3.4 DNA sequence analysis

Sequencing data was obtained using a Chromas Lite 2.01 and copied into Vector NTI Suite 8 (Invitrogen). DNA sequence was aligned and compared with expected sequence with Vector NTI Suite 8 or blasted with NCBI Nucleotide Blast.

2.3.5 Purification of DNA from gel

The GeneJET™ Gel Extraction Kit (Fermentas) was used to purify DNA from gels following separation by agarose electrophoresis. Briefly, the labelled DNA band was cut from the agarose gel by imaging with ultra-violet light and placed in a 1.5 ml sterilized Eppendorf tube. The excised gel fragment was weighed. If the band exceeded 400 mg, it was divided into two fragments. 1:1 volume of Binding Buffer was added to the gel slice (volume:weight, i.e. 100 µl binding buffer for 100 mg of agarose gel). The gel mixture was incubated for at 50°C for 10 min or until the gel mixture is completely dissolved. When the gel was dissolved completely, the solutions were removed into a GeneJET™ purification column with a collection tube. The columns were centrifuged at 13,000 rpm for 30-60 s, during which time the DNA binds to the matrix. Discarding the flow through, 700 µl wash buffer was added to the column with centrifugation at 13,000 rpm for 30-60 s. Discarding the flow through, the column was centrifuged at 13,000 rpm for 1 min again to remove any residual wash buffer. The spin column was placed in a clean 1.5 ml micro-centrifuge tube. 50 µl elution buffer was added to the centre of the column. The column was incubated at room temperature for 1 min and centrifuged at 13,000 rpm for 1 min. The purified DNA was processed as required or stored at -20°C.

2.3.6 Plasmids DNA extraction and purification

The Fermentas GeneJET™ Plasmid Miniprep Kit was used to extract plasmid DNA. Firstly, a colony was inoculated to 5 ml LB with appropriate antibiotic. After overnight culture at 37°C with shaking at 200 rpm, the culture was centrifuged at 4,000 rpm for 5 min at room temperature. Discarding the supernatant, the pellets were resuspended in 250 µl Resuspension Solution and transferred to a 1.5 ml Eppendorf tube. A 250 µl aliquot of Lysis Solution was added and mixed thoroughly by inverting the tube 4-6 times until the

solution became viscous and begins to clear (alkaline lysis). Then 350 µl Neutralization Buffer was added and mixed immediately and thoroughly by inverting the tube 4-6 times. Centrifugation was carried out at 13,000 rpm for 5 mins at room temperature. The supernatant was removed to a GeneJET™ spin column by decanting or pipetting and centrifuged at 13,000 rpm for 1 min. Discarding the flow through, the column was washed with 500 µl Wash Solution and then centrifuged at 13,000 rpm for 1 min. The wash step was repeated and an additional centrifugation was carried out to remove the residual wash buffer. The column was then placed in a clean 1.5 ml micro-centrifuge tube with 50 µl elution buffer added to the center of GeneJET™ spin column. After 2 min incubation at room temperature, the columns were centrifuged for 2 min to collect the plasmid DNA. The columns were discarded and DNA stored at 20°C.

2.3.7 Electro-transformation

2.3.7.1 Preparation of competent cell

Bacteria were cultured in LB with appropriate antibiotic to an optical density at 600 nm of 0.4-0.6. Cultures were transferred to 50 ml tubes and cooled on ice for 30 min. Following centrifugation at 4,000g for 7 min at 4 °C in a pre-chilled centrifuge, the pellets were washed in a 0.5 volume of 10% chilled glycerol and re-centrifuged at 4,000 g for 7 min at 4°C. The pellets were again washed in a 0.25 X original volume of 10% chilled glycerol and centrifuged at 4,000 g for another 7 min at 4 °C. Finally, pellets were suspended in a 0.01 X original volume (0.5 ml for a 50 ml culture) of 10% chilled glycerol and distributed into 60 µl aliquots and stored at -70 °C.

2.3.7.2 Electro-transformation

The competent cells were kept on ice for 5-10 min after removal from -70°C storage. Plasmid DNA (1-3 µl) was added to each 60 µl competent cell aliquot. The mixed reaction was left on ice for 10-15 min. Electro-transformation was carried out at 2500 V for 0.005 s. Then 400 µl Super Optimal broth with Catabolite repression (SOC) was added to each reaction for recovery. After incubation at 37 °C 110rpm for 1 h (at least two

hours for the pIB307-based plasmids as these are cultured at 28-30 °C), 100 µl of cells were spread gently per plate containing appropriate antibiotic(s).

2.3.8 Chemical transformation

2.3.8.1 Preparation of calcium-chloride competent bacteria

A 1 ml overnight culture was added to 100 ml LB (a dilution of 1:100) broth. This 100 ml LB culture was incubated at the appropriate temperature at 200 rpm to reach 0.4-0.6 at OD₆₀₀ nm, the bacteria were chilled on ice for 30min in 50 ml tubes. The cell culture was pelleted at 4000 x rpm for 10 min at 4°C in a chilled centrifuge. For this and each subsequent step the bacteria need to be treated gently. The pellets were resuspended in 0.4 x the volume of ice-cold TFB I, i.e. 40 ml for a 100 ml culture. The bacteria were chilled on ice for 10 min and pelleted by centrifugation at 4000 x rpm for 10 min in a chilled centrifuge. The bacteria were suspended in 0.04 x volume (4 ml for a 100 ml culture) of TFB II. The suspension was kept on ice for at least 30 min before aliquoting (200 µl), then stored at -70 °C.

SOC medium

Bacto-tryptone	20 g
Bacto-yeast extract	5 g
NaCl	20 g
1M KCl	2.5ml

Dissolved in 1000 ml distilled water, adjust pH to 7.0 with 10N NaOH and autoclave to sterilize. Add 20 ml sterile 1 M glucose immediately before use.

TFB I Solution (1 litre)

30mM KoAc	2.94 g
10mM CaCl ₂ .2H ₂ O	1.47 g
100mM KCl	7.45 g
15% Glycerol	150 ml

Dissolved in 900 ml distilled water and autoclaved, 100 ml of autoclaved 500 mM MnCl₂ (50 mM final concentration) was then added.

TFB II Solution (1 liter)

75mM CaCl₂·2H₂O 11.03 g

10mM KCl 0.745 g

15% Glycerol 150 ml

Diluted in 900 ml distilled water and autoclaved, then 100 ml of autoclaved 100 mM Na-MOPs pH7.0 (2.09 g MOPs with 10 mM NaOH) was added.

2.3.8.2 Chemical transformation

Briefly, 10 µl ligation product was added to 200 µl chemical competent cells. Then it was kept on ice for 30 minutes, and heat-shocked at 42 °C for 1 minute and then put back on ice for 2 minutes. 1 ml SOC was added to each tube and incubated at 37 °C for 1 hour (80 rpm). 100 µl of cells were spread gently per plate containing appropriate antibiotic(s).

2.4 Construction of mutants

2.4.1 The construction of ZAP198 mutants in genes involved in aerobic and anaerobic respiration

λ-Red recombineering technology has been used extensively in *E. coli* for PCR product-mediated generation of deletion mutants. The λ Red recombination system uses Bet (a ssDNA annealing protein) and Exo (a 5'-3' dsDNA exonuclease) to promote gene

replacement of linear DNA substrates that are electroporated into the required *E. coli* strain (Murphy KC, Campellone KG, 2003.). Bet and Exo are introduced into the required strain background on a plasmid (pKM201, Table 2.2) by transformation. Murphy and co-workers (Murphy KC, Campellone KG, 2003) reported that EHEC deletion mutants can be easily and precisely achieved by using PCR-generated product consisting of antibiotic markers flanked by 40 bp of target DNA.

2.4.1.1 Preparation of electrocompetent hyper-rec EHEC carrying λ -Red functions on pKM201

Plasmid pKM201 was electro-transformed into the strain to be manipulated as described in Section 2.7 and cultured at 30 °C on LB-AMP plates. A single fresh colony was placed into 5ml LB with AMP and cultured overnight at 30 °C. Then the overnight culture was diluted into fresh prewarmed medium at 1:100. When the bacteria have grown to an optical density at 600 nm of 0.3, the bacteria were induced with 4mM IPTG for 60 min. The culture was then heat-shocked at 42 °C for 15 min and chilled on ice for 10 min. Bacteria were centrifuged at 4000 g at 4 °C and suspended in 5 ml cold 20% glycerol. The centrifugation step was repeated and the cells were re-suspended in 2 ml cold 20% glycerol. The cells were divided into 90 μ l aliquots. The competent cells were either used straight away or stored at -70 °C for future use.

2.4.1.2 Electro-transformation of PCR products into EHEC strains containing pKM201

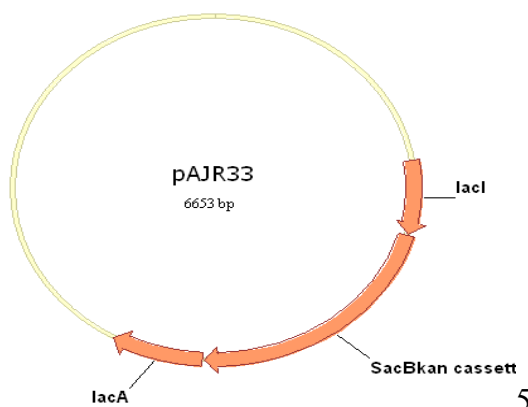
PCR-generated DNA substrates were amplified by using the relevant primer sets detailed in Table 2.3. Individually, primer pair 5-*ArcA* and 3-*ArcA* were used to amplify DNA fragments for the *arcA* deletion; primer pair 5-*Fnr* and 3- *Fnr* were used for construction of the *fnr* deletion; primer pair 5-*NarX* and 3- *NarX* were used for generation of the *narX* deletion, and primer pair 5-*NarP* and 3- *NarP* were used to construct a *narP* mutant. Prior to electroporation, cuvettes (VWR) with a 1 mm gap were cooled in an ice-water

bath for at least 10 min prior to use. DNA samples containing either 0.05–1 µg of purified DNA fragments were added to 90 µl of competent cells in an electroporation cuvette, and incubated on ice for 10 min. The cuvette was quickly dried and the cells shocked at 2200V for 0.005 sec. Following electroporation, SOC was immediately added to a total volume and 1 ml transferred to a culture tube and incubated with shaking at 30 °C for 2 hour. The bacteria were then plated onto LB plates containing 10–15 µg/ml CAM. Following subculture, PCR primers (Table 2.3) were used to screen for deletions.

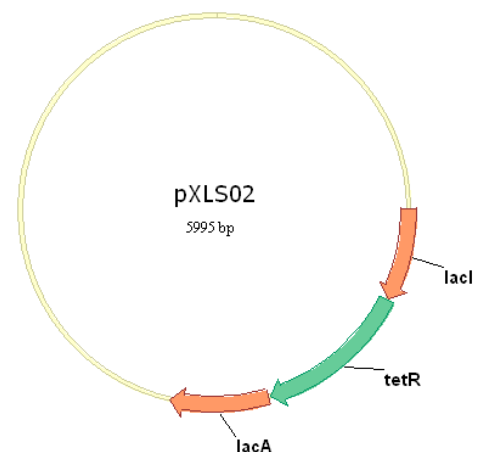
2.4.2 The creation of LEE1 promoter constructs

The aim is to construct a LEE1 promoter artificially controlled by adding aTc inducer. Briefly, the original LEE1 chromosomal promoter will be replaced by the *tet* promoter using allelic exchange. This promoter is controlled by *tetR* and the *tetR* will be placed in *lacZY* location by the same method. Therefore, LEE1 expression would be quantitatively expressed by using aTc and then LEE2-LEE5 expression and other effector expression could be investigated with a constant LEE1 expression system. The experimental process is demonstrated below.

A.



B.



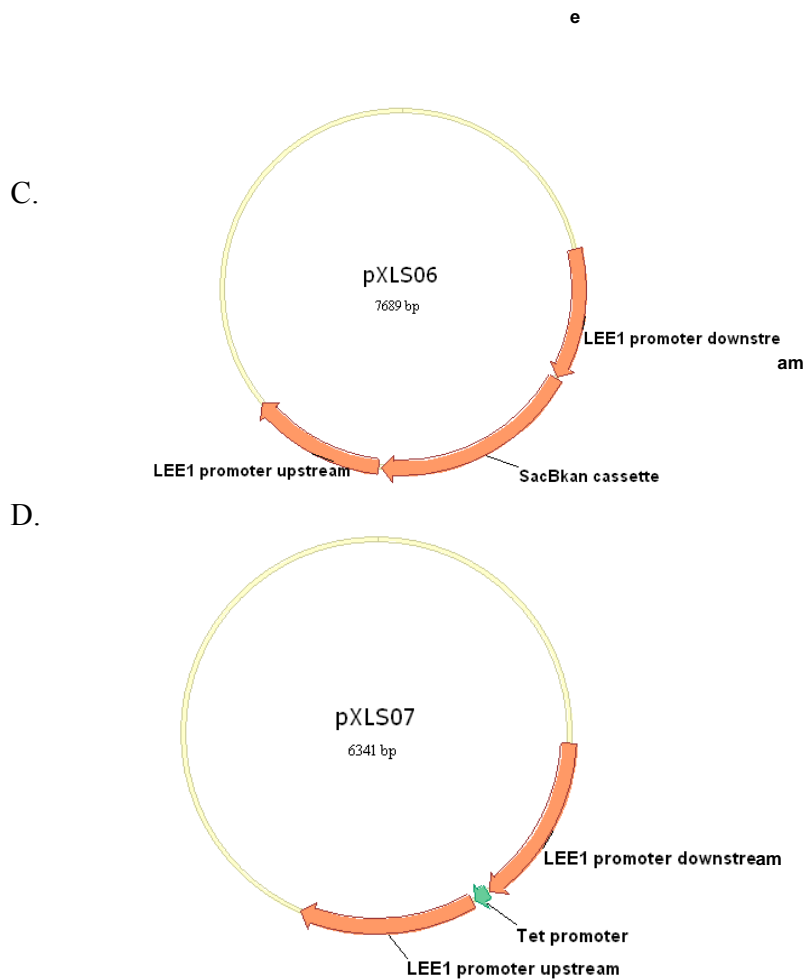


Fig. 2.1 Summary diagram of constructs for LEE1 constructions (A-D)
 pAJR33 is used to produce ZAP1212 with *lacYZ* replaced by *sacBkan* cassette. pXLS02 is designed to construct ZAP1213. pXLS06 is used to produce ZAP1213 with LEE1 promoter replaced by *sacBkan* cassette in first construction. pXLS07 is constructed for ZAP1213 with LEE1 promoter replaced by tet promoter in first construction.

2.4.2.1 Constructs for allelic exchange

pAJR 33 was used to replace *lacYZ* genes with *sacBkan* cassette. To construct a strain with *sacBkan* cassette in *lacYZ* loci replaced by *TetR* gene, a plasmid containing *tetR* gene in pAJR27 was made. PZS4Int-*laci/tetR* plasmids contain the *tetR* gene controlled by a constitutive promoter (PN25). PN25&*tetR* was PCR amplified from PZS4Int-*laci/tetR* plasmid by using primer pairs 5-PN25-BamHI and 3-PN25-BamHI (Table 2.3), then cloned into pAJR27 in the *BamH* I site creating pXLS02 to allow the exchange for *sacBkan* cassette.

In order to construct plasmids facilitating exchange of LEE1 promoter with *tet* promoter, plasmid with LEE1 promoter flanking regions was obtained. According to LEE1 promoter and *tet* promoter structure, two constructs will be made. The first construction will keep the original transcriptional start site and -10 region of LEE1 operon promoter, while the -35 regions will be replaced by AT rich DNA sequence synthesized artificially. For the second construct, only the original transcriptional start site will be kept with -35 and -10 regions replaced. Briefly, PCR fragments were amplified from TUV93-0 using the primer pairs shown in Table 2.3: 5-*LEE1* UP FR XmaI and 3-*LEE1* UP FR BamHI for upstream flanking region, 5-*LEE1* down FR 1st and 3-*LEE1* down FR for downstream flanking region for the first construction and 5-*LEE1* down FR 2nd and 3-*LEE1* down FR for downstream flanking region for the second construction. These PCR fragments were digested with proper enzymes and cloned into PIB307. The resultant plasmids containing both flanking regions for the first and the second construction were termed as pXLS04 and pXLS05 respectively. Then a *sacBkan* cassette cut from pAJR32 was cloned into pXLS04 at *BamH* I site. This plasmid was termed as pXLS06. In addition, *tet* promoter which was PCR synthesized by using primer pairs 5-Tet promoter BamHI 1st 3-Tet promoter BamHI 1st (Table 2.3) was inserted into pXLS04 at *BamH* I site producing pXLS07.

2.4.2.2 The construction of mutants for LEE1 constructions

- (1) The exchange of *lacYZ* genes with *sacBkan* cassette. To replace *lacZY*, the plasmid pAJR33 was used that contains *lacIA* flanking regions cloned into pIB307 with a *sacBkan* cassette. The method of Hamilton *et al* (Hamilton *et al.*, 1989) was applied for the allelic exchange in this study. Briefly, the plasmid containing the appropriate flanking regions was electroporated into the strain to be manipulated and cultured at 30 °C on LB-CAM plates. Ten transformants were then inoculated into pre-warmed LB-KAN at 42 °C and passaged repeatedly in LB-KAN broth at 42 °C to obtain cointegrates. The culture was further passaged at 30 °C in LB-KAN broth in which a secondary recombination event resulted in the *lacYZ* being replaced by the *sacBkan* cassette. The correct replacement strain (ZAP1212) was determined by KAN resistance and CAM sensitivity further confirmed by PCR with primer pairs in Table 2.3: 5-*lacI* and 3-*lacA* for outside *lacYZ*, 5-*lacY* and 3-*lacZ* for inside *lacYZ*.

- (2) The exchange of *sacBkan* cassette with *PN25&tetR* in *lacYZ* location. To generate the exchange of the *sacBkan* cassette with *PN25&tetR*, plasmid pXLS02 was electroporated into ZAP1212 and the above process repeated with the following differences: the second of cultures at 30 °C was performed without antibiotic selection, and the correct clones were identified by sensitivity to both KAN and CAM on replica plates, and confirmed by PCR using primer pair 5-*PN25*-BamHI and 3-*PN25*-BamHI (Table 2.3) for *PN25&tetR*, primer pair 5-*lacI* and 3-*lacA* (Table 2.3) for flanking the region. The strain obtained from this exchange is named as ZAP1213.

- (3) The exchange of LEE1 promoter with *sacBkan* cassette. The exchange method was used as described in Materials and Methods. Specifically, pXLS06 was electro-transformed into ZAP1213 and cultured at 30 °C on LB-CAM plates separately. Ten transformants were then inoculated into pre-warmed LB-CAM at 42 °C and

passed repeatedly in LB-CAM broth at 42 °C to obtain cointegrates. The culture was further passed at 30 °C in LB-KAN broth in which a selection of LEE1 promoter replaced by the *sacBkan* cassette was carried out. The correct replacement strain was determined by KAN resistance and CAM sensitivity. Further confirmation were carried out by PCR with primer pairs in Table 2.3: 5-*LEE1* test and 3-*LEE1* test for inside of LEE1 promoter, 5-SacB and 3-SacB for inside of *sacBkan* cassette and 5-*LEE1* UP FR XmaI and 3-SacB for cross junction of *sacBkan* cassette and chromosome.

- (4) The exchange of *sacBkan* cassette with *tet* promoter in LEE1 promoter location. Once the *sacBkan* cassette is placed on LEE1 promoter region, plasmids pXLS07 was transformed into the strain to be manipulated. The same procedure will be performed as mentioned in “The exchange of *sacBkan* cassette with PN25&*TetR* in *lacYZ* location”. The resultant colonies were screened by PCR with primer pair 5-SacB and 3-SacB (Table 2.3) for inside of *sacBkan* cassette, primer pair 5-PN25-BamHI and 3-PN25-BamHI (Table 2.3) for PN25&*tetR* (Table 2.3), primer pair 5-Tet promoter BamHI 1st and 3-*LEE1* down FR XbaI cross junction of *tet* promoter and chromosome.

2.4.2.3 Testing aTc induction efficiency by TetR using GFP measurement

In order to test the aTc induction efficiency and allelic exchange for replacing *lacYZ* with *TetR*, the *tet* promoter was PCR amplified by using primer pair 5-Tet promoter-XbaI and 3-Tet promoter-XbaI (Table 2.3), then cloned into pKC26 plasmid in XbaI site creating plasmid pXLS03. This plasmid places GFP under control of the *tet* promoter. pXLS03 was transformed into ZAP1213 by standard electro-transformation as mentioned above. The resultant transformants were grown overnight in LB containing appropriate antibiotics. For the total GFP measurement, the overnight was diluted into fresh LB with appropriate antibiotics to reach an OD₆₀₀ value of 0.05. According to the preliminary experiment, a concentration of 200ngml⁻¹ was used to induce the maximum induction. Normally, 25 ml media with bacteria was cultured in Erlenmeyer flasks with shaking at 200 rpm at 37°C in dark to protect aTc activity. The optical density of the cultures was

measured at OD₆₀₀ every one hour and analyzed by testing 100 µl aliquots of culture with a fluorescent plate reader (Fluorostar Optima; BMG). ZAP198, ZAP1213 and promoterless plasmids pKC26 in ZAP1213 were used as a negative control for background fluorescence.

2.4.3 The construction of EDL933 mutants in Stx1&2 phage and *cII* genes

2.4.3.1 Constructs for allelic exchange.

In order to construct plasmids that would facilitate chromosomal exchange, flanking regions of the *z1449* (*cII_{stx2}*) genes and Stx1 and Stx2 phages were PCR amplified and cloned into the temperature-sensitive plasmid pIB307 (Table 2.2). Primer pairs as described in Table 2.3 *z3357* up 5', *z3357* up3' and *z3357* down 5', *z3357* down 3' ; *z1449* up 5', *z1449* up3' and *z1449* down 5', *z1449* down 3'; *stx1* up 5', *stx1* up3' and *stx1* down 5', *stx1* down 3'; *stx2* up 5', *stx2* up3' and *stx2* down 5', *stx2* down 3 were used to amplify *z3357*, *z1449* Stx1 phage and Stx2 phage flanking regions sequences from *E. coli* O157:H7 EDL933. These products were cleaned with a Invitrogen PCR purification kit, digested with *Bam*H I and *Hind* III or *Sac* I, or *Sal* I , re-cleaned, and then ligated with digested PIB307(Table 2.2) to obtain pXLS10, pXLS11, pXLS12 and pXLS15 containing flanking regions of *z3357*, *z1449*, *stx1* phage, and *stx2* genes respectively. To produce plasmids for exchange, a *sacBkan* cassette was cloned into the *Bam*H I sites of pXLS11, pXLS10 and pXLS12 creating pXLS13, pXLS14 and pXLS16 that would allow the chromosomal replacement of *z1449*, *z3357* and *stx1* genes respectively with a selectable marker and a counterselection gene.

2.4.3.2 Mutant construction

The method of Emmerson *et al.* was used for allelic exchange (Emmerson *et al.*, 2006). Plasmids pXLS13 was transformed into EDL933 to obtain the intermediate strain with *z1449* (*cII_{stx2}*) replaced by *sacBkan* cassette. Briefly, pXLS13 was electroporated into EDL933 (Table 2.1) and cultured at 30°C on LB-C plates. Ten transformants were then inoculated into pre-warmed LB-C at 42°C and passaged repeatedly in LB-C broth at 42°C to obtain co-integrates. The culture was further passaged at 3°C in LB-K broth to select for the complete exchange. The kanamycin resistant and chloramphenicol sensitive

strain was confirmed by PCR with primer pairs z1449 5' and z1449 3' for inside of *z1449*, z1449 external 5' and z1449 external 3' for outside of *z1449*, sacB 5' and sacB 3' for *sacBkan* cassette (Primer Table 2.3). The resultant strain was termed as ZAP1321. ZAP1321 was then transformed with plasmids pXLS15 and pXLS11 and allelic exchange carried out to generate strains with Stx2 phage and *z1449* (*cII_{stx2}*) clean deletions. These allelic exchanges were as above except that the cultures at 30 °C did not contain any antibiotic selection. The required clones were identified by sensitivity to both KAN and CAM and confirmed by PCR using primer pairs: wrbA and intW plus z1503 and z1504 for the junction sites of Stx2; wrbA and Z1504 for a region inside the Stx2 phage; z1449 5' and z1449 3' for inside of *z1449* (*cII_{stx2}*), z1449 external 5' and z1449 external 3' for outside of *z1449*, sacB 5' and sacB 3' for *sacBkan* cassette. The clean *stx2* and *z1449* deletion strain were termed ZAP1322 and ZAP1323 respectively (Table 2.1). In order to construct a strain deleted for both Stx1 and Stx2 phages, ZAP1322 was used to create strain with *stx1* replaced with *sacBkan* cassette using pXLS16. The required strain by exchanger was determined by KAN resistance and CAM sensitivity; further confirmed by PCR with primer pairs yehU and z3305 for left end of Stx1 phage, intV and yehV for right end of Stx1 phage, SLT-I-1 and SL-1 for inside of Stx1 phage, sacB 5' and sacB 3' for *sacBkan* cassette (Primer Table 2.3). The resultant strain was termed ZAP1326 (EDLStx1&2⁻). To construct a strain with both *z1449* (*cII_{stx2}*) and *z3357* (*cII_{stx1}*) deleted, ZAP1323 was used for allelic exchange. pXLS14 was transformed into ZAP 1323 and exchange was done as described above to produce strain with *z3357* replaced by *sacBkan* cassette using. The strain obtained by exchanger was determined by KAN resistance and CAM sensitivity; further confirmed by PCR with primer pairs z3357 5' and z3357 3' for inside of *z3357*, sacB 5' and sacB 3' for *sacBkan* cassette (Primer Table 2.3). This resultant strain was termed as ZAP1324.

2.5 Quantification of population fluorescence levels

Strains were electro-transformed with pAJR70–71 (Table 2.2) under standard conditions. The resultant transformants were cultured overnight in LB broth and then diluted 1:100 into fresh, MEM-HEPES with appropriate antibiotics. Typically, 30 ml was cultured in Erlenmeyer flasks shaken at 200 rpm, 37°C. The optical density of the cultures was monitored by determination of the OD₆₀₀. Cultures were sampled every hour for optical density and GFP measurement. The total fluorescence produced by the population was determined by analyzing 100 ul aliquots of culture with a fluorescent plate reader (Fluorostar Optima; BMG). Promoterless plasmid pAJR70 acted as a control for background fluorescence.

2.6 Preparation of bacterial and epithelial cell cultures for infection assays

For routine cultures, EHEC strains were grown in LB medium at 37°C. Prior to cell challenge, the required strains were cultured to saturation in LB overnight, then diluted and cultured in MEM-Hepes starting at an optical density at 600 nm of 0.05. Embryonic bovine lung (EBL) cells were cultured in Minimum Essential Medium Eagle (Sigma) supplemented with 10% heat inactivated foetal bovine serum (FBS) (Sigma), 100U/ml penicillin, 100 µg/ml streptomycin (Gibco) and 2 mM L-glutamine (Gibco). Cells were maintained at 37°C in 5% CO₂.

2.7 Bacterial infection assays and immunofluorescence microscopy

To assess cell binding and actin pedestal formation by *E. coli* O157 strains, EBL cells were used that had been seeded (5×10^4 cells/well) into 8-well chamber slides (BD) the day prior to carrying out the assay. One hour before addition of the bacteria, the EBL cells were washed and cultured with pre-warmed bacterial culture medium MEM-Hepes to remove the antibiotics. Then EBL cells were infected with a 2×10^6 bacteria in MEM-Hepes for 3 hrs. Monolayers were washed two times with PBS, fixed for 20 min with PBS + 2.5% paraformaldehyde (PFA), permeabilized for 5 min with PBS + 0.1% Triton X-100, washed three times with PBS and treated with anti *E. coli* O157:H7 rabbit antibody (MAST ASSURE) diluted in PBS 1:50 for 35 min. Monolayers were then washed three times, incubated with Alexa 568-conjugated anti-mouse IgG (Molecular Probes) at a dilution of 1:1000 for 30 min. The chamber slides were then washed three times and stained with $1 \mu\text{g ml}^{-1}$ TRITC-Phalloidin (Sigma) for 30 min, washed two times with PBS and mounted with mounting medium (Invitrogen). These are left to set for at least one night and then examined by fluorescence and light microscopy. The cell-binding frequencies of EHEC strains were quantified by counting the number of bacteria (identified by anti-O157-staining) associated with randomly chosen fields of view. Twenty fields of view were examined per strain for cell binding and actin pedestal formation assays. Pedestal formation frequencies were quantified by counting the number of localized F-actin pedestals (identified by intense phalloidin staining) on randomly chosen EBL cells.

2.8 Comparative genomic hybridization (CGH)

A total of 12 IPRAVE strains (6 for PT21/28 and PT 32) were selected for CGH based on T3 profile. Genomic DNA was extracted with Invitrogen ChargeSwitch gDNA Mini Bacteria Kit (Invitrogen). Labeling was carried out with Bioprime Plus Array CGH

Genomic Labelling System (Invitrogen). Protocol for pre-hybridization, hybridization and washing for ultragaps slides was from UBEC project (School of Biosciences, University of Birmingham). Briefly, array slides were washed twice in Wash Buffer II (0.1% SDS, 0.1x saline-sodium citrate (SSC), each time for 30S. Then slides were transferred in pre-hybridization buffer (0.1% BSA, 0.1% SDS, 5x SSC) for 120 min. After washing in Wash Buffer II and III (0.1 unit SSC), the denatured hybridization probe mixture (30% formamide, 5x SSC, 0.1% SDS, 0.1mg/ml Salmon sperm DNA, 1x Denhardt's Solution (Sigma) and 80 pmoles Cy3 and Cy5 dye (Invitrogen) probe) was added to slides and incubated for overnight. Next day, the array slides were washed in Wash Buffer I (0.1% SDS, 2x SSC), II and III and scanned in Axon scanner. With the help of Jai Tree in the ZAP laboratory, CGH was carried out and data was analyzed.

2.9 PCR to identify Stx2 and Stx2c phage

Genomic DNA for 62 tested strains was extracted with the Invitrogen Charge Switch gDNA Mini Bacteria Kit. The concentration of the genomic DNA was measured by a nanodrop. The method of Wang *et al.* (Wang *et al.*, 2002) was used for PCR to determine Stx2 and Stx2c phage. A mount of 100 ng genomic DNA was used for each PCR reaction. A size of 115 bp specific DNA fragment was amplified from Stx2 phage, while a 124 bp DNA fragment was designed for Stx2c phage according to the specific gene sequence for each phage.

2.10 Preparation of secreted proteins and bacterial fractions for protein analyses

Bacteria were cultured in 30 ml of MEM-HEPES at 37°C (200 rpm) to an OD₆₀₀ of 0.8 unless specifically stated. The bacterial cells were pelleted by centrifugation at 4000 x g for 15 min, and supernatants were passed through filters (0.45 µm). Supernatant proteins were precipitated overnight with 10% TCA, and separated by centrifugation at 4000 x g for 30 min (4°C); the proteins were suspended in 100 µl of 1.5 M Tris (pH 8.8). The bacterial pellet was initially suspended in 50 µl laemmli sample buffer (Sigma) and 50 µl molecular water. Proteins were separated by SDS-PAGE using standard methods and

Western blotting performed as described previously (Naylor *et al.*, 2005; Roe *et al.*, 2003b). Antibodies used specifically recognized EspD (Gift from Prof. T. Chakraborty, University of Giessen), EscJ (Gift from Dr Ando and Prof. Abe), RecA (Stressgen/Enzo Life Sciences).

2.11 Sodium dodecyl sulphate-polyacrylamide gel electrophoresis (SDS-PAGE)

Secreted proteins and bacterial fractions were separated on SDS-PAGE gel using Bio-Rad Mini Protein II gen apparatus (Bio-Rad). Protein Samples were diluted into 2 X loading buffer (Sigma) and boiled for 5 mins in water bath. Prepared samples were loaded in a 5% stacking gel (5% acrylamide-bisacrylamide, 0.125 Tris-HCL (pH 6.8), 0.1% SDS, 0.1% ammonium persulfate (APS), 0.001% N, N, N', N'-tetramethylethylenediamine (TEMED)) and resolved in a 12% resolving gel (12% acrylamide-bisacrylamide, 0.375 Tris-HCl (pH 8.8), 0.1% SDS, 0.1% ammonium APS, 0.001% TEMED) by electrophoresis. Electrophoresis was performed in Tris-glycine running buffer (25 mM Tris-HCl (pH 8.3, 192 mM glycine, 0.1% SDS) at 150 B for 1 hour.

2.12 Colloidal coomassie blue staining of SDS-PAGE gels

Gels were stained by colloidal coomassie blue stain (Severn Biotech) for overnight. De-staining was carried out in distilled water. Gels were viewed and imaged by a Flowgen Multi Image light cabinet and Chemi Image 4000i v.4.04 software.

2.13 Western blotting

Firstly, SDS PAGE was carried out as described above. The stacking gel was removed. If required for orientation, one corner was removed from the resolving gel. Four sheets of gel-sized filter paper and one gel-sized piece of nitrocellulose (Amersham Hybond ECL) and two pieces of gel-sized sponge were soaked in transfer buffer. The blot was assembled in the order: Black Plate – sponge – 2x filter paper - gel – nitrocellulose – 2x filter paper – sponge – Clear Plate. The tank was filled with transfer buffer and blotting was carried out at 60 V for 1.5 hours or 10 V for overnight. If running at 60 V a frozen water block (stored at -20°C) was included in the running tank to prevent overheating. The nitrocellulose was incubated with blocking buffer (8 % (w/w) milk in PBS) for at least 1 hour at room temperature or overnight at 4 °C. The blot was washed 3 times with washing buffer (0.05 % (v/v) Tween-20 in PBS) on a “gyro rocker” at room temperature for 15 mins. Primary EspD antibody was added (1: 5000 dilution) in testing buffer (0.05 % (v/v) Tween-20 in PBS), with incubation for at least 2 hours on a “gyro rocker” at room temperature. The wash steps were then repeated. Secondary antibody (horseradish peroxidase labeled, 1: 4000) in testing buffer was added with incubation of 1 hour on a “gyro rocker” at room temperature. Wash as before. Equal volumes of ECL Solutions 1&2 were mixed and added to the blot and left for 5 mins at room temperature. The ECL signal is short-lived (<1 h.) The blot was sealed in clingfilm and taped inside a film exposure cassette, exposed to Amersham Hybond ECL film for the required time (usually <1 min) and developed in the film processor.

2.14 Statistical analysis

2.14.1 Statistical analysis in Chapter 3

The cell binding data and A/E lesions data was analyzed by F-test and t-test. F-test (two sample variance) was performed for each pair of data with tested sample and wild type. $P < 0.05$ from F-test indicated an unequal variance and in turn two sample assuming unequal variances was applied for t-test. In contrast, if $P > 0.05$ from F-test, two sample assuming equal variances was carried out for t-test. $P < 0.05$ (two tail) from t-test was considered to indicate statistical significance.

2.14.2 Statistical analysis in Chapter 7

This work was carried out by Dr. Darren J. Shaw. Differences in the level of fluorescence from the PT32 strains compared to PT21/28 strains and strains containing both Stx2 or Stx2c prophages compared to strains only containing one were compared by standard two-sample t-tests on \log_{10} transformed values. Standard two-sample t-tests were also performed to compare relative fluorescence in specific TUV, EDL and K-12 strains. All analyses were carried out in R (© R Development Core Team (2009). R version 2.10.1 (© Foundation for Statistical Computing, Vienna, Austria. ISBN 3-900051-07-0, URL <http://www.R-project.org>). $P < 0.05$ was taken to indicate statistical significance.

3 Chapter 3 The T3SS & respiration regulation

3.1 Introduction

Cattle are known as a main source of human infection with *E. coli* O157:H7 (Hancock *et al.*, 1994; Orskov *et al.*, 1987). *E. coli* O157:H7 mainly colonizes at the terminal rectum in which a T3SS is essential (Naylor *et al.*, 2003). Ando and coworkers reported (Ando *et al.*, 2007) that the activation of anaerobic respiratory system accelerates the maturation of the functional T3S apparatus under anaerobic growth conditions. The hypothesis to be tested is that the tropism is driven by when the secretion system is expressed in the animal under changes in anaerobic/aerobic conditions in the gastrointestinal tract. To investigate the effect of the respiration regulatory system on T3SS expression, *arcA*, *fnr*, *narX* and *narP* deletion mutants were constructed by λ Red recombination in the background of the *E. coli* O157:H7 ZAP198 strain. λ Red recombination has been used extensively in *E. coli* for PCR-mediated generation of deletion mutants. Murphy and co-workers reported that EHEC deletion mutants can be easily and precisely achieved by using PCR-generated products containing drug markers flanked by 40 bp of target homologous (Murphy & Campellone, 2003). Once the mutants were obtained, the T3S profiles and T3S levels of these mutants were examined as well as the capacity of the strains to form A/E lesions on embryonic bovine lung (EBL) cells by phalloidin staining of actin.

3.2 Results

3.2.1 The deletion of *E. coli* O157 respiration regulators

Four mutants were obtained by λ Red recombination including ZAP198 $\Delta arcA$, ZAP198 Δfnr , ZAP198 $\Delta narX$ and ZAP198 $\Delta narP$. These mutants were confirmed by PCR. Each deletion construction and confirmation is now described.

3.2.1.1 The construction of an *arcA* deletion

By using PCR primer pair 5-ArcA and 3-ArcA (Table 2.3), a DNA fragment containing the CAM cassette flanked with 40bp of *arcA* upstream and downstream was amplified (Fig. 3.2A). This PCR product was electroporated into ZAP198 carrying pKM201 that encodes the λ Red recombinase. The *arcA* gene locus and correct recombinants with designed primers were shown in Fig. 3.1. The resultant strain was verified by PCR with primer pair 5-KO-ArcA and 3-KO-ArcA (Table 2.3) for the CAM cassette (Fig. 3.2B), 5-ArcA and 3-ArcA (Table 2.3) for detecting *arcA* (Fig. 3.2C), 5-up-ArcA and 3-down-ArcA (Table 2.3) for outside of the *arcA* (Fig. 3.2D). 4 colonies contained the CAM cassette, but only one of them had lost the *arcA* gene (Fig. 3.2B-C). That colony was confirmed by PCR using primers outside of *arcA* indicating the recombinant is approximately 200 bp larger than the wild type sequence (Fig. 3.2D). This is the expected size difference between the CAM cassette (900 bp) and the *arcA* gene (717bp). Colony 2 was taken forward for analysis.

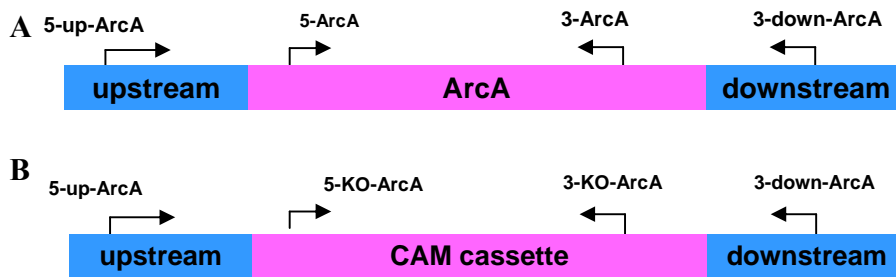


Fig. 3.1 A: Structure diagram of *arcA* locus and primers in ZAP198

B: Structure diagram of CAM cassette and primers in *arcA* mutant

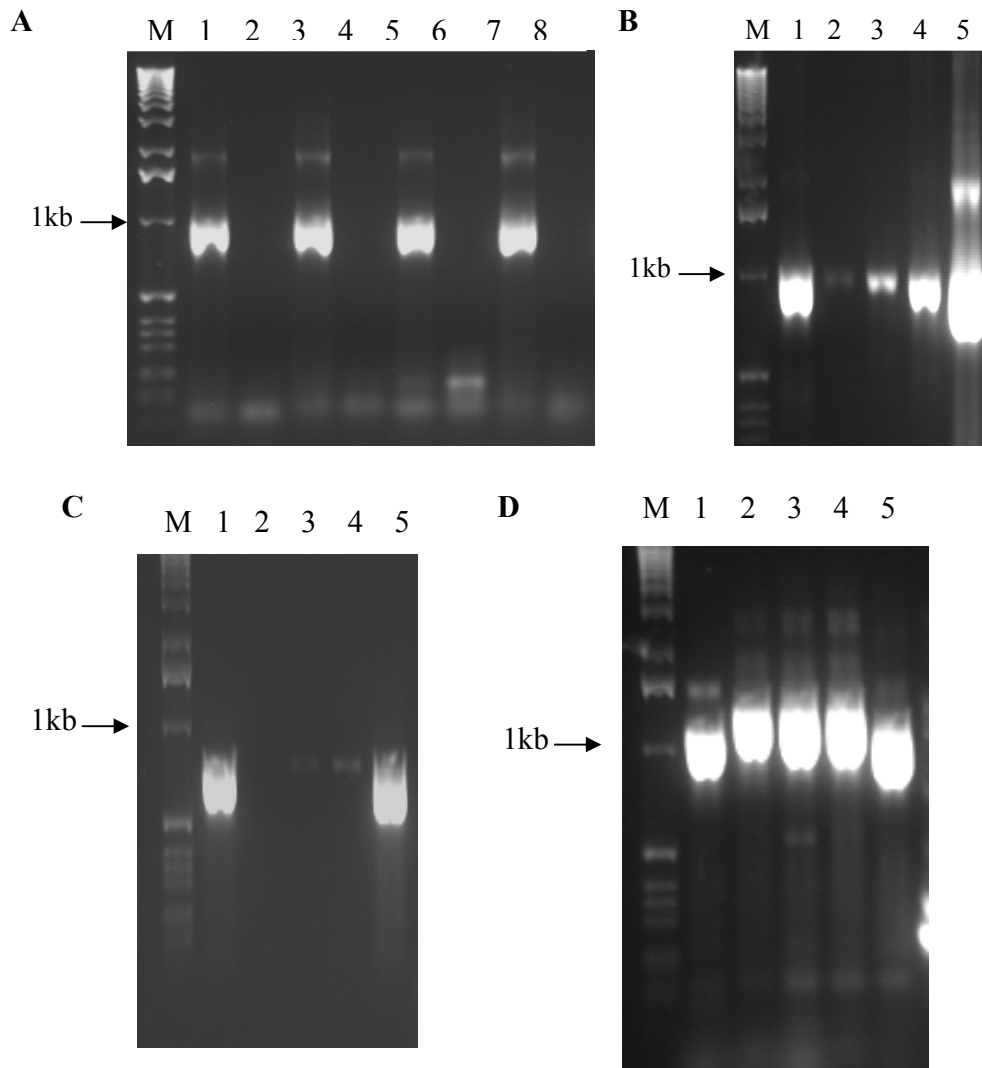


Fig. 3.2 PCR for generation of the deletion cassette with *arcA*, *fnr*, *narX*, *narP* flanking regions and for screening of *arcA* recombination

(A) PCR fragments for construction of deletion mutants: Lane M: 1kb ladder, Lane1: *arcA*, Lane 3: *fnr* Lane 5: *narX* Lane 7: *narP*, Lane 2,4,6,8: negative control

(B-D) Screening of recombinant colonies for deletion of *arcA* Lane M: 1kb ladder

Lanes 1-4 contain amplified products from tested colonies 1-4 respectively; Lane 5 contains products amplified from *E. coli* O157:H7 ZAP 198 as a control unless otherwise stated. .

(B) PCR screening of recombination of CAM cassette to replace *arcA*; the 4 colonies all contain the CAM cassette with pTP883 (CAM⁺) as a positive control. (C) Screening of

recombinant colonies for deletion of *arcA*. Colony 2 has no detectable *arcA* with ZAP198 used as a positive control. (D) PCR screening of recombinant colonies across the *arcA*

region. Colony 2-4 show the size difference between CAM cassette (900bp) and the *arcA* (717bp). ZAP198 was used as a control.

3.2.1.2 *fnr* deletion

The same method was used to generate an *fnr* deletion. The CAM cassette with flanking regions for *fnr* was amplified by primer pair 5-KO-Fnr and 3-KO-Fnr (Table 2.3) (Fig. 3.2A). The *fnr* gene locus and correct recombinants with designed primers were shown in Fig. 3.3. To determine the right replacement, primer pair 5-KO-Fnr and 3-KO-Fnr (Table 2.3) were used to detect the CAM cassette (Fig. 3.4A), primer pair 5-Fnr and 3-Fnr (Table 2.3) were used to identify the presence of the *fnr* gene (Fig. 4B), and primer pair 5-up-Fnr and 3-down-Fnr (Table 2.3) for amplifying across the *fnr* region (Fig. 3.4C). As shown in Fig. 3.2A, colony 1 contained a CAM cassette with *fnr* removed. The correct recombinant, colony 1 was further confirmed by PCR across the *fnr* gene region (Fig. 3.4C) with a 150bp distinction which is consistent with the difference between wild type and *fnr* mutant replaced by CAM cassette.

A.



B.

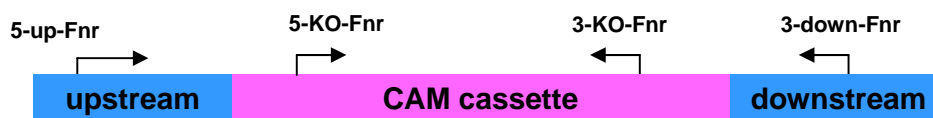


Fig. 3.3 A: Structure diagram of *fnr* locus and primers in ZAP198

B: Structure diagram of CAM cassette and primers in *fnr* mutant

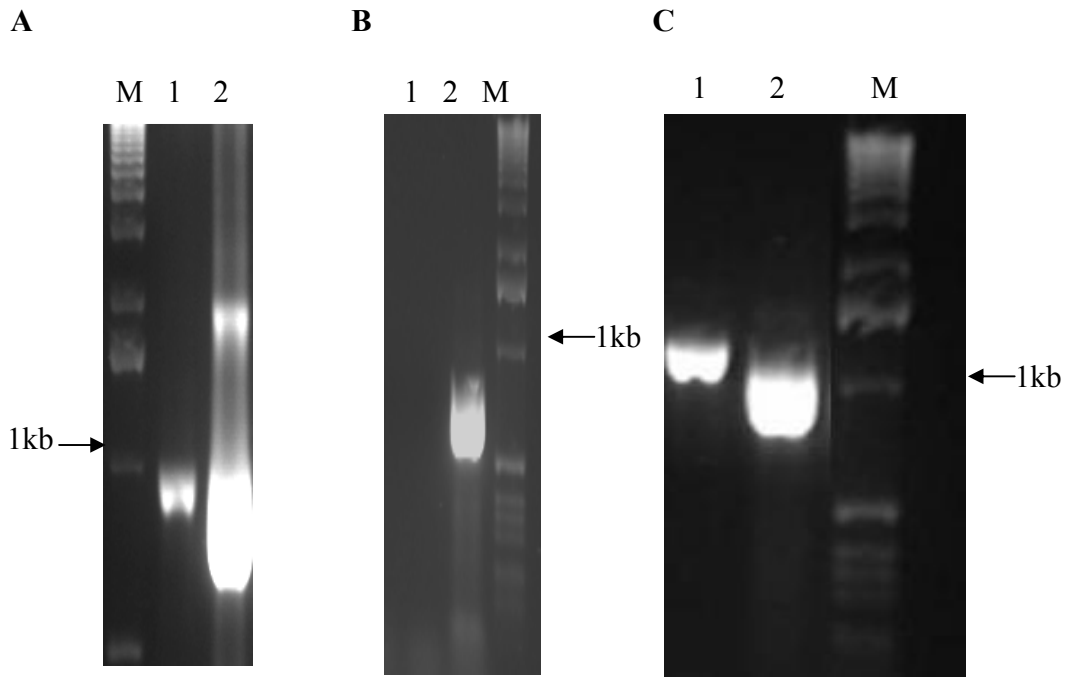


Fig. 3.4 PCR screening of recombinant colony 1
Lane M: 1kb ladder; Lane 1: colony 1; Lane 2: control as stated:
(A) PCR screening for CAM cassette with pTP883 (CAM⁺) as a positive control, colony 1 contains the CAM cassette.
(B) PCR screening for the *fnr* gene, expected size is 753bp, colony 1 contains no amplified product for *fnr*. The control is *E. coli* O157 ZAP198.
(C) PCR screening across *fnr*; the PCR product from colony 1 is larger than for the wild type control (ZAP 198) as expected for the difference between amplifying across the CAM cassette (900bp) vs. *fnr* (753bp).

3.2.1.3 *narX* deletion

As showed in Fig. 3.1A, the PCR generated DNA substrate was amplified by using 5-KO-NarX and 3-KO-NarX (Table 2.3). The *narX* gene locus and correct recombinants with designed primers were shown in Fig. 3.5. To identify a gene replacement, primer pair 5-KO-NarX and 3-KO-NarX (Table 2.3) was used to test the presence of the CAM cassette (Fig. 3.6A), primer pair 5-NarX and 3-NarX (Table 2.3) were used to identify the presence of *narX* (Fig. 3.6B), and primer pair 5-up-NarX and 5-down-NarX (Table 2.3) were used to amplify across the *narX* gene (Fig. 3.6C). Fig. 3.3.A indicates that both colonies 1 and 2 contained the CAM cassette (900bp). From further tests, it was demonstrated that colony 1 has lost the *narX* gene (1797bp) (Fig. 3.6B) and colony 1 amplified a product across the regions that was approximately 900bp smaller than expected for the wild type region from *E. coli* O157 ZAP198, indicating *narX* has been replaced by the CAM cassette in this strain (Fig. 3.6C).

A.



B.

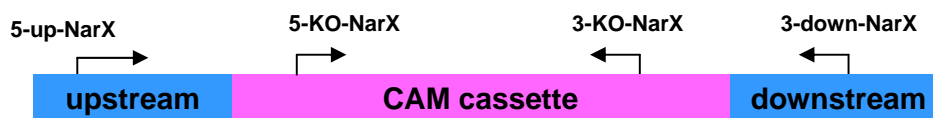


Fig. 3.5 A: Structure diagram of *narX* locus and primers in ZAP198

B: Structure diagram of CAM cassette and primers in *narX* mutant

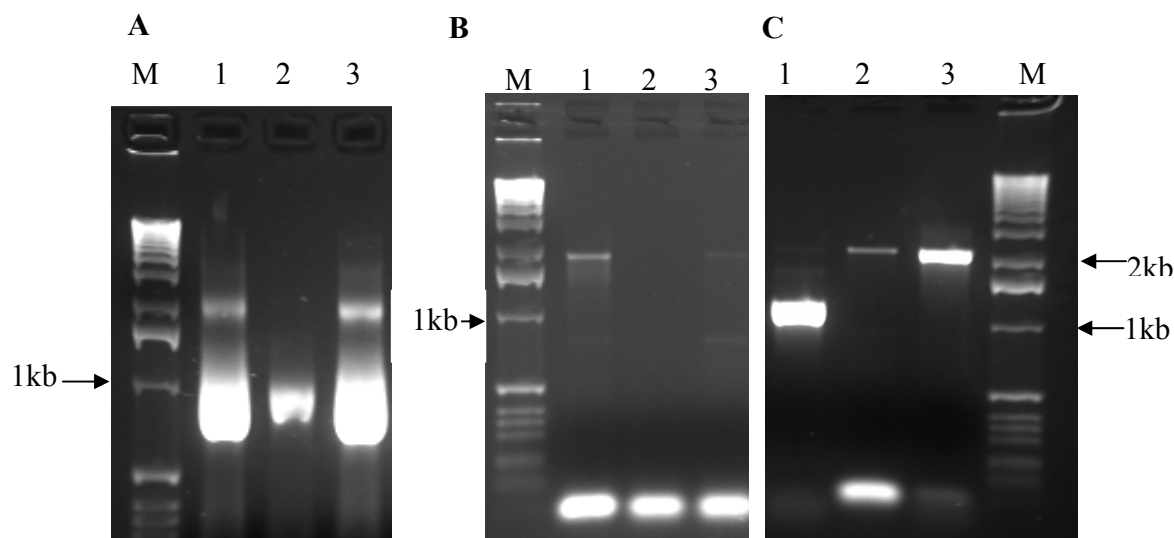


Fig. 3.6 PCR screening of colonies for replacement of *narX* with a CAM cassette (A-B): Lane M: 1kb ladder; Lane 1: colony 2; Lane 2: colony 1; Lane 3: positive control. (A): Screening for the CAM cassette, two colonies were isolated that contained the CAM cassette, the expected size is 900bp. (B): Screening for *narX* deletion, only colony 1(Lane 2) has no amplified product indicating loss of *narX* (1797bp). (C): Screening across the *narX* region: Lane M: 1kb ladder. Lane 1 contains colony 1; Lane 2 contains colony 2; Lane 3 uses ZAP198 as a template. The PCR product from colony 1 (lane 1) is smaller than from the WT ZAP198 and these sizes are consistent with the expected difference between insertion of the CAM cassette (900bp) and the wild type *narX* (1797bp).

3.2.1.4 *narP* deletion

The same procedure was used to delete *narP* using 5-KO-NarP and 3-KO-NarP (Table 2.3). The *narP* gene locus and correct recombinants with designed primers were shown in Fig. 3.7. CAM resistant colonies were analysed by PCR tests with primer pair 5-KO-NarP and 3-KO-NarP (Table 2.3) for the CAM cassette, 5-NarP and 3-NarP (Table 2.3) for *narP*, and 5-up-NarP and 5-down-NarP (Table 2.3) for a region across *narP*. The PCR results showed that colonies 1-6 all possess the CAM cassette (Fig. 3.8A), but only colony 3 does not amplify a *narP* product (Fig. 3.8B). The insertion of the CAM genes was verified by PCR across the region indicating a 250bp difference between the isolate with the replacement CAM cassette (900bp) and across wild type *narP* (648bp) (Fig. 3.8C).

A.



B.

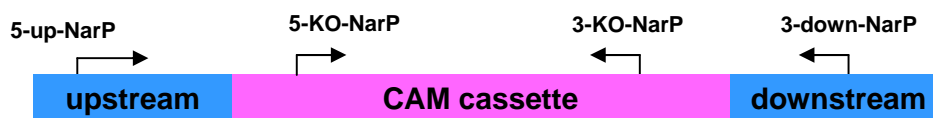


Fig. 3.7 A: Structure diagram of *narP* locus and primers in ZAP198

B: Structure diagram of CAM cassette and primers in *narP* mutant

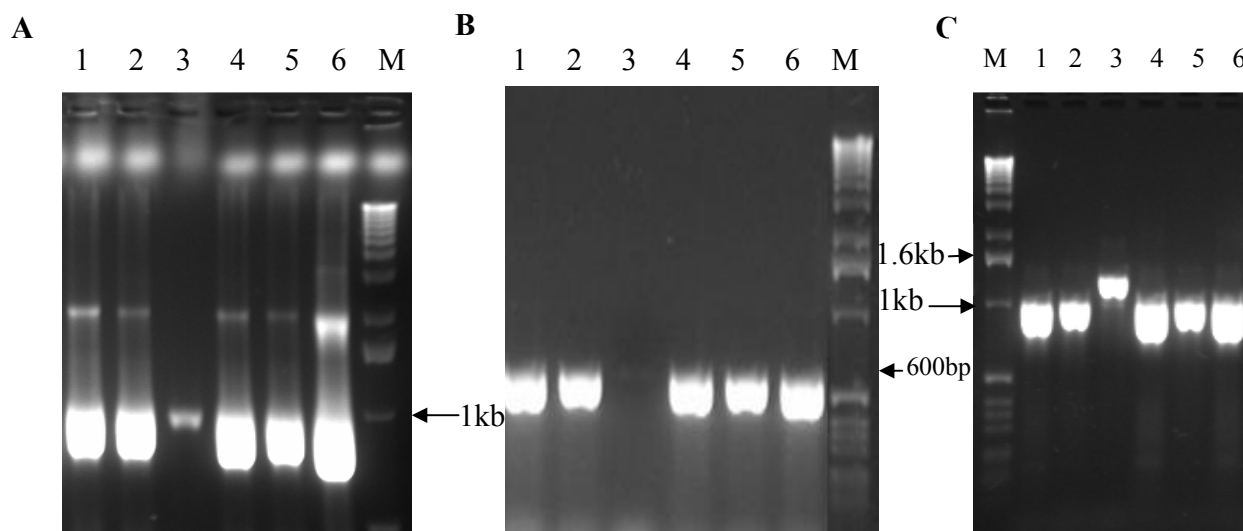


Fig. 3.8 Screening of colonies for deletion of *narP*

Lane M: 1kb ladder Lanes 1-5; colonies 1-5; Lane 6 contains control template as defined.

- (A) PCR screening for the CAM cassette, the expected size is 900bp, all colonies generated an amplified product of the expected size for this CAM screening PCR.
- (B) Screening for *narP*, only colony 3 did not generate a product of the expected size if *narP* is present; ZAP198 template was used as a positive control.
- (C) Screening of colonies for outside of *narP*, colony 3 was verified by size difference between CAM cassette (900bp) and *narP* (648bp).

3.2.2 Growth of ZAP198 and mutant strains

To test the growth defect of the constructed mutants, growth optical density were measured for each mutant strain and the parent strain (ZAP198) in triplicate. Time of one generation for each strain was determined by half of the time gap between OD 0.15 and 0.6 at 600_{nm} (Fig. 3.9). The results showed that the time of one generation for ZAP198, ZAP198 Δ *arcA*, ZAP198 Δ *fnr*, ZAP198 Δ *narX*, ZAP198 Δ *narP* is 1 hour (hr) 15 min, 1 hr 45 min, 1 hr 7 min, 1 hr 35min and 1 hr 40 min respectively. It demonstrated that the deletion of ArcA, NarX and NarP all led to growth defect in MEM-Hepes medium. However, no defective effect was found in Fnr mutant. In contrast, the growth rate in *fnr* mutant was increased compared to the wild type. Significant differences ($P < 0.001$) were found in the time of two generation in all four mutants by comparing with the wild type using F-test and t-test statistical methods.

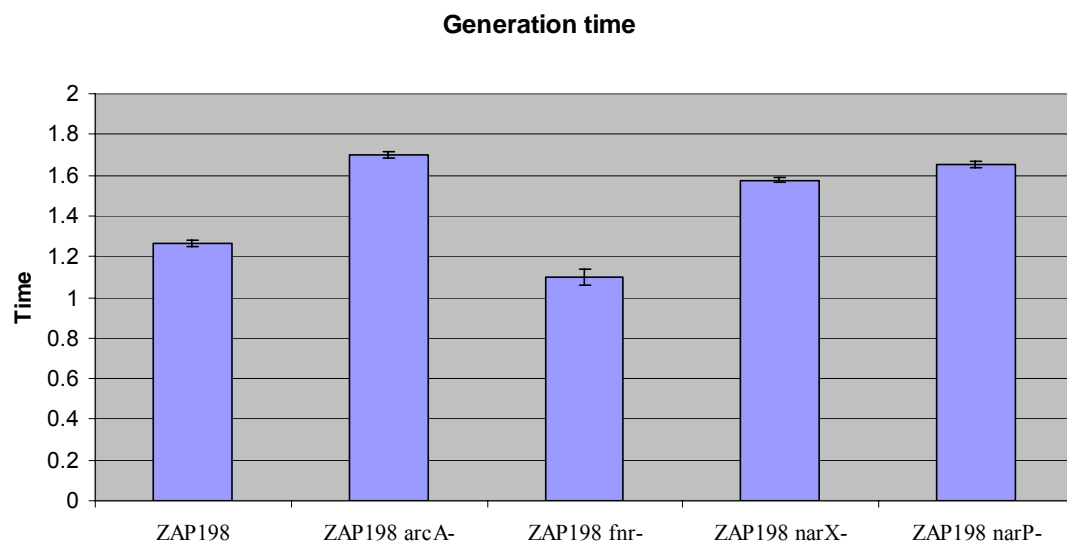


Fig. 3.9 One generation time of the four mutants and wild type (ZAP198)

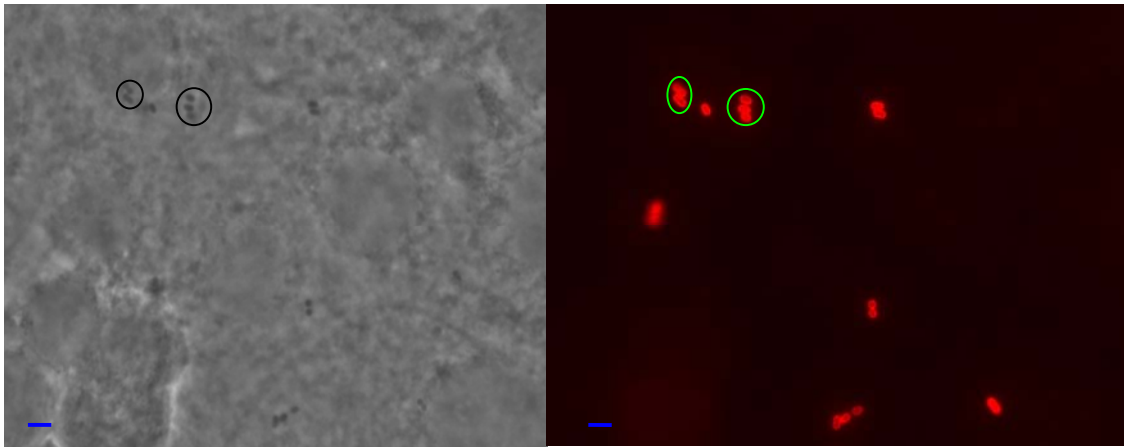
The LB cultures were incubated overnight and inoculated in MEM-Hepes with a start value 0.02 at OD₆₀₀. The cultures were measured at different time points and the time

graph plotted. Calculation of mean generation times indicate doubling time of each strain. The results indicated an increase in *fnr* mutant and a decrease in other mutants in growth. These differences in the mutants already indicated that there were going to be difficult issues dissecting effects based on growth rate changes from any impact the regulation may have on T3S. Certainly this variation needed to be taken into consideration with the phenotyping assays shown below.

3.2.3 Cell binding assay of ZAP198 and mutant strains on EBL cells

To assess the cell binding capacity of ZAP198 and the four regulatory mutants obtained as described above, the EHEC strains were cultured overnight in LB broth and diluted in MEM-Hepes with glucose and iron additions to reach an optical density at 600_{nm} of 0.5-0.6. EBL cells were infected with 2×10^6 bacteria and incubated for 3 hours in MEM-Hepes medium. The EBL cells were fixed and then stained with anti-O157 antibody to identify bacteria as described in Materials and Methods (Fig. 3.10A). The number of adherent bacteria per mammalian cell was determined by microscopy. The results showed that the binding efficiency of *arcA*, *narX* and *narP* mutants was significantly decreased compared to ZAP198 (wild type) after 3 hours of infection (Fig. 3.10B). All the mutants demonstrated some reduction in adherence level, while *arcA* and *narX* mutants showed a significant decrease ($P < 0.01$). The binding ability in *narP* mutant was decreased significantly as well ($P < 0.05$).

A



B

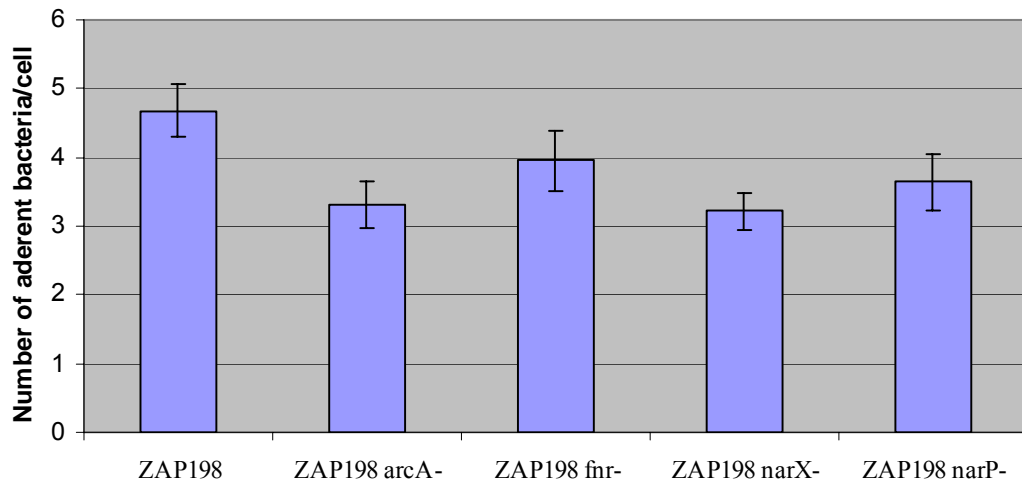


Fig. 3.10. Cell binding of *E. coli* O157: H7 ZAP198 and isogenic mutants in *arcA*, *fnr*, *narX* and *narP*.

A-B. EHEC strains were cultured in LB overnight and diluted in MEM-Hepes, and then used to infect EBL cells. Infected cells were treated by anti-O157 antibody to identify bacteria. Bacteria were indicated in circles. C. Cell binding capacity of ZAP198 and defined mutants. All the four mutants exhibit lower binding capacity compared to ZAP198, while *arcA* and *narX* mutants showed significant decrease ($P < 0.01$). The binding ability in *narP* mutant also decreased significantly ($P < 0.05$). Scale bar in A represents 5 μm .

3.2.4 A/E lesion formation by ZAP198 and isogenic strains with deletions in specific respiration-associated genes

To investigate whether the ZAP198 respiration regulators affect A/E lesion formation and T3SS within cultured EBL cells, fluorescent actin staining was performed as described in Materials and Methods after EHEC infection, and the number of condensed actin pedestals was quantified microscopically. Consistent with the adherence results, the numbers of A/E lesions associated with all four regulatory mutants was decreased compared with the wild type strain, especially for the *arcA* and *narX* mutants ($P < 0.01$) (Fig. 3.11).

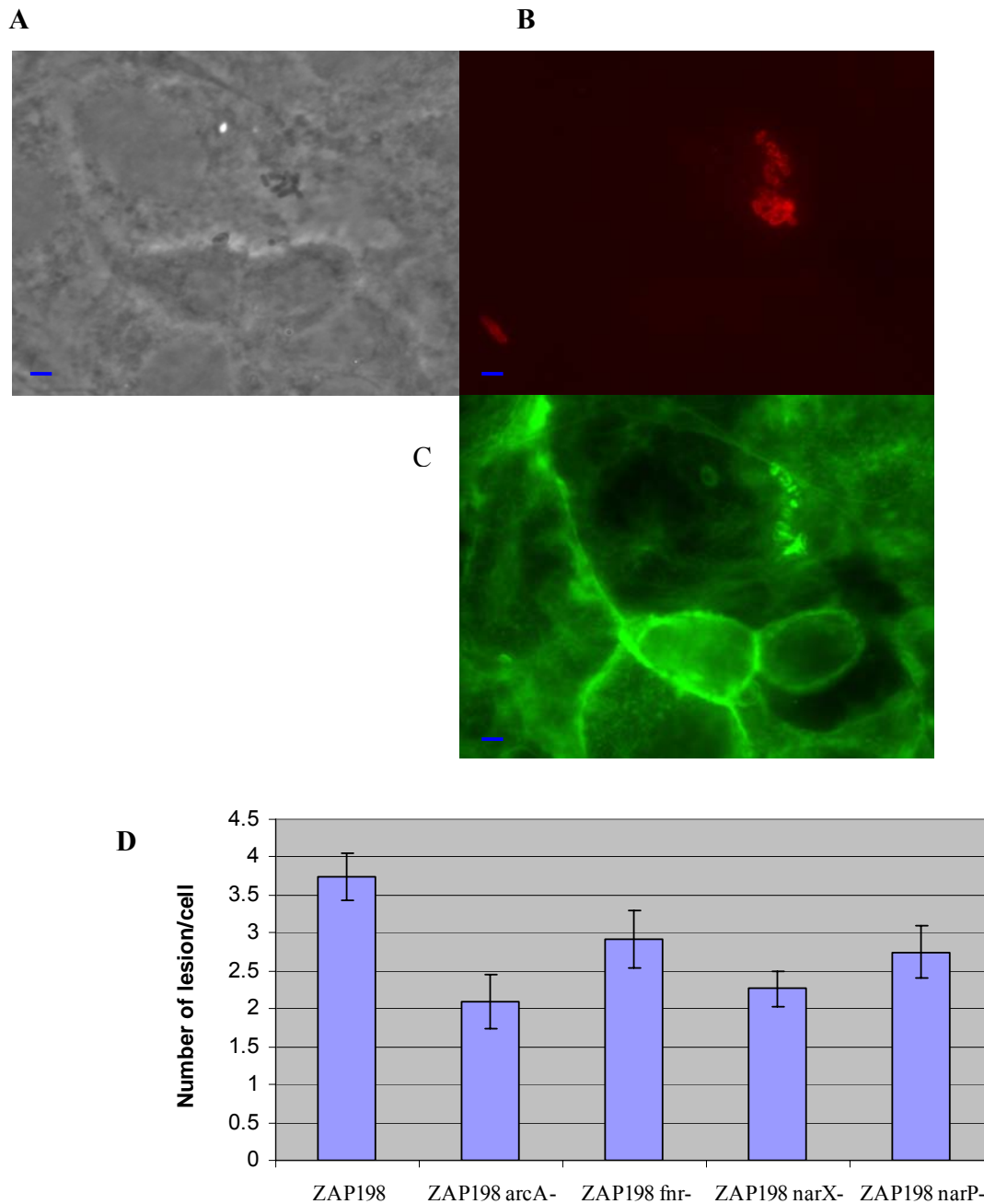


Fig. 3.11 A/E lesion formation by ZAP198 and defined respiration-associated mutants.

A-C. Infected cells were co-stained using anti-O157 antibody (B) and TRITC-Phalloidin (C) to identify bacteria and actin respectively (as described in Materials and Methods). D. The number of condensed actin pedestals per cell. All the four mutants display a lower capacity to generate A/E lesions by comparison with the WT ZAP198 strains, especially in *arcA*, and *narX* mutants ($P < 0.01$). Scale bar in A-C represent 5 μm .

3.2.5 T3S level in ZAP198 and the respiration regulation mutants

ZAP198 and the defined mutants were cultured in LB overnight and inoculated into MEM-Hepes to examine the T3S profile and relative secretion levels. The cultures were incubated in an anaerobic cabinet and harvested at OD 0.8 after centrifugation at 4000 rpm for 15 min. A final concentration of 10% trichloroacetic acid and 4 $\mu\text{g ml}^{-1}$ bovine serum albumin were added to supernatant and left at 4 °C for overnight. The proteins were recovered by centrifugation at 4000 rpm for 30 min at 4 °C. SDS-PAGE was performed as described in Materials and Methods. A demonstration gel was illustrated in Chapter 1 Introduction (Fig. 1.9) The result indicates that an *fnr* mutant possesses lower T3S levels when compared to ZAP198 with no obvious secretion differences indicated for the other mutants (Fig. 3.12). Because no significant difference was found in T3S profile gel in the four mutants, Western blotting has been performed to identify smaller changes in the secreted proteins.

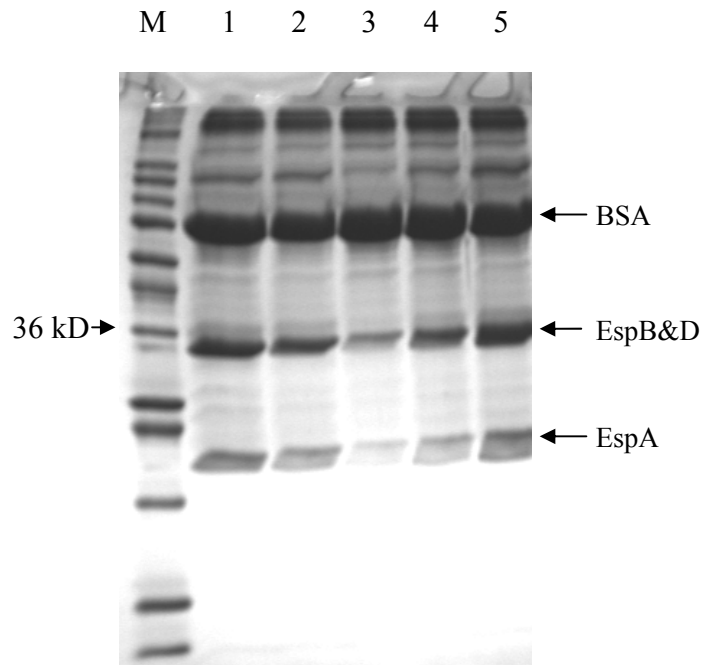


Fig. 3.12 SDS-PAGE analysing supernatant proteins of ZAP198 and isogenic mutants deleted for specific respiration-associated genes. M-wide range marker ;: ZAP198. lane 2 - *arcA* mutant ; lane 3 - *fnr* mutant ; lane 4 - *narX* mutant ; lane 5 - *narQ* mutant. The precipitation control (BSA) and putative identification of other protein bands are indicated.

3.3 Discussion

Cattle are the main source of the transmission for EHEC O157:H7 (Gansheroff & O'Brien, 2000). EHEC O157:H7 was demonstrated to have a colonization tropism in cattle. The organism colonizes the terminal rectum of the animal's gastrointestinal tract with little apparent disease (Naylor *et al.*, 2003; Rice *et al.*, 2003). High colonisation of this site is associated with high-level shedding individuals (super-shedders) and these animals are considered to be important for maintenance of EHEC O157:H7 in the host population (Matthews *et al.*, 2006). This tropism was supported by long term culture of *E. coli* O157:H7 in the bovine gastrointestinal tract (Lim *et al.*, 2007). It was revealed that recto-anal junction mucosa is the main region of the gastrointestinal tract supporting the growth of *E. coli* O157:H7 (Lim *et al.*, 2007). Colonization of the gastrointestinal tract is promoted by attachment to epithelial cells. This attachment requires the outer membrane adhesin intimin and its translocated receptor Tir. These two factors are both expressed from the LEE5 operon. Previous research has demonstrated that the LEE4 operon is required for terminal rectum colonization as deletion of LEE4 negates colonization of cattle (Naylor *et al.*, 2005). The LEE4 operon encodes EspA, B, and D that form a filamentous channel through which Tir and other factors are translocated into host cells. Therefore, the T3S system is essential for terminal rectum colonization in cattle in EHEC.

The assembly and regulation of the T3S system are very complex. It can be affected by many regulators and factors including pH, glucose, iron and temperature (Laaberki *et al.*, 2006). Ando *et al.* demonstrated that T3S apparatus was matured with the activation of the anaerobic respiratory system (Ando *et al.*, 2007).

Under my research, the hypothesis to be tested is that the tropism is driven, in part, by when the secretion system is expressed in the animal. One aspect of this will be the amount of oxygen available, either as a consequence of being at the very end of the gastrointestinal tract and/or due to proximity to epithelial cells. The T3S system and colonization was increased under microaerobic conditions in EHEC (Schuller & Phillips, 2010). In this study, four mutants were constructed in established regulators of

respiratory-linked systems, including ZAP198 $\Delta arcA$, ZAP198 Δfnr , ZAP198 $\Delta narX$ and ZAP198 $\Delta narP$, all involved in controlling the switch between aerobic and anaerobic growth.

These four mutants were successfully made using the λ Red recombinase technique (Murphy & Campellone, 2003) resulting in the replacement of the target regulatory genes with a CAM resistance cassette. This CAM resistance provides a simple selectable marker followed by PCR screening to confirm the allele replacement.

E. coli responds to availability of oxygen and the presence of other electron acceptors via a large number of sensing/regulation systems such as the one-component Fnr protein, and the two-component Arc system (Guest JR, 1996; Gunsalus, 1992; Lin & Iuchi, 1991; Park & Gunsalus, 1995; Unden *et al.*, 1995). The Arc system consists of two global regulators ArcA, the cytosolic response regulator, and ArcB, the transmembrane histidine kinase sensor. After switching from aerobic to micro-anaerobic growth conditions, ArcB is stimulated and remains in the activated state. ArcA is activated by ArcB through a His \rightarrow Asp \rightarrow His \rightarrow Asp phosphorelay (Georgellis *et al.*, 1999). Interestingly, it has been recently shown that *arcA* is required for motility by interacting with *FliA* which controls motility-related genes (Kato *et al.*, 2007). Motility was totally abolished in an *arcA* mutant *E. coli* BW25113 (Kato *et al.*, 2007). However, FlhDC regulators and ArcB were not involved in this interaction. It has been shown that the H7 serotype flagella of EHEC O157 acts as an initial colonization factor on primary cells cultured from the bovine terminal rectum (Erdem *et al.*, 2007; Mahajan *et al.*, 2009). As T3S is co-ordinated with flagella expression via the GrlR–GrlA regulatory system (Iyoda *et al.*, 2006), any effect of *arcA* on T3S could be through an impact on flagella expression. However, results showed that no obvious effect on T3S in the *arcA* mutant under both aerobic (data not shown) and anaerobic conditions. It indicates that *arcA* in ZAP198 strain doesn't affect the T3S system directly. However, Alexeeva *et al* have demonstrated that *arcA* functions as a redox regulator only under micro-aerobic growth conditions (Alexeeva *et al.*, 2003). In addition, it was shown that *arcA* regulates the expression of genes related to oxygen regulation and the glycolysis pathway when incubated under micro-aerobic conditions

(Shalel-Levanon *et al.*, 2005). In addition, it was recently reported that bacterial colonization of polarized human colon carcinoma cells was increased under micro-aerobic conditions (Schuller & Phillips, 2010). Future work could address the effect of *arcA* deletion on T3S system by culturing the bacteria under micro-aerobic conditions or on tissue explants with controlled oxygen tensions.

Fnr functions as a redox sensor containing a Fe-S cluster (Shalel-Levanon *et al.*, 2005). It is regulated by the concentration of iron-sulfur cluster assembly proteins and the protease ClpXP which also degrades a LEE activator, GrlA (Tolla & Savageau, 2010). Fnr is only considered active during anaerobic growth conditions inducing the expression of genes that allow *E. coli* to grow anaerobically. It also represses genes expressed under aerobic condition. So the *fnr* mutant was cultured under anaerobic conditions in an anaerobic cabinet in order to examine the T3 secretion profile. A decrease in the level of T3S was found in the *fnr* mutant compared to the wild type ZAP198. This effect might be due to a higher ClpXP concentration in the mutant with increased degradation of the T3S-activator GrlA. Future work could address the mechanistic basis of this regulation.

NarX and NarP belong to NarX-NarL and NarQ-NarP two-component regulatory systems respectively. NarX-NarL and NarQ-NarP two component regulatory systems are responsible to control transcriptional response to nitrate and nitrite (Stewart *et al.*, 2003; Stewart, 1995). The phosphorylation of the NarL and NarP regulators is determined by the NarX and NarQ sensors in response to signal nitrate, nitrite and ligands. A previous study demonstrated that a cross interaction may exist between these two systems (Stewart, 1995). They are all related to the synthesis of anaerobic respiratory enzymes. The effect of *narX* and *narP* on T3S under anaerobic condition is tested in this study. The results showed that no significant differences were found in the *narX* and *narP* mutants with respect to T3S level in comparison to the wild type. It indicates that *narX* and *narP* are not connected with the regulation of T3S under the conditions examined.

The formation of A/E lesions depends on T3SS (Jarvis *et al.*, 1995), the outer membrane adhesive protein intimin (Jerse *et al.*, 1990) and Tir, which is translocated into the host cell after attachment (Kenny *et al.*, 1997). Therefore, consistent with the T3S level, a minor decrease was detected in binding to and A/E lesion formation on EBL cells in the four constructed mutants compared to the wild type. This result demonstrated that the T3S level did correlate to some extent with binding efficiency and A/E lesion formation *in vitro*.

In conclusion, T3S profile, cell binding capacity and A/E lesions were investigated in the four constructed mutants. Minor reductions in binding efficiency were observed in all four mutants with significant differences in *arcA*, *narP* and *narX* mutants ($P < 0.05$). This result correlated with a decrease in A/E lesion formation. *arcA* and *narX* mutants showed significantly lower levels of A/E lesions compared with the wild type, with minor reductions in the *fnr* and *narP* mutants. However, the growth rates were all affected significantly ($P < 0.05$) in these four mutants. The *arcA*, *narP* and *narX* mutants had reduced growth rates compared to the wild type. While the *fnr* mutant had a decreased doubling time under the conditions tested. The reduction in adherence and A/E lesions of *arcA*, *narP* and *narX* mutants might be due to the slow growth, and this issue really leads to stopping this line of research at a relatively early stage. Interestingly, the *fnr* regulatory system might be a significant controller of T3S. Recent work by Dr Jai Tree in our research group has examined post transcriptional control of LEE4 expression, in particular of the substrate switch protein SepL (Wang *et al.*, 2008). *sepl*/LEE4 translation is dependent on Hfq which acts as a chaperone to bring mRNA and small RNAs together. From his work, FnrS is predicted to interact with the LEE4 transcript (Jair Tree, personal communication).

Taken together, while it was evident that altering control of aerobic/anerobic respiration in EHEC O157 did have some impact on binding and A/E lesion formation capacity, the impact on T3S was minimal, with the possible exception of Fnr, under the conditions tested. Given that the mutations also affected growth rates and will have other multiple

effects on other pathways, it was decided not to continue this work by testing the mutants in cattle, as this could not be justified. Consider trying to manipulate T3S regulation specifically might be more fruitful. My PhD work switched to construct an inducible T3SS to test the regulation of T3SS and examine the T3S effect on the colonization in cattle with the constructed inducible T3SS strain.

4 Chapter 4 The Construction of an Inducible LEE1 Promoter

4.1 Introduction

The regulation of T3S is complex and controlled by many genes and effectors as described in the main Introduction. The aim of the work in this chapter was to try and override normal inputs into LEE1 promoter by replacing this promoter with one that is inducible. This construct could then be used to examine the link between the tropism of O157 for the terminal rectum of cattle and the regulation of T3S. If successful, this construct could also be used to test whether heterogeneous expression of LEE4 and LEE5 (Roe *et al.*, 2003b) is completely independent of normal inputs at LEE1 and whether the expression level at LEE1 alters the proportion of bacteria expressing a functional T3SS.

The approach was to replace the main LEE1 promoter with the inducible tetracycline (Tc) promoter. Bacteria resistance against widely used antibiotics has caused severe problems in contemporary medicine (Parkinson, 1993). Resistance against the broad-spectrum antibiotic Tc and its chemically-modified analogues is one of the best known examples of bacterial resistance. The inducible system using the Tet repressor (*tetR*) is broadly applied in molecular genetics (Saenger *et al.*, 2000). When Tc and its analogues diffuse through the cytoplasmic membrane into bacteria, they chelate a divalent cation, preferentially Mg^{2+} . The complex $[MgTc]^+$ binds to the small (30S) prokaryotic ribosomal subunit, thereby inhibiting protein biosynthesis and preventing the growth of bacteria (Epe & Woolley, 1984). The main established resistance mechanism against the Tc-type antibiotics involves proteins that export Tc out of the bacterial cell (Eckert & Beck, 1989; Tovar K, 1988). Tc-resistance determinants encode active efflux pumps of the drug and are widely distributed in Gram negative bacteria and unique with respect to genetic organization and regulation of expression. Each determinant consists of tet activator gene (*tetA*) and *tetR*. The resistance protein TetA is a tetracycline/metal-proton antiporter located in the cytoplasmic membrane, while the regulatory protein TetR is a tetracycline (tc) inducible repressor of the system. The expression of TetA is tightly regulated by TetR.

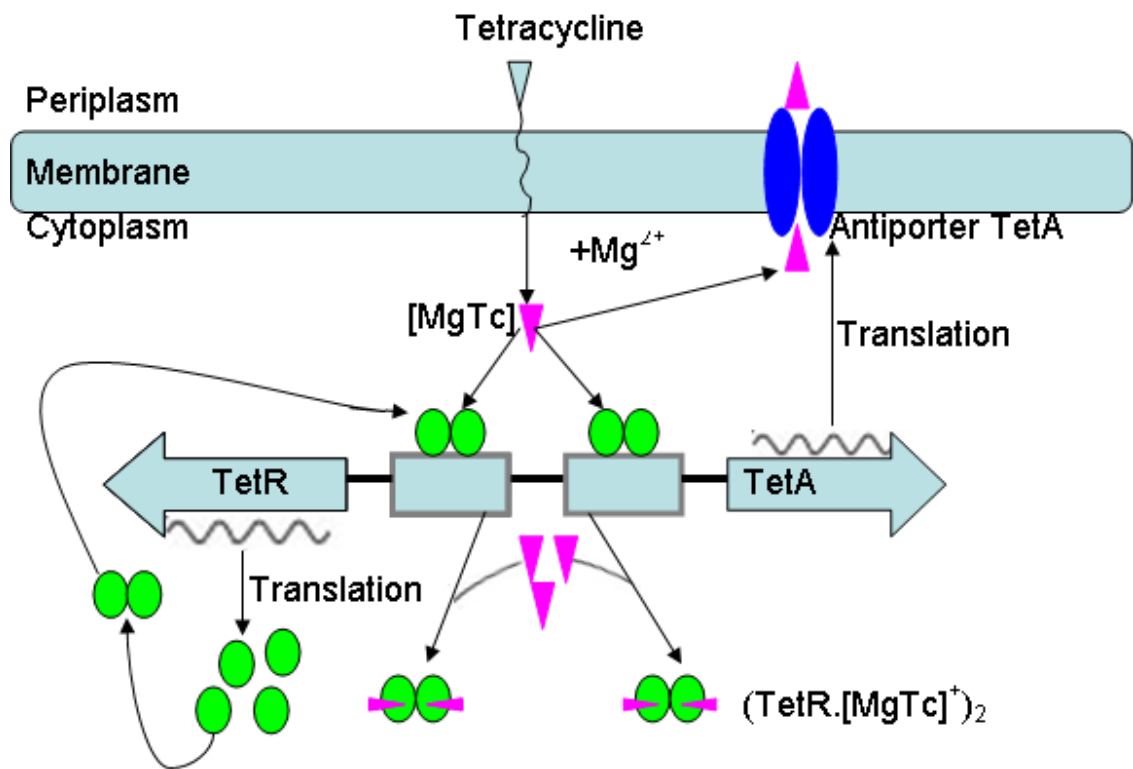


Fig. 4.1 Schematic description of tetracycline (Tc) resistance. (Originally from Saenger *et al.*, 2000)

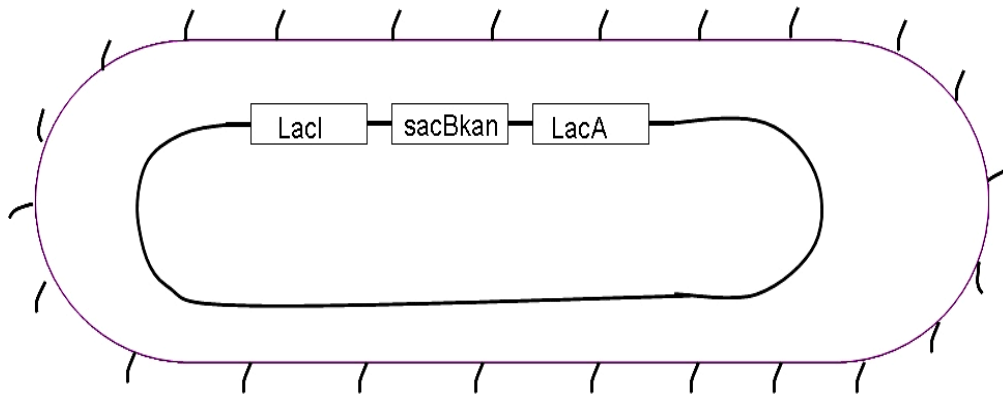
The tetracycline repressor acts as the homodimer $(TetR)_2$ in which two identical helix-turn-helix (HTH) motifs bind in the absence of $[MgTc]^+$. $(TetR)_2$ has only a low affinity to nonspecific DNA sequences but binds tightly to two specific DNA operator sequences, *tetO1* and *tetO2* forming a $[(TetR)_2. tetO]$ complex. This complex composed by TetR (shown as green spheres) binds at *tetO1* and *tetO2* forming a homodimer to repress the expression of *tetA*. Tc (lt. blue triangle) distributes into the (bacterial) cell and forms a $[MgTc]^+$ complex (pin triangles) with Mg^{2+} . When $[MgTc]^+$ binds to $[(TetR)_2. tetO]$

homodimer, it leads to a conformational change forming $(\text{TetR} \cdot [\text{MgTc}]^+)_2$ complexes which release the *tetO*. Therefore, transcription of genes *tetR* and *tetA* are triggered (wavy lines represent mRNA). After translation, TetA protein is inserted into the cytoplasmatic membrane and translocates $[\text{MgTc}]^+$ out of the cell to avoid the attacking to the ribosome.

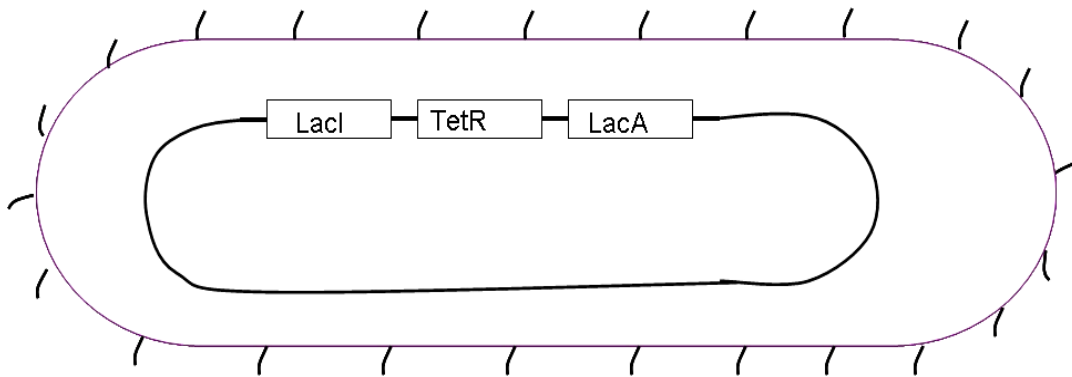
Tet repressor blocks the transcription of the gene *tetR* (controlled by the operator *tetO1*), which encodes for TetR itself, and of the gene *tetA* (controlled by operator *tetO1* and *tetO2*), which encodes for the resistance protein TetA. When Tc or its analogues diffuse into a resistant bacterial cell carrying the genes *tetR* and *tetA*, a chelate $[\text{MgTc}]^+$ is formed with Mg^{2+} . This chelate binds to the $[(\text{TetR})_2 \cdot \text{tetO}]$ complex and leads to the structural changes in $(\text{TetR})_2$ which reduces its affinity to *tetO*. A complex $(\text{TetR} \cdot [\text{MgTc}]^+)_2$ formed by $(\text{TetR})_2$ and two inducers $[\text{MgTc}]^+$ releases *tetO*, then genes *tetR* and *tetA* can be expressed. The antiporter protein TetA is located in the cytoplasmic membrane and transfers $[\text{MgTc}]^+$ to outside the cell, therefore preventing interaction of $[\text{MgTc}]^+$ with the ribosomal 30S subunit.

This well-defined switching between the two states relevant for regulation of gene expression is applied for molecular genetics to control the expression of other genes. According to the report by Lutz and Bujard (Lutz & Bujard, 1997), induction is mediated by a tetracycline-metal complex and requires only nanomolar concentrations of the drug. In the presence of anhydrotetracycline (aTc), *tetR* is induced and detaches from its cognate DNA sequence *tetO*. The regulation of gene expression over a 5000-fold range was achieved with promoter PL_{tetO1} (Tet operator, responsible for *tetR* expression) (Lutz & Bujard, 1997). The aim of this study was to replace the LEE1 chromosomal promoter with the *tetO2* operator (Tet promoter) by allelic exchange. *tetR* will also be introduced into the chromosome at *lac*. Thereby *tetO2* expression level can be regulated by aTc via TetR. The construction process was depicted in Fig 4.2. Four steps (Fig. 4.2 step1-4) were carried out to achieve the aTc inducible construction. This construction should allow controlled induction of LEE1 and hopefully the T3S system.

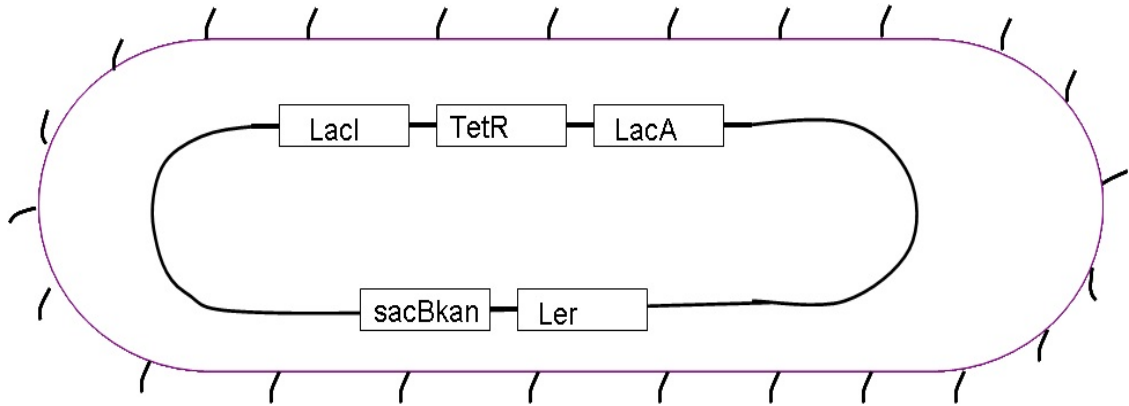
Step 1 *lacY&Z* was replaced by *sacBkan* cassette by allelic exchange



Step 2 *sacBkan* cassette at *lacY&Z* was exchanged by constitutive *tetR* using allelic exchange, the resultant strain termed ZAP1213



Step 3 LEE1 promoter was replaced by *sacBkan* cassette by allelic exchange, the resultant strain termed ZAP1327



Step 4 *sacBkan* cassette at LEE1 promoter was exchanged by *tet* promoter using allelic exchange

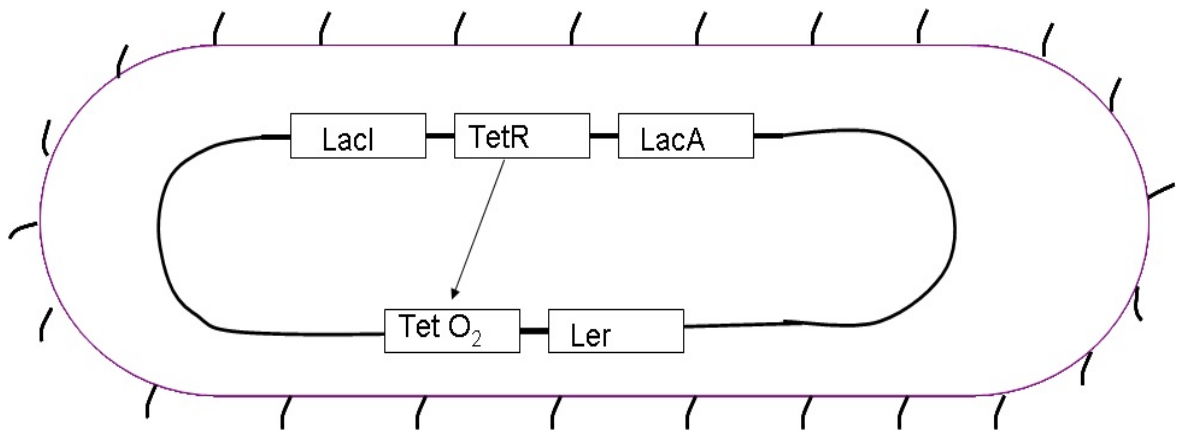


Fig. 4.2 Four steps used to construct an inducible LEE1 promoter, each step indicating one allelic exchange process, the arrow showed the TetR repression of *tet* promoter.

4.2 Results

4.2.1 Construction of an *E. coli* O157:H7 strain with *tetR* exchanged into the *lac*

To obtain a strain containing *tetR*, two allelic exchange steps were used. The first exchange was to replace *lacZY* with the *sacBkan* cassette and the second one was to exchange the *sacBkan* cassette with *tetR*. This two step process takes advantage of counter-selectable SacB expression in the second step as detailed previously (Blomfield *et al.*, 1991).

4.2.1.1 Replacement of *lacZY* with the *sacBkan* cassette in ZAP198 (Step 1 Fig. 4.2)

For the first exchange, a previously constructed plasmid, pAJR33 (Roe *et al.*, 2003b), was used that contains the appropriate *lac* flanking regions. The process was performed as described in Materials and Methods. To identify the correct replacement, primer pair 5-*lacY* and 3-*lacZ* (Table 5) were designed to test the presence or absence of *lacZY*. Primer pair 5-*lacI* and 3-*lacA* (Table 5) was used to PCR across the whole *lacZY* region. PCR with primer pair 5-SacB and 3-SacB (Table 5) was carried out to determine whether the *sacBkan* cassette was present and primer pair 5-*lacI* and 3-SacB (Table 5) was used to test the conjunction of the *sacBkan* cassette and *lacI*. The genetic annealing sites of these primers was shown in Fig. 4.3. The PCR results showed the three colonies tested all acquired *sacBkan* cassette (Fig. 4.4) and had lost the *lacZY* genes (Fig. 4.4). To confirm the replacement, PCR from outside of *lacZY* genes using 5-*lacI* and 3-*lacA* (Table 5) indicated that the *sacBkan* cassette was inserted between *lacI* and *lacA* genes compared to a control, pAJR33 (Fig. 4.6). For further confirmation, PCR for conjunction of the cassette and *lacA* genes using primer pair 3-*lacA* and 3-SacB (Table 5) was carried out and demonstrated that the *sacBkan* cassette was integrated into the *lac* locus as anticipated (Fig. 4.7).

A.



B.

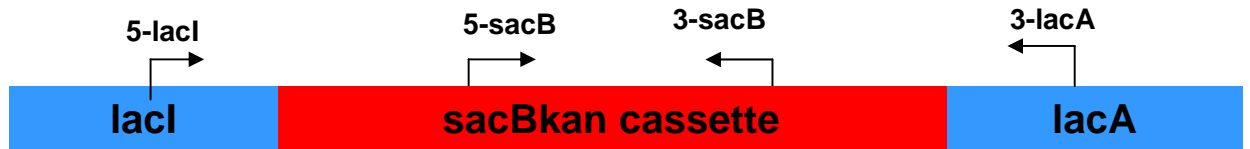


Fig. 4.3 A: Structure diagram of *lacYZ* locus and primers in ZAP198

B: Structure diagram of *sacBkan* cassette and primers in *lacYZ* mutant

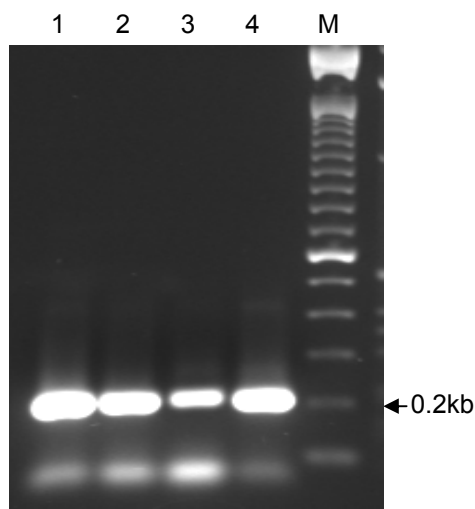


Fig. 4.4 PCR for screening the *sacBkan* cassette: Lanes 1-3 are from colonies 1-3 respectively and Lane4 used pAJR 33 DNA as a template. Lane M: 100bp ladder PCR shows that colony 1-3 all got *SacB* with the size of 210bp.

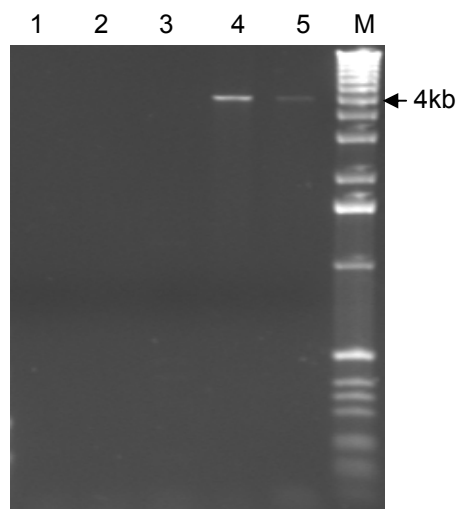


Fig. 4.5 PCR for screening the *lacZY* genes. Lane 1-3: colony 1-3; Lane 4: pAJR 33 as templates for the PCR. Lane 5: ZAP198; Lane M: 1 kb ladder. PCR shows that all three colonies have potentially lost *lacZY* with ZAP198 as positive control. The expected region from ZAP198 is 4351bp.

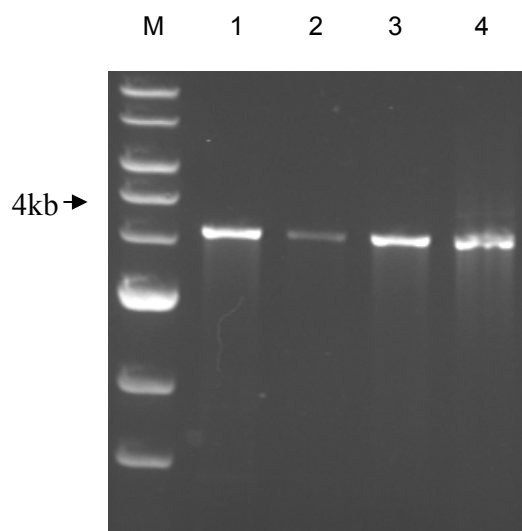


Fig. 4.6 PCR for screening the outside *lacZY* genes using 5-*lacI* and 3-*lacA*
Lane M - 1 kb ladder: Lane1-3 - colony 1-3:
Lane 4 - pAJR33 as a positive control.
PCR substrate for pAJR33 is 4458bp.

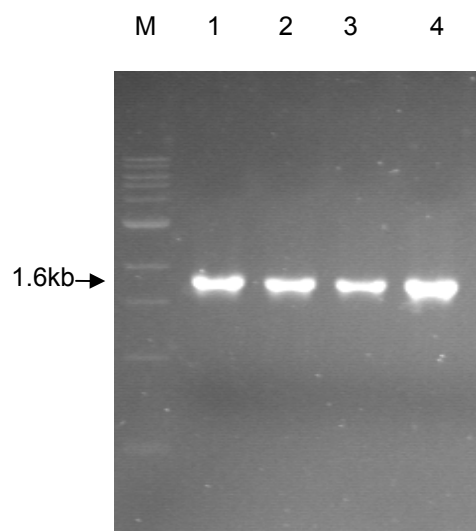


Fig. 4.7 PCR for screening the conjunction of *lacI* and *sacBkan* cassette
Lane M - 1 kb ladder: Lane1-3 - colony 1-3:
Lane 4 - PCR amplified from pAJR33 as a positive control.

4.2.1.2 The exchange of the *sacBkan* cassette with PN25&*tetR* at *lacZY* (Step 2 Fig. 4.2)

To replace the *sacBkan* cassette at *lac* with *tetR*, a plasmid containing PN25&*tetR* with the same flanking regions as pAJR33 in PIB307 was constructed. The plasmid pAJR27 created by Andrew J. Roe (Roe *et al.*, 2003b) without the *sacBkan* cassette was used and PN25&*tetR* was inserted into the *BamH* I site. PN25&*tetR* was amplified from commercial plasmids PZS4*Int-laci/tetR* in which a promoter (PN25) in front of *tetR* gives constitutive expression of *tetR*. The allelic exchange procedure was performed as described in Materials and Methods.

4.2.1.2.1 The construction of a plasmid suitable for the exchange of the *sacBkan* cassette with PN25TetR at *lac*

PN25&*tetR* was PCR amplified from PZS4*Int-laci/tetR* with a size of 764bp using primer pair 5-PN25-BamHI and 3-PN25-BamHI (Table 5, Fig. 4.8). Then the PCR product was cloned into the *BamH* I site in pAJR27, and verified by *BamH* I digestion (Fig. 4.9) and termed pXLS02. Fig. 4.8 shows that the size of plasmid from the clone is larger than pAJR27 and the expected band was obtained by *BamH* I digestion. pXLS02 was then sequenced for a further confirmation (data not shown).

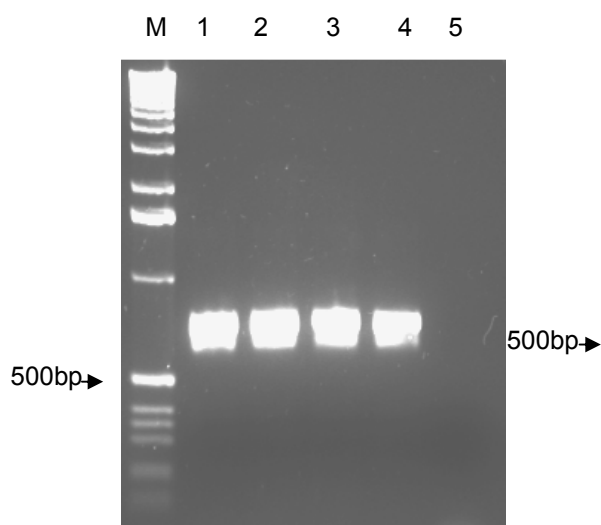


Fig. 4.8 PCR for PN25&*tetR* from PZS4*Int-lacI/tetR* plasmid. Lane1-4 - PCR substrate from PZS4*Int-lacI/tetR*:Lane5 - negative control: Lane M - 1kb ladder. Expected PCR product size is 764bp.

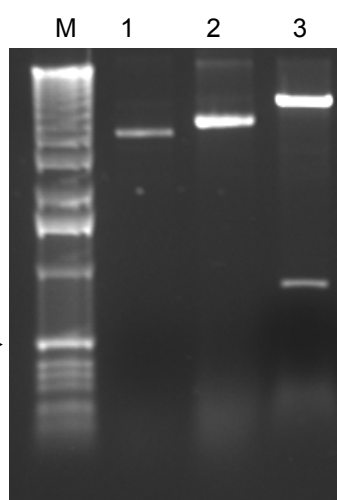


Fig. 4.9 *Bam*H I digestion of PN25&*tetR* in pAJR27. Lane1 - pAJR27: Lane2 - PN25&*tetR* in pAJR27: Lane3 - pXU02 digested by *Bam*H I: Lane M - 1 kb ladder. A right size was obtained by *Bam*H I digestion

4.2.1.2.2 The exchange of *sacBkan* cassette with *tetR*

To replace the *sacBkan* cassette with *tetR* in pXLS02, the plasmid was eletroporated into ZAP1212. The exchange was carried out as described in Materials and Methods. The resultant colonies were screened by PCR with primer pair 5-*PN25*-BamHI and 3-*PN25*-BamHI (Table 5) for PN25&*tetR*, primer pair 5-*lacI* and 3-*lacA* (Table 5) for flanking the region. The loci of these primers on the genome was shown in Fig. 4.10. The PCR results indicated that one colony acquired PN25&*tetR* (Fig. 4.11) and this was confirmed by primer pair 5-*lacI* and 3-*lacA* (Fig. 4.12). The map for the correct exchange is shown in Fig. 4.2 Step2. The strain with *tetR* was successfully constructed and designated ZAP1213.



Fig. 4.10 Structure diagram of *tetR* and primers in ZAP1213

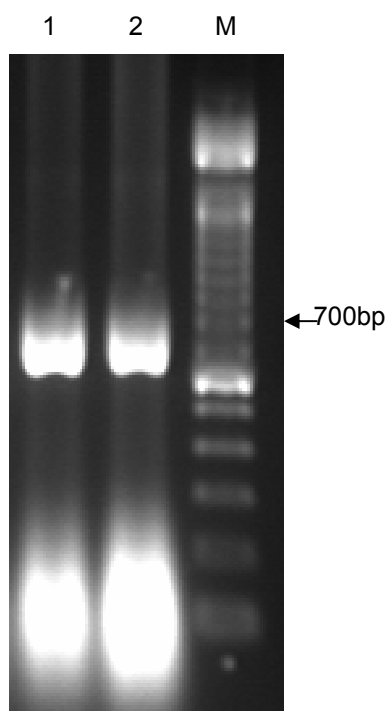


Fig. 4.11 PCR screening for PN25&*tetR*
 Lane 1: colony 1
 Lane2: pXLS01 as a positive control
 Lane M: 100bp ladder
 It shows one colony from the allelic exchange acquired PN25&*tetR* gene.

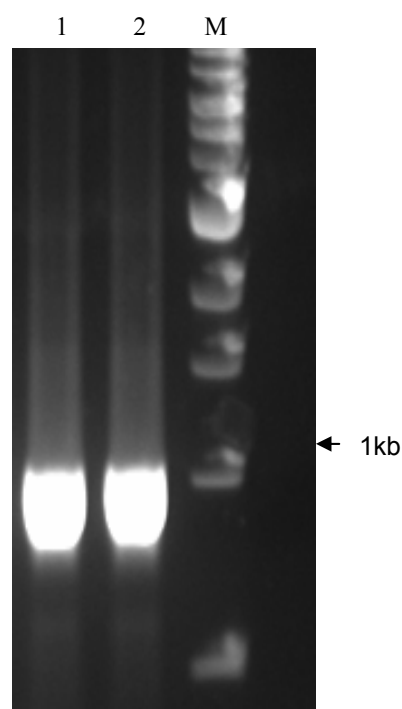


Fig. 4.12 PCR screening for outside *lacZY*
 Lane 1: colony 1
 Lane2: pXLS01 as a positive control
 Lane M: 1kb ladder.

4.2.2 Testing aTc induction of GFP expression in ZAP1213

To investigate the aTc induction efficiency via *TetR* on the *tet* promoter, the promoter was cloned into pKC26 at *Xba*I site creating pXLS03. Then the pXLS03 was transformed into ZAP1213 containing *TetR* and aTc was applied for induction of *tet* promoter by acting on Tet repressor. Thereby the induction efficiency can be tested by measuring GFP levels (expressed by pKC26) which represents *tet* promoter expression level controlled by *TetR*.

4.2.2.1 The construction of pXLS03

In order to determine if the TetR repressor would function as anticipated on the *tet* promoter, a plasmid was constructed in which *tet* promoter was placed in front of *egfp*+. So this constructed plasmids can be induced with the presence of aTc. Firstly, the *tet* promoter was PCR amplified by annealing primer pair 5-Tet promoter-*Xba*I and 3-Tet promoter-*Xba*I (without a template) (Fig. 4.13). The sequence for the *tet* operator was as published (Lutz and Bujard, 1997). The cleaned PCR fragment was digested with *Xba*I and cloned into pKC26 in the *Xba*I restriction site. The correct clone was verified by *Xba*I digestion (Fig. 4.14) and termed as pXLS03.

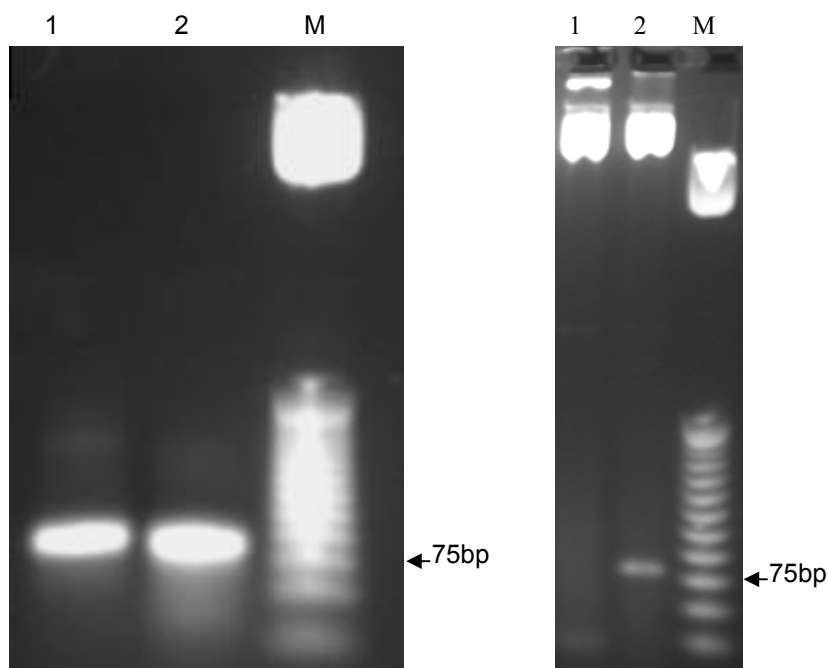


Fig. 4.14 *Xba* I digestion for *tetO1* cloning

Lane 1: pKC26 as a negative control
Lane 2: Colony obtained from cloning

Fig. 4.13 PCR synthesis of *tetO1*
Lane 1-2: *tetO1*
Lane M: 25bp ladder
It shows *tetO1* was amplified
with a size of 81bp by PCR.

4.2.2.2 GFP measurement following aTc induction

pXLS03, containing the *tet* promoter controlling *gfp+*, was transformed into ZAP1213 (contains the Tet repressor - *tetR*) to determine whether aTc addition could induce GFP expression by removing TetR repression. Controls included pXLS03 in ZAP1213 without aTc as a negative control and pXLS03 in ZAP198 as a positive control as it does not have any TetR repression. The result showed that the GFP expression level in ZAP1213 with pXLS03 without aTc was very low which indicated that *tet* promoter was tightly repressed by the Tet repressor in ZAP1213 compared to wild type ZAP198 (Fig. 4.15). When a concentration of 200 ngml⁻¹ aTc was added to ZAP1213 with pXLS03, the GFP expression reached a similar level as the positive control group, i.e. pXLS03 in ZAP198 (without *TetR*). It demonstrated that aTc can induce *tet* promoter expression to a very high expression level compared to the negative control and close to the positive control. To prove the induction was produced by inducing the *tet* promoter, a control plasmid pKC26 (blank plasmid without *tet* promoter insertion) was also transformed into ZAP1213 and GFP fluorescence level measured. Fig. 4.16 demonstrated that when a high induction level was induced by adding aTc in *tet* promoter group (pXLS03), the fluorescence in the control plasmids pKC26 (parent plasmids) group kept in low level.

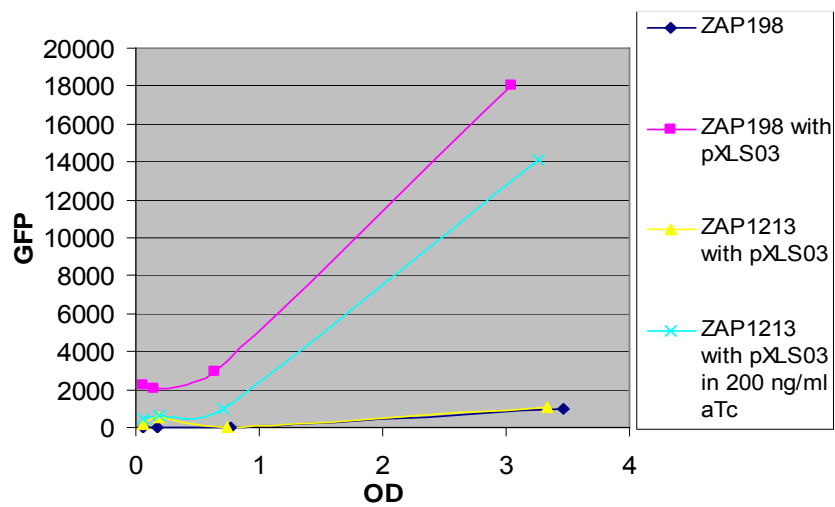


Fig. 4.15 aTc induction for Tet repressor with *tetO1* operator
 With a concentration of 200 ngml^{-1} aTc, pXLS03 GFP expression level in ZAP1213 is similar as its expression in ZAP198.

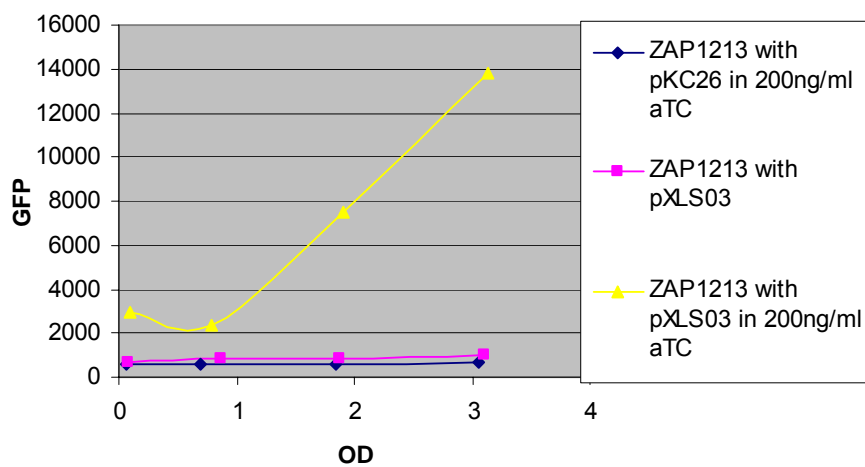


Fig. 4.16 aTc induction for Tet repressor with *tetO1* operator
pXLS03 GFP expression level in ZAP1213 reaches a high level with a blank pKC26 background.

4.2.3 Creation of strains with LEE1 promoter replaced by *tet* promoter in ZAP1213

As described in Materials and Methods, two constructs were designed. The genetic organization of LEE1 promoter is shown in Fig. 4.17. The first construction keeps the original transcriptional start site and -10 region of the native LEE1 operon promoter, while the -35 regions are replaced by AT rich DNA sequence (*tet* promoter) synthesized artificially (Fig. 4.18). For the second construct, only the original transcriptional start site was kept with -35 and -10 regions replaced by a synthesized *tet* promoter (Fig. 4.19). To obtain a strain with *tet* promoter in front of LEE1 operon instead of the native LEE1 promoter, two exchanges were carried out in each construct. The first exchange was to replace the native LEE1 promoter with *sacBkan* cassette to produce an intermediate strain for the exchange of *tet* promoter. Since the second construct deletes 25 bp more from the -35 region more than first construct, the intermediate strain from first construct can be used for the second exchange of the second construct. In the second exchange, the *sacBkan* cassette was replaced by the synthesized *tet* promoters in the two different constructed exchange plasmids. This *tet* promoter can be controlled by *tetR* gene in the same strain.

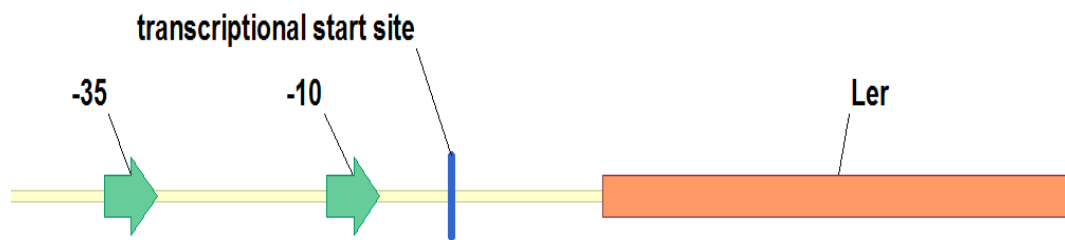


Fig. 4.17 Genetic organization of LEE1 promoter

-10 and -35 elements were shown in green with arrow; transcriptional start site was labelled in blue. Opening reading frame of *ler* was shown in red.

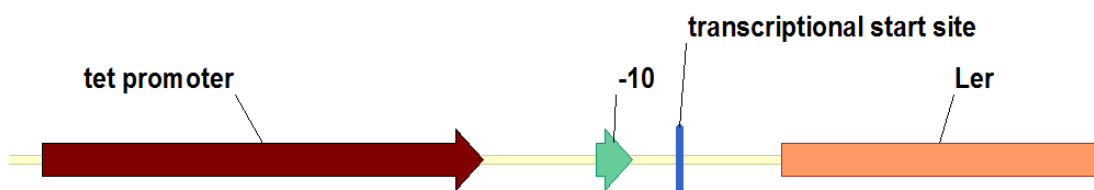


Fig. 4.18 Genetic organization of first construction

tet promoter and -10 element were shown in brown and green with arrow respectively; transcriptional start site was labelled in blue. Opening reading frame of *ler* was shown in red.

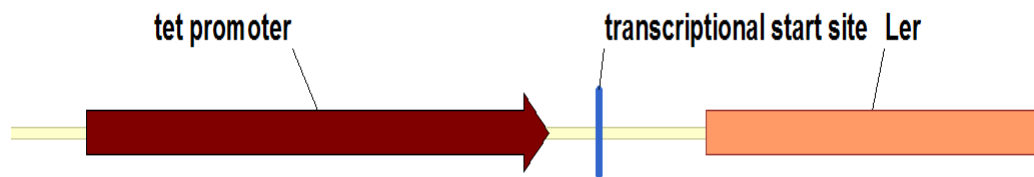


Fig. 4.19 Genetic organization of second construction

tet promoter was shown in brown with arrow; transcriptional start site was labelled in blue. Opening reading frame of *ler* was shown in red.

4.2.3.1 First exchange: The exchange of the LEE1 promoter with *sacBkan* cassette producing intermediate strains for both constructions (Step 3, Fig. 4.2)

The aim of the first exchange is to obtain an intermediate strain for the exchange of LEE1 promoter with *tet* promoter. As the second construction is only 25 bp more deletion than the first construction, the intermediate strain for first construction can also be used for second construction. Therefore only one strain was needed for the first exchange. Then in the second exchange, plasmids with different flanking region fragments were applied resulting in a different deletion of LEE1 promoter.

4.2.3.1.1 The construction of plasmids suitable for the exchange of the LEE1 promoter with *sacBkan* cassette

In the first exchange, a plasmid containing LEE1 promoter flanking regions with the *sacBkan* cassette in PIB307 was produced for each construct. Briefly, two downstream flanking region fragments for each construct were PCR amplified from TUV93-0 using primer pairs 5-*LEE1* down FR 1st BamHI & 3-*LEE1* down FR XbaI and 5-*LEE1* down FR 2nd BamHI & 3-*LEE1* down FR XbaI (Fig. 4.20). These two flanking region fragments were digested by *Xba* I and *Bam*H I and then cloned into the same sites in PIB307. Fig. 4.21 showed insertions digested by *Xba* I and *Bam*H I from PIB307. The clone was also sequenced (Data not shown). Then a downstream PCR fragment amplified from TUV93-0 using 5-*LEE1* UP FR XmaI & 3-*LEE1* UP FR BamHI was cloned into *Xma* I and *Bam*H I sites into the two plasmids containing downstream flanking region for each construct (Fig.4.22). These two clones were digested with *Xma* I and *Bam*H I to prove the insertions were the expected size (Fig.4.23) and then sequenced (data not

shown). The plasmid with both downstream and upstream flanking region insertions for first construct was termed pXLS04 and for second construct pXLS05. The *sacBkan* cassette was cloned into the *Bam*H I site in pXLS04 producing pXLS06 and as only one intermediate strain was required for both proposed final constructs. Fig. 4.24 demonstrated that the required plasmid was produced.

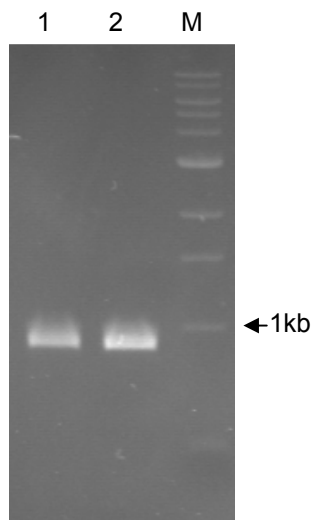


Fig.4.20 PCR for downstream flanking region fragments for first and second constructions

Lane 1: first construction, 907bp
Lane 2: second construction, 901bp
Lane M: 1 kb ladder.

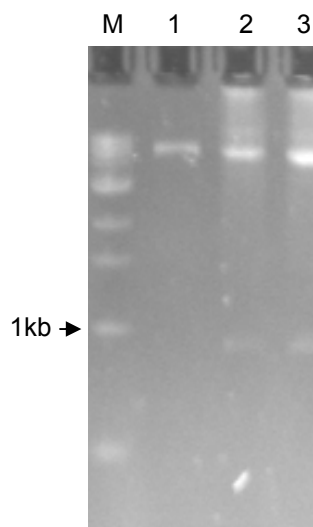


Fig. 4.21 *Xba* I and *Bam*H I digestion for downstream cloning

Lane 1: pIB 307 as a negative control
Lane 2: First construction
Lane 3: Second construction
Lane M: 1 kb ladder
The expected fragment was obtained by *Xba* I and *Bam*H I digestion.

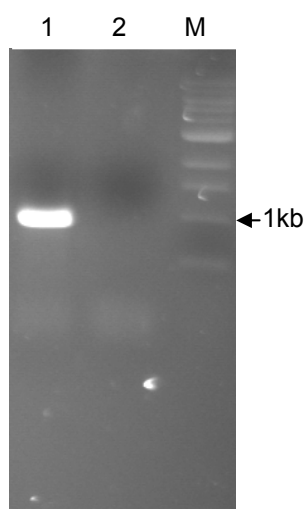


Fig.4.22 PCR for upstream flanking region fragment for first and second constructions
Lane 1: upstream flanking region PCR fragment for first construction, 932bp
Lane M: 1 kb ladder.

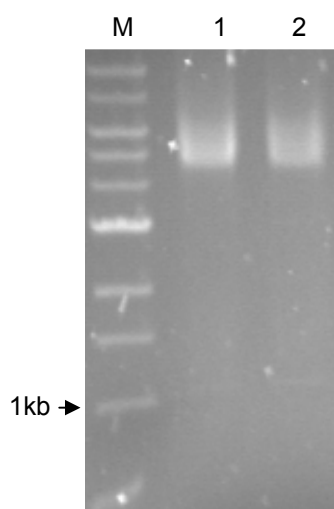


Fig. 4.23 *Xma* I and *Bam*H I digestion for upstream cloning
Lane 1: First construction
Lane 2: Second construction
Lane M: 1 kb ladder
A 932 bp fragment was detected following *Xma* I and *Bam*H I digestion.

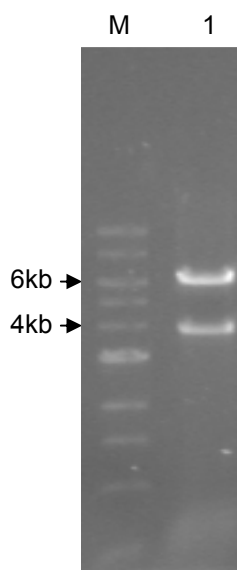
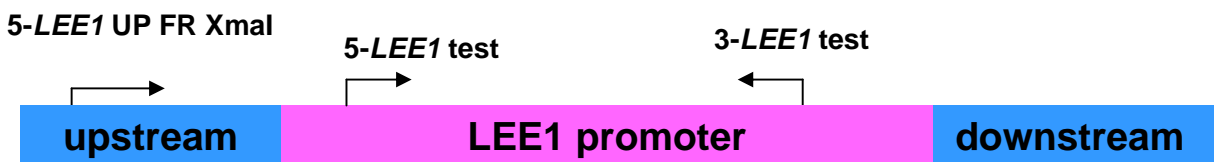


Fig. 4.24 *Bam*H I digestion for *sacBkan* cassette cloning
Lane 1: First construction
Lane M: 1 kb ladder
A 3.9 kb *sacBkan* cassette was detected by *Bam*H I digestion.

4.2.3.2 The exchange of the LEE1 promoter with *sacBkan* cassette

The exchange method was used as described in Materials and Methods. Specifically, pXLS06 was electro-transformed into ZAP1213 and cultured at 30°C on LB-CAM plates separately. Ten transformants were then inoculated into pre-warmed LB-CAM at 42 °C and passaged repeatedly in LB-CAM broth at 42 °C to obtain co-integrates. The culture was further passaged at 30 °C in LB-KAN broth in which the exchange of the LEE1 for the *sacBkan* cassette was carried out. The correct replacement strain was determined by KAN resistance and CAM sensitivity. Further confirmation was carried out by PCR with primer pairs 5-*LEE1* test and 3-*LEE1* test for inside of the LEE1 promoter; 5-SacB and 3-SacB for inside of *sacBkan* cassette and 5-*LEE1* UP FR XmaI and 3-SacB for a cross junction of the *sacBkan* cassette and that specific chromosomal region (Fig. 4.25). The LEE1 promoter is absent in tested sample (Fig.4.26); the *sacBkan* cassette was present (Fig.4.27) and in the expected site in the chromosome (Fig.4.28). The resultant strain is termed ZAP1327.

A.



B.

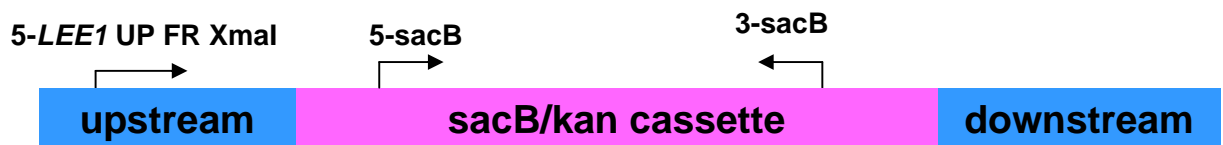


Fig. 4.25 A: Structure diagram of LEE1 promoter locus and primers in ZAP198

B: Structure diagram of *sacBkan* cassette and primers in ZAP1327

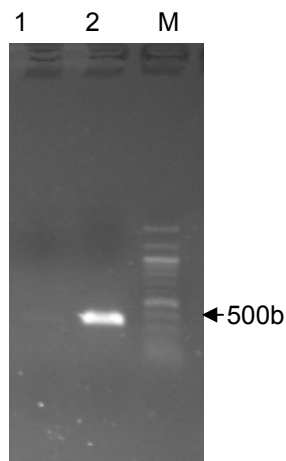


Fig.4.26 PCR for testing inside LEE1 promoter

Lane 1: Colony PCR from exchange
Lane 2: ZAP198 as a positive control
Lane M: 1 kb ladder

The expected size was 336 bp, the LEE1 promoter was absent in the tested colony from the exchange.

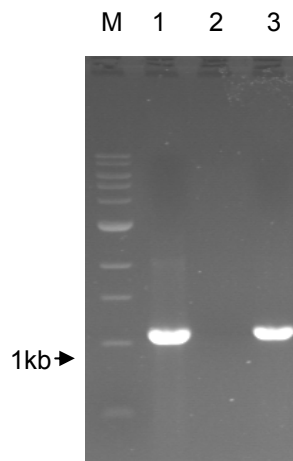


Fig.4.27 PCR for *sacBkan* cassette

Lane 1: positive control
Lane 2: negative control
Lane 3: Colony from exchange
Lane M: 1KB ladder

The expected size was 1.1 kb, the *sacBkan* cassette was present in the tested colony.

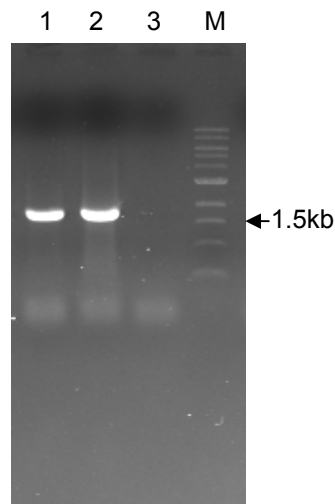


Fig.4.28 PCR for testing the junction of *sacBkan* cassette

Lane 1: colony from exchange
Lane 2: plasmids for exchange as a positive control
Lane 3: negative control
Lane M: 1kb ladder

A right size was obtained compared to the positive control indicating *sacBkan* cassette was exchanged in the loci of LEE1 promoter.

4.2.3.3 The second exchange: the exchange of the *sacBkan* cassette with *tet* promoter (Step 4, Fig. 4.2)

To exchange the the *sacBkan* cassette for the *tet* promoter, one plasmid for each construct was made based on pXLS04 and pXLS05. Then these two plasmids were used for exchange of the *sacBkan* cassette with the *tet* promoter in the intermediate strain.

4.2.3.3.1 The construction of plasmids suitable for the exchange of the *sacBkan* cassette with *tet* promoter

The *tet* promoters were PCR synthesized by using primer pairs 5-Tet promoter BamHI 1st 3-Tet promoter BamHI 1st and 5-Tet promoter BamHI 2nd and 3-Tet promoter BamHI 2nd. The PCR fragments for the two constructs are shown in Fig.4.29. These two PCR fragments were digested by *BamH* I and cloned into pXLS04 and pXLS05 respectively. The insertions were confirmed by PCR using primers flanking the cloning site on PIB 5-PIB test and 3-PIB test (Fig.4.30 and Fig.4.31). For the first construction, the sequencing result was 100% as expected from the design. The resultant plasmid for the first construction was termed pXLS07. However there was 1 bp missing in the second amplified *tet* promoter. Several further attempts were made to produce this construct but were unsuccessful. Another approach included cloning the product in a DH5 α Z1 strain containing Tet repressor to limit any expression from this promoter, but even in this case there were changes from the anticipated sequence, usually based around the sequences encoding the *tetO2* when the sequences were obtained. This operator is bound by TetR as described above.

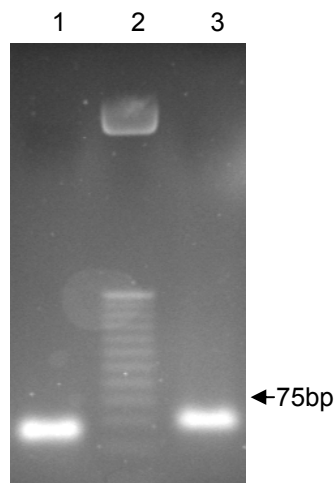


Fig.4.29 PCR for Tet promoter synthesis
 Lane 1: Tet promoter for the 1st construction, 56bp, lane 2: 25 bp ladder,
 lane 3: Tet promoter for the 2nd construction, 77bp
 PCR products of the anticipated size were obtained.

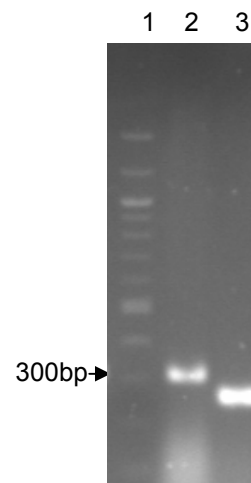


Fig.4.30 PCR for testing Tet promoter cloning for 1st construcion
 Lane 1: 100 bp ladder
 Lane 2: tested colony sample (315bp)
 Lane 3: negative control (259 bp)
 The positive sample contained a product of the expected size.

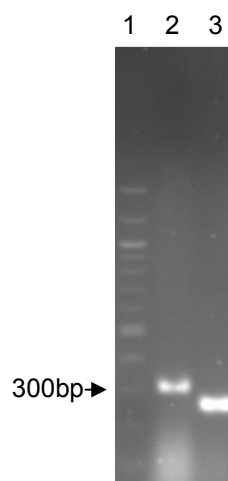


Fig.4.31 PCR for testing Tet promoter cloning for 2nd construcion
 Lane 1: 100 bp ladder
 Lane 2: tested colony sample (319bp)
 Lane 3: negative control (253 bp)
 The size from the positive sample was as anticipated.

4.2.3.3.2 The exchange of the *sacBkan* for the *tet* promoter

To replace the *sacBkan* cassette with the *tet* promoter, pXLS07 was electroporated into ZAP1213 that contains the LEE1 promoter replaced by the *sacBkan* cassette. The exchange was carried out as described in Materials and Methods. The resultant colonies were screened by PCR with primer pair 5-SacB and 3-SacB (Table 5) for inside of the *sacBkan* cassette, primer pair 5-Tet promoter BamHI 1st and 3-Tet promoter BamHI 1st (Table 5) for *tet* promoter (Table 5), primer pair 5-Tet promoter BamHI 1st and 3-*LEE1* down FR XbaI cross junction of *tet* promoter and chromosome (Fig. 4.32). The PCR results indicated that one colony had lost the *sacBkan* cassette (Fig. 4.33) and acquired PN25&*tetR* (Fig. 4.34). The results from a PCR across the junction of the *tet* promoter and the chromosome confirmed the exchange (Fig. 4.35). Another plasmid containing the *tet* promoter with LEE1 promoter flanking regions in pIB 307 for the second construction was also electro-transformed into ZAP1213 and the same exchange process was carried out.

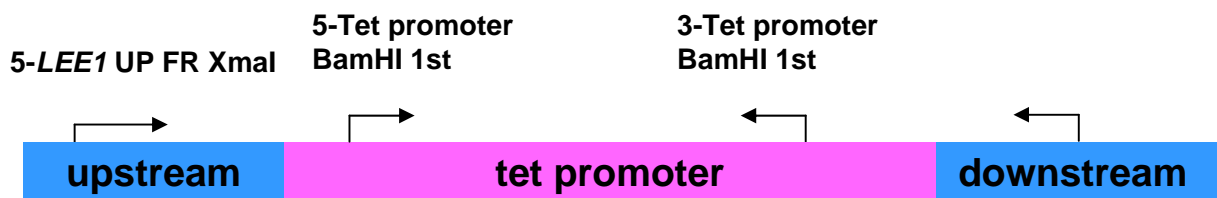


Fig. 4.32 Structure diagram of *tet* promoter and primers in ZAP1327 with LEE1 promoter replaced by *tet* promoter

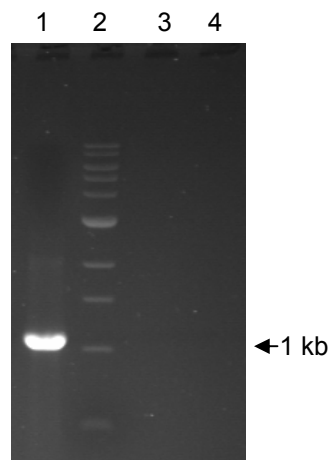


Fig.4.23 PCR for *sacBkan* cassette for exchange *sacBkan* cassette for *tet* promoter
 Lane 1: positive control
 Lane 2: 1 kb ladder
 Lane 3: negative control
 Lane 4: sample from exchange. The *sacBkan* cassette was absent in the tested strain.

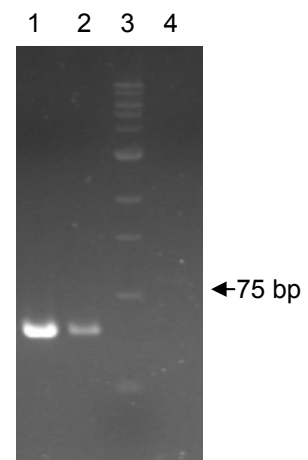


Fig. 4.34 PCR for *tet* promoter
 Lane 1: sample from exchange
 Lane 2: positive control
 Lane 3: 25 bp ladder
 Lane 4: negative control
 The *tet* promoter was present in the tested colony.

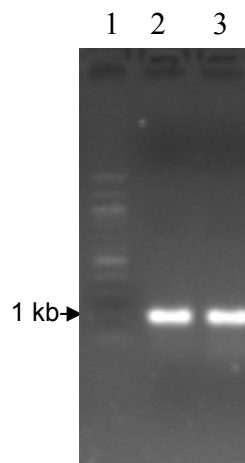


Fig. 4.35 PCR crossing junction of *tet* promoter and chromosome
 Lane 1: 1 kb ladder
 Lane 2: positive control
 Lane 3: sample from exchange
 Tested colony showed a 992 bp PCR fragment was obtained with a positive control.

4.2.3.4 Testing induction of the *tet* promoter in ZAP1213 with the LEE1 promoter replaced by the two *tet* promoter constructs

The resultant strains with the LEE1 promoter exchanged for the *tet* promoter controlled by the *tet* repressor was achieved as described above. To test the *tet* promoter induction, 200ng/ml aTC was added to the MEM-HEPES cultures. The secreted proteins samples were prepared as described in Materials and Methods. Results from SDS-PAGE gel (Fig. 4.36) and anti-EspD (Fig. 4.37) Western Blotting showed that there was no increase of T3S with aTC induction in the constructed strain for the first construct compared to the wild type. Similarly, the strain for the second construction also showed no increase with aTC induction.

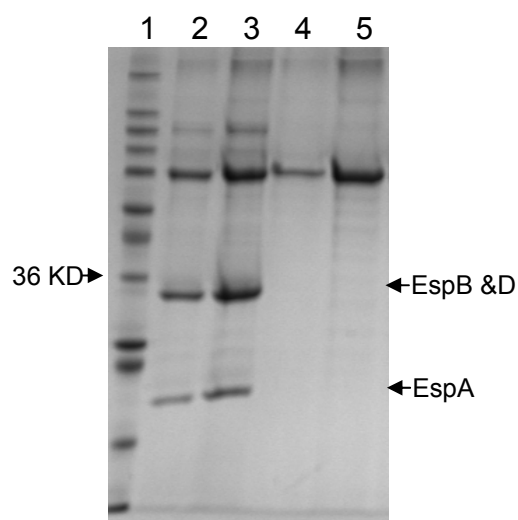


Fig. 4.36 SDS-PAGE gel results

Lane 1: wide range Marker
 Lane 2: ZAP198
 Lane 3: ZAP198 with aTC
 Lane 4: sample strain
 Lane 5: sample strain with aTC
 No T3S protein was found with aTC induction in sample strain.



Fig. 4.37 Anti-EspD Western Blotting results

Lane 1: ZAP198
 Lane 2: ZAP198 with aTC
 Lane 3: sample strain
 Lane 4: sample strain with aTC
 No EspD protein was detected by anti- EspD Western Blotting

4.2.4 The control of T3S in ZAP1327

I was very upset about the unsuccessful induction of T3S in the first construction, because it took me a lot of time in my PhD journey. With this disappointed mood, I didn't keep this final strain (LEE1 promoter first construction). Otherwise, more work such as using RT-PCR to measure the transcriptional level of *ler* could be carried out in the future. But based on the results produced by my colleagues described below, the final exchange might be repeated to get the strain of first construction as long as the constructed plasmids were stored. However, interesting result was found by other colleagues in the intermediate strain I made as detailed below. The control of T3S in ZAP1327 (ZAP198 with LEE1 promoter replaced by *sacBkan* cassette) described as above in Section 4.3.2 was investigated by three experiments including measuring LEE1 promoter activity by pLEE1-GFP reporter (this measurement was carried out by Maryia Karpiyevich), determining the *ler* transcriptional expression levels by RT-PCR (this work was done by Jai Tree), examining the EspD secretion level by Western blotting (this work was done by Allen Flockhart). LEE1 promoter transcriptional activity was high compared to the negative control (pKC26) in ZAP1327 (Fig. 4.38). The T3S regulator, ECs1581 showed a higher *ler* expression. This was confirmed by the RT-PCR measurement of *ler* transcriptional expression in ZAP1327 with a low expression of *ler* detected in ZAP1004 (Ler deletion mutant) (Fig. 4.39). It was demonstrated that *sacBkan* cassette controlled *ler* transcription expressed in an equivalent level to the wild type (ZAP198). However, no EspD was detected in ZAP1327 (Fig. 4.40). This *sacBkan* controlled Ler expression can be overridden by adding *ler* plasmids (with *ler* ORF inserted) (Fig. 4.40).

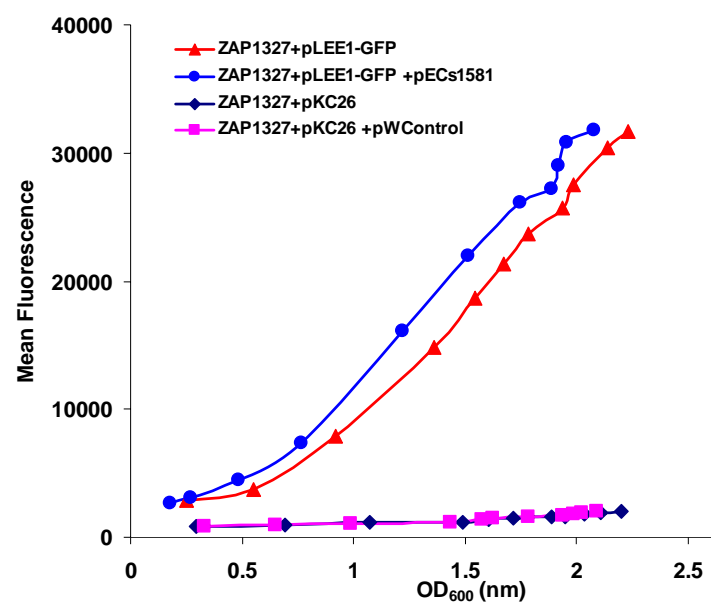


Fig. 4.38 Measurement of LEE1 promoter activity in ZAP1327

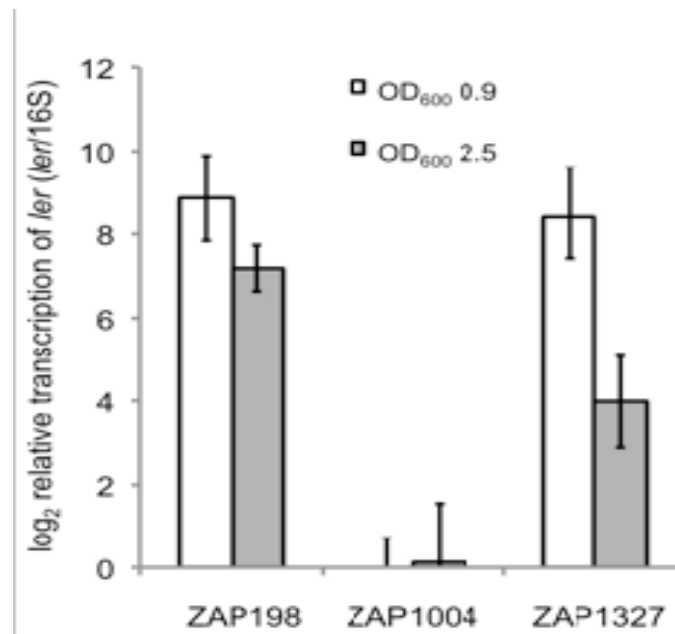


Fig. 4.39 RT-PCR measurement of *ler* expression levels in EHEC strains ZAP198, ZAP1004 and ZAP1327

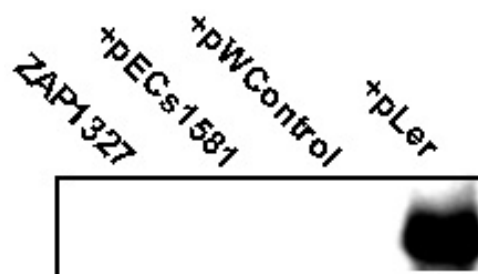


Fig. 4.40 Western blot of EspD secretion in ZAP1327 with and without Ler

4.3 Discussion

From genome analysis it is evident that EHEC strains contain a number of prophages and degenerated prophage regions that contribute to pathogenesis and host colonisation (Hayashi *et al.*, 2001; Perna *et al.*, 2001). EHEC are defined by the expression of Shiga toxins, encoded from integrated prophages, and the delivery of effector proteins via a type III secretion (T3S) system that is expressed from a degenerate prophage element, the locus of enterocyte effacement (LEE). The T3SS is essential for forming intestinal attaching and effacing (A/E) lesions allowing colonization of intestinal epithelium in ruminant hosts and in humans. The LEE possesses five main operons (LEE1-5) (Elliott *et al.*, 1998). *LEE1-3* encodes components of the basal apparatus of the T3SS including EscC, J, R, S, T, U, V (Bustamante *et al.*, 2001; Garmendia *et al.*, 2005; Sperandio *et al.*, 2003), the CesAB chaperone and the EspH effector (EPEC EHEC LEE1). LEE4 encodes the translocon proteins plus SepL (Kresse *et al.*, 2000) and EscF (Wilson *et al.*, 2001); and LEE5 encodes an outer membrane adhesin called intimin, its translocated receptor Tir, and a chaperone known as CesT for intimin (Sanchez-SanMartin *et al.*, 2001).

There are multiple regulatory inputs that govern the expression of T3S involving environmental sensing and regulators that act on these signals by activating or repressing transcription (Laaberki *et al.*, 2006). Most of the published regulation feeds into the promoter of the LEE1 operon and is passed through to the expression of the other LEE operons by the LEE-encoded regulator (Ler). The LEE1 regulatory region is controlled by many regulators, including IHF, Fis, H-NS, QseA, BipA, GadX, DksA, Hha, EtrA, EivF and Pch together with Ler itself (Hansen & Kaper, 2009; Mellies *et al.*, 2007) (Tree *et al.*, 2009b) (Kendall *et al.*, 2010). The nucleoid-associated protein H-NS, a global inhibitor of virulence-related genes in Gram negative bacteria, represses the expression of LEE1 which is particularly apparent at temperatures below 30°C. H-NS also negatively regulates LEE2 through LEE5 promoters in a temperature-independent way. However this effect is overcome by the related Ler protein (Bustamante *et al.*, 2001; Sanchez-SanMartin *et al.*, 2001) (Umanski *et al.*, 2002), and in turn has multiple inputs into the rest of LEE regulation. A second nucleoid-associated protein, integration host factor, IHF,

activates the expression of LEE1-3 and LEE5 by directly binding to the *ler* promoter and is essential for efficient expression of LEE (Friedberg *et al.*, 1999). Another nucleoid-associated protein (Fis), is also required for LEE1 expression. However this regulation by Fis was not transmitted to the rest of the downstream LEE operons (Goldberg *et al.*, 2001). As the first gene of LEE PAI, *Ler*, is a regulator related to the H-NS family of nucleoid-associated proteins, which therefore activates the expression of LEE2, LEE3, LEE5 ((Elliott *et al.*, 2000; Friedberg *et al.*, 1999; Mellies *et al.*, 1999; Sperandio *et al.*, 2000). In addition, *GrlR* and *GrlA*, encoded by a bi-cistronic operon *grlRA* located between LEE1 and LEE2, positively regulate the expression of LEE operons through *Ler* expression (Barba *et al.*, 2005; Deng *et al.*, 2004) (Jimenez *et al.*, 2010). Taken together it is apparent that many regulators and signals which affect T3S do so through LEE1 and in particular *Ler* expression.

Previous work has demonstrated that T3S in EHEC O157:H7 can be controlled at LEE4 in a post-transcriptional manner and that clear differences in this regulation occur between strains and may be important in the epidemiology (Naylor *et al.*, 2005). If expression can be controlled or fixed at LEE1 then this will allow assessment of how independent this LEE4 regulation is and may help define the regulatory mechanism, especially if LEE1 can be induced. Therefore, the aim of this study is to construct an inducible T3SS by controlling LEE1 promoter with a TetR-aTc system. In addition, it is proposed that the multiple regulatory inputs into the LEE may be an important factor in driving the rectal tropism in cattle. So quorum sensing in the large bowel (as high density of bacteria) plus sensing of specific ions, pH, oxygen tension and possibly particular carbohydrate sources, all may contribute flowing through LEE1 to switch on T3S, and then access to the rectal mucosa may be easiest on epithelium associated with lymphoid follicles so have M-like cells with less mucus coverage. So, if T3S expression can be induced constantly or earlier in the gut, rectal tropism might be changed. aTc could be used in an animal so possible with the construct being made here.

In *Yersinia*, the timing of T3S induction can be studied by altering the calcium concentration so that you can get a 'synchronized' culture allowing dissection of the

regulation (Torruellas *et al.*, 2005). For EHEC, there is no established single transition signal (perhaps not surprising given the points being made in 1 and 2 about multiple inputs), so again an inducible LEE1 construct would provide insights into the temporal regulation of T3S in EHEC.

In most *E. coli* promoters, the key sequences required for activity are the -10 and -35 hexamer elements, which are recognized by different domains of the RNA polymerase factors (McClure, 1985). The binding of transcription factors, DNA helicase, RNA polymerase, activators and repressors with this core promoter initiates transcription and in turn translation. Thus if this promoter is controlled 'manually', the expression of LEE can be controlled artificially. In this work, two constructs to replace the LEE1 promoter were designed in order to be able to induce LEE1 expression. The first construct keeps the original transcriptional start site and -10 region of LEE1 operon promoter, while the -35 region will be replaced by AT rich DNA sequence (*tet promoter*) synthesized artificially (Fig. 4.18). For the second construct, only the original transcriptional start site will be kept with -35 and -10 regions replaced (Fig. 4.19).

As shown in results, a strain containing the first construct strain was achieved. However, when induction with aTc was tested in this no T3S was detected by comparison with wild type levels. Relief of repressor activity was proven in this strain by demonstrating aTc induction of GFP from pXLS03 in ZAP1213 (Tet repressor exchanged at lac). One explanation for the failure to induce detectable T3S levels may lie with expression levels. For GFP expression, the plasmid copy number will be 15-20 (Sambrook, 1989) So increased GFP measurement was detected indicating increased expression of *tet* promoter in .Potentially, the levels of mRNA produced from the LEE1 promoter were too low to give enough translated products leading to detectable T3S. A second possibility can be due to the unspecific binding or interaction of aTc with other chemicals or reagents other than Mg⁺ in O157 background. This unspecific reaction might block the release of TetR repression. Therefore, aTc induction can not be achieved as planned and in turn T3S was not detected.

Another possibility might be the construction issue, i.e. the specific promoter sequence used. As described above, the original -10 region sequence was kept in the first construct. It indicated that the original repression by H-NS and other factors still existed and was passed to the promoter including -10 element. This promoter could control the expression of LEE and T3S causing undetectable level in the constructed strain even after inducing with aTc. A fourth reason why the first construction did not work might be the natural regulation of T3SS. Because a post transcriptional regulation after LEE1 promoter exists (Roe *et al.*, 2003b), T3S expression level still can not be detected even with fully induced *tet* promoter.

In the process of trying to obtain the second promoter region, mutations were always found in the inserted *tet* promoter which was cloned into pIB307 with both flanking regions of the original LEE1 promoter. It indicated that this *tet* promoter can't be expressed, or maybe even cloned, in the vector with both LEE1 flanking regions which include the regulator Ler protein. One reason might be that the deleted -10 and -35 hexamer elements led to the uninhibited expression of T3S causing toxic cell effect. In the absence of -10 and -35 elements, the expression of Ler, which is located down stream of *tet* promoter cloning site, might be very high. As an essential regulator, it can lead to enormous influence which might include toxic biological effect to the bacteria. In addition, *tet* promoter is a high activity promoter (Lutz & Bujard, 1997) with an increase of 5000 fold when the repression is released by aTc. Such a high expression of T3S proteins must be toxic to cells. Thus, in the process of cloning *tet* promoter into pIB307 with both flanking region of LEE1 promoter, no successful vector was selected.

Although the control of T3S in the obtained strain for the first construct did not induce detectable T3S levels and the construction of the strain with the designed 2nd construct could not be achieved, there is significant application for these and future application of the constructs.

For example, lab colleague, Allen Flockhart (Mariya, Jai Tree as well) used the intermediate strain, ZAP1327 (LEE1 promoter replaced by *sacBkan* cassette), to identify

the mechanism of the phage regulator, ECs1581, effect on LEE and LEE1 promoter. From the results of three experiments as described in Section 4.5, it was demonstrated that comparatively high transcriptional level of LEE1 promoter (*sacBkan*) was found in ZAP1327. However, the secretion level of T3S proteins was not detectable in ZAP1327. This indicated that the translation level of T3S proteins keeps low even with an equivalent transcriptional LEE1 promoter expression level to the wild type. However, this control of *sacBkan* on T3S can be overridden by the present of Ler (plasmids of *ler* containing the ORF of *ler*). As the original -10 region and transcriptional start site were kept, the transcription of *ler* could not be induced any further, because a comparatively high transcriptional *ler* expression was found in ZAP1327 and the LEE1 regulatory region it normally auto-induces is no longer there. It implied that additional factors or regulation is required at post transcription level of *ler* to switch on T3S. The resultant strain should be controlled by aTc as expected. Surprisingly, no detectable T3S protein was found with aTc induction in the first construction. However, it could still be the case that the *tet* promoter was being induced but that this did not result in T3S for reasons that are not currently understood. That is might be one of the reasons why no T3S proteins were detected in the first construction with aTc induction.

In addition, ZAP1213 (*lacY* and *lacZ* genes replaced by Tet repressor) can also be used for other inducible constructions. Future work can address to resolve the difficulties in cloning *tet* promoter in front of *ler* or find substitute promoter for *tet* promoter. For example, the λ Red recombineering technology can be used to exchange the LEE1 promoter with *tet* promoter. Briefly, an antibiotic cassette plus *tet* promoter with a short flanking region of LEE1 promoter will be designed. An anticipated strain with LEE1 promoter replaced by *tet* promoter with antibiotic cassette will be created. In this method, LEE1 promoter will be exchanged with *tet* promoter directly without any cloning needed. Another way is to find another promoter as a substitute for the *tet* promoter.

5 Chapter V Phage Regulation of T3S

5.1 Introduction

Bacteria such as *E. coli* that colonise the mammalian gastrointestinal tract are exposed to a constant onslaught of bacterial viruses, known as bacteriophages (Kaper *et al.*, 2004). Many bacteriophages inject their genetic material and use the bacterial host simply to produce more phage in a lytic cycle. Other, temperate phages, can insert their genetic material into the bacterial genome (Hacker *et al.*, 1997; Kaper *et al.*, 2004; Lim *et al.*, 2010). In this lysogenic state the phage genome is amplified along with the dividing bacteria (Friedman & Court, 2001). Lysogenic phages have evolved to initiate their replication and escape from the bacterial host by using the stress or SOS response of the bacterium (Waldor & Friedman, 2005). The integration of phage genomes and their subsequent degeneration is important in the evolution of many bacterial genera, for example *Salmonella*, *Staphylococcus* and *Escherichia* (Boyd & Brussow, 2002), (Brussow *et al.*, 2004).

Enterohaemorrhagic *Escherichia coli* (EHEC) are a subset of *E. coli* strains defined by the integration of lambdoid bacteriophages into their genomes that encode Shiga toxin (Stx) (Ogura *et al.*, 2009) and the capacity of the strains to form characteristic attaching and effacing lesions on epithelial cells in the gastrointestinal tract as a result of type III secretion of effector proteins (Kenny *et al.*, 1997; Kenny & Jepson, 2000; Nataro & Kaper, 1998). The different Stx types belong to a family of A₁B₅ exotoxins comprising of a single A subunit that is non-covalently associated with pentameric B subunits that are responsible for toxin binding to its receptor, the glycosphingolipid Gb3 (globotriaosylceramide; CD77) (Lindberg *et al.*, 1987; Lingwood, 1999; Sandvig, 2001).

The A subunit of Stx is an N-glycosidase which cleaves the N-glycosidic bond of a specific adenine residue of the 28S rRNA in the 60S ribosomal subunit. This inhibits protein synthesis by interfering with the elongation factor 1-dependent binding of aminoacyl-tRNA to the 60S ribosomal subunit (Law, 2000). Severe EHEC infections in humans are characterised by bloody diarrhoea and capillary damage in the kidneys and brain as a result of Stx activity with potential fatal consequences or long term morbidity (Kaper *et al.*, 2004; Proulx F, 2001; Tarr *et al.*, 2005).

Humans though are an incidental host for the majority of EHEC strains and it is apparent that ruminants (Cherifi *et al.*, 1994; Hancock *et al.*, 1994), in particular cattle are the main reservoir for the principle EHEC serotypes associated with human infection, in particular EHEC O157:H7 and EHEC O26:H11 (Geue *et al.*, 2009; Orskov *et al.*, 1987). The success of the organism therefore needs to be considered in the context of the ruminant host in terms of selective factors that drive its evolution. In contrast to the situation in humans, there is little evidence for pathology associated with EHEC infection in mature, immuno-competent cattle or other reservoir hosts which typically carry EHEC asymptomatically (Chapman *et al.*, 1993; Synge, 2000). This is related, in part, to differences in Gb3 receptor distribution in cattle versus humans and differences in how internalised toxin is trafficked in the cell (Hoey *et al.*, 2002; Hoey *et al.*, 2003) (Pruimboom-Brees *et al.*, 2000). If phage insertion can confer an advantage to the bacterium then this will also increase the survival chances of the integrated phage DNA. Studies on Shiga toxin activity have provided some insight into possible benefits for EHEC in the ruminant host, even though a subset of the bacteria must lyse to release the toxin. Advantages for colonisation include the redistribution of nucleolin to the epithelial cell surface where it aids bacterial attachment via interaction with the bacterial outer membrane protein intimin (Robinson *et al.*, 2006). Stx has also been shown to have immuno-modulatory functions, including the suppression of inflammatory responses and repression of B cell/T cell proliferation (Gu *et al.*, 2009; Neal *et al.*, 2011; Rojas *et al.*, 2010).

Epidemiological studies have shown that particular strain types emerge that are more likely to be associated with human disease. In the USA, Clade 8 is associated with more serious human disease (Manning *et al.*, 2008) and in Europe particular phage types are more commonly associated with human infections (Pearce *et al.*, 2009). In a previous study, Chase-Topping *et al* (Chase-Topping *et al.*, 2007b) investigated fecal pat samples from 481 farms throughout Scotland for the presence of *E. coli* O157:H7. Three main phage types were identified, 21/28 (46%), 32 (19%), and 8 (12%). Previous research had shown that cattle colonized at the terminal rectum can shed bacteria at higher levels than transient colonization, leading to the concept of ‘super-shedders’. Low or high-level shedding was defined by whether the *E. coli* O157 counts were below or above 10^3 CFU g⁻¹ feces respectively. PT 21/28 strains were more likely to be associated with high shedding and PT 32 with low-level shedding samples. PT 21/28 strains are the predominant type associated with human infection in the UK (Chase-Topping *et al.*, 2008). The initial aim of this study was to identify genetic differences between PT 21/28 and PT32 strains. The research indicated that Stx bacteriophage carriage was different between the two as was the regulation of T3 secretion. This led us to determine the impact of Stx phage lysogeny on T3S regulation in EHEC with the conclusion that the bacteriophage usurps control of this essential colonization factor and propose that this modulation further limits immune stimulation and recognition in the host animal.

5.2 Results

5.2.1 Comparative genomic hybridization of PT 21/28 and PT 32 strains

In order to investigate genomic differences between the two phage types, twelve strains (six of each type) were analyzed by comparative genomic hybridization (CGH) as detailed in Materials and Methods. The strains were chosen to include the variation in type III secretion (T3S) profiles apparent by colloidal blue staining of culture supernatants and strains originating from faecal pats with both high and low bacterial counts. Full details of the strains are provided in Tables 5.1. While multiple differences in gene content were identified between the phage types, the most consistent difference

was in hybridization to the Stx2 bacteriophage immunity region, with 1/6 PT32 strains showing hybridization to this region and 6/6 PT21/28 strains (Table 5.1). The array design is based on the *E. coli* O157:H7 Sakai sequence (Table 5.1), which contains both Stx1 and Stx2 phages but not the Stx2c phage.

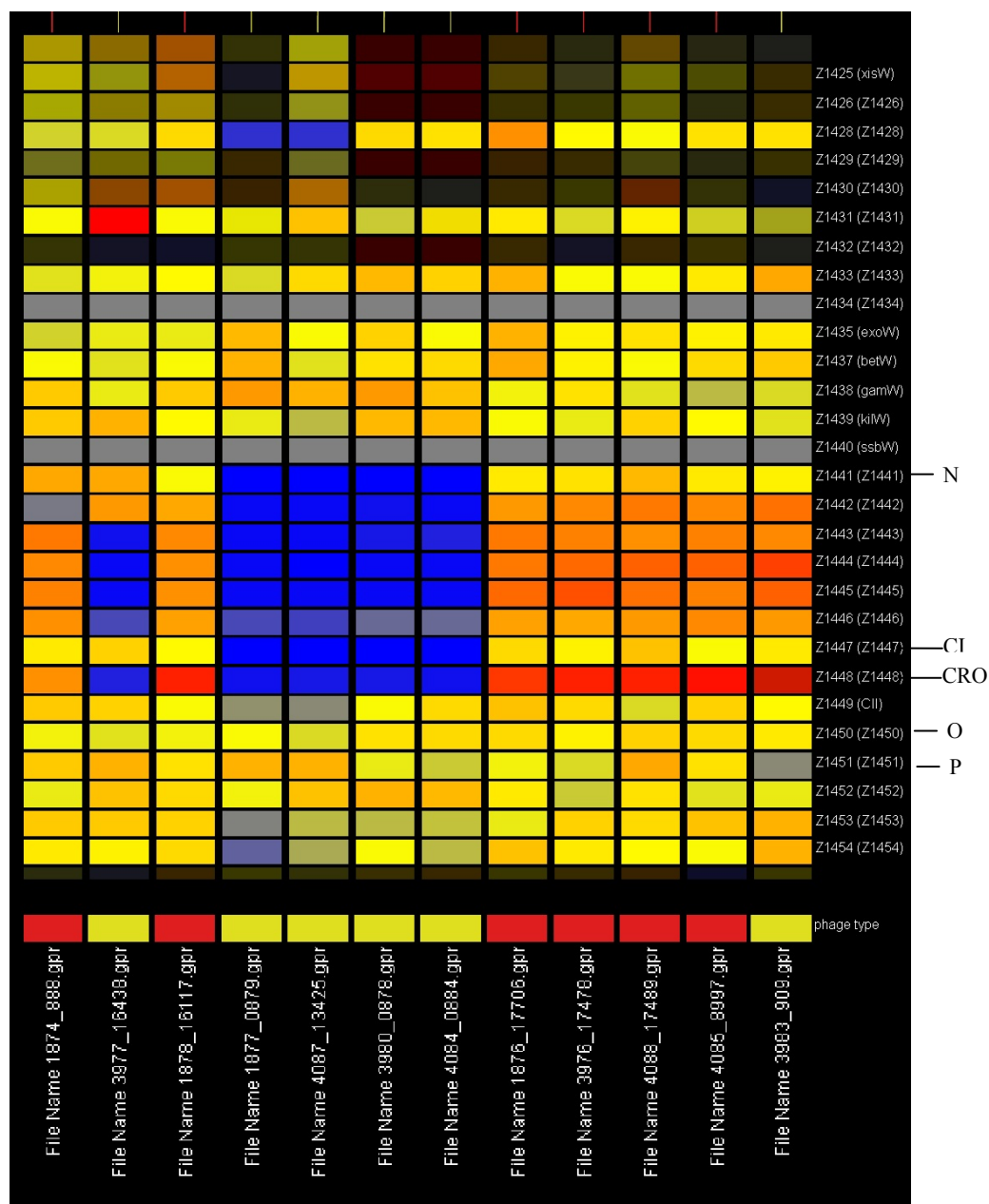


Fig. 5.1 Analysis of CGH data for Stx2 phage for PT 21/28 and PT 32 (Jai Tree)

Upper panel: The copy number of each gene increased in the order of blue, grey, yellow and red. Blue indicates absence of gene. Gray means lower copy number than Sakai. Yellow indicates similar copy as Sakai. Red means higher copy number than Sakai. Bottom panel: PT 32 was indicated in red with PT/28 in yellow. The numbers shown in the bottom are strain numbers.

5.2.2 Identification of Stx2 and Stx2c phage

Previous characterization of the strains had already determined that they all contained at least one type of Stx2 phage (IPRAVE study), so to investigate whether Stx2 vs Stx2c prophages could account for the hybridization differences, genomic DNA preparations from strains (n=62) were analyzed for these prophages by PCR (Materials and Methods). While the majority of all the strains analyzed contained the Stx2c prophage (87%), the main difference was in the distribution of the Stx2 prophage. With respect to strains isolated from cattle, PT 21/28 strains were more likely to contain Stx2 compared to PT 32 strains ($P<0.01$) (Table 5.1). However, PT 32 strains from humans were more likely ($p=0.01$) to contain Stx2 than the PT 32 bovine isolates (75% versus 25%), while the majority of 21/28 strains from either source contained Stx2 (Table 5.1). This indicates that PT32 strains associated with human disease appear more likely to be lysogenized with Stx2 phage and PT21/28 strains, which are the main human disease associated phage type in the United Kingdom, generally harbor both Stx2 and Stx2c phages.

Table 5.1 EHEC O157:H7 PT21/28 and PT32 strains and properties

Source	Phage Type	Fecal count (CFU)	Super-shedder >1000 CFU	LEE1-GFP (RFU)	Stx1	Stx2	Stx2c
Bovine	21/28	<50	no	7692	-	+	+
Bovine	21/28	<50	no	11923	-	+	+
Bovine	21/28	<50	no	12692	-	+	+
Bovine	21/28	<50	no	15000	-	+	+
Bovine	21/28	<50	no	3078	-	+	+
Bovine	21/28	300000	yes	5000	-	+	+
Bovine	21/28	686400	yes	6154	-	+	+
Bovine	21/28	150000	yes	10769	-	+	+
Bovine	21/28	384000	yes	12692	-	+	+
Bovine	21/28	269200	yes	12692	-	+	+
Bovine	21/28	77600	yes	24615	-	+	+
Bovine	21/28	16100	yes	NT	-	+	+
Bovine	21/28	59300	yes	5385	-	+	+
Bovine	21/28	11500	yes	NT	-	+	+
Bovine	21/28	42400	yes	10385	-	+	+
Bovine	21/28	150000	yes	NT	-	+	-
Bovine	21/28	46000	yes	NT	-	+	+
Bovine	21/28	21000	yes	NT	-	+	+
Bovine	32	36150000	yes	28461	-	+	+
Bovine	32	NK	unknown	20000	-	-	+
Bovine	32	<50	no	20385	-	-	+
Bovine	32	<50	no	18846	-	-	+
Bovine	32	<50	no	16923	-	-	+
Bovine	32	<50	no	16923	-	+	-
Bovine	32	900	no	NT	-	-	+
Bovine	32	<50	no	14231	-	-	+
Bovine	32	<50	no	12692	-	-	+
Bovine	32	<50	no	21538	-	-	+
Bovine	32	<50	no	NT	-	-	+
Bovine	32	<50	no	19230	-	-	+

Bovine	32	<50	no	NT	-	+	+
--------	----	-----	----	----	---	---	---

Bovine	32	119600	yes	28845	-	+	+
Bovine	32	<50	no	13078	-	-	+
Bovine	32	<50	no	NT	-	-	+
Bovine	32	<50	no	NT	-	+	+
Bovine	32	<50	no	13846	-	-	+
Bovine	32	<50	no	11923	-	-	+
Bovine	32	<50	no	13846	-	-	+
Human	21/28	-		13461	-	+	+
Human	21/28	-		NT	-	+	+
Human	21/28	-		NT	-	+	+
Human	21/28	-		NT	-	+	-
Human	21/28	-		NT	-	+	+
Human	21/28	-		NT	-	+	-
Human	21/28	-		NT	-	+	+
Human	21/28	-		NT	-	+	+
Human	21/28	-		NT	-	+	+
Human	21/28	-		NT	-	+	+
Human	21/28	-		NT	-	+	+
Human	21/28	-		NT	-	+	+
Human	32	-		36155	-	+	-
Human	32	-		20385	+	-	+
Human	32	-		NT	-	-	+
Human	32	-		NT	-	+	+
Human	32	-		NT	-	+	-
Human	32	-		NT	-	+	+
Human	32	-		NT	-	+	+
Human	32	-		NT	-	+	-
Human	32	-		NT	-	+	+
Human	32	-		NT	-	-	+
Human	32	-		NT	-	+	+
	32			NT	-	+	-

5.2.3 T3S levels in PT 21/28 and PT 32 strains

5.2.3.1 EspD and EscJ levels in PT 21/28 and PT32 strains

The secretion profiles of thirty strains of each phage type were analyzed, including Western blotting for the translocon protein EspD (a subset of strains is shown in Fig 5.2). From these initial profiles it was evident that more PT32 strains were secreting higher levels of EspD. The strains also produced variable levels of EscJ, with higher levels of the T3S apparatus protein EscJ correlating with higher levels of EspD secretion (Fig 5.2). Anti-RecA blotting was used as control for lysis. A same level of RecA from whole cell preparation indicated a similar level of lysis.

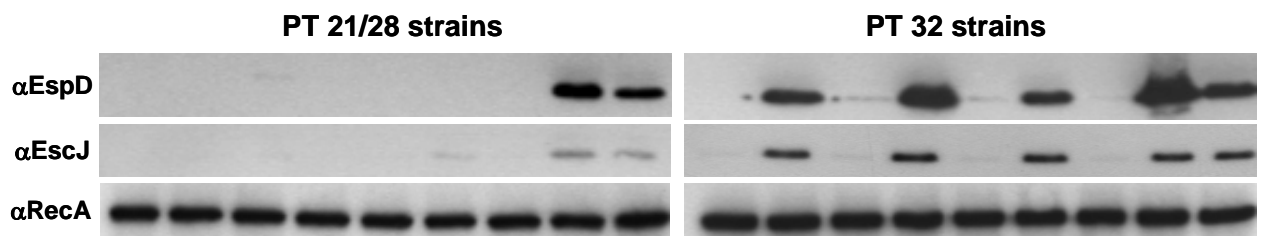


Fig. 5.2 Western blot analysis of a subset of PT21/28 and PT32 strains.

EspD was detected from bacterial supernatants and EscJ and RecA from whole cell samples prepared as described in Materials and Methods.

5.2.3.2 LEE1 promoter expression levels in PT 21/28 and PT32 strains

In order to quantify any differences in the expression of the T3S system in the two phage types, a subset of the strains (n=31) were transformed with a LEE1::egfp reporter construct (Roe *et al.*, 2003b). Fluorescence levels were then measured for the different strains during standard growth curves. For statistical analyses, fluorescence values were determined from multiple experiments for $OD_{600} = 1.0$ (Table 5.1). PT32 strains had a significantly higher median level of expression compared to the PT21/28 strains (Fig 5.3). As an alternative analysis, strains exhibiting expression levels over the mean of 13,000 fluorescence units were grouped separately from those with lower values. On this basis, PT32 strains were more likely to express the LEE1 fusion at higher levels than the PT21/28 strains ($p < 0.01$), consistent with the secretion profiles and Western blotting data.

There was no correlation between T3S expression and single point shedding levels of the strain obtained from the faecal pat at the time of sampling (Table 5.1).

Based on the observation that PT 21/28 was more likely to contain two types of Stx2 phage (Stx2 and Stx2C) and generally demonstrated lower levels of T3S, we compared LEE1 expression levels with Stx2 and Stx2c carriage. Strains containing both Stx2 and Stx2c phages were significantly more likely ($p=0.016$) to have lower LEE1 expression levels than strains containing just one Stx2 phage (Fig 5.4). All bar one of these strains did not contain a Stx1 phage.

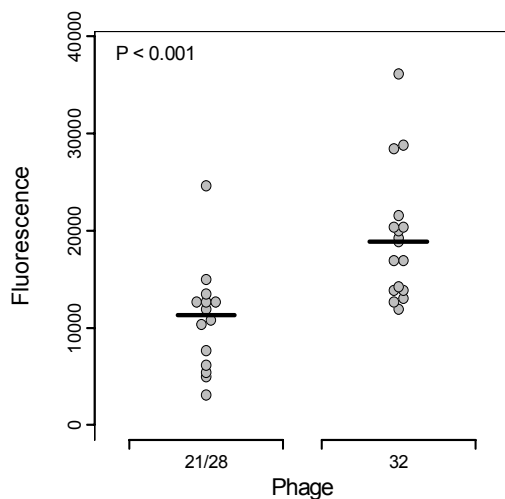


Fig. 5.3 Relative fluorescence levels from a LEE1-GFP reporter construct transformed into 20 PT21/28 and 20 PT32 strains with levels measured at $OD_{600}=1$ (produced with collaboration with David Gally). The median level of fluorescence from the PT32 strains is significantly higher than for the PT21/28 ($p<0.001$), the variability in expression levels correlates with the Western blotting data in part Fig 5.4.

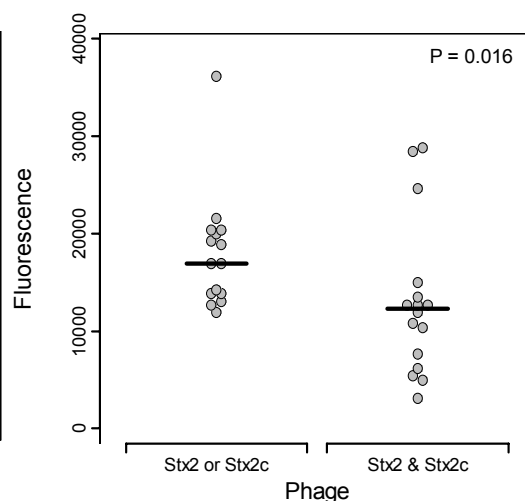


Fig. 5.4 LEE1-GFP expression levels compared between strains containing either one or both Stx2 or Stx2c prophages (produced with collaboration with David Gally). Strains containing both Stx2 phages have a significantly reduced median level of LEE1 expression determined at $OD_{600}=1$ cultured in MEM-Hepes medium.

5.2.4 Comparison of T3S expression in the presence and absence of Stx phages

5.2.4.1 Comparison of EDL933 and TUV93-0

In order to investigate whether the expression of the T3S system is repressed by the presence of Stx prophages, secretion profiles and LEE1 expression levels in pairs of EHEC strains, with and without integrated Stx2 prophages, were analyzed. The sequenced isolate EDL933 was compared with a published Stx1 and Stx2 phage-cured derivative TUV93-0 (Fig 5.5). Higher levels of EspD secretion were detected in bacterial supernatants of TUV93-0 compared with EDL933 (Fig 5.5). This correlated with higher levels of the apparatus protein, EscJ, in the whole cell fractions compared with RecA as a control (Fig 5.5). Again, to quantify this difference, the LEE1 promoter fusion was introduced into both strains. The expression in TUV93-0 was higher than EDL933 throughout the growth curve with a significance difference for values determined at $OD_{600} = 0.9$ (Fig 5.6-7). As both the EDL933 and TUV93-0 strains used have been cultured in a number of different laboratories and EDL933 was also subject to genetic manipulation during which phage excision occurred (Campellone *et al.*, 2007), there may be other genetic changes, in addition to the absence of the Stx phages, that may account for the increased level of T3S in TUV93-0. To investigate this, two approaches were taken. In the first, a Stx2 phage marked with a kanamycin resistance cassette from a derivative *E. coli* O157 Sakai strain (Sakai stx-, Table 2.1) was conjugated into TUV93-0 (This work is carried out by Sean McAteer) and EspD secretion level, EscJ expression and LEE1-GFP expression determined (Fig 5.5-6). This conjugation partially restored repression of T3S but not to the level demonstrated for EDL933. It is appreciated that

this conjugation may introduce additional non-phage DNA from the Sakai strain and also acts on a background that may already contain other genetic changes. As a second approach, another series of strains were generated from EDL933 in which the Stx2 phage and then the Stx1 phage were deleted by allelic exchange to generate another Stx phage negative derivative of EDL933. This strain also exhibited increased levels of T3S and LEE1 expression by comparison with the isogenic EDL933 parent, but at lower levels than shown for TUV93-0 (Fig. 5.5-8). Taken together, it is evident that the presence of Stx prophages in the EHEC O157 chromosome can limit T3S by repressing LEE1 expression. However, other uncharacterized changes between our laboratory stocks of EDL933 and TUV93-0 also contribute to T3S differences between these strains.

To examine if Stx phage excision has an effect on T3S in another EHEC serotype, two pairs of published *E. coli* O26:H11 strains were obtained from Dr Helge Karch (Table 2.1). Both pairs are considered isogenic apart from the presence and absence of Stx2 prophages (Mellmann *et al.*, 2008), the phages were lost during culture of the bacteria. For one pair, T3S increased significantly in the absence of Stx phage (Fig 5.5), while for the other no T3S was detectable for either strain under the conditions tested (data not shown). For the pair with detectable T3S, the LEE1-GFP reporter was transformed into both strains and levels of expression measured throughout the growth curve. Again the presence of the Stx2 phage correlated with significant repression of LEE1 expression in agreement with the Western blotting profile for EspD secretion and EscJ apparatus production (Fig 5.5).

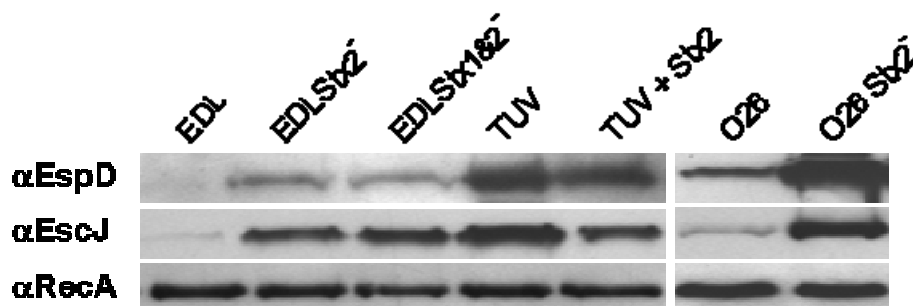


Fig. 5.5 Western blot analysis of paired *E. coli* O157 and O26 strains.

EspD was detected from bacterial supernatants and EscJ and RecA from whole cell samples prepared as described in Materials and Methods. EDL is the sequenced EDL933 strain and this was originally compared with a published Stx1/2 derived strain TUV93-0 (lane 4), which shows higher secretion levels and EscJ expression. Both Stx1 and Stx1/2 were deleted from EDL933 (lanes 2 and 3 respectively) leading to increased T3S. A marked Stx2 phage was conjugated into TUV93-0 (lane 5) resulting in a reduction in T3S and Esc expression. The final two lanes contain samples from a published isogenic pair of EHEC O26 strains from which one has lost the Stx2 phage leading to a marked increase in T3S.

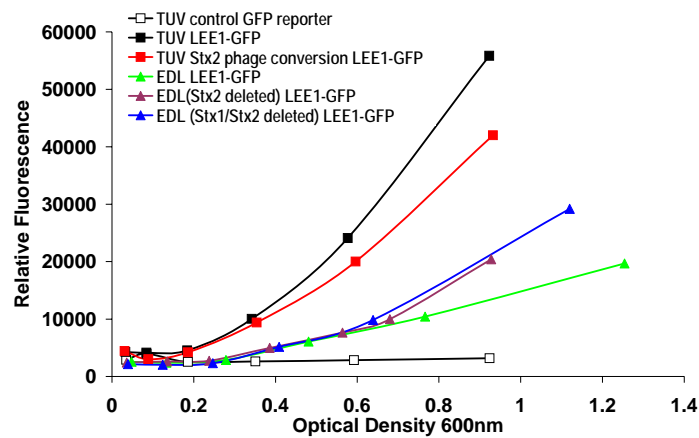


Fig. 5.6 LEE1-GFP measurement of the same strain sets as in Fig 5.5 (produced with collaboration with David Gally)

To quantify differences in T3S expression, the same strain sets as in Fig 5.5, were transformed with a LEE1-GFP construct and fluorescence measured throughout the growth curve. This was repeated three times with one experiment shown in Fig 5.6.

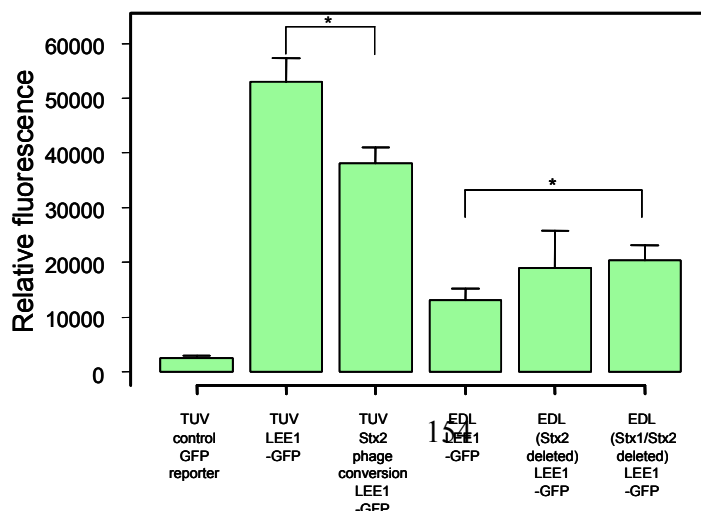


Fig 5.7 A minimum of three values were determined from the expression curves for $OD_{600}=0.9$ and plotted in Fig 5.7. $p<0.001$ for the TUV strains and $p=0.001$ for the EDL strains compared (produced with collaboration with David Gally).

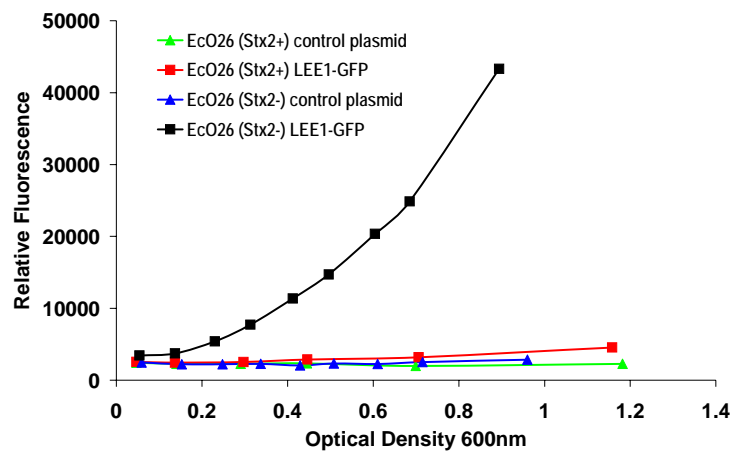


Fig. 5.8 LEE1-GFP expression of *E. coli* O26 pair of strains

The *E. coli* O26 pair of strains blotted in Fig 5.5 (Table 2.1) were transformed with the LEE1-GFP expression construct or a control plasmid and population fluorescence levels measured through the growth curve (produced with collaboration with David Gally). Taken together the data demonstrates that lysogeny with a Stx phage represses T3S expression.

5.2.4.2 Plasmid constructs to create deletion mutants

To obtain the Shiga toxin phage and CII deletion strains, a series of plasmids were constructed as described in Materials and Methods. pXLS11, pXLS12, pXLS13, pXLS15 and pXLS16 were used to obtain Stx phage deletion strains. Briefly, flanking regions of *z1449* (*cII_{stx2}*), Stx1, Stx2 were PCR amplified from EDL933, cloned into pIB307 and confirmed by restriction with the appropriate enzyme; the plasmids were termed pXLS11 (Fig. 5.9-10) , pXLS12 (Fig. 5.12-13), and pXLS15 (Fig. 5.15-16) respectively. Then a *sacBkan* cassette was cloned into both pXLS11 and pXLS12 at the *BamH* I site producing pXLS13 (Fig. 5.11) and pXLS16 respectively (Fig. 5.14).

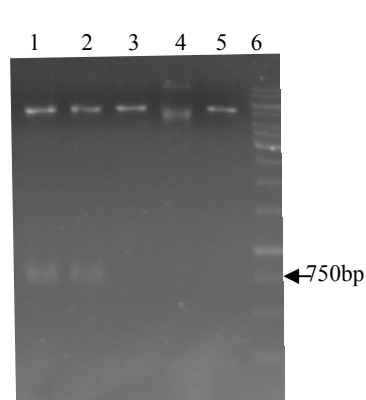


Fig. 5.9 pIB307 with the *zI449* digestion with *BamH* I and *Hind* III. Lane1-2: positive sample, lane 3-4: negative sample, lane 5: negative control lane 6: 1 kb ladder

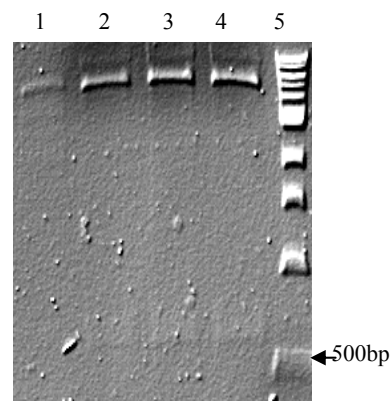


Fig. 5.10 pXLS11 digested by *BamH* I and *Sal* I to check for cloning the downstream flanking region of *zI449*. Lane1: negative control, lane 2-4: positive sample lane 5: 1 kb ladder

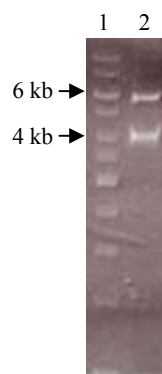


Fig. 5.11 pXLS13 digested by *BamH* I to demonstrate the insertion of the *sacBkan* cassette. Lane1: 1 kb ladder, lane 2: positive sample

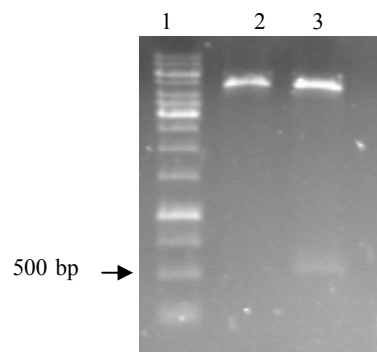


Fig. 5.12 pIB307 with *stxI* upstream flanking region inserted; digested with *BamH* I and *Hind* III. Lane1: 1 kb ladder, lane 2: negative control, lane 3: positive sample

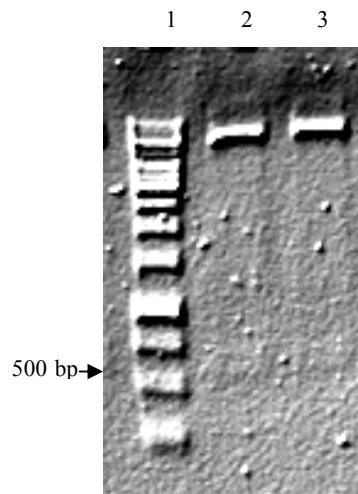


Fig. 5.13 pXLS12 digested by *Bam*H I and *Sal* I to cut out the downstream flanking region of *stx1*. Lane1: 1 kb ladder, lane 2-3: positive sample

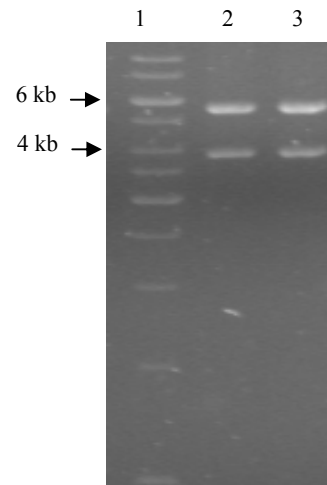


Fig. 5.14 pXLS16 digested by *Bam*H I to detect *sacBkan* cassette. Lane1: 1 kb ladder, lane 2-3: positive sample

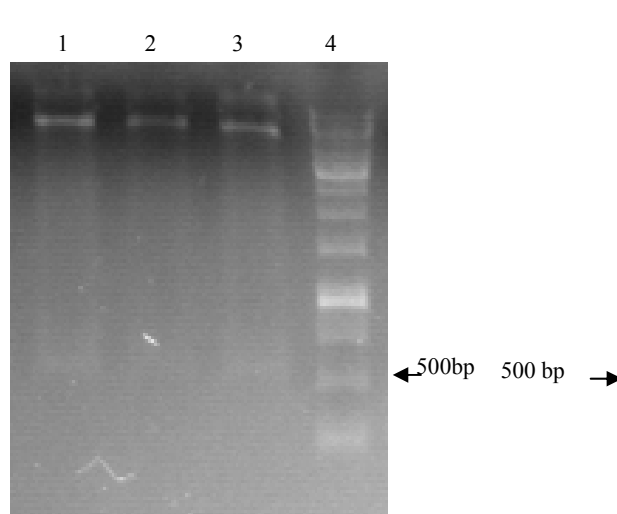


Fig. 5.15 pIB with the *stx2* upstream flanking region inserted; digested with *Bam*H I and *Hind* III. Lane1-3: positive samples, lane 4: 1 kb ladder

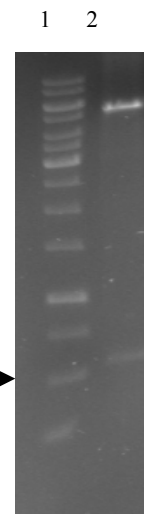


Fig. 5.16 pXLS15 digested by *Bam*H I and *Sal* I to show the insertion of the *stx2* downstream flanking region. Lane1: 1 kb ladder lane 2: positive sample

5.2.4.3 Construction of Stx phage deletion strains in EDL933

To obtain a *stx2* clean deletion mutant, an intermediate strain with *z1449* (*cII_{stx2}*) replaced by the *sacBkan* cassette was constructed. As detailed in Materials and Methods, plasmid pXLS13 (Table 2.2) was used for this construction. A flow of constructed strains and plasmids used to create these strains were shown in Fig. 5.17. The replacement of *z1449* with *sacBkan* cassette was confirmed by PCR with primer pairs *z1449* 5' and *z1449* 3' for the inside of *z1449* (Fig. 5.23), *z1449* external 5' and *z1449* external 3' for outside of *z1449* (Fig. 5.24), *sacB* 5' and *sacB* 3' for *sacBkan* cassette (Fig. 5.25). These primers positions on the genome were demonstrated in Fig. 5.18 and Fig. 5.19. PCR results indicated that *z1449* was replaced by *sacBkan* properly (Fig. 5.23-25). The resultant strain was termed as ZAP1321. ZAP1321 was then transformed with plasmids pXLS15 and allelic exchange carried out to generate strains with Stx2 phage clean deletions. The required clones were identified by sensitivity to both kanamycin and chloramphenicol and confirmed by PCR using primer pairs: *wrbA* and *intW* plus *z1503* and *z1504* for the junction sites of Stx2 (Fig. 5.26-27); *stx2* F and *stx2* R for a region inside the Stx2 phage (Fig. 5.28). PCR primers for Stx2 phage were shown in Fig. 5.20. The clean *stx2* deletion strain was termed ZAP1322 (Table 2.1). In order to construct a strain deleted for both Stx1 and Stx2 phages, ZAP1322 was used to create a strain with *stx1* replaced with the *sacBkan* cassette using pXLS16 (Table 2.2). The required strain was selected on the basis of KAN resistance and CAM sensitivity; further confirmation was carried out by PCR with primer pairs *yehU* and *z3305* for the left end of the Stx1 phage (Fig. 5.29), *intV* and *yehV* for right end of the Stx1 phage (Fig. 5.29), *stx1* 5' and *stx1* 3' for inside of Stx1 phage (Fig. 5.30), *yehU* and *yehV* for outside of Stx1 phage (Fig. 5.31), *sacB* 5' and *sacB* 3' for *sacBkan* cassette (Fig. 5.32) (Table 2.3). These PCR primers positions on the genome were depicted in Fig. 5.21 and Fig. 5.22. The resultant strain was designated ZAP1326 (EDLStx1&2).

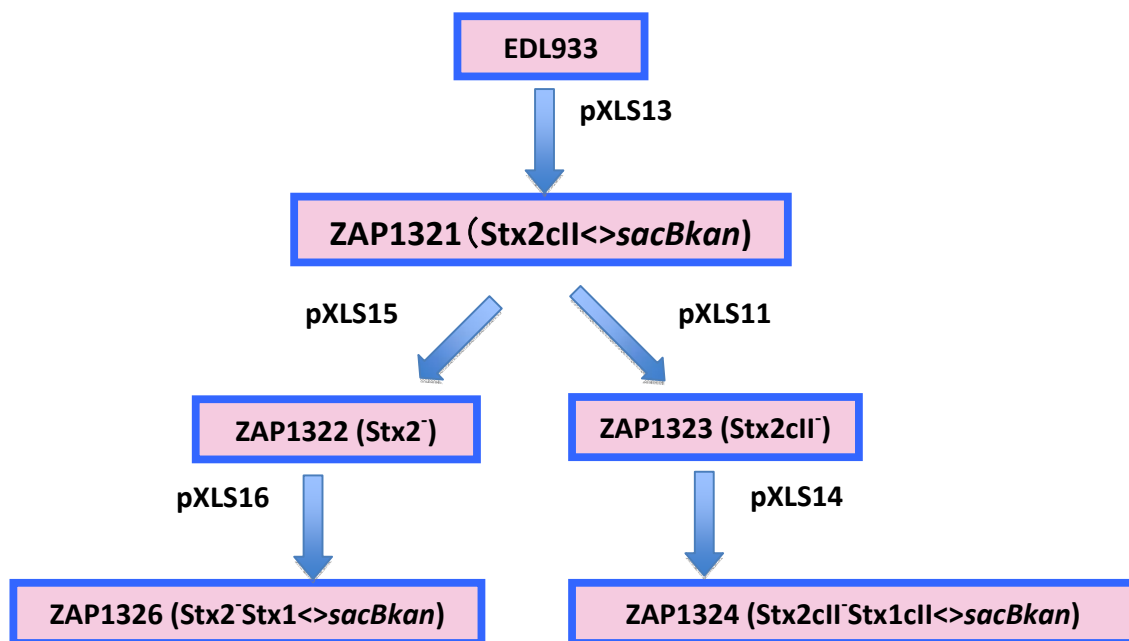


Fig. 5.17 Schematic diagram of strains construction

Strains were shown in rectangle. Plasmids were depicted beside the arrow.



Fig. 5.18 Structure diagram of z1449 locus and primers in EDL933

Genes were shown in rectangle and primes were depicted with directional arrow.

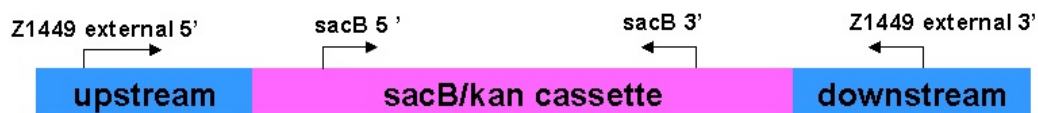


Fig. 5.19 Structure diagram of z1449 locus and primers in ZAP1321

Genes were shown in rectangle and primes were depicted with directional arrow.

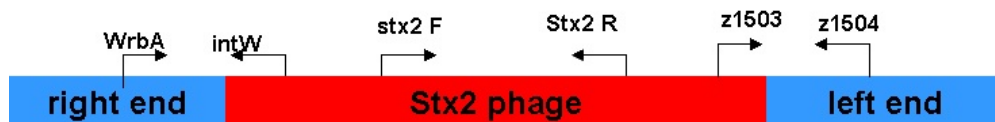


Fig. 5.20 Structure diagram of Stx2 phage locus and primers in EDL933

Genes were shown in rectangle and primes were depicted with directional arrow.

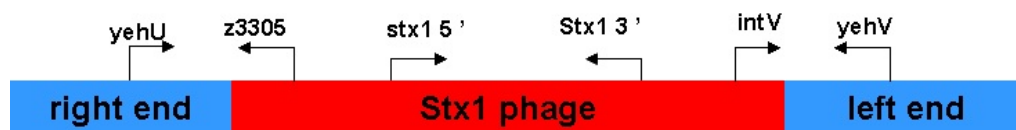


Fig. 5.21 Structure diagram of Stx1 phage locus and primers in EDL933

Genes were shown in rectangle and primes were depicted with directional arrow.

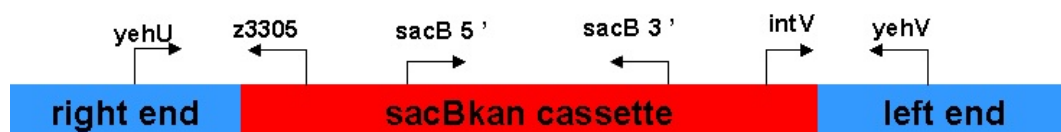


Fig. 5.22 Structure diagram of Stx1 phage locus and primers in ZAP1326
Genes were shown in rectangle and primes were depicted with directional arrow.

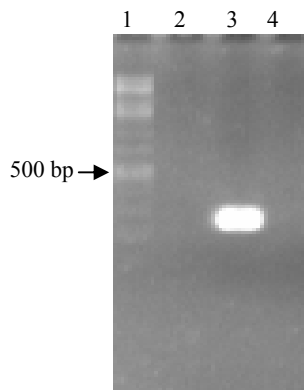


Fig. 5.23 Internal PCR of *z1449*

Lane 1: 1 kb ladder, lane 2: negative control, lane 3: positive control (EDL933), lane 4: tested sample. PCR indicated *z1449* was lost in the tested sample.

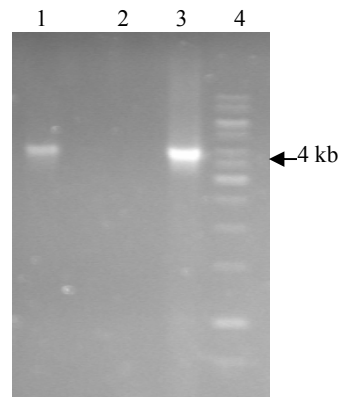


Fig. 5.24 External PCR of *z1449*

Lane 1: tested sample, lane 2: negative control, lane 3: positive control (pXLS13) lane 4: 1 kb ladder. It was demonstrated that *sacBkan* cassette replaced *z1449* in the right chromosome site.

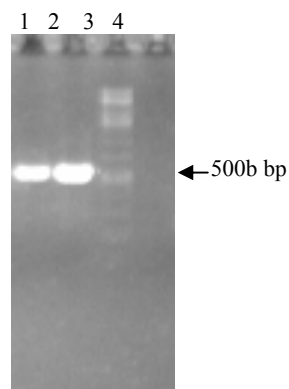


Fig. 5.25 PCR of *sacBkan* cassette for exchange of *z1449* for *sacBkan* cassette

Lane 1: positive sample, lane 2: positive control, lane 3: 1 kb ladder, lane 4: negative control. It was showed *sacBkan* cassette was present in the tested sample (lane 1).

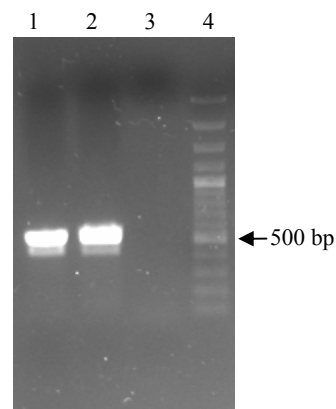


Fig. 5.26 PCR of junction of Stx2 using primer pair *wrbA* and *intW*

Lane 1: positive control (EDL933), lane 2: tested sample 1, lane 3: tested sample 2, lane 4: 100 bp ladder. PCR indicated that sample 2 might have lost Stx2 phage.

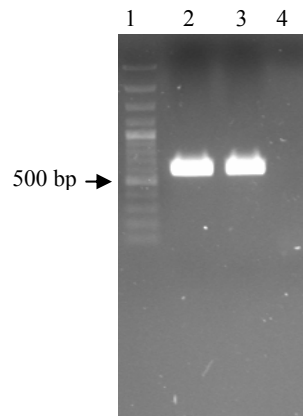


Fig. 5.27 PCR of junction of Stx2 using primer pair z1503 and z1504
Lane 1: 100 bp ladder, lane 2: positive control (EDL933), lane 3: tested sample 1, lane 4: tested sample 2. PCR showed that sample 2 might have lost Stx2 phage. Thus sample 2 was taken for next steps.

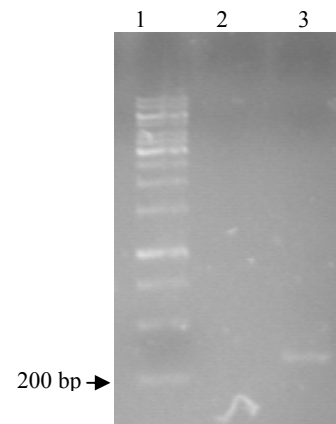


Fig. 5.28 PCR of inside of Stx2 using primer pair stx2F and stx2R
Lane 1: 100 bp ladder, lane 2: tested sample, lane 3: positive control (EDL933). PCR result showed that sample 2 didn't contain Stx2 A unit.

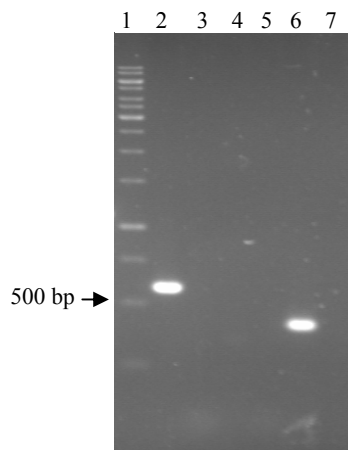


Fig. 5.29 PCR of left end and right end of Stx1 phage
Lane: 1 kb ladder, lane 2-4: PCR of left end of Stx1, lane 2: positive control (EDL933), lane 3: negative control, lane 4: tested sample; lane 5-7: PCR of right end of Stx1, lane 5: negative control, lane 6: positive control (EDL933), lane 7: tested sample. PCR results showed that Stx1 was lost in tested sample.

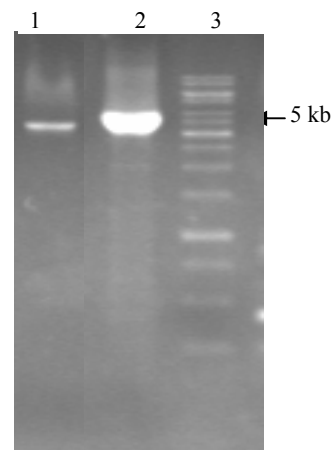


Fig. 5.30 PCR of outside of Stx1
Lane 1: tested sample, lane 2: positive control, lane 3: 1 kb ladder. PCR indicated that *sacBkan* cassette was replaced in Stx1 phage loci on the chromosome.

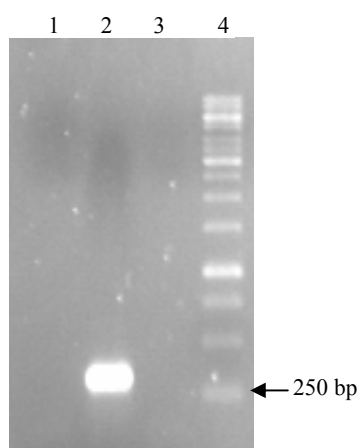


Fig. 5.31 PCR of inside of Stx1 with primers stx1 5' and stx1 3'. Lane 1: negative control, lane 2: positive control (ELD933), lane 3: tested sample, lane 4: 1 kb ladder. PCR result showed that Stx1 subunit A was absent in tested sample.

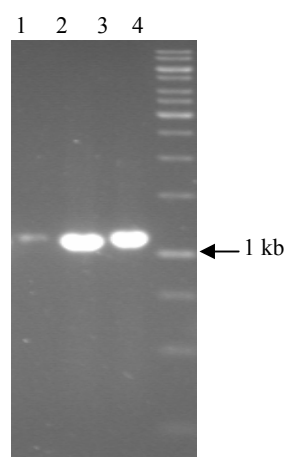


Fig. 5.32 PCR of *sacBkan* cassette. Lane 1: negative control, lane 2: positive control, lane 3: tested sample. It indicated that tested sample obtained *sacBkan* cassette.

5.2.5 Repression of LEE1 promoter activity in *E. coli* K12 transduced with a Stx2 bacteriophage

In order to determine whether the repression of T3S expression by Stx prophages could also be detected in a distinct genetic background; the marked Stx2 phage induced from *E. coli* O157:H7 Sakai was used to transduce *E. coli* K12 MG1655. This transduction was achieved and the establishment of a lysogen in *E. coli* K-12 confirmed by selectable markers and PCR assays (this strain was constructed by Sean McAteer). The recipient strain was Lac negative and Nalidixic acid resistant making it easy to distinguish from the original Sakai strain and the final strain was also shown to contain *stx2* genes and not intimin (data not shown). This *E. coli* K-12 Stx2 lysogen and the parental MG1655 strain were then transformed with the LEE1::egfp promoter fusion plasmid and fluorescence levels measured throughout the growth curve (Fig. 5.33A). While there was some detectable expression from the LEE1 promoter there was no significant difference in LEE1 expression levels between the strains (Fig. 5.33A). However, neither of these strains contains the LEE-encoded regulator (Ler) which is known to relieve H-NS repression of the LEE1 and other LEE promoters to activate T3S expression. To examine Ler induction of LEE1 in the two backgrounds, *ler* was cloned into the inducible pWSK29 vector and this was transformed into the same pair of K-12 strains containing the reporter for LEE1. Induction of Ler was carried out using IPTG and fluorescence levels measured throughout the growth curve. As anticipated Ler induction significantly increased expression from the LEE1 promoter fusion in the *E. coli* K-12 strain (Fig. 5.33A). However, this *ler*-dependent activation did not occur to the same extent in the *E. coli* K-12 derivative containing the Stx2 lysogen (Fig. 5.33A). This result implied that Stx2-based repression of T3S involved inhibition of Ler activation of the LEE1 promoter. To confirm that Ler was induced by IPTG induction to a similar level in the two backgrounds, *ler* was cloned into pWSK29 with a carboxy-terminal six histidine tag to allow levels to be determined by Western blotting. This construct was also able to induce LEE expression in *E. coli* MG1655 but not to the same extent as the strain transduced with the Stx2 phage (Fig. 5.34). Whole cell protein samples were blotted for detection of 6xHis-Ler and the isogenic Stx2⁺ and Stx2⁻ K-12 strains containing the LEE1-GFP reporter (Fig 5.35, lanes 6 & 8) contained equivalent levels of the tagged Ler protein

when compared to RecA levels as a control. This implied that although Ler was induced and present its capacity to act on the LEE1 promoter was limited by the presence of the integrated Stx2 phage in the chromosome.

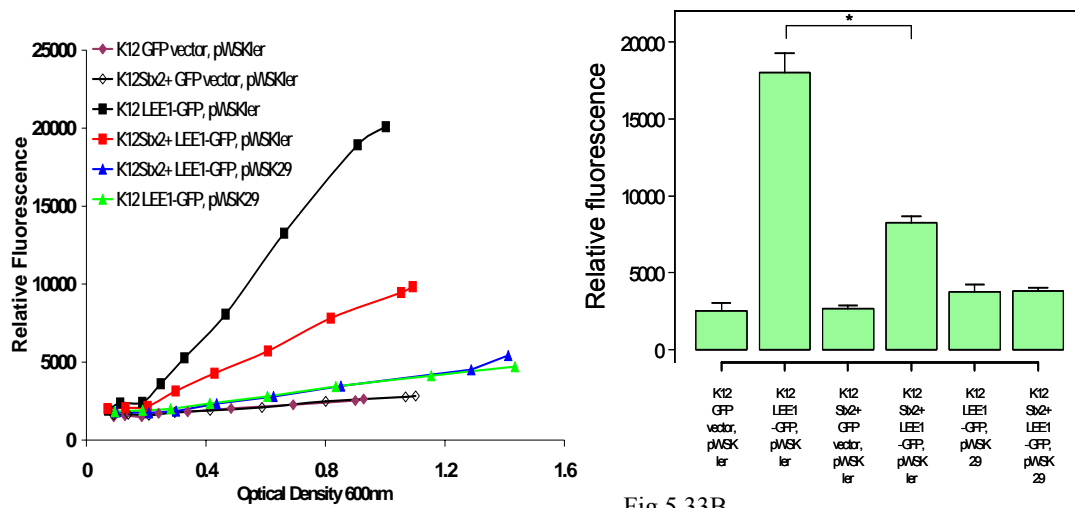


Fig 5.33A

Fig 5.33B

Fig. 5.33 LEE1-GFP measurement of K12 and K12 Stx2⁺ (produced with collaboration with David Gally)

(A) A marked Stx2 phage was transduced into *E. coli* K-12 MG1655 as described in Materials and Methods. Expression of the LEE1-GFP reporter, or from a control GFP plasmid (GFP vector) were then compared in the Stx⁺ and Stx⁻ K-12 strains with and without induction of the LEE-encoded regulator (pWSKler) or control plasmid (pWSK29) with 1mM IPTG. This experiment was repeated four times and fluorescence values determined at OD₆₀₀=0.9 used in (B). Stx2 lysogeny significantly reduced LEE1-GFP expression levels ($p<0.001$) following Ler

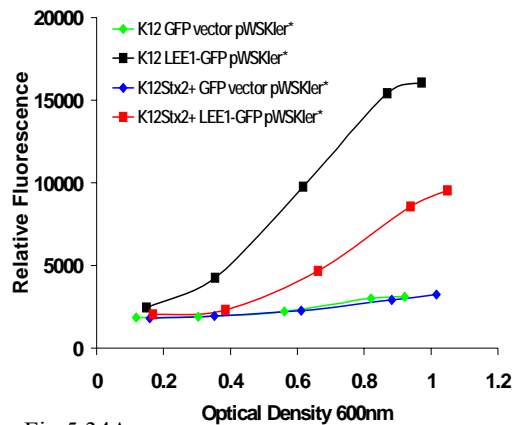


Fig 5.34A

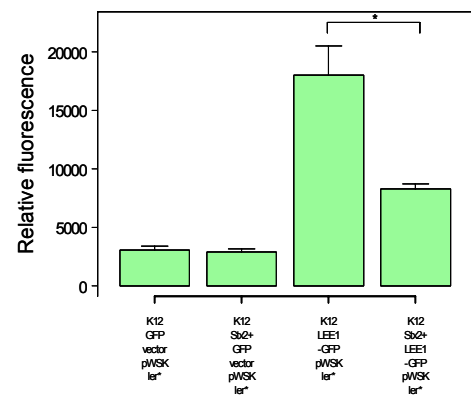


Fig 5.34B

Fig. 5.34 LEE1-GFP measurement of K12 and K12 Stx2⁺ with plasmids *ler*(produced with collaboration with David Gally)

The experiments were repeated with a 6xHis-tagged Ler construct (pWSKler*) to determine if Ler was present in equivalent levels in both K-12 strains (Fig 5.35). Again Ler induction led to significantly reduced levels ($p=0.002$) of population fluorescence in the K-12 Stx2 lysogen (red and black squares in (A) when compared at OD₆₀₀=0.9 in (B).

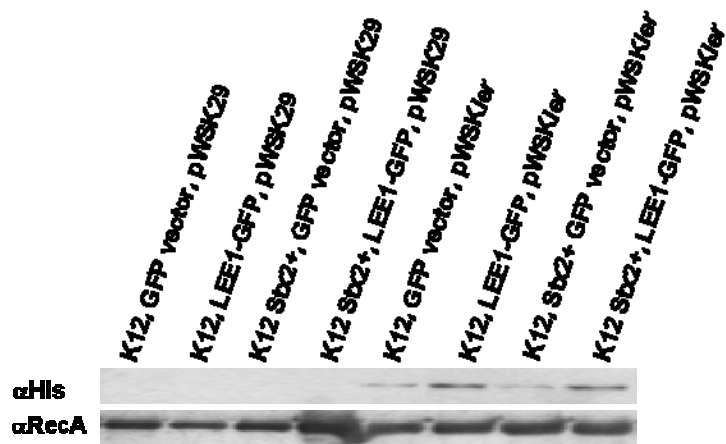


Fig. 5.35 6xHis-tagged Ler levels were compared with RecA in the different strains by Western blotting from whole cell samples taken at $OD_{600}=0.9$. Both strains containing the LEE1-GFP fusion and the induced pWSKler contained equivalent levels of the induced 6xHis-tagged Ler protein, lanes 6 & 8.

5.2.6 The lysogeny regulator CII can repress type III secretion

One explanation for the failure of Ler to induce LEE1 expression in the presence of the Stx2 lysogen is that a regulator or regulators expressed from the Stx2 lysogen repress Ler activity on the LEE1 promoter. Several of the key lysis/lysogeny regulators characterized for phage lambda were cloned from the EDL933 Stx2 phage into the arabinose inducible vector pBAD18. These clones were sequenced and confirmed as identical to the published Stx2 (BP933-W) genes (NCBI). The clones were electroporated into the Stx phage negative *E. coli* O157:H7 strain TUV93-0 and the T3S profiles determined from supernatants following arabinose induction (Fig 5.36). Only the clone of *cII* showed any evidence of T3S repression. However, it is established that CII induction can be toxic for cells and we observed reduced growth rates when expressing *cII*. It is also apparent that in this case even though EspD levels are reduced, EscJ expression is not, indicating a different regulatory pathway. Of note though was that the same reduced growth rate was measured when *cII* was induced in EPEC O127 E2348/69, but in this case there was no repression of T3S (data not shown), indicating a regulatory difference in this Stx phage negative background. To determine the relevance of *cII* to repression of T3S at physiological levels, the *cII* gene was deleted from both the Stx2 phage and from the Stx1 phage in *E. coli* O157 EDL933. Western blotting for T3S proteins as well as fluorescence levels from the LEE1-GFP reporter transformed into the strain demonstrated significantly increased LEE1 expression and T3S in the absence of *cII* (Fig. 36-37). The induction and deletion experiments with *cII* confirm a role in T3S control following Stx phage integration.

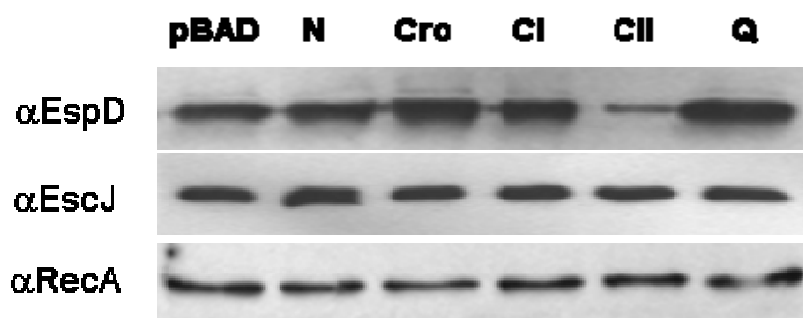


Fig. 5.36 Western blot detection of EspD from bacterial supernatants and EscJ & RecA from whole cell samples.

The defined bacteriophage lysis/lysogeny regulators were cloned into the pBAD vector and induced in *E. coli* TUV93-0 which does not contain any Stx prophages.

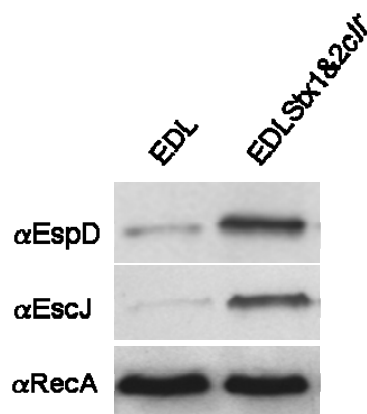


Fig. 5.37 Western blot analysis of the same proteins from *E. coli* EDL933 and an isogenic strain from which both the Stx1 phage *cII* gene and the Stx2 *cII* gene had been deleted by allelic exchange as described in Materials and Methods.

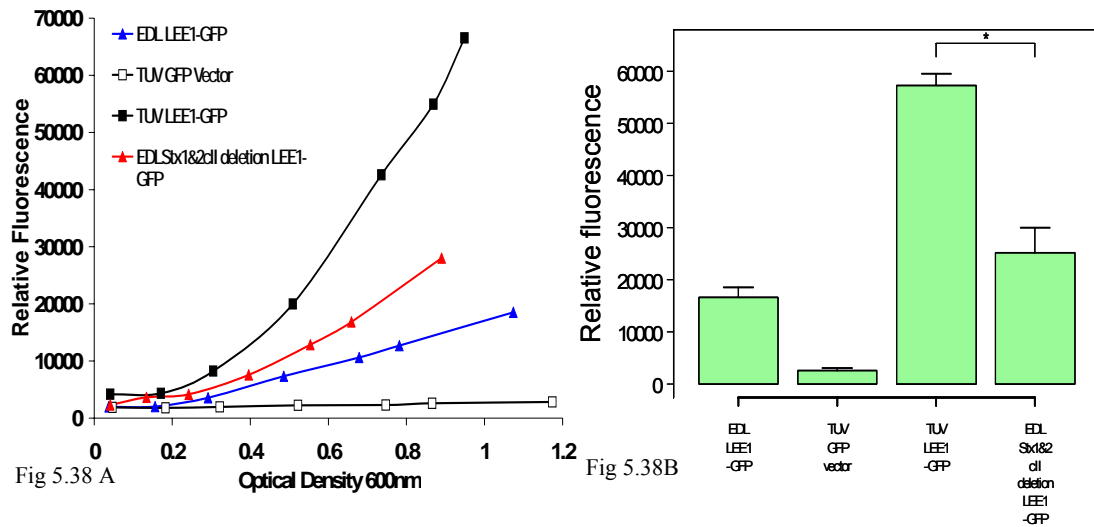


Fig. 5.38 LEE1-GFP measurement of EDL933, TUV93-0 and TUV Stx1&2*cII* deletion (produced with collaboration with David Gally)

(A) Population fluorescence from the LEE1-GFP reporter, or control plasmid, were examined in EDL933 and the double *cII* deletion. Deletion of both *cII* genes led to a significant increase ($p < 0.001$) in population fluorescence levels at $OD_{600} = 0.9$ (B).

5.2.6.1 Constructs for allelic exchange

In order to construct plasmids that would facilitate chromosomal exchange, flanking regions of the *z1449* (*cII_{stx2}*) (described above) and *z3357* (*cII_{stx1}*) genes were PCR amplified and cloned into the temperature-sensitive plasmid pIB307 (Table 2.2). These products were cleaned with a Invitrogen PCR purification kit, digested with *Bam*H I and *Hind* III or *Sac* I, or *Sal* I, re-cleaned, and then ligated with digested pIB307 (Table 2.2) to obtain pXLS10 (Fig. 5.39- Fig. 5.40) and pXLS11 (Fig. 5.9-10) containing flanking regions of *z3357* and *z1449* genes respectively. To produce plasmids for exchange, a *sacBkan* cassette was cloned into the *Bam*H I sites of pXLS11 and pXLS10 creating pXLS13 (Fig. 5.11) and pXLS14 (Fig. 5.41) that would allow the chromosomal replacement of *z1449* and *z3357* genes respectively with a selectable marker and a counter-selection gene.

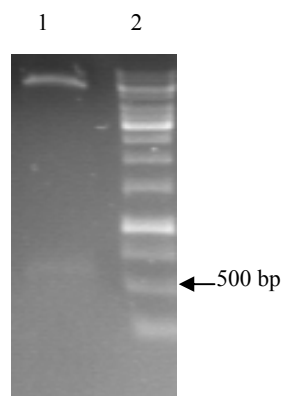


Fig. 5.39 *z3357* downstream flanking region inserted into pIB307 digested by *BamH* I and *Hind* III
Lane 1: tested sample, lane 2: 1 kb ladder. *z3357* downstream fragment was detected by *BamH* I and *Hind* III digestion.

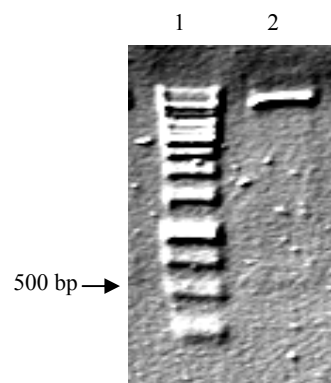


Fig. 5.40 pXLS10 digested by *BamH* I and *Sal* I
Lane 1: 1 kb ladder, lane 2: tested sample. *z3357* upstream fragment was detected from pXLS10 by *BamH* I and *Sal* I digestion.

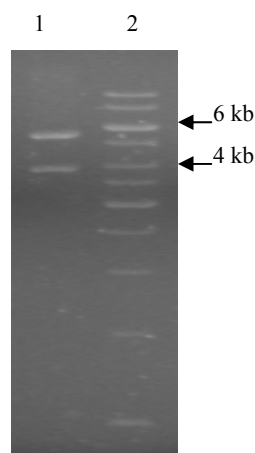


Fig. 5.41 PXLS14 digested by *BamH* I
Lane 1: tested sample, lane 2: 1 kb ladder. *sacBkan* cassette was detected by *BamH* I digestion.

5.2.6.2 Strain construction

The method of Emmerson *et al.* was used for allelic exchange (Emmerson *et al.*, 2006). Plasmid pXLS13 (Table 2.2) was transformed into ZAP1321 (described above) to obtain *z1449* (*cII_{stx2}*) clean deletion. Briefly, pXLS13 was electroporated into ZAP1321 (Table 2.1) and cultured at 30°C on LB-C plates. Ten transformants were then inoculated into pre-warmed LB-C at 42°C and passaged repeatedly in LB-C broth at 42°C to obtain co-integrates. The culture was further passaged in at 30°C in LB broth to select for the complete exchange. The kanamycin sensitive and chloramphenicol sensitive strain was confirmed by PCR with primer pairs *z1449* external 5' and *z1449* external 3' for outside of *z1449* (Fig. 5.44), *sacB* 5' and *sacB* 3' for *sacBkan* cassette (Primer Table) (Fig. 5.45). PCR primer locations on the genome were shown in Fig. 5.18. The resultant strain was termed as ZAP1323. ZAP1323 was then transformed with plasmids pXLS14 and allelic exchange carried out to generate ZAP1324 with *z3357* (*cII_{stx1}*) replaced with *sacBkan* cassette. This allelic exchange was carried out as above except that the cultures at 30°C contain kanamycin antibiotic selection. The required clones were identified by

kanamycin resistance and chloramphenicol sensitivity and confirmed by PCR using primer pairs: z3357 external 5' and z3357 external 3' for outside of z3357 (Fig. 5.46), sacB 5' and sacB 3' for *sacBkan* (Fig. 5.47), and cassette z3357 3' for inside of z3357 (Fig. 5.48). These PCR primer locations on the genome were shown in Fig. 5.42-43.



Fig. 5.42 Structure diagram of z3357 locus and primers in EDL933

Genes were shown in rectangle and primes were depicted with directional arrow.

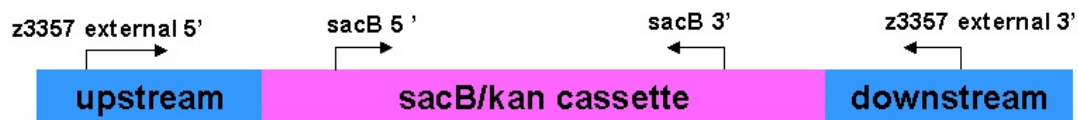


Fig. 5.43 Structure diagram of *z3357* (replaced by *sacB/kan* cassette) locus and primers in ZAP1324, Genes were shown in rectangle and primes were depicted with directional arrow.

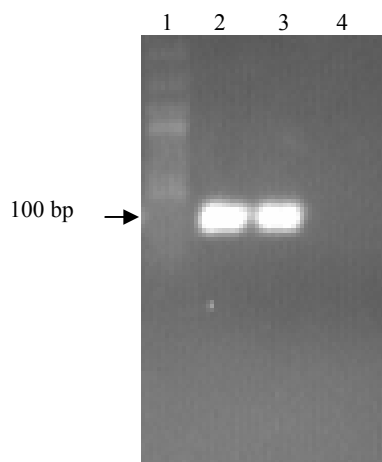


Fig. 5.44 External PCR of *z1449* in ZAP1323
Lane 1: 100 bp ladder, lane 2: tested sample 1, lane 3: tested sample 2, lane 4: negative control. It indicated that tested samples lost *sacBkan* cassette and *z1449*.

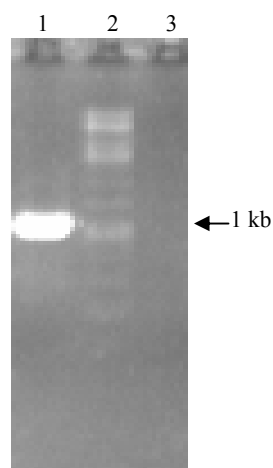


Fig 5.45 PCR of *sacBkan* cassette in ZAP1323
Lane 1: positive control, lane 2: 1 kb ladder, lane 3: tested sample. It indicated that tested sample lost *sacBkan* cassette.

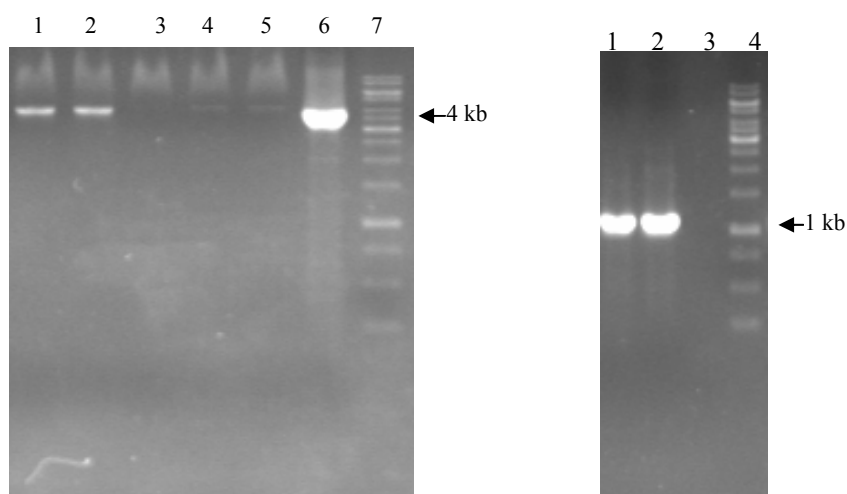


Fig. 5.46 Internal PCR of *z3357* in ZAP1324

Lane 1,2,4,5: tested samples, lane 3: control, lane 6: positive control, lane 7: 1kb ladder. It indicated *z3357* was present in tested samples.

Fig. 5.47 PCR of *sacBkan* cassette in ZAP1324

Lane 1: tested sample, lane 2: positive control, lane 3: negative control, lane 4: 1kb ladder. PCR result showed that *sacBkan* cassette was present in tested sample

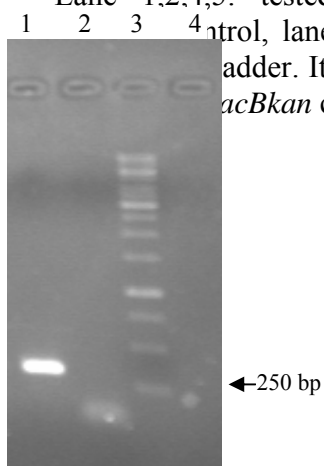


Fig. 5.48 Internal PCR of *z3357* in ZAP1324

Lane 1: positive control, lane 2 negative control, lane 3: 1 kb ladder, lane 4: tested sample.

The result indicated that *z3357* was absent in tested sample.

5.3 Discussion

EHEC strains are characterised by the integration of lambdoid-like phages into their chromosome that encode Shiga toxins (Ogura *et al.*, 2009; Perna *et al.*, 2001). EHEC O157 strains can be lysogenized by different types of Stx phage, but those associated with Stx2 and Stx2c are considered the most important in terms of human virulence (Garcia-Aljaro *et al.*, 2005; Muniesa *et al.*, 2004). Some strains carry multiple Stx phages indicating some differences in phage exclusion regulation beyond that characterised for classical lambda (Dobrindt *et al.*, 2010). A key question is what evolutionary advantage can Stx phage lysogeny have for the EHEC strain, and do these underpin the epidemiology of EHEC O157 strains? A large epidemiological study of farms in Scotland demonstrated that PT21/28 strains were more likely to be associated with higher level faecal counts compared with PT32 strains. In addition, PT21/28 strains over that period were the most prevalent phage type associated with human infection (Chase-Topping *et al.*, 2008; Chase-Topping *et al.*, 2007b). The initial aim of this study was to compare PT21/28 and PT32 strains in terms of genomic differences to determine how these inform the epidemiology.

Comparative genomic hybridisation (CGH) analysis of 12 strains indicated that one of the main differences between the phage types was with Stx phage carriage. Based on the CGH, PCR was used to determine the presence of Stx2 and Stx2c in 60 strains. PT21/28 strains generally carried both Stx2 and Stx2c bacteriophages, irrespective of whether the strains were sourced from cattle or humans. By contrast, nearly all the bovine PT32

strains analysed carried only the Stx2c phage. The situation for the limited number of human PT32 strains was more complex, but these were significantly more likely to contain a Stx2 phage in comparison to the bovine strains. This data indicates that strains carrying both Stx2 and Stx2c phages are more likely to be associated with human infection. This result is in line with recently published research on Clade 8 strains in the USA that are considered to be more virulent. Clade 8 strains were significantly more likely to carry both the *stx2* and *stx2c* genes in comparison to the other clades containing *stx2c* (Manning *et al.*, 2008). All clade 8 strains tested had *stx2*, and 57.6% had *stx2c*. Whether this association for both relates to differences in toxicity of the strains or other phenotypes associated with the strains is not known, although more recent work has indicated that levels of Stx2 production alone are likely to be important, irrespective of lineage, in terms of association with human clinical disease (Zhang *et al.* 2009).

As type III secretion (T3S) is essential for cattle colonisation and variation in its regulation may associate with differences in shedding level from cattle (Pearce *et al.*, 2009), we investigated T3S levels between PT32 and PT21/28 by Western blotting bacterial supernatants for the secreted translocon protein EspD and whole cell fractions for the T3S apparatus protein EscJ. LEE1 expression was also measured by determining fluorescence levels from a previously published LEE1-GFP reporter (Roe *et al.*, 2003a). Levels of T3S varied markedly between strains in agreement with our previous work on T3S profiles of EHEC O157 strains (Roe *et al.*, 2004). T3S levels were low in the majority of PT21/28 strains compared with the PT32 strains. Extensive research has defined multiple regulatory inputs for T3S and it is likely that the variation observed will be due to a complex combination of alleles. For example, use of a LEE1 reporter readout in different lineages of EHEC O157 strains has yielded a complex and widely distributed pattern of expression with no clear association with particular integrated O-islands or S-loops (Yang *et al.*, 2009). However, the finding in the present study that strains with both Stx2 and Stx2c phages had on average lower levels of LEE1 expression than strains with a single Stx2 bacteriophage prompted us to test strain pairs with and without Stx bacteriophages. Analysis of these strains demonstrated that Stx phage insertion into the chromosome leads to repression on T3S (Fig. 5.5-8), this was also apparent in a pair of

O26 strains, including one from which the Stx2 phage had been naturally cured Bielaszewska ref at end. As stated there are likely to be multiple variable inputs into T3S expression and this was confirmed by analysis of the potentially isogenic EDL933 and TUV93-0 strains. While Stx bacteriophage insertion and deletion repressed and activated T3S respectively, other differences between the strains also account for the marked difference in T3S levels between these strains. Further research using information on the sequences of multiple strains in comparison with T3S profile should help clarify the main alleles responsible for this variation.

To confirm and study the Stx2 bacteriophage repression in another background, the sequenced *E. coli* K12 MG1655 strain was lysogenised with a marked Stx2 phage from the sequenced *E. coli* O157:H7 Sakai strain (Table 3). Without the presence of the LEE-encoded regulator (Ler) there was no difference in the expression levels from the LEE1-GFP reporter transformed into these two strains, indicating that there was no inherent difference in these backgrounds affecting the basal level of GFP detected. However, upon induction of Ler, expression of LEE1 was always significantly lower in the K-12 strain containing the Stx2 lysogen. To rule out that the lower level of expression may be due to reduced Ler expression, the experiments were repeated using a 6xHis-Ler construct with nearly identical results (Fig. 5.37-38). This set of experiments demonstrates that the capacity of Ler to induce LEE1 expression is reduced in the presence of the Stx2 lysogen. Attempts were made to examine T3S in the K-12 backgrounds by transforming in a full length LEE clone (McDaniel & Kaper, 1997), but this clone failed to express any detectable T3-related proteins in either background (data not shown). Our results are in line with recently published work examining the impact of Stx phage insertion on gene expression in *E. coli* K-12 by micro-array (Su *et al.* 2010). Of 166 genes found to be differentially expressed, 62 were down-regulated and 104 of these were up-regulated, including motility and acid-resistance associated genes. GadE is known to be involved in repression of T3S so increased *gadE* expression following Stx phage lysogeny may well account for some of the reduced expression (Kailasan Vanaja *et al.*, 2009; Tatsuno *et al.*, 2003). In addition, there is established reciprocal cross-talk between motility and T3S governed by GrlA/R and so a decrease in T3S may lead to an

increase in motility, although this cannot be the molecular basis for the increase in motility in *E. coli* K-12 (Su *et al.* 2010).

Previous work has established that the LEE2/3 operons, but not LEE1 are subject to repression by LexA in EPEC with activation following SOS induction (Mellies *et al.*, 2007). The repression of Ler activity on LEE1 may be the result of established lambda lysogeny regulators and/or regulators encoded elsewhere in the bacteriophages. To test established lambda phage regulators, *cI*, *cII*, *cro*, anti-terminators N and Q were cloned and induced in TUV93-0. CI was a potential regulator as this is the main phage encoded-protein known to be expressed constitutively during lysogeny (Oppenheim *et al.*, 2005) but its induction had no impact on T3S. CII was the only induced regulator that had an effect, but in this case the growth rate of the cells was also reduced and there was not the concomitant reduction in EscJ levels as seen for lysogeny with the whole phage. De-regulated CII expression is established to have effects on growth rates through the cell cycle (Kedzierska *et al.*, 2003) and so the T3S changes may have been due to indirect effects. For example, ClpX activity is increased in stressed bacteria and this is known act predominately on LEE4/5 and so would affect T3S levels of the LEE4-encoded EspD but not EscJ expressed from LEE3 (Iyoda & Watanabe, 2005). To test the potential importance of *cII*, both copies were deleted from the Stx1 and Stx2 phages in EDL933. For this mutant T3S was increased indicating a role of *cII* in the control of T3S regulation. This result is however incongruous with the established regulation and function of CII, which is thought to only be expressed to establish the lambda lysogen (Oppenheim *et al.*, 2005). While this appears to be the case for bacteriophage Lambda there may well be differences in the regulation between classic lambda and Stx lambdoid bacteriophages. In addition, we cannot rule out that other Stx phage-based regulators may also contribute to repression of T3S following lysogeny and investigating this will be the basis of future work in this area.

A key question is why is this repression of T3S associated with Stx phage lysogeny? In the host, the bacterium will be subject to multiple stresses that will lead to a subset of the bacterial signalling and relocating nucleolin to the epithelial cell surface where it binds to

the EHEC adhesin, intimin, expressed from LEE5 (Robinson *et al.*, 2006) population undergoing lysis (Liu *et al.*, 2010). Shiga toxins released from the lytic subset of the bacterial population have been shown to provide a colonisation advantage both by reducing inflammatory). This function of Stx directly links Stx phage regulation/lysis control and LEE-promoted adherence. The findings of the present study have demonstrated that Stx2 bacteriophage integration represses T3S. We propose that Stx phages repress LEE1 expression to effectively take control of this critical colonisation factor. The Stx bacteriophage, through this regulation, ensures that bacterial colonisation and persistence become dependent on the bacteriophage. It is interesting that EHEC strains, by comparison with the sequenced EPEC strain O127:H6 strain have a greater number of T3S effector proteins expressed from a variety of cryptic prophages (Ogura *et al.*, 2009; Tobe *et al.*, 2006). More than 60 effectors from Sakai O157:H7 genomes were identified in which 39 proteins were proved to be experimentally functional (Toru Tobe, 2006, PNAS). The majority of these functional genes are located on the prophages of Sakai O157:H7 strain. These effectors can be classified into many proteins family such as NleG, NleA, NleH, NleB, NleC, LRR, EspF, PerC family etc. Seven homologue genes of PerC are encoded within OIs in EHEC including PchA-E, PchX and PchY. The effect of these effector proteins are mediated via PchA/B regulators that act by increasing expression from LEE1 (Abe *et al.*, 2008). It is considered that prophages can contribute to the change of phenotype or fitness of host bacteria. Consequently, these resulted bacteria are more competitive in host and environment, and even more pathogenic to animals and human. We propose that Stx phages provide a selective advantage in EHEC strains for colonisation and persistence in cattle not just through the effects of Shiga toxin but also through repressing T3S expression favoring the selection of multiple prophage units encoding effector proteins with regulators that overcome this repression (Fig 5.49-51). As a consequence, it is the network of prophage-based repressors and activators controlling T3S that is important for EHEC strains (Tree *et al.*, 2009b).

It is established that EHEC strains vary markedly in their capacity to produce Stx toxins (Zhang *et al.*, 2009), a phenotype that is intricately associated with Stx phage carriage and levels of lysis induction. The lysis/lysogeny decision will be affected by the

genotype of the strain, number of Stx phages and possible cross-talk between phage regulators. The heterogeneous nature of lysis induction means that for the subset of cells that do not lyse, then the remaining subset may have induced T3S ready to benefit from Stx priming of the epithelium. In this way, the Stx phage and effector prophage repertoire of an EHEC strain are intimately associated with excretion level from the animal host (Fig 5.49-51).

Additional work could be carried out on the confirmation of Stx phage and *cII* regulation on T3SS. Using single copy of *ler* with GFP, the plasmids multiple copy number effect on the measurement of expression in bacteria can be excluded. Other work also could focus on the *cII* transcription level in different strains such as Stx[±] strains to confirm *cII* effect of T3SS.

Some future work will examine the mechanism of the Stx phage regulation of T3SS. Firstly, *cII*, as a potential regulator on T3S, will be investigated in the binding with LEE1 promoter and *ler*. Briefly, cII protein will be purified. Then the electrophoretic mobility shift assay will be used to test the binding between CII and LEE1 promoter region and *ler*. If interaction is indentified, then specific mutations will be designed to figure out the exact binding site on LEE1 promoter region and or *ler*. If no binding is detected, future work will address on the question which genes are responsible for the regulation of T3SS on Stx2 phage. Deletions of the candidate genes on conjugated Stx2 phage in K12 can be constructed. The expression of LEE1 promoter indicating the level of T3S can be measured by GFP reading. If any gene is identified, further work including protein-protein interaction, structure analysis, functional domain study etc can be carried out.

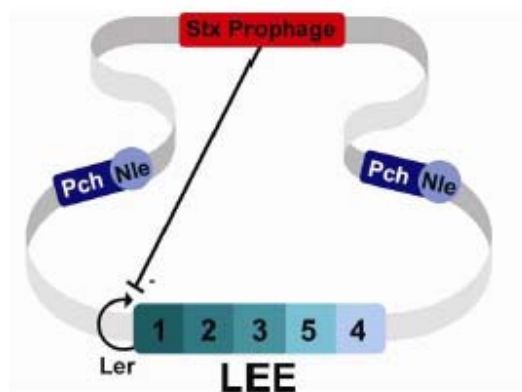


Fig. 5.49 Schematic diagram showing that the integrated Shiga toxin prophage represses type III secretion (T3S) by blocking Ler activation at LEE1 (This graph was produced by Eliza Wolfson).

Under the conditions shown there is no expression of the PchA/B regulators associated with other integrated prophages that express effector proteins secreted by the T3S system.

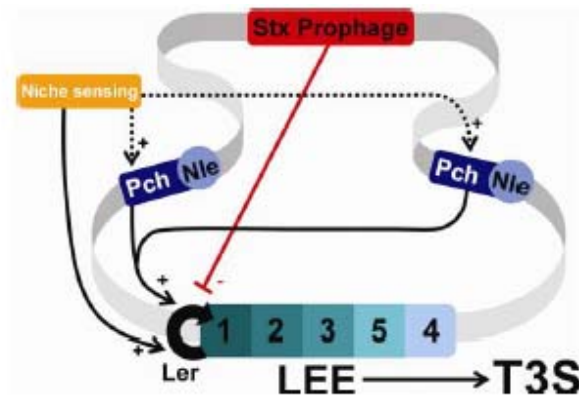


Fig. 5.50 Schematic diagram showing that the repressive control of the Stx prophage is overridden by the activity of activators such as Ler, and PchA/B that are induced following sensing of niche specific signals in the animal host (This graph was produced by Eliza Wolfson). While a number of environmental signals are known to control T3S at LEE1 there is less information on environmental control of Pch regulator induction.

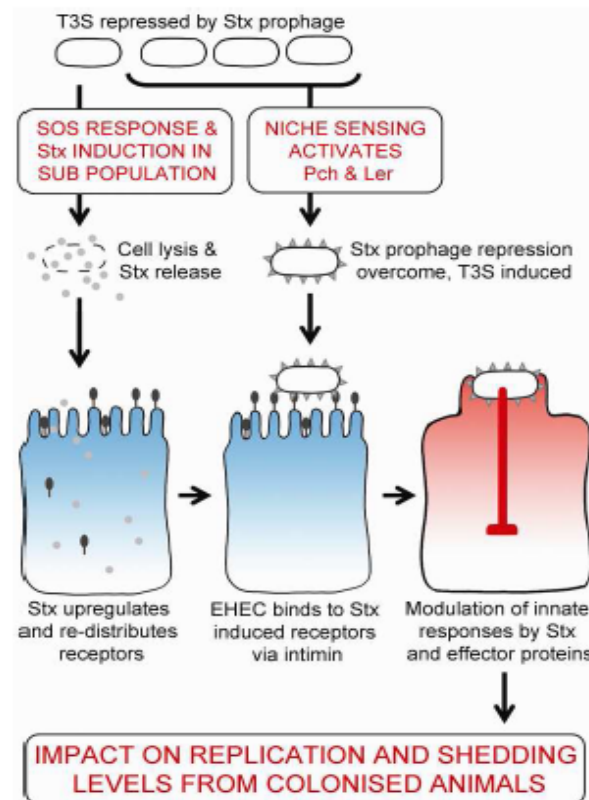


Fig.5.51 A model for EHEC interaction with the epithelium (produced by Eliza Wolfson). SOS stress responses result in prophage induction and Stx release in a subset of the population. Potentially certain stresses associated with the interaction with epithelial cells may induce this response. The released toxin induces the expression and redistribution of receptors to the epithelial cell surface. T3S is repressed but can be induced by Pch activators (Tree *et al.*, 2009a; Yang *et al.*, 2009) present on cryptic lambdoid prophages that ensure co-ordination of effector protein expression with production of the T3S system (Fig. 5. 49-50). The induction of T3S includes intimin expression on the outer membrane of the bacteria allowing binding to Stx-induced receptors, including nucleolin (Kenny *et al.*, 1997). This leads to intimate attachment and lesion formation. Secreted effector proteins can repress inflammation as can Stx. It is proposed that the degree and nature of this modulation will be different between strain types impacting on bacterial replication and therefore the extent of excretion from the animal.

E. coli O157:H7 is a devastating pathogen causing serious diseases including bloody diarrhea, HC, HUS and even death. The latest biggest outbreak occurred in Germany leading to over 800 HUS cases (including over 30 fatalities) reported in Germany with over 36 HUS cases (at least 1 fatality) and 66 EHEC cases (none fatal) from other European countries. HUS develops from released Stx binding to Gb3 expressing endothelial cells in the kidney and the subsequent host responses to repair the killed cells. Stx phages are key prophages acquired into the chromosome during the evolution of *E. coli* O157:H7 (Filee *et al.*, 2003; Perna *et al.*, 2001). Cattle are considered as the main reservoir of *E. coli* O157:H7 (Perna *et al.*, 2001). T3S is essential to the colonization of *E. coli* O157:H7 in the terminal rectum (Naylor *et al.*, 2005). Bacteria utilize the T3SS to export effectors into host cell and the open conduit may even allow the import of essential nutrients. These secreted effectors affect host cell signal transduction pathways and drive the formation of A/E lesions. However, the tropism of *E. coli* O157:H7 for the terminal rectum in cattle is not understood. One hypothesis proposed in this study is that variant oxygen levels in different parts of the gastrointestinal tract may influence the maturation of T3SS. This is supported by a report demonstrating that the maturation of T3SS was enhanced by the activation of anaerobic system (Ando *et al.*, 2007). T3SS responds to many regulators and factors such as pH value, glucose, iron and temperature (Laaberki *et al.*, 2006). Previous work has demonstrated marked variation in the levels of T3S among EHEC O157 strains. The aim of this research was to further investigate the regulation of T3S towards two objectives: (1) to understand the localization of EHEC O157 at the terminal rectum of cattle; (2) to understand the strain variation in T3S and whether this might be related to differences in strain epidemiology.

In relation to rectal and mucosal colonization, I investigated the importance of four aerobic/anaerobic regulators (ArcA, Fnr, NarX and NarP) on T3SS. Four deletion mutants were constructed by λ recombination technology in the *E. coli* O157:H7 Walla 3 (ZAP198) background. Adherence efficiency, A/E lesions formation, growth rate and T3S level, were examined in these four mutants as well as the wild type (ZAP198). All the four mutants showed some reduction in adherence level, while *arcA*, *narX* and *narP* mutants showed a significant decrease ($P < 0.05$). A/E lesions are formed by the T3SS

following colonization and attachment to intestinal mucosa. Consistent with the binding data, A/E lesions in the four regulatory mutants were also decreased compared with the wild type strain, especially for the *arcA* and *narX* mutants ($P < 0.01$). However, the results from growth basic growth rate determinations indicated that the *arcA*, *narX* and *narP* mutants were affected. In contrast, the *fnr* mutant grew faster than the wild type. These results indicated that the adherence and A/E lesions reduction in *arcA*, *narX* and *narP* mutants might due to growth issues with these strains. Slower growth can cause less adherence and A/E lesion formation in the same time period. Interestingly, the *fnr* mutant showed decreased adherence and A/E lesion level with a shorter generation time compared to the wild type. This may indicate that Fnr can enhance attachment and A/E lesion formation by up-regulating the T3SS directly or indirectly. Recent work by Dr Jai Tree in our group has demonstrated that FnrS (Fnr sRNA) is predicted to interact with the LEE4 transcript (Jai Tree, personal communication). Further work may address Fnr regulation of T3S, but my PhD research switched to an alternative approach involving the construction of an inducible LEE1 promoter to allow induction of T3S by addition of the chemical inducer.

The aim of this second section of work was to override normal signal inputs into the promoter by replacing this promoter with *tet* promoter which can be induced with aTc. This construct could then be used to examine the link between the tropism of O157 for the terminal rectum of cattle and the regulation of T3S, as aTc could be administered to animals or a constitutive promoter used in its place. If successful, this construct could also be used to test whether heterogeneous of LEE4 and LEE5 (Roe *et al.*, 2003b) is completely independent of normal inputs at LEE1 and whether the expression level at LEE1 alters the proportion of bacteria expressing a functional T3SS. Two constructs were designed. The first construction kept the original transcriptional start site and -10 region of the native LEE1 operon promoter, while the -35 regions are replaced by AT rich DNA sequence (*tet* promoter) synthesized artificially (Fig. 4.16). For the second construct, only the original transcriptional start site was kept with -35 and -10 regions replaced by a synthesized *tet* promoter (Fig. 4.17). The first construction was successfully obtained by allelic exchange with LEE1 promoter -35 region replaced by the *tet* promoter.

The resultant strain should be controlled by aTc as expected. Surprisingly, no detectable T3S protein was found with aTc induction in this strain. However, it could still be the case that the *tet* promoter was being induced but that this did not result in T3S for reasons that are not currently understood. Based on subsequent work using my ZAP1327 strain (ZAP198 with the LEE1 promoter replaced by *sacBkan* cassette), Allen Flockhart, Jai Tree and Mariya demonstrated that a comparatively high level of transcription of LEE1 is occurring from this cassette into the LEE1 operon, but that despite this there is no T3S detected by Western blotting. Interestingly, the introduction of a plasmid containing *ler* and its promoter region lead to T3S being detectable from ZAP1327. Given that *ler* should not be able to induce LEE1 any further in this strain (as the LEE1 regulatory region it normally auto-induces is no longer there) then this T3S must be the result of the introduced additional *ler* acting on LEE2-5 and/or a controlling factor present upstream of *ler*, such as an sRNA, that is also required for T3S. It does though indicate that even with successful aTc induction from my construct it is unlikely that I would have induced T3S. Future work will examine by RT-PCR whether the aTc induction is producing increased levels of the LEE1 transcript. In attempting to obtain the second construction strain, I had difficulties in cloning *tet* promoter in front of *ler*. I tried many times in cloning the *tet* promoter into pIB307 with both LEE1 promoter flanking regions including *ler*. But mutations were always detected in the cloned *tet* promoter. This might be due to a high expression levels from the *tet* promoter in the cloning vector leading to an extremely high expression of *Ler* which could be lethal to the bacteria and therefore selected against. So only defective *tet* promoter regions could be selected in the process of cloning. Although the constructed strain (first construction) can not be used for the designed purposes, the intermediate strains, such as ZAP1213 (ZAP198 with *lazY&Z* replaced by *tetR*) and ZAP1327 (ZAP1213 with LEE1 promoter replaced by *sacBkan* cassette), can be used for other related work and other constructions using the inducible TetR system. My PhD work moved on to investigate variable T3S levels in different strains.

An IPRAVE (Wellcome Trust funded) study reported that PT21/28 strains were more likely to be associated with higher level faecal counts compared with PT32 strains in

cattle. In addition, PT21/28 strains over that period were the most prevalent phage type associated with human infection (Chase-Topping *et al.*, 2008; Chase-Topping *et al.*, 2007b). The initial aim was to compare PT21/28 and PT32 strains in terms of genomic differences and phenotypes including T3SS to determine how these inform the epidemiology.

CGH analysis of 12 strains indicated that one of the main differences between the PT 21/28 and 32 strains was with Stx phage carriage. Based on the CGH, PCR was used to determine the presence of Stx2 and Stx2c in 60 strains. Results indicated that PT21/28 strains generally carried both Stx2 and Stx2c bacteriophages, irrespective of whether the strains were sourced from cattle or humans. By contrast, nearly all the bovine PT32 strains analyzed carried only the Stx2c phage. The situation for the limited number of human PT32 strains was more complex, but these were significantly more likely to contain a Stx2 phage in comparison to the bovine strains. This data indicates that strains carrying both Stx2 and Stx2c phages are more likely to be associated with human infection. This result is in line with recently published research on Clade 8 strains in the USA that are considered to be more virulent. Clade 8 strains were significantly more likely to carry both the *stx2* and *stx2c* genes in comparison to the other clades containing *stx2c* (Manning *et al.*, 2008). All clade 8 strains tested had *stx2*, and 57.6% had *stx2c*. Whether this association for both relates to differences in toxicity of the strains or other phenotypes associated with the strains is not known, although more recent work has indicated that levels of Stx2 production alone are likely to be important, irrespective of lineage, in terms of association with human clinical disease (Zhang *et al.* 2009).

To identify the T3S levels in these two phage types, we investigated for the secreted translocon protein EspD and T3S apparatus protein EscJ by Western blotting. LEE1 expression was also measured by determining fluorescence levels from a previously published LEE1-GFP reporter (Roe *et al.*, 2003a). T3S levels were low in the majority of PT21/28 strains compared with the PT32 strains. The results also demonstrated that both Stx2 and Stx2c phages had on average lower levels of LEE1 expression than strains with

a single Stx2 bacteriophage. Analysis of strain pairs demonstrated that Stx phage insertion into the chromosome leads to repression on T3S (Fig. 5.5-8), this was also apparent in a pair of O26 strains, including one from which the Stx2 phage had been naturally cured Bielaszewska ref at end. While Stx bacteriophage insertion and deletion repressed and activated T3S respectively, other differences between the strains also account for the marked difference in T3S levels between these strains. Further research using information on the sequences of multiple strains in comparison with T3S profile should help clarify the main alleles responsible for this variation.

To confirm and study the Stx2 bacteriophage repression in another background, the sequenced *E. coli* K12 MG1655 strain was lysogenised with a marked Stx2 phage from the sequenced *E. coli* O157:H7 Sakai strain (Table 3, this work is done by Sean McAteer) and LEE1 transcription levels were measured this constructed strain and MG1655. It was revealed that expression of LEE1 was significantly repressed in the K-12 strain containing the Stx2 lysogen. GadE is known to be involved in repression of T3S so increased *gadE* expression following Stx phage lysogeny may well account for some of the reduced expression (Kailasan Vanaja *et al.*, 2009; Tatsuno *et al.*, 2003). The repression of Ler activity on LEE1 may be the result of established lambda lysogeny regulators and/or regulators encoded elsewhere in the bacteriophages. To test established lambda phage regulators, *cI*, *cII*, *cro*, anti-terminators N and Q were cloned and induced in TUV93-0. CII was the only induced regulator that had an effect on T3S, but in this case the growth rate of the cells was also reduced and there was not the concomitant reduction in EscJ levels as seen for lysogeny with the whole phage. To test the potential importance of *cII*, both copies were deleted from the Stx1 and Stx2 phages in EDL933. For this mutant T3S was increased indicating a role of *cII* in the control of T3S regulation. This result is however incongruous with the established regulation and function of CII, which is thought to only be expressed to establish the lambda lysogen (Oppenheim *et al.*, 2005). While this appears to be the case for bacteriophage Lambda there may well be differences in the regulation between classic lambda and Stx lambdoid bacteriophages. In addition, I cannot rule out that other Stx phage-based regulators may also contribute to

repression of T3S following lysogeny and investigating this will be the basis of future work in this area.

Some future work will examine whether increased persistence or excretion of strains in/from cattle is associated with integration of multiple Stx phages and increased Stx toxin levels, with the obvious negative ramifications for human EHEC infections. Briefly, paired strains including Stx positive and negative such as 1238 (Stx2⁺) and 1239 (Stx2⁻), EDL933 and TUV93-0 will be used to infect cattle. The shedding levels will be measured in the following weeks. In the end, the colonization persistence and tropism in the cattle will be examined. At the same time, the A/E lesions and toxin production levels of these tested strains will be measured in the lab.

Additional future work can address further the regulatory mechanisms working between the Stx phage and the T3SS. To investigate the mechanism of CII regulation on T3S, the interaction of CII with the *ler*/LEE1 promoter could be examined. Briefly, expressed CII proteins would be used to examine with the interaction with *ler* DNA including the promoter of *ler* by electrophoretic mobility shift assay. Further work would be carried out to investigate the the specific site on *ler* to which CII binds. If no interaction is found between CII and *ler*, future work could address other regions to which it may bind such as *grlA/R* and the *gadE* promoters. Other phage based controlling factors could be screened for by deleting Stx phage regions from the K12 Stx2 phage lysogen and the effect on T3S induction measured with a LEE1-GFP reporter.

Overall the key finding of my work is that the Stx bacteriophage ‘takes control’ of the key EHEC colonisation system, potentially allowing selection of other prophage elements that are able to reverse this repression using Pch positive regulators.

7 References

- Abe, H., Abo, T. & Aiba, H. (1999).** Regulation of intrinsic terminator by translation in *Escherichia coli*: transcription termination at a distance downstream. *Genes Cells* **4**, 87-97.
- Abe, H., Miyahara, A., Oshima, T., Tashiro, K., Ogura, Y., Kuhara, S., Ogasawara, N., Hayashi, T. & Tobe, T. (2008).** Global regulation by horizontally transferred regulators establishes the pathogenicity of *Escherichia coli*. *DNA Res* **15**, 25-38.
- Acheson, D. W. (1992).** Enterotoxins in acute infective diarrhoea. *J Infect* **24**, 225-245.
- Agency, H. P. (2005).** Verotoxin-producing E.coli O157 (VTEC O157) at a school in the south Wales valleys. *Commun Dis Rep CDR Wkly* **15**, 38.
- Alexeeva, S., Hellingwerf, K. J. & Teixeira de Mattos, M. J. (2003).** Requirement of ArcA for redox regulation in *Escherichia coli* under microaerobic but not anaerobic or aerobic conditions. *J Bacteriol* **185**, 204-209.
- Ando, H., Abe, H., Sugimoto, N. & Tobe, T. (2007).** Maturation of functional type III secretion machinery by activation of anaerobic respiration in enterohaemorrhagic *Escherichia coli*. *Microbiology* **153**, 464-473.
- Asadulghani, M., Ogura, Y., Ooka, T., Itoh, T., Sawaguchi, A., Iguchi, A., Nakayama, K. & Hayashi, T. (2009).** The defective prophage pool of *Escherichia coli* O157: prophage-prophage interactions potentiate horizontal transfer of virulence determinants. *PLoS Pathog* **5**, e1000408.
- Banuett, F., Hoyt, M. A., McFarlane, L., Echols, H. & Herskowitz, I. (1986).** hflB, a new *Escherichia coli* locus regulating lysogeny and the level of bacteriophage lambda cII protein. *J Mol Biol* **187**, 213-224.

Barba, J., Bustamante, V. H., Flores-Valdez, M. A., Deng, W., Finlay, B. B. & Puente, J. L. (2005). A positive regulatory loop controls expression of the locus of enterocyte effacement-encoded regulators Ler and GrlA. *J Bacteriol* **187**, 7918-7930.

Bearson SM, Albrecht JA, Gunsalus RP. (2002). Oxygen and nitrate-dependent regulation of dmsABC operon expression in *Escherichia coli*: sites for Fnr and NarL protein interactions. *BMC Microbiol* **2**, 2:13.

Beery, J. T., Doyle, M. P. & Schoeni, J. L. (1985). Colonization of chicken cecae by *Escherichia coli* associated with hemorrhagic colitis. *Appl Environ Microbiol* **49**, 310-315.

Bentley, R. & Meganathan, R. (1982). Biosynthesis of vitamin K (menaquinone) in bacteria. *Microbiol Rev* **46**, 241-280.

Besser, R. E., Griffin, P. M. & Slutsker, L. (1999). *Escherichia coli* O157:H7 gastroenteritis and the hemolytic uremic syndrome: an emerging infectious disease. *Annu Rev Med* **50**, 355-367.

Bettelheim, K. A., Breadon, A., Faiers, M. C., O'Farrell, S. M. & Shooter, R. A. (1974). The origin of O serotypes of *Escherichia coli* in babies after normal delivery. *J Hyg (Lond)* **72**, 67-70.

Bettelheim, K. A., Bensink, J. C. & Tambunan, H. S. (2000). Serotypes of verotoxin-producing (Shiga toxin-producing) *Escherichia coli* isolated from healthy sheep. *Comp Immunol Microbiol Infect Dis* **23**, 1-7.

Blomfield, I. C., Vaughn, V., Rest, R. F. & Eisenstein, B. I. (1991). Allelic exchange in *Escherichia coli* using the *Bacillus subtilis* sacB gene and a temperature-sensitive pSC101 replicon. *Mol Microbiol* **5**, 1447-1457.

Boyce, T. G., Swerdlow, D. L. & Griffin, P. M. (1995). *Escherichia coli* O157:H7 and the hemolytic-uremic syndrome. *N Engl J Med* **333**, 364-368.

Boyd, E. F. & Brussow, H. (2002). Common themes among bacteriophage-encoded virulence factors and diversity among the bacteriophages involved. *Trends Microbiol* **10**, 521-529.

Brussow, H., Canchaya, C. & Hardt, W. D. (2004). Phages and the evolution of bacterial pathogens: from genomic rearrangements to lysogenic conversion. *Microbiol Mol Biol Rev* **68**, 560-602.

Bustamante, V. H., Santana, F. J., Calva, E. & Puente, J. L. (2001). Transcriptional regulation of type III secretion genes in enteropathogenic *Escherichia coli*: Ler antagonizes H-NS-dependent repression. *Mol Microbiol* **39**, 664-678.

Cain, R. J., Hayward, R. D. & Koronakis, V. (2008). Deciphering interplay between Salmonella invasion effectors. *PLoS Pathog* **4**, e1000037.

Campellone, K. G., Roe, A. J., Lobner-Olesen, A. & other authors (2007). Increased adherence and actin pedestal formation by dam-deficient enterohaemorrhagic *Escherichia coli* O157:H7. *Mol Microbiol* **63**, 1468-1481.

Canchaya, C., Fournous, G., Chibani-Chennoufi, S., Dillmann, M. L. & Brussow, H. (2003). Phage as agents of lateral gene transfer. *Curr Opin Microbiol* **6**, 417-424.

Chapman, P. A., Siddons, C. A., Wright, D. J., Norman, P., Fox, J. & Crick, E. (1993). Cattle as a possible source of verocytotoxin-producing *Escherichia coli* O157 infections in man. *Epidemiol Infect* **111**, 439-447.

Chase-Topping, M., Gally, D., Low, C., Matthews, L. & Woolhouse, M. (2008). Super-shedding and the link between human infection and livestock carriage of *Escherichia coli* O157. *Nat Rev Microbiol* **6**, 904-912.

Chase-Topping, M. E., Gunn, G., Strachan, W. D., Edwards, S. A., Smith, W. J., Hillman, K., Stefopoulou, S. N. & Thomson, J. R. (2007a). Epidemiology of porcine non-specific colitis on Scottish farms. *Vet J* **173**, 353-360.

Chase-Topping, M. E., McKendrick, I. J., Pearce, M. C. & other authors (2007b). Risk factors for the presence of high-level shedders of *Escherichia coli* O157 on Scottish farms. *J Clin Microbiol* **45**, 1594-1603.

Chattopadhyay, S., Garcia-Mena, J., DeVito, J., Wolska, K. & Das, A. (1995). Bipartite function of a small RNA hairpin in transcription antitermination in bacteriophage lambda. *Proc Natl Acad Sci U S A* **92**, 4061-4065.

Cherifi, A., Contrepolis, M., Picard, B., Goullet, P., Orskov, I. & Orskov, F. (1994). Clonal relationships among *Escherichia coli* serogroup O78 isolates from human and animal infections. *J Clin Microbiol* **32**, 1197-1202.

Committee, I. I. (2010). Review of the major outbreak of *E. coli* O157 in Surrey, 2009.

Cowan, L. A., Hertzke, D. M., Fenwick, B. W. & Andreasen, C. B. (1997). Clinical and clinicopathologic abnormalities in greyhounds with cutaneous and renal glomerular vasculopathy: 18 cases (1992-1994). *J Am Vet Med Assoc* **210**, 789-793.

Crane, J. K., McNamara, B. P. & Donnenberg, M. S. (2001). Role of EspF in host cell death induced by enteropathogenic *Escherichia coli*. *Cell Microbiol* **3**, 197-211.

Creasey, E. A., Delahay, R. M., Daniell, S. J. & Frankel, G. (2003). Yeast two-hybrid system survey of interactions between LEE-encoded proteins of enteropathogenic *Escherichia coli*. *Microbiology* **149**, 2093-2106.

Crepin, V. F., Prasannan, S., Shaw, R. K., Wilson, R. K., Creasey, E., Abe, C. M., Knutton, S., Frankel, G. & Matthews, S. (2005). Structural and functional studies of the enteropathogenic *Escherichia coli* type III needle complex protein EscJ. *Mol Microbiol* **55**, 1658-1670.

Dahan, S., Knutton, S., Shaw, R. K., Crepin, V. F., Dougan, G. & Frankel, G. (2004). Transcriptome of enterohemorrhagic *Escherichia coli* O157 adhering to eukaryotic plasma membranes. *Infect Immun* **72**, 5452-5459.

Dahan, S., Wiles, S., La Ragione, R. M. & other authors (2005). EspJ is a prophage-carried type III effector protein of attaching and effacing pathogens that modulates infection dynamics. *Infect Immun* **73**, 679-686.

Daniell, S. J., Takahashi, N., Wilson, R. & other authors (2001). The filamentous type III secretion translocon of enteropathogenic *Escherichia coli*. *Cell Microbiol* **3**, 865-871.

Datta, A. B., Panjikar, S., Weiss, M. S., Chakrabarti, P. & Parrack, P. (2005a). Structure of lambda CII: implications for recognition of direct-repeat DNA by an unusual tetrameric organization. *Proc Natl Acad Sci U S A* **102**, 11242-11247.

Datta, A. B., Roy, S. & Parrack, P. (2005b). Role of C-terminal residues in oligomerization and stability of lambda CII: implications for lysis-lysogeny decision of the phage. *J Mol Biol* **345**, 315-324.

Dean-Nystrom, E. A., Stoffregen, W. C., Bosworth, B. T., Moon, H. W. & Pohlenz, J. F. (2008). Early attachment sites for Shiga-toxigenic *Escherichia coli* O157:H7 in experimentally inoculated weaned calves. *Appl Environ Microbiol* **74**, 6378-6384.

Dean, P. & Kenny, B. (2004). Intestinal barrier dysfunction by enteropathogenic *Escherichia coli* is mediated by two effector molecules and a bacterial surface protein. *Mol Microbiol* **54**, 665-675.

Degnan, P. H., Michalowski, C. B., Babic, A. C., Cordes, M. H. & Little, J. W. (2007). Conservation and diversity in the immunity regions of wild phages with the immunity specificity of phage lambda. *Mol Microbiol* **64**, 232-244.

Delahay, R. M., Knutton, S., Shaw, R. K., Hartland, E. L., Pallen, M. J. & Frankel, G. (1999). The coiled-coil domain of EspA is essential for the assembly of the type III secretion translocon on the surface of enteropathogenic *Escherichia coli*. *J Biol Chem* **274**, 35969-35974.

Deng, W., Puente, J. L., Gruenheid, S. & other authors (2004). Dissecting virulence: systematic and functional analyses of a pathogenicity island. *Proc Natl Acad Sci U S A* **101**, 3597-3602.

Dobrindt, U., Chowdary, M. G., Krumbholz, G. & Hacker, J. (2010). Genome dynamics and its impact on evolution of *Escherichia coli*. *Med Microbiol Immunol* **199**, 145-154.

Eaton, K. A., Friedman, D. I., Francis, G. J., Tyler, J. S., Young, V. B., Haeger, J., Abu-Ali, G. & Whittam, T. S. (2008). Pathogenesis of renal disease due to enterohemorrhagic *Escherichia coli* in germ-free mice. *Infect Immun* **76**, 3054-3063.

Ebel, F., Podzadel, T., Rohde, M., Kresse, A. U., Kramer, S., Deibel, C., Guzman, C. A. & Chakraborty, T. (1998). Initial binding of Shiga toxin-producing *Escherichia coli* to host cells and subsequent induction of actin rearrangements depend on filamentous EspA-containing surface appendages. *Mol Microbiol* **30**, 147-161.

Eckert, B. & Beck, C. F. (1989). Overproduction of transposon Tn10-encoded tetracycline resistance protein results in cell death and loss of membrane potential. *J Bacteriol* **171**, 3557-3559.

Elliott, S. J., Wainwright, L. A., McDaniel, T. K., Jarvis, K. G., Deng, Y. K., Lai, L. C., McNamara, B. P., Sonnenberg, M. S. & Kaper, J. B. (1998). The complete sequence of the locus of enterocyte effacement (LEE) from enteropathogenic *Escherichia coli* E2348/69. *Mol Microbiol* **28**, 1-4.

Elliott, S. J., Hutcheson, S. W., Dubois, M. S., Mellies, J. L., Wainwright, L. A., Batchelor, M., Frankel, G., Knutton, S. & Kaper, J. B. (1999). Identification of CesT, a chaperone for the type III secretion of Tir in enteropathogenic *Escherichia coli*. *Mol Microbiol* **33**, 1176-1189.

Elliott, S. J., Sperandio, V., Giron, J. A., Shin, S., Mellies, J. L., Wainwright, L., Hutcheson, S. W., McDaniel, T. K. & Kaper, J. B. (2000). The locus of enterocyte effacement (LEE)-encoded regulator controls expression of both LEE- and non-LEE-encoded virulence factors in enteropathogenic and enterohemorrhagic *Escherichia coli*. *Infect Immun* **68**, 6115-6126.

Emmerson, J. R., Gally, D. L. & Roe, A. J. (2006). Generation of gene deletions and gene replacements in *Escherichia coli* O157:H7 using a temperature sensitive allelic exchange system. *Biol Proced Online* **8**, 153-162.

Epe, B. & Woolley, P. (1984). The binding of 6-demethylchlortetracycline to 70S, 50S and 30S ribosomal particles: a quantitative study by fluorescence anisotropy. *EMBO J* **3**, 121-126.

- Erdem, A. L., Avelino, F., Xicohtencatl-Cortes, J. & Giron, J. A. (2007).** Host protein binding and adhesive properties of H6 and H7 flagella of attaching and effacing *Escherichia coli*. *J Bacteriol* **189**, 7426-7435.
- Ewing, P. R. E. W. H. (1972).** Identification of *Enterobacteriaceae*: Burgess Publishing Co., Minneapolis, Minn.
- Fang, T. J. (2005).** Bacterial contamination of ready to eat foods: concern for human toxicity. *Reviews in Food and Nutrition Toxicity* **6**: 143-171.
- Fattah, K. R., Mizutani, S., Fattah, F. J., Matsushiro, A. & Sugino, Y. (2000).** A comparative study of the immunity region of lambdoid phages including Shiga-toxin-converting phages: molecular basis for cross immunity. *Genes Genet Syst* **75**, 223-232.
- Feng, P., Lampel, K. A., Karch, H. & Whittam, T. S. (1998).** Genotypic and phenotypic changes in the emergence of *Escherichia coli* O157:H7. *J Infect Dis* **177**, 1750-1753.
- Feng, P. C., Monday, S. R., Lacher, D. W. & other authors (2007).** Genetic diversity among clonal lineages within *Escherichia coli* O157:H7 stepwise evolutionary model. *Emerg Infect Dis* **13**, 1701-1706.
- Filee, J., Forterre, P. & Laurent, J. (2003).** The role played by viruses in the evolution of their hosts: a view based on informational protein phylogenies. *Res Microbiol* **154**, 237-243.
- Fogg, P. C., Gossage, S. M., Smith, D. L., Saunders, J. R., McCarthy, A. J. & Allison, H. E. (2007).** Identification of multiple integration sites for Stx-phage Phi24B in the *Escherichia coli* genome, description of a novel integrase and evidence for a functional anti-repressor. *Microbiology* **153**, 4098-4110.
- Fogg, P. C., Allison, H. E., Saunders, J. R. & McCarthy, A. J. (2010).** Bacteriophage lambda: a paradigm revisited. *J Virol* **84**, 6876-6879.
- Frankel, G., Phillips, A. D., Rosenshine, I., Dougan, G., Kaper, J. B. & Knutton, S. (1998).** Enteropathogenic and enterohaemorrhagic *Escherichia coli*: more subversive elements. *Mol Microbiol* **30**, 911-921.
- Friedberg, D., Umanski, T., Fang, Y. & Rosenshine, I. (1999).** Hierarchy in the expression of the locus of enterocyte effacement genes of enteropathogenic *Escherichia coli*. *Mol Microbiol* **34**, 941-952.
- Friedman, D. I. & Court, D. L. (2001).** Bacteriophage lambda: alive and well and still doing its thing. *Curr Opin Microbiol* **4**, 201-207.

Friedrich, A. W., Zhang, W., Bielaszewska, M., Mellmann, A., Kock, R., Fruth, A., Tschape, H. & Karch, H. (2007). Prevalence, virulence profiles, and clinical significance of Shiga toxin-negative variants of enterohemorrhagic *Escherichia coli* O157 infection in humans. *Clin Infect Dis* **45**, 39-45.

Gansheroff, L. J. & O'Brien, A. D. (2000). *Escherichia coli* O157:H7 in beef cattle presented for slaughter in the U.S.: higher prevalence rates than previously estimated. *Proc Natl Acad Sci U S A* **97**, 2959-2961.

Garcia-Aljaro, C., Muniesa, M., Blanco, J. E., Blanco, M., Blanco, J., Jofre, J. & Blanch, A. R. (2005). Characterization of Shiga toxin-producing *Escherichia coli* isolated from aquatic environments. *FEMS Microbiol Lett* **246**, 55-65.

Garcia, A., Marini, R. P., Feng, Y., Vitsky, A., Knox, K. A., Taylor, N. S., Schauer, D. B. & Fox, J. G. (2002). A naturally occurring rabbit model of enterohemorrhagic *Escherichia coli*-induced disease. *J Infect Dis* **186**, 1682-1686.

Garcia, A., Bosques, C. J., Wishnok, J. S., Feng, Y., Karalius, B. J., Butters, J. R., Schauer, D. B., Rogers, A. B. & Fox, J. G. (2006). Renal injury is a consistent finding in Dutch Belted rabbits experimentally infected with enterohemorrhagic *Escherichia coli*. *J Infect Dis* **193**, 1125-1134.

Garg, A. X., Clark, W. F., Salvadori, M., Macnab, J., Suri, R. S., Haynes, R. B. & Matsell, D. (2005). Microalbuminuria three years after recovery from *Escherichia coli* O157 hemolytic uremic syndrome due to municipal water contamination. *Kidney Int* **67**, 1476-1482.

Garmendia, J., Frankel, G. & Crepin, V. F. (2005). Enteropathogenic and enterohemorrhagic *Escherichia coli* infections: translocation, translocation, translocation. *Infect Immun* **73**, 2573-2585.

Gauthier, A., Puente, J. L. & Finlay, B. B. (2003). Secretin of the enteropathogenic *Escherichia coli* type III secretion system requires components of the type III apparatus for assembly and localization. *Infect Immun* **71**, 3310-3319.

Georgellis, D., Kwon, O. & Lin, E. C. (1999). Amplification of signaling activity of the arc two-component system of *Escherichia coli* by anaerobic metabolites. An in vitro study with different protein modules. *J Biol Chem* **274**, 35950-35954.

Geue, L., Klare, S., Schnick, C., Mintel, B., Meyer, K. & Conraths, F. J. (2009). Analysis of the clonal relationship of serotype O26:H11 enterohemorrhagic *Escherichia coli* isolates from cattle. *Appl Environ Microbiol* **75**, 6947-6953.

Ghosh, P. (2004). Process of protein transport by the type III secretion system. *Microbiol Mol Biol Rev* **68**, 771-795.

- Gillespie, I. A., O'Brien, S. J., Adak, G. K., Cheasty, T. & Willshaw, G. (2005).** Foodborne general outbreaks of Shiga toxin-producing *Escherichia coli* O157 in England and Wales 1992-2002: where are the risks? *Epidemiol Infect* **133**, 803-808.
- Goldberg, M. D., Johnson, M., Hinton, J. C. & Williams, P. H. (2001).** Role of the nucleoid-associated protein Fis in the regulation of virulence properties of enteropathogenic *Escherichia coli*. *Mol Microbiol* **41**, 549-559.
- Goosney, D. L., de Grado, M. & Finlay, B. B. (1999).** Putting *E. coli* on a pedestal: a unique system to study signal transduction and the actin cytoskeleton. *Trends Cell Biol* **9**, 11-14.
- Greenblatt, J., Mah, T. F., Legault, P., Mogridge, J., Li, J. & Kay, L. E. (1998).** Structure and mechanism in transcriptional antitermination by the bacteriophage lambda N protein. *Cold Spring Harb Symp Quant Biol* **63**, 327-336.
- Griffin, P. M. (1995).** *Escherichia coli* O157:H7 and other enterohemorrhagic *Escherichia coli*. New York: Raven Press.
- Gruenheid, S., Sekirov, I., Thomas, N. A. & other authors (2004).** Identification and characterization of NleA, a non-LEE-encoded type III translocated virulence factor of enterohaemorrhagic *Escherichia coli* O157:H7. *Mol Microbiol* **51**, 1233-1249.
- Gu, J., Liu, Y., Yu, S. & other authors (2009).** Enterohemorrhagic *Escherichia coli* trivalent recombinant vaccine containing EspA, intimin and Stx2 induces strong humoral immune response and confers protection in mice. *Microbes Infect* **11**, 835-841.
- Guest JR, G. J., Irvine AS, Spiro S. (1996).** The FNR modulon and FNRregulated gene expression In: Lin, ECC.; Lynch, AS., editors. Regulation of Gene Expression in *Escherichia coli*. New York, NY: Champman and Hall, 317-342.
- Gunsalus, R. P. (1992).** Control of electron flow in *Escherichia coli*: coordinated transcription of respiratory pathway genes. *J Bacteriol* **174**, 7069-7074.
- Gunzer, F., Bohm, H., Russmann, H., Bitzan, M., Aleksic, S. & Karch, H. (1992).** Molecular detection of sorbitol-fermenting *Escherichia coli* O157 in patients with hemolytic-uremic syndrome. *J Clin Microbiol* **30**, 1807-1810.
- Guo, J. & Roberts, J. W. (2004).** DNA binding regions of Q proteins of phages lambda and phi80. *J Bacteriol* **186**, 3599-3608.
- Hacker, J., Blum-Oehler, G., Muhldorfer, I. & Tschape, H. (1997).** Pathogenicity islands of virulent bacteria: structure, function and impact on microbial evolution. *Mol Microbiol* **23**, 1089-1097.
- Hacker, J. & Kaper, J. B. (2000).** Pathogenicity islands and the evolution of microbes. *Annu Rev Microbiol* **54**, 641-679.

Hamilton, C. M., Aldea, M., Washburn, B. K., Babitzke, P. & Kushner, S. R. (1989). New method for generating deletions and gene replacements in *Escherichia coli*. *J Bacteriol* **171**, 4617-4622.

Hancock, D. D., Besser, T. E., Kinsel, M. L., Tarr, P. I., Rice, D. H. & Paros, M. G. (1994). The prevalence of *Escherichia coli* O157:H7 in dairy and beef cattle in Washington State. *Epidemiol Infect* **113**, 199-207.

Hansen, A. M. & Kaper, J. B. (2009). Hfq affects the expression of the LEE pathogenicity island in enterohaemorrhagic *Escherichia coli*. *Mol Microbiol* **73**, 446-465.

Hartland, E. L., Daniell, S. J., Delahay, R. M., Neves, B. C., Wallis, T., Shaw, R. K., Hale, C., Knutton, S. & Frankel, G. (2000). The type III protein translocation system of enteropathogenic *Escherichia coli* involves EspA-EspB protein interactions. *Mol Microbiol* **35**, 1483-1492.

Hayashi, T., Makino, K., Ohnishi, M. & other authors (2001). Complete genome sequence of enterohemorrhagic *Escherichia coli* O157:H7 and genomic comparison with a laboratory strain K-12. *DNA Res* **8**, 11-22.

Herman, C., Ogura, T., Tomoyasu, T., Hiraga, S., Akiyama, Y., Ito, K., Thomas, R., D'Ari, R. & Boulloc, P. (1993). Cell growth and lambda phage development controlled by the same essential *Escherichia coli* gene, *ftsH/hflB*. *Proc Natl Acad Sci U S A* **90**, 10861-10865.

Herman, C., Thevenet, D., D'Ari, R. & Boulloc, P. (1997). The HflB protease of *Escherichia coli* degrades its inhibitor lambda cIII. *J Bacteriol* **179**, 358-363.

Hoey, D. E., Currie, C., Else, R. W., Nutikka, A., Lingwood, C. A., Gally, D. L. & Smith, D. G. (2002). Expression of receptors for verotoxin 1 from *Escherichia coli* O157 on bovine intestinal epithelium. *J Med Microbiol* **51**, 143-149.

Hoey, D. E., Sharp, L., Currie, C., Lingwood, C. A., Gally, D. L. & Smith, D. G. (2003). Verotoxin 1 binding to intestinal crypt epithelial cells results in localization to lysosomes and abrogation of toxicity. *Cell Microbiol* **5**, 85-97.

Holden, N., Blomfield, I. C., Uhlin, B. E., Totsika, M., Kulasekara, D. H. & Gally, D. L. (2007). Comparative analysis of FimB and FimE recombinase activity. *Microbiology* **153**, 4138-4149.

Hoyt, M. A., Knight, D. M., Das, A., Miller, H. I. & Echols, H. (1982). Control of phage lambda development by stability and synthesis of cII protein: role of the viral cIII and host *hflA*, *himA* and *himD* genes. *Cell* **31**, 565-573.

Hueck, C. J. (1998). Type III protein secretion systems in bacterial pathogens of animals and plants. *Microbiol Mol Biol Rev* **62**, 379-433.

Iyoda, S. & Watanabe, H. (2004). Positive effects of multiple pch genes on expression of the locus of enterocyte effacement genes and adherence of enterohaemorrhagic *Escherichia coli* O157 : H7 to HEP-2 cells. *Microbiology* **150**, 2357-2571.

Iyoda, S. & Watanabe, H. (2005). ClpXP protease controls expression of the type III protein secretion system through regulation of RpoS and GrlR levels in enterohemorrhagic *Escherichia coli*. *J Bacteriol* **187**, 4086-4094.

Iyoda, S., Koizumi, N., Satou, H., Lu, Y., Saitoh, T., Ohnishi, M. & Watanabe, H. (2006). The GrlR-GrlA regulatory system coordinately controls the expression of flagellar and LEE-encoded type III protein secretion systems in enterohemorrhagic *Escherichia coli*. *J Bacteriol* **188**, 5682-5692.

Jackson, M. P., Newland, J. W., Holmes, R. K. & O'Brien, A. D. (1987). Nucleotide sequence analysis of the structural genes for Shiga-like toxin I encoded by bacteriophage 933J from *Escherichia coli*. *Microb Pathog* **2**, 147-153.

Jain, D., Kim, Y., Maxwell, K. L., Beasley, S., Zhang, R., Gussin, G. N., Edwards, A. M. & Darst, S. A. (2005). Crystal structure of bacteriophage lambda cII and its DNA complex. *Mol Cell* **19**, 259-269.

Jarvis, K. G., Giron, J. A., Jerse, A. E., McDaniel, T. K., Donnenberg, M. S. & Kaper, J. B. (1995). Enteropathogenic *Escherichia coli* contains a putative type III secretion system necessary for the export of proteins involved in attaching and effacing lesion formation. *Proc Natl Acad Sci U S A* **92**, 7996-8000.

Jerse, A. E., Yu, J., Tall, B. D. & Kaper, J. B. (1990). A genetic locus of enteropathogenic *Escherichia coli* necessary for the production of attaching and effacing lesions on tissue culture cells. *Proc Natl Acad Sci U S A* **87**, 7839-7843.

Jimenez, R., Cruz-Migoni, S. B., Huerta-Saquero, A., Bustamante, V. H. & Puente, J. L. (2010). Molecular characterization of GrlA, a specific positive regulator of ler expression in enteropathogenic *Escherichia coli*. *J Bacteriol* **192**, 4627-4642.

Kailasan Vanaja, S., Bergholz, T. M. & Whittam, T. S. (2009). Characterization of the *Escherichia coli* O157:H7 Sakai GadE regulon. *J Bacteriol* **191**, 1868-1877.

Kang, G., Pulimood, A. B., Koshi, R., Hull, A., Acheson, D., Rajan, P., Keusch, G. T., Mathan, V. I. & Mathan, M. M. (2001). A monkey model for enterohemorrhagic *Escherichia coli* infection. *J Infect Dis* **184**, 206-210.

Kaper, J. B., Nataro, J. P. & Mobley, H. L. (2004). Pathogenic *Escherichia coli*. *Nat Rev Microbiol* **2**, 123-140.

- Karch, H., Janetzki-Mittmann, C., Aleksic, S. & Datz, M. (1996).** Isolation of enterohemorrhagic *Escherichia coli* O157 strains from patients with hemolytic-uremic syndrome by using immunomagnetic separation, DNA-based methods, and direct culture. *J Clin Microbiol* **34**, 516-519.
- Karch, H., Bielaszewska, M., Bitzan, M. & Schmidt, H. (1999).** Epidemiology and diagnosis of Shiga toxin-producing *Escherichia coli* infections. *Diagn Microbiol Infect Dis* **34**, 229-243.
- Karmali, M. A., Steele, B. T., Petric, M. & Lim, C. (1983).** Sporadic cases of haemolytic-uraemic syndrome associated with faecal cytotoxin and cytotoxin-producing *Escherichia coli* in stools. *Lancet* **1**, 619-620.
- Karmali, M. A. (1989).** Infection by verocytotoxin-producing *Escherichia coli*. *Clin Microbiol Rev* **2**, 15-38.
- Karpman, D., Connell, H., Svensson, M., Scheutz, F., Alm, P. & Svanborg, C. (1997).** The role of lipopolysaccharide and Shiga-like toxin in a mouse model of *Escherichia coli* O157:H7 infection. *J Infect Dis* **175**, 611-620.
- Kato, Y., Sugiura, M., Mizuno, T. & Aiba, H. (2007).** Effect of the *arcA* mutation on the expression of flagella genes in *Escherichia coli*. *Biosci Biotechnol Biochem* **71**, 77-83.
- Kauffmann, F. (1947).** The serology of coli group. *J Immunol* **57**, 71-100.
- Kedzierska, B., Glinkowska, M., Iwanicki, A., Obuchowski, M., Sojka, P., Thomas, M. S. & Wegrzyn, G. (2003).** Toxicity of the bacteriophage lambda cII gene product to *Escherichia coli* arises from inhibition of host cell DNA replication. *Virology* **313**, 622-628.
- Kendall, M. M., Rasko, D. A. & Sperandio, V. (2010)** The LysR-type regulator QseA regulates both characterized and putative virulence genes in enterohaemorrhagic *Escherichia coli* O157:H7. *Mol Microbiol* **76**, 1306-1321.
- Kenny, B., DeVinney, R., Stein, M., Reinscheid, D. J., Frey, E. A. & Finlay, B. B. (1997).** Enteropathogenic *E. coli* (EPEC) transfers its receptor for intimate adherence into mammalian cells. *Cell* **91**, 511-520.
- Kenny, B. & Jepson, M. (2000).** Targeting of an enteropathogenic *Escherichia coli* (EPEC) effector protein to host mitochondria. *Cell Microbiol* **2**, 579-590.
- Khakhriaa, R., D., D. and H. Liora (1990).** Extended phage-typing scheme for *Escherichia coli* O157:H7. *Epidemiology and Infection* **105**, 211-520.

Kihara, A., Akiyama, Y. & Ito, K. (1997). Host regulation of lysogenic decision in bacteriophage lambda: transmembrane modulation of FtsH (HflB), the cII degrading protease, by HflKC (HflA). *Proc Natl Acad Sci U S A* **94**, 5544-5549.

Kim, M., Ogawa, M., Fujita, Y. & other authors (2009). Bacteria hijack integrin-linked kinase to stabilize focal adhesions and block cell detachment. *Nature* **459**, 578-582.

Knutton, S., Baldini, M. M., Kaper, J. B. & McNeish, A. S. (1987). Role of plasmid-encoded adherence factors in adhesion of enteropathogenic *Escherichia coli* to HEp-2 cells. *Infect Immun* **55**, 78-85.

Knutton, S., Baldwin, T., Williams, P. H. & McNeish, A. S. (1989). Actin accumulation at sites of bacterial adhesion to tissue culture cells: basis of a new diagnostic test for enteropathogenic and enterohemorrhagic *Escherichia coli*. *Infect Immun* **57**, 1290-1298.

Knutton, S., Rosenshine, I., Pallen, M. J., Nisan, I., Neves, B. C., Bain, C., Wolff, C., Dougan, G. & Frankel, G. (1998). A novel EspA-associated surface organelle of enteropathogenic *Escherichia coli* involved in protein translocation into epithelial cells. *EMBO J* **17**, 2166-2176.

Kobiler, O., Koby, S., Teff, D., Court, D. & Oppenheim, A. B. (2002). The phage lambda CII transcriptional activator carries a C-terminal domain signaling for rapid proteolysis. *Proc Natl Acad Sci U S A* **99**, 14964-14969.

Kornitzer, D., Altuvia, S. & Oppenheim, A. B. (1991). The activity of the CIII regulator of lambdoid bacteriophages resides within a 24-amino acid protein domain. *Proc Natl Acad Sci U S A* **88**, 5217-5221.

Kresse, A. U., Schulze, K., Deibel, C., Ebel, F., Rohde, M., Chakraborty, T. & Guzman, C. A. (1998). Pas, a novel protein required for protein secretion and attaching and effacing activities of enterohemorrhagic *Escherichia coli*. *J Bacteriol* **180**, 4370-4379.

Kresse, A. U., Rohde, M. & Guzman, C. A. (1999). The EspD protein of enterohemorrhagic *Escherichia coli* is required for the formation of bacterial surface appendages and is incorporated in the cytoplasmic membranes of target cells. *Infect Immun* **67**, 4834-4842.

Kresse, A. U., Beltrametti, F., Muller, A., Ebel, F. & Guzman, C. A. (2000). Characterization of SepL of enterohemorrhagic *Escherichia coli*. *J Bacteriol* **182**, 6490-6498.

Krinke, L. & Wulff, D. L. (1990). RNase III-dependent hydrolysis of lambda cII-O gene mRNA mediated by lambda OOP antisense RNA. *Genes Dev* **4**, 2223-2233.

Krinke, L., Mahoney, M. & Wulff, D. L. (1991). The role of the OOP antisense RNA in coliphage lambda development. *Mol Microbiol* **5**, 1265-1272.

Kurioka, T., Yunou, Y. & Kita, E. (1998). Enhancement of susceptibility to Shiga toxin-producing *Escherichia coli* O157:H7 by protein calorie malnutrition in mice. *Infect Immun* **66**, 1726-1734.

Laaberki, M. H., Janabi, N., Oswald, E. & Repoila, F. (2006). Concert of regulators to switch on LEE expression in enterohemorrhagic *Escherichia coli* O157:H7: interplay between Ler, GrlA, HNS and RpoS. *Int J Med Microbiol* **296**, 197-210.

Larzabal, M., Mercado, E. C., Vilte, D. A., Salazar-Gonzalez, H., Cataldi, A. & Navarro-Garcia, F. (2010). Designed coiled-coil peptides inhibit the type three secretion system of enteropathogenic *Escherichia coli*. *PLoS One* **5**, e9046.

Law, D. (2000). Virulence factors of *Escherichia coli* O157 and other Shiga toxin-producing *E. coli*. *J Appl Microbiol* **88**, 729-745.

Lim, J. Y., Li, J., Sheng, H., Besser, T. E., Potter, K. & Hovde, C. J. (2007). *Escherichia coli* O157:H7 colonization at the rectoanal junction of long-duration culture-positive cattle. *Appl Environ Microbiol* **73**, 1380-1382.

Lim, J. Y., Yoon, J. & Hovde, C. J. (2010). A brief overview of *Escherichia coli* O157:H7 and its plasmid O157. *J Microbiol Biotechnol* **20**, 5-14.

Lin, E. C. & Iuchi, S. (1991). Regulation of gene expression in fermentative and respiratory systems in *Escherichia coli* and related bacteria. *Annu Rev Genet* **25**, 361-387.

Lindberg, A. A., Brown, J. E., Stromberg, N., Westlingryd, M., Schultz, J. E. & Karlsson, K. A. (1987). Identification of the Carbohydrate Receptor for Shiga Toxin Produced by *Shigella-Dysenteriae* Type-1. *Journal of Biological Chemistry* **262**, 1779-1785.

Lingwood, C. A. (1999). Glycolipid receptors for verotoxin and *Helicobacter pylori*: role in pathology. *Biochimica Et Biophysica Acta-Molecular Basis of Disease* **1455**, 375-386.

Lior, L., Litt, M., Hockin, J. & other authors (1996). Vancomycin-resistant enterococci on a renal ward in an Ontario hospital. *Can Commun Dis Rep* **22**, 125-128.

Liu, B., Yin, X., Feng, Y., Chambers, J. R., Guo, A., Gong, J., Zhu, J. & Gyles, C. L. (2010). Verotoxin 2 enhances adherence of enterohemorrhagic *Escherichia coli* O157:H7 to intestinal epithelial cells and expression of {beta}1-integrin by IPEC-J2 cells. *Appl Environ Microbiol* **76**, 4461-4468.

Louise, C. B. & O'Brig, T. G. (1995). Specific interaction of *Escherichia coli* O157:H7-derived Shiga-like toxin II with human renal endothelial cells. *J Infect Dis* **172**, 1397-1401.

Lutz, R. & Bujard, H. (1997). Independent and tight regulation of transcriptional units in *Escherichia coli* via the LacR/O, the TetR/O and AraC/I1-I2 regulatory elements. *Nucleic Acids Res* **25**, 1203-1210.

Lynch, A. S. & Lin, E. C. (1996). Transcriptional control mediated by the ArcA two-component response regulator protein of *Escherichia coli*: characterization of DNA binding at target promoters. *J Bacteriol* **178**, 6238-6249.

Mahajan, A., Currie, C. G., Mackie, S. & other authors (2009). An investigation of the expression and adhesin function of H7 flagella in the interaction of *Escherichia coli* O157 : H7 with bovine intestinal epithelium. *Cell Microbiol* **11**, 121-137.

Mahajna, J., Oppenheim, A. B., Rattray, A. & Gottesman, M. (1986). Translation initiation of bacteriophage lambda gene cII requires integration host factor. *J Bacteriol* **165**, 167-174.

Mainil, J. G., Duchesnes, C. J., Whipp, S. C., Marques, L. R., O'Brien, A. D., Casey, T. A. & Moon, H. W. (1987). Shiga-like toxin production and attaching effacing activity of *Escherichia coli* associated with calf diarrhea. *Am J Vet Res* **48**, 743-748.

Manning, S. D., Motiwala, A. S., Springman, A. C. & other authors (2008). Variation in virulence among clades of *Escherichia coli* O157:H7 associated with disease outbreaks. *Proc Natl Acad Sci U S A* **105**, 4868-4873.

Matthews, L., Low, J. C., Gally, D. L. & other authors (2006). Heterogeneous shedding of *Escherichia coli* O157 in cattle and its implications for control. *Proc Natl Acad Sci U S A* **103**, 547-552.

McClure, W. R. (1985). Mechanism and control of transcription initiation in prokaryotes. *Annu Rev Biochem* **54**, 171-204.

McDaniel, T. K., Jarvis, K. G., Donnenberg, M. S. & Kaper, J. B. (1995). A genetic locus of enterocyte effacement conserved among diverse enterobacterial pathogens. *Proc Natl Acad Sci U S A* **92**, 1664-1668.

McDaniel, T. K. & Kaper, J. B. (1997). A cloned pathogenicity island from enteropathogenic *Escherichia coli* confers the attaching and effacing phenotype on *E. coli* K-12. *Mol Microbiol* **23**, 399-407.

McNamara, B. P., Koutsouris, A., O'Connell, C. B., Nougayrede, J. P., Donnenberg, M. S. & Hecht, G. (2001). Translocated EspF protein from enteropathogenic *Escherichia coli* disrupts host intestinal barrier function. *J Clin Invest* **107**, 621-629.

Mead, P. S. & Griffin, P. M. (1998). *Escherichia coli* O157:H7. *Lancet* **352**, 1207-1212.

Mellies, J. L., Elliott, S. J., Sperandio, V., Donnenberg, M. S. & Kaper, J. B. (1999). The Per regulon of enteropathogenic *Escherichia coli*: identification of a regulatory cascade and a novel transcriptional activator, the locus of enterocyte effacement (LEE)-encoded regulator (Ler). *Mol Microbiol* **33**, 296-306.

Mellies, J. L., Haack, K. R. & Galligan, D. C. (2007). SOS regulation of the type III secretion system of enteropathogenic *Escherichia coli*. *J Bacteriol* **189**, 2863-2872.

Mellmann, A., Bielaszewska, M., Kock, R., Friedrich, A. W., Fruth, A., Middendorf, B., Harmsen, D., Schmidt, M. A. & Karch, H. (2008). Analysis of collection of hemolytic uremic syndrome-associated enterohemorrhagic *Escherichia coli*. *Emerg Infect Dis* **14**, 1287-1290.

Melton-Celsa, A. R., Darnell, S. C. & O'Brien, A. D. (1996). Activation of Shiga-like toxins by mouse and human intestinal mucus correlates with virulence of enterohemorrhagic *Escherichia coli* O91:H21 isolates in orally infected, streptomycin-treated mice. *Infect Immun* **64**, 1569-1576.

Mills, E., Baruch, K., Charpentier, X., Kobi, S. & Rosenshine, I. (2008). Real-time analysis of effector translocation by the type III secretion system of enteropathogenic *Escherichia coli*. *Cell Host Microbe* **3**, 104-113.

Mogridge, J., Mah, T. F. & Greenblatt, J. (1995). A protein-RNA interaction network facilitates the template-independent cooperative assembly on RNA polymerase of a stable antitermination complex containing the lambda N protein. *Genes Dev* **9**, 2831-2845.

Mohawk, K. L., Melton-Celsa, A. R., Zangari, T., Carroll, E. E. & O'Brien, A. D. (2000). Pathogenesis of *Escherichia coli* O157:H7 strain 86-24 following oral infection of BALB/c mice with an intact commensal flora. *Microb Pathog* **48**, 131-142.

Morelli, M. J., Ten Wolde, P. R. & Allen, R. J. (2009). DNA looping provides stability and robustness to the bacteriophage lambda switch. *Proc Natl Acad Sci U S A* **106**, 8101-8106.

Muniesa, M., Blanco, J. E., De Simon, M., Serra-Moreno, R., Blanch, A. R. & Jofre, J. (2004). Diversity of stx2 converting bacteriophages induced from Shiga-toxin-producing *Escherichia coli* strains isolated from cattle. *Microbiology* **150**, 2959-2971.

Murphy, K. C., Campellone, K. G. & Poteete, A. R. (2000). PCR-mediated gene replacement in *Escherichia coli*. *Gene* **246**, 321-330.

Murphy, K. C. & Campellone, K. G. (2003). Lambda Red-mediated recombinogenic engineering of enterohemorrhagic and enteropathogenic *E. coli*. *BMC Mol Biol* **4**, 11.

Nadler, C., Baruch, K., Kobi, S. & other authors (2010). The type III secretion effector NleE inhibits NF-kappaB activation. *PLoS Pathog* **6**, e1000743.

Nagai, T., Abe, A. & Sasakawa, C. (2005). Targeting of enteropathogenic *Escherichia coli* EspF to host mitochondria is essential for bacterial pathogenesis: critical role of the 16th leucine residue in EspF. *J Biol Chem* **280**, 2998-3011.

Nakanishi, N., Abe, H., Ogura, Y., Hayashi, T., Tashiro, K., Kuhara, S., Sugimoto, N. & Tobe, T. (2006). ppGpp with DksA controls gene expression in the locus of enterocyte effacement (LEE) pathogenicity island of enterohaemorrhagic *Escherichia coli* through activation of two virulence regulatory genes. *Mol Microbiol* **61**, 194-205.

Napoli, C. & Staskawicz, B. (1987). Molecular characterization and nucleic acid sequence of an avirulence gene from race 6 of *Pseudomonas syringae* pv. *glycinea*. *J Bacteriol* **169**, 572-578.

Nataro, J. P. & Kaper, J. B. (1998). Diarrheagenic *Escherichia coli*. *Clin Microbiol Rev* **11**, 142-201.

Naylor, S. W., Low, J. C., Besser, T. E., Mahajan, A., Gunn, G. J., Pearce, M. C., McKendrick, I. J., Smith, D. G. & Gally, D. L. (2003). Lymphoid follicle-dense mucosa at the terminal rectum is the principal site of colonization of enterohemorrhagic *Escherichia coli* O157:H7 in the bovine host. *Infect Immun* **71**, 1505-1512.

Naylor, S. W., Roe, A. J., Nart, P., Spears, K., Smith, D. G., Low, J. C. & Gally, D. L. (2005). *Escherichia coli* O157: H7 forms attaching and effacing lesions at the terminal rectum of cattle and colonization requires the LEE4 operon. *Microbiology* **151**, 2773-2781.

Neal, L. M., McCarthy, E. A., Morris, C. R. & Mantis, N. J. (2011). Vaccine-induced intestinal immunity to ricin toxin in the absence of secretory IgA. *Vaccine* **29**, 681-689.

Neely, M. N. & Friedman, D. I. (1998). Arrangement and functional identification of genes in the regulatory region of lambdoid phage H-19B, a carrier of a Shiga-like toxin. *Gene* **223**, 105-113.

Neves, B. C., Knutton, S., Trabulsi, L. R., Sperandio, V., Kaper, J. B., Dougan, G. & Frankel, G. (1998). Molecular and ultrastructural characterisation of EspA from different enteropathogenic *Escherichia coli* serotypes. *FEMS Microbiol Lett* **169**, 73-80.

Newton, H. J., Pearson, J. S., Badea, L. & other authors (2010). The type III effectors NleE and NleB from enteropathogenic *E. coli* and OspZ from *Shigella* block nuclear translocation of NF-kappaB p65. *PLoS Pathog* **6**, e1000898.

Nougayrede, J. P. & Donnenberg, M. S. (2004). Enteropathogenic *Escherichia coli* EspF is targeted to mitochondria and is required to initiate the mitochondrial death pathway. *Cell Microbiol* **6**, 1097-1111.

O'Connell, C. B., Creasey, E. A., Knutton, S. & other authors (2004). SepL, a protein required for enteropathogenic *Escherichia coli* type III translocation, interacts with secretion component SepD. *Mol Microbiol* **52**, 1613-1625.

O'Brien, J. B. K. a. A. D. (1998). *Escherichia coli* O157:H7 and Other Shiga Toxin-Producing *E. coli* Strains. Washington, DC, USA: ASM Press.

Ogino, T., Ohno, R., Sekiya, K., Kuwae, A., Matsuzawa, T., Nonaka, T., Fukuda, H., Imajoh-Ohmi, S. & Abe, A. (2006). Assembly of the type III secretion apparatus of enteropathogenic *Escherichia coli*. *J Bacteriol* **188**, 2801-2811.

Ogura, Y., Kurokawa, K., Ooka, T. & other authors (2006). Complexity of the genomic diversity in enterohemorrhagic *Escherichia coli* O157 revealed by the combinational use of the O157 Sakai OligoDNA microarray and the Whole Genome PCR scanning. *DNA Res* **13**, 3-14.

Ogura, Y., Ooka, T., Iguchi, A. & other authors (2009). Comparative genomics reveal the mechanism of the parallel evolution of O157 and non-O157 enterohemorrhagic *Escherichia coli*. *Proc Natl Acad Sci U S A* **106**, 17939-17944.

Oppenheim, A. B., Kobiler, O., Stavans, J., Court, D. L. & Adhya, S. (2005). Switches in bacteriophage lambda development. *Annu Rev Genet* **39**, 409-429.

Orskov, F., Orskov, I. & Villar, J. A. (1987). Cattle as reservoir of verotoxin-producing *Escherichia coli* O157:H7. *Lancet* **2**, 276.

Pallen, M. J., Beatson, S. A. & Bailey, C. M. (2005a). Bioinformatics analysis of the locus for enterocyte effacement provides novel insights into type-III secretion. *BMC Microbiol* **5**, 9.

Pallen, M. J., Beatson, S. A. & Bailey, C. M. (2005b). Bioinformatics, genomics and evolution of non-flagellar type-III secretion systems: a Darwinian perspective. *FEMS Microbiol Rev* **29**, 201-229.

Pallen, M. J., Penn, C. W. & Chaudhuri, R. R. (2005c). Bacterial flagellar diversity in the post-genomic era. *Trends Microbiol* **13**, 143-149.

Park, S. J. & Gunsalus, R. P. (1995). Oxygen, iron, carbon, and superoxide control of the fumarase fumA and fumC genes of *Escherichia coli*: role of the arcA, fnr, and soxR gene products. *J Bacteriol* **177**, 6255-6262.

Parkinson, J. S. (1993). Signal transduction schemes of bacteria. *Cell* **73**, 857-871.

Paton, J. C. & Paton, A. W. (1998). Pathogenesis and diagnosis of Shiga toxin-producing *Escherichia coli* infections. *Clin Microbiol Rev* **11**, 450-479.

Peacock, S. & Weissbach, H. (1985). *Escherichia coli* integration host factor inhibits the NusA stimulation of RNA polymerase sigma subunit synthesis in vitro. *Arch Biochem Biophys* **243**, 315-319.

Pearce, M. C., Chase-Topping, M. E., McKendrick, I. J. & other authors (2009). Temporal and spatial patterns of bovine *Escherichia coli* O157 prevalence and comparison of temporal changes in the patterns of phage types associated with bovine shedding and human *E. coli* O157 cases in Scotland between 1998-2000 and 2002-2004. *BMC Microbiol* **9**, 276.

Pearson, J. S., Riedmaier, P., Marches, O., Frankel, G. & Hartland, E. L. (2011). A type III effector protease NleC from enteropathogenic *Escherichia coli* targets NF-kappaB for degradation. *Mol Microbiol* **80**, 219-230.

Perna, N. T., Plunkett, G., 3rd, Burland, V. & other authors (2001). Genome sequence of enterohaemorrhagic *Escherichia coli* O157:H7. *Nature* **409**, 529-533.

Pickering, L. K., Obrig, T. G. & Stapleton, F. B. (1994). Hemolytic-uremic syndrome and enterohemorrhagic *Escherichia coli*. *Pediatr Infect Dis J* **13**, 459-475; quiz 476.

Porter, M. E., Mitchell, P., Roe, A. J., Free, A., Smith, D. G. & Gally, D. L. (2004). Direct and indirect transcriptional activation of virulence genes by an AraC-like protein, PerA from enteropathogenic *Escherichia coli*. *Mol Microbiol* **54**, 1117-1133.

Porter, M. E., Mitchell, P., Free, A., Smith, D. G. & Gally, D. L. (2005). The LEE1 promoters from both enteropathogenic and enterohemorrhagic *Escherichia coli* can be activated by PerC-like proteins from either organism. *J Bacteriol* **187**, 458-472.

Proulx F, S. E., Karpman D. (2001). Pathogenesis of Shiga toxin-associated hemolytic uremic syndrome. *Pediatr Res* **50**, 163-171.

Pruimboom-Brees, I. M., Morgan, T. W., Ackermann, M. R., Nystrom, E. D., Samuel, J. E., Cornick, N. A. & Moon, H. W. (2000). Cattle lack vascular receptors for *Escherichia coli* O157:H7 Shiga toxins. *Proc Natl Acad Sci U S A* **97**, 10325-10329.

Rattray, A., Altuvia, S., Mahajna, G., Oppenheim, A. B. & Gottesman, M. (1984). Control of bacteriophage lambda CII activity by bacteriophage and host functions. *J Bacteriol* **159**, 238-242.

Reid, E., Cole, J. & Eaves, D. J. (2001). The *Escherichia coli* CcmG protein fulfils a specific role in cytochrome c assembly. *Biochem J* **355**, 51-58.

Renwick, S. A., Wilson, J. B., Clarke, R. C. & other authors (1993). Evidence of direct transmission of *Escherichia coli* O157:H7 infection between calves and a human. *J Infect Dis* **168**, 792-793.

Rice, D. H., Hancock, D. D. & Besser, T. E. (2003). Faecal culture of wild animals for *Escherichia coli* O157:H7. *Vet Rec* **152**, 82-83.

Riley, L. W., Remis, R. S., Helgerson, S. D. & other authors (1983). Hemorrhagic colitis associated with a rare *Escherichia coli* serotype. *N Engl J Med* **308**, 681-685.

Robinson, C. M., Sinclair, J. F., Smith, M. J. & O'Brien, A. D. (2006). Shiga toxin of enterohemorrhagic *Escherichia coli* type O157:H7 promotes intestinal colonization. *Proc Natl Acad Sci U S A* **103**, 9667-9672.

Roe, A. J., Yull, H., Naylor, S. W., Woodward, M. J., Smith, D. G. & Gally, D. L. (2003a). Heterogeneous surface expression of EspA translocon filaments by *Escherichia coli* O157:H7 is controlled at the posttranscriptional level. *Infection and Immunity* **71**, 5900-5909.

Roe, A. J., Yull, H., Naylor, S. W., Woodward, M. J., Smith, D. G. & Gally, D. L. (2003b). Heterogeneous surface expression of EspA translocon filaments by *Escherichia coli* O157:H7 is controlled at the posttranscriptional level. *Infect Immun* **71**, 5900-5909.

Roe, A. J., Naylor, S. W., Spears, K. J. & other authors (2004). Co-ordinate single-cell expression of LEE4- and LEE5-encoded proteins of *Escherichia coli* O157:H7. *Mol Microbiol* **54**, 337-352.

Rojas, R. L., Gomes, P. A., Bentancor, L. V., Sbrogio-Almeida, M. E., Costa, S. O., Massis, L. M., Ferreira, R. C., Palermo, M. S. & Ferreira, L. C. (2010). Salmonella enterica serovar Typhimurium vaccine strains expressing a nontoxic Shiga-like toxin 2 derivative induce partial protective immunity to the toxin expressed by enterohemorrhagic *Escherichia coli*. *Clin Vaccine Immunol* **17**, 529-536.

Saenger, W., Orth, P., Kisker, C., Hillen, W. & Hinrichs, W. (2000). The Tetracycline Repressor-A Paradigm for a Biological Switch. *Angew Chem Int Ed Engl* **39**, 2042-2052.

Sambrook, J., Fritsch, E.F., and Maniatis, T. (1989). Molecular Cloning. New York: Cold Spring Harbor Laboratory Press.

Sanchez-SanMartin, C., Bustamante, V. H., Calva, E. & Puente, J. L. (2001). Transcriptional regulation of the orf19 gene and the tir-cesT-eae operon of enteropathogenic *Escherichia coli*. *J Bacteriol* **183**, 2823-2833.

- Sanderson, M. W., Gay, J. M., Hancock, D. D., Gay, C. C., Fox, L. K. & Besser, T. E. (1995).** Sensitivity of bacteriologic culture for detection of *Escherichia coli* O157:H7 in bovine feces. *J Clin Microbiol* **33**, 2616-2619.
- Sandvig, K. & van Deurs, B. (1994).** Endocytosis and intracellular sorting of ricin and Shiga toxin. *FEBS Lett* **346**, 99-102.
- Sandvig, K. (2001).** Shiga toxins. *Toxicon* **39**, 1629-1635.
- Schuller, S. & Phillips, A. D. (2010).** Microaerobic conditions enhance type III secretion and adherence of enterohaemorrhagic *Escherichia coli* to polarized human intestinal epithelial cells. *Environ Microbiol* **12**, 2426-2435.
- Shalel-Levanon, S., San, K. Y. & Bennett, G. N. (2005).** Effect of ArcA and FNR on the expression of genes related to the oxygen regulation and the glycolysis pathway in *Escherichia coli* under microaerobic growth conditions. *Biotechnol Bioeng* **92**, 147-159.
- Shames, S. R., Deng, W., Guttman, J. A. & other authors (2010).** The pathogenic *E. coli* type III effector EspZ interacts with host CD98 and facilitates host cell prosurvival signalling. *Cell Microbiol* **12**, 1322-1339.
- Shimizu, K., Asahara, T., Nomoto, K., Tanaka, R., Hamabata, T., Ozawa, A. & Takeda, Y. (2003).** Development of a lethal Shiga toxin-producing *Escherichia coli*-infection mouse model using multiple mitomycin C treatment. *Microb Pathog* **35**, 1-9.
- Shotland, Y., Koby, S., Teff, D. & other authors (1997).** Proteolysis of the phage lambda CII regulatory protein by FtsH (HflB) of *Escherichia coli*. *Mol Microbiol* **24**, 1303-1310.
- Shukla, R., Slack, R., George, A., Cheasty, T., Rowe, B. & Scutter, J. (1995).** *Escherichia coli* O157 infection associated with a farm visitor centre. *Commun Dis Rep CDR Rev* **5**, R86-90.
- Smith, H. R. & Scotland, S. M. (1993).** ACP Broadsheet 135: January 1993. Isolation and identification methods for *Escherichia coli* O157 and other Vero cytotoxin producing strains. *J Clin Pathol* **46**, 10-17.
- Smith, H. R. (1998).** *Escherichia coli* O157 infections: the Scottish experience. *Hosp Med* **59**, 164.
- Spears, K. J., Roe, A. J. & Gally, D. L. (2006).** A comparison of enteropathogenic and enterohaemorrhagic *Escherichia coli* pathogenesis. *FEMS Microbiol Lett* **255**, 187-202.
- Sperandio, V., Mellies, J. L., Delahay, R. M., Frankel, G., Crawford, J. A., Nguyen, W. & Kaper, J. B. (2000).** Activation of enteropathogenic *Escherichia coli* (EPEC) LEE2 and LEE3 operons by Ler. *Mol Microbiol* **38**, 781-793.

Sperandio, V., Li, C. C. & Kaper, J. B. (2002). Quorum-sensing *Escherichia coli* regulator A: a regulator of the LysR family involved in the regulation of the locus of enterocyte effacement pathogenicity island in enterohemorrhagic *E. coli*. *Infect Immun* **70**, 3085-3093.

Sperandio, V., Torres, A. G., Jarvis, B., Nataro, J. P. & Kaper, J. B. (2003). Bacteria-host communication: the language of hormones. *Proc Natl Acad Sci U S A* **100**, 8951-8956.

Stewart, V., Chen, L. L. & Wu, H. C. (2003). Response to culture aeration mediated by the nitrate and nitrite sensor NarQ of *Escherichia coli* K-12. *Mol Microbiol* **50**, 1391-1399.

Stewart, V. R., RS. (1995). Dual sensors and dual response regulators interact to control nitrate- and nitrite-responsive gene expression in *Escherichia coli*. Washington D. C: ASM Press.

Strachan, N. J., Dunn, G. M., Locking, M. E., Reid, T. M. & Ogden, I. D. (2006). *Escherichia coli* O157: burger bug or environmental pathogen? *Int J Food Microbiol* **112**, 129-137.

Zheng J, Cui S, Teel LD, Zhao S, Singh R, O'Brien AD, Meng J. (2008) Identification and characterization of Shiga toxin type 2 variants in *Escherichia coli* isolates from animals, food, and humans. *Appl Environ Microbiol*, 74(18):5645-52.

Su, L. K., Lu, C. P., Wang, Y., Cao, D. M., Sun, J. H. & Yan, Y. X. (2010). [Lysogenic infection of a Shiga toxin 2-converting bacteriophage changes host gene expression, enhances host acid resistance and motility]. *Mol Biol (Mosk)* **44**, 60-73.

Sueyoshi, M. & Nakazawa, M. (1994). Experimental infection of young chicks with attaching and effacing *Escherichia coli*. *Infect Immun* **62**, 4066-4071.

Synge, B. A. (2000). Verocytotoxin-producing *Escherichia coli*: a veterinary view. *Symp Ser Soc Appl Microbiol*, 31S-37S.

Tarr, P. I., Gordon, C. A. & Chandler, W. L. (2005). Shiga-toxin-producing *Escherichia coli* and haemolytic uraemic syndrome. *Lancet* **365**, 1073-1086.

Tatsuno, I., Nagano, K., Taguchi, K., Rong, L., Mori, H. & Sasakawa, C. (2003). Increased adherence to Caco-2 cells caused by disruption of the yhiE and yhiF genes in enterohemorrhagic *Escherichia coli* O157:H7. *Infect Immun* **71**, 2598-2606.

Taylor, F. B., Jr., Tesh, V. L., DeBault, L., Li, A., Chang, A. C., Kosanke, S. D., Pysher, T. J. & Siegler, R. L. (1999). Characterization of the baboon responses to

Shiga-like toxin: descriptive study of a new primate model of toxic responses to Stx-1. *Am J Pathol* **154**, 1285-1299.

te Loo, D. M., Monnens, L. A., van Der Velden, T. J., Vermeer, M. A., Preyers, F., Demacker, P. N., van Den Heuvel, L. P. & van Hinsbergh, V. W. (2000). Binding and transfer of verocytotoxin by polymorphonuclear leukocytes in hemolytic uremic syndrome. *Blood* **95**, 3396-3402.

Tobe, T., Ando, H., Ishikawa, H., Abe, H., Tashiro, K., Hayashi, T., Kuhara, S. & Sugimoto, N. (2005). Dual regulatory pathways integrating the RcsC-RcsD-RcsB signalling system control enterohaemorrhagic *Escherichia coli* pathogenicity. *Mol Microbiol* **58**, 320-333.

Tobe, T., Beatson, S. A., Taniguchi, H. & other authors (2006). An extensive repertoire of type III secretion effectors in *Escherichia coli* O157 and the role of lambdoid phages in their dissemination. *Proc Natl Acad Sci U S A* **103**, 14941-14946.

Tolla, D. A. & Savageau, M. A. (2010). Regulation of aerobic-to-anaerobic transitions by the FNR cycle in *Escherichia coli*. *J Mol Biol* **397**, 893-905.

Torruellas, J., Jackson, M. W., Pennock, J. W. & Plano, G. V. (2005). The *Yersinia pestis* type III secretion needle plays a role in the regulation of Yop secretion. *Mol Microbiol* **57**, 1719-1733.

Tovar K, E. A., Hillen W (1988). Identification and nucleotide sequence of the class E tet regulatory elements and operator and inducer binding of the encoded purified Tet repressor. *Mol Gen Genet* **215**, 76-80.

Tree, J. J., Wang, D., McNally, C. & other authors (2009a). Characterization of the effects of salicylidene acylhydrazide compounds on type III secretion in *Escherichia coli* O157:H7. *Infect Immun* **77**, 4209-4220.

Tree, J. J., Wolfson, E. B., Wang, D., Roe, A. J. & Gally, D. L. (2009b). Controlling injection: regulation of type III secretion in enterohaemorrhagic *Escherichia coli*. *Trends Microbiol* **17**, 361-370.

Tree, J. J., Roe, A. J., Flockhart, A. & other authors (2011). Transcriptional regulators of the GAD acid stress island are carried by effector protein-encoding prophages and indirectly control type III secretion in enterohemorrhagic *Escherichia coli* O157:H7. *Mol Microbiol* **80**, 1349-1365.

Tu, X., Nisan, I., Yona, C., Hanski, E. & Rosenshine, I. (2003). EspH, a new cytoskeleton-modulating effector of enterohaemorrhagic and enteropathogenic *Escherichia coli*. *Mol Microbiol* **47**, 595-606.

Tzipori, S., Wachsmuth, I. K., Chapman, C., Birden, R., Brittingham, J., Jackson, C. & Hogg, J. (1986). The pathogenesis of hemorrhagic colitis caused by *Escherichia coli* O157:H7 in gnotobiotic piglets. *J Infect Dis* **154**, 712-716.

Umanski, T., Rosenshine, I. & Friedberg, D. (2002). Thermoregulated expression of virulence genes in enteropathogenic *Escherichia coli*. *Microbiology* **148**, 2735-2744.

Unden, G., Becker, S., Bongaerts, J., Holighaus, G., Schirawski, J. & Six, S. (1995). O₂-sensing and O₂-dependent gene regulation in facultatively anaerobic bacteria. *Arch Microbiol* **164**, 81-90.

Unkmeir, A. & Schmidt, H. (2000). Structural analysis of phage-borne stx genes and their flanking sequences in shiga toxin-producing *Escherichia coli* and *Shigella dysenteriae* type 1 strains. *Infect Immun* **68**, 4856-4864.

Viswanathan, V. K., Koutsouris, A., Lukic, S., Pilkinton, M., Simonovic, I., Simonovic, M. & Hecht, G. (2004). Comparative analysis of EspF from enteropathogenic and enterohemorrhagic *Escherichia coli* in alteration of epithelial barrier function. *Infect Immun* **72**, 3218-3227.

Vossenkamper, A., Marches, O., Fairclough, P. D. & other authors (2010). Inhibition of NF-kappaB signaling in human dendritic cells by the enteropathogenic *Escherichia coli* effector protein NleE. *J Immunol* **185**, 4118-4127.

Wachter, C., Beinke, C., Mattes, M. & Schmidt, M. A. (1999). Insertion of EspD into epithelial target cell membranes by infecting enteropathogenic *Escherichia coli*. *Mol Microbiol* **31**, 1695-1707.

Wadolowski, E. A., Burris, J. A. & O'Brien, A. D. (1990). Mouse model for colonization and disease caused by enterohemorrhagic *Escherichia coli* O157:H7. *Infect Immun* **58**, 2438-2445.

Waldor, M. K. & Friedman, D. I. (2005). Phage regulatory circuits and virulence gene expression. *Curr Opin Microbiol* **8**, 459-465.

Wang, D., Roe, A. J., McAteer, S., Shipston, M. J. & Gally, D. L. (2008). Hierarchical type III secretion of translocators and effectors from *Escherichia coli* O157:H7 requires the carboxy terminus of SepL that binds to Tir. *Mol Microbiol* **69**, 1499-1512.

Wang, G., Clark, C. G. & Rodgers, F. G. (2002). Detection in *Escherichia coli* of the genes encoding the major virulence factors, the genes defining the O157:H7 serotype, and components of the type 2 Shiga toxin family by multiplex PCR. *J Clin Microbiol* **40**, 3613-3619.

Wasteson, Y. (2001). Zoonotic *Escherichia coli*. *Acta Vet Scand Suppl* **95**, 79-84.

Wilson, R. K., Shaw, R. K., Daniell, S., Knutton, S. & Frankel, G. (2001). Role of EscF, a putative needle complex protein, in the type III protein translocation system of enteropathogenic *Escherichia coli*. *Cell Microbiol* **3**, 753-762.

Wu, B., Skarina, T., Yee, A. & other authors (2010). NleG Type 3 effectors from enterohaemorrhagic *Escherichia coli* are U-Box E3 ubiquitin ligases. *PLoS Pathog* **6**, e1000960.

Yang, Z., Kim, J., Zhang, C., Zhang, M., Nietfeldt, J., Southward, C. M., Surette, M. G., Kachman, S. D. & Benson, A. K. (2009). Genomic instability in regions adjacent to a highly conserved pch prophage in *Escherichia coli* O157:H7 generates diversity in expression patterns of the LEE pathogenicity island. *J Bacteriol* **191**, 3553-3568.

Zadik, P. M., Chapman, P. A. & Siddons, C. A. (1993). Use of tellurite for the selection of verocytotoxigenic *Escherichia coli* O157. *J Med Microbiol* **39**, 155-158.

Zhang, L., Chaudhuri, R. R., Constantinidou, C. & other authors (2004). Regulators encoded in the *Escherichia coli* type III secretion system 2 gene cluster influence expression of genes within the locus for enterocyte effacement in enterohemorrhagic *E. coli* O157:H7. *Infect Immun* **72**, 7282-7293.

Zhang, Y., Laing, C., Zhang, Z. & other authors (2009). Lineage and host source are both correlated with levels of Shiga toxin 2 production by *Escherichia coli* O157:H7 strains. *Appl Environ Microbiol* **76**, 474-482.

Zhou, Z., Li, X., Liu, B. & other authors (2010). Derivation of *Escherichia coli* O157:H7 from its O55:H7 precursor. *PLoS One* **5**, e8700.

Zotta, E., Lago, N., Ochoa, F., Repetto, H. A. & Ibarra, C. (2008). Development of an experimental hemolytic uremic syndrome in rats. *Pediatr Nephrol* **23**, 559-567.